Development of biosenseors for the detection of glyphosate and thiabendazole pesticides in water.

Mohamed Amine Berkal

Université de Pau et de Pays de l'Adour (UPPA)

Doctoral school of exact sciences and their applications (ED211)

Presented and defended on October 25, 2023

by **Mohamed Amine BERKAL**

To obtain the degree of Doctor of the Université de Pau et de Pays de l'Adour

Speciality: Biotechnology and Analytical Chemistry

Development of biosensors for the detection of glyphosate and thiabendazole pesticides in water

Jury composition

Dr. Franck Molina: Director of the public-private research centre at Sys2Diag (Montpellier-France) Rapporteur

Dr. Fouzia Boulmedais: CNRS research director (Strasbourg, France) Rapporteur

Prof. Bruno Grassl: UPPA-IPREM (Pau, France) Jury president

Prof. Jean-Jacques Toulmé: Scientific director of Novaptech (Bordeaux, France) Invited member

Prof. Corinne Nardin: Supervisor, UPPA-IPREM (Pau, France)

Remerciements

Chères collègues, chers collègues, amis et famille,

Je tiens à exprimer ma profonde gratitude envers chacun d'entre vous pour votre soutien indéfectible et votre précieuse présence tout au long de mon parcours doctoral. Cette thèse marque une étape cruciale de ma vie académique, et je reconnais pleinement que sans votre contribution exceptionnelle, ce voyage aurait été impossible.

Je souhaite tout particulièrement adresser mes remerciements les plus sincères à ma directrice de thèse, Corinne Nardin. Votre mentorat exemplaire, votre infinie patience et la confiance que vous avez placée en moi ont été les fondements essentiels de mon succès dans ce projet de grande envergure. Votre guidance éclairée a illuminé mon chemin, et je vous suis profondément reconnaissant.

Je tiens également à exprimer ma gratitude envers toute l'équipe du projet Captain Ad Hoc, en particulier Corinne Parat, Luisa Ronga, Christine Lartigau-Dagron, Estelle Ricard et Quentin Palas. Votre collaboration fructueuse, vos idées stimulantes et votre approche réfléchie ont considérablement enrichi mon expérience de recherche.

J'aimerais également exprimer ma sincère gratitude envers l'entreprise Novaptech pour m'avoir accueilli au sein de leur organisation, et plus spécifiquement, je tiens à remercier chaleureusement Jean-Jacques Toulmé, le directeur scientifique, ainsi que Marine Faussillon-Laville, présidente de Novaptech. Votre formation initiale m'a fourni les compétences cruciales nécessaires pour avancer dans ce projet de thèse avec assurance.

À mes parents, bien que les mots ne puissent jamais suffire à exprimer ma gratitude, vous méritez une mention spéciale pour votre soutien indéfectible, vos encouragements permanents, ainsi que vos prières pour moi, jour et nuit.

Youcef, mon frère aîné, je te remercie pour toutes les sorties en bateau que nous avons partagées lors des étés précédents, même si je n'ai malheureusement pas eu l'occasion d'en profiter cet été.

Je tiens également à remercier mes sœurs : Sarah, Rifka et ma jumelle Zohra. Nos conversations incessantes sur les réseaux sociaux m'ont toujours fait sentir proche de chez vous. Merci infiniment d’être toujours à mes côtés.

Mon frère Ammar, je te remercie du fond de mon cœur pour ton aide précieuse et ton soutien qui ont été des facteurs déterminants dans ma capacité à vivre cette expérience exceptionnelle et à devenir la personne que je suis aujourd'hui.

Imène, ma femme, je t'adresse mes remerciements les plus profonds pour ta présence constante à mes côtés lors des moments les plus exigeants de ce périple et surtout pour ta compréhension dans les moments stressants.

J'aimerais également étendre mes gratitudes à mes cousins et mes meilleurs amis, Imad et Islam. Nos souvenirs sont empreints de moments précieux, d'aventures mémorables et, bien sûr, de nos disputes inlassables qui ont forgé notre lien spécial.

Enfin, je souhaite exprimer ma profonde gratitude envers l'université, les organismes de financement et toutes les personnes qui ont contribué, de près ou de loin, à la réalisation de cette thèse remarquable.

Ce travail représente le fruit de nombreuses années de recherche, de réflexion profonde et d'efforts inlassables, et je suis profondément fier de le partager avec vous tous. Votre présence à mes côtés tout au long de cette aventure a été un cadeau inestimable.

Merci encore pour votre soutien inébranlable et votre amitié sincère.

Avec toute ma gratitude et cordialement,

Mohamed Amine Berkal

Résumé général

Ce travail de thèse s'inscrit dans le cadre du projet CAPTAIN AD HOC, dont l'objectif est la détection des pesticides émergents présents dans les eaux environnementales. En collaboration avec l'agence de l'eau de Pau, une liste des pesticides les plus fréquemment détectés dans ces eaux a été établie. Parmi ces pesticides, deux ont été choisis pour une détection spécifique : le glyphosate, l'herbicide le plus utilisé au monde et en France, ainsi que le thiabendazole, principalement employé comme fongicide mais également comme additif de conservation dans l'industrie alimentaire, est également une cible d'intérêt pour ce projet.

L'objectif principal de cette thèse était de détecter ces pesticides sur le terrain, en temps réel, grâce à des biocapteurs spécifiques. Un biocapteur est constitué d'une molécule de bioreconnaissance telle qu'une enzyme, un anticorps, un aptamère ou une cellule, et d'une plateforme de détection électrochimique ou optique. La molécule de bioreconnaissance interagit avec la molécule cible à détecter, générant ainsi des changements physico-chimiques mesurables par la plateforme de détection, permettant ainsi la détection et la quantification de la molécule ciblée.

Parmi les différentes molécules de bioreconnaissance, les aptamères présentent des avantages significatifs par rapport aux anticorps et aux enzymes, notamment leur stabilité, disponibilité et coût de développement relativement bas. Dans cette optique, la première étape des activités de recherche présentées dans cette thèse a consisté à développer des aptamères spécifiques pour les deux pesticides sélectionnés. Trois aptamères spécifiques du glyphosate, nommés GLY1, GLY2 et GLY3, ont été identifiés dans la littérature. Pour le thiabendazole, un aptamère a été fourni par l'entreprise Novaptech, avec laquelle une collaboration a été établie dans le cadre de cette thèse.

Pour les aptamères anti-glyphosate, et après avoir étudié leur interaction avec le glyphosate en utilisant une méthode de digestion enzymatique, aucune interaction spécifique n'a été observée. Cependant, une découverte intéressante a été faite : l'inhibition de l'activité de l'exonucléase I par le glyphosate. Cela a conduit au développement d'un biocapteur de fluorescence basé sur cette inhibition de l'activité enzymatique, permettant ainsi la détection rapide et spécifique du glyphosate dans une gamme linéaire, avec une limite de détection (LOD) supérieure à 16.9 mg L^{-1}.

Seul l'aptamère du thiabendazole montrant une interaction spécifique avec cette petite molécule est disponible, et par conséquent, cet aptamère a été utilisé dans le cadre du développement

d’une plateforme électrochimique. Lors des tentatives ultérieures d'immobilisation de cet aptamère sur une plateforme électrochimique en vue de la détection du thiabendazole, aucune variation significative du signal électrochimique n'a pu être obtenue. Plusieurs hypothèses ont été formulées pour expliquer ce résultat, la plus plausible suggérant que le changement de conformation de l'aptamère lors de son interaction avec le thiabendazole n’est pas suffisamment important pour entraîner une variation significative des propriétés de conductivité à la surface de l'électrode. En revanche, contrairement aux petites molécules, la thrombine, considérée comme une grande molécule et étudiée dans ce projet, a induit des variations électrochimiques significatives via la plateforme électrochimique développée lors de l’étude de son interaction avec l’aptamère correspondant, conduisant ainsi à sa détection. Ceci est dû au fait que la thrombine est spécifiquement retenue à la surface de l'électrode de travail via l’aptamère, ce qui restreint le flux d’électrons, entraînant ainsi une diminution du signal détecté. Il est ainsi très probable que le changement de conformation de l’aptamère en réponse à l’interaction avec la thrombine est plus prononcé, ce qui contribue à un changement du signal.

Bien que la plateforme électrochimique n'ait pas permis la détection du thiabendazole, un aptacapteur de fluorescence a pu être développé en utilisant la méthode de digestion enzymatique avec l'exonucléase I et la spectroscopie de fluorescence. Ce biocapteur présente plusieurs avantages, notamment une rapidité d'analyse, une spécificité élevée pour la détection du thiabendazole, ainsi qu'une grande sensibilité. Il a permis la détection linéaire du thiabendazole sur une plage allant de 0 à 20 mg L^{-1}, avec une LOD de 0.2 mg L^{-1} et un coefficient de détermination (R^2) de 0.9595. Cet aptacapteur de fluorescence ouvre ainsi des perspectives prometteuses pour son utilisation dans la détection rapide, sur place et en temps réel de différents types de cibles pour lesquelles il existe un aptamère spécifique.

General Summary

This doctoral work is part of the CAPTAIN AD HOC project, which aims at detecting emerging pesticides in environmental waters. A list of the most frequently detected pesticides in these waters has been compiled in collaboration with the Pau Water Agency in France. Among these pesticides, two were selected for specific detection: glyphosate, the most widely used herbicide worldwide and in France, and thiabendazole, primarily used as a fungicide but also as a preservative additive in the food industry, making it an interesting target for this project.

The main objective of this thesis was to detect these pesticides on-site and in real-time using specific biosensors. A biosensor consists of a biorecognition molecule such as an enzyme, an antibody, an aptamer, or a cell, and a detection platform such as an electrochemical or optical system. The biorecognition molecule interacts with the target molecule to be analyzed, generating detectable physicochemical changes by the detection platform, allowing for the detection and quantification of the targeted molecule.

Among the various biorecognition molecules, aptamers have significant advantages over antibodies and enzymes, including their stability, availability, and relatively low development cost. In this regard, the first step of the research activities conducted during this doctoral work was to develop specific aptamers for the two selected pesticides. Three specific aptamers for glyphosate, named GLY1, GLY2, and GLY3, were identified in the literature. For thiabendazole, an aptamer was provided by the Novaptech company, with which a collaboration has been established in the frame of this doctoral research activity.

Regarding the anti-glyphosate aptamers, and after studying their interaction with glyphosate using an enzymatic digestion method, no specific interaction was observed. However, an interesting discovery was made: the inhibition of exonuclease I activity by glyphosate. This led to the development of a fluorescence biosensor based on this enzymatic activity inhibition, enabling the rapid and specific detection of glyphosate in a linear range, with a detection limit (LOD) exceeding 16.9 mg L^{-1}.

Only the thiabendazole aptamer, showing a specific interaction with this small molecule, is available, and consequently, this aptamer was used for the development of the electrochemical platform. However, during subsequent attempts to immobilize this aptamer on an electrochemical platform for detection, no significant variation in the electrochemical signal could be obtained. Several hypotheses were formulated to explain this result, with the most plausible suggesting that the conformational change of the aptamer during its interaction with

thiabendazole was not significant enough to induce a measurable variation in conductivity properties at the surface of the electrochemical electrode. In contrast, unlike small molecules, thrombin, considered a large molecule and studied in this project, induced significant electrochemical signal variations through the developed electrochemical platform during its interaction with its corresponding aptamer, leading to its detection. The conformational change of the aptamer in response to thrombin is likely pronounced enough to contribute to the signal decrease.

Although the electrochemical platform did not enable the detection of thiabendazole, a fluorescence aptasensor was successfully developed using the enzymatic digestion method with exonuclease I and fluorescence spectroscopy. This biosensor offers several advantages, including rapid analysis, high specificity for thiabendazole detection, and high sensitivity. It enabled the linear detection of thiabendazole over a range of 0 to 20 mg L^{-1}, with an LOD of 0.2 mg L^{-1} and a determination coefficient (R^2) of 0.9595. This fluorescence aptasensor thus holds promises for use in the rapid, on-site, and real-time detection of different types of targets having their specific aptamers.

Table of Contents

Figures list

Supplementary figures list

Table list

Supplementary table list

General introduction

In 2021, 355,175 tons of pesticides were sold in the European Union (EU), 2.7% more than in 2020 (346,000 tones)[1]. With 20% of purchases in the EU, France is the 2nd highest consumer of pesticides, or "phytosanitary products" for those used in industry, in Europe (after Spain - 21%). Since their introduction, pesticides have provided significant health and economic benefits. At the same time, their widespread use has created serious problems related to their effects on the environment[2,3] and human health[4,5]. The Law on Water and Aquatic Environments in France oblige phytosanitary product distributors to declare their annual sales. This declaration should enable the monitoring of sales within the country (sales traceability) to better evaluate and manage the pesticide-associated risks and also to establish the amount of the fee for diffuse pollution that can be established for each of these distributors. According to the Public Water Information Service (SIE), more than 497 pesticides were sold in France in 2019. The Solgaro Association's iterative card, introduced in June 2022 (**Figure 1**), illustrates the frequency of pesticide utilization across various metropolitan municipalities in France[6].

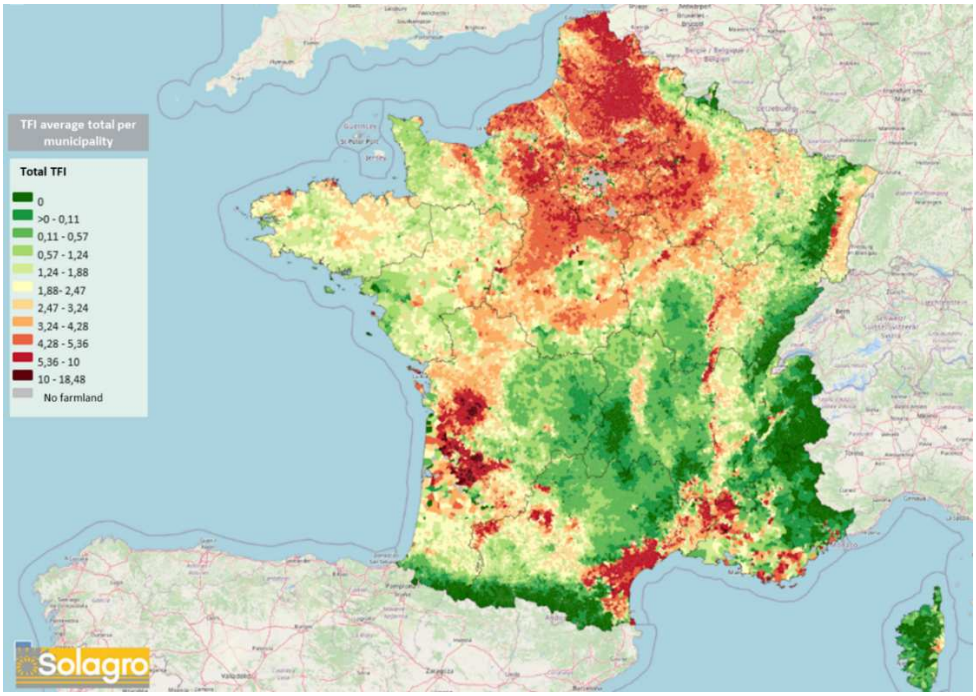

Figure 1. Frequency of pesticide utilization across various metropolitan municipalities in France. Treatment Frequency Indicator (TFI) corresponds to the number of doses of plant protection products applied per hectare during a crop year[6].

The Landes area is the first region of consumption of pesticides in France, particularly herbicides due to the massive culture of corn and in which pesticides are necessary to kill weeds that disturb the harvest.

After their use, pesticides can contaminate surface waters (groundwater, river water, tap water, lakes…) in different ways, including seepage, volatilization, runoff...etc.

To protect the consumer from the dangers of pesticide residue use, the European Water Framework Directive (98/83/EC) has established safety measures to control the quality of drinking water. The amount of each pesticide is therefore regulated and must not exceed a threshold of 0.1 µg L^{-1}, and 0.5 µg L^{-1} for total pesticides i.e., the sum of all pesticides detected in a sample. Following the implementation of this directive, national and international reference laboratories have developed techniques for the analysis of pesticides in surface waters. Generally, the identification and quantification of pesticides are done by liquid[7] (HPLC) or gas chromatography[8] (GC) coupled with mass spectrometry (MS) or other types of detectors. These conventional techniques are sensitive and present strong specificity allowing trace analysis of pesticides in environmental samples. However, these techniques are associated with several limitations: they do not allow on-site and real-time analysis since samples are analyzed in sophisticated laboratories and they require long pretreatment steps before analysis. Moreover, those techniques require highly qualified technicians which makes the analysis expensive.

Researchers thus moved towards the development of sensors which would allow the real-time analysis of pesticides in environmental waters. Sensors can be defined as devices that allow to capture a physical phenomenon and transduce it in a measurable signal. Various pesticide sensors have been developed[9–13]. To enhance the specificity of sensors against pesticides, several biorecognition molecules (antibodies, aptamers, enzymes…) were integrated into those sensors. These, that use a biorecognition molecule as the capture-probe are called ‘‘biosensors’’. A biosensor is defined as the combination of the biomolecule of recognition and a platform of detection which could be optical (colorimetric, fluorometric, photoluminescent…) or electrochemical. Biosensors are largely studied for the detection of pesticide residues in environmental samples[14–18]. Among all biosensors, electrochemical ones are the most prominent due to their high sensitivity and specificity as well as their ability to be easily transported on-site for real-time analysis. They have been widely used for the detection of pesticides[19–22].

Electrochemical biosensors are divided, according to the recognition biomolecule used, into three categories: electrochemical aptasensors using aptamers, electrochemical immunosensors

for those using antibodies, and electrochemical enzymosensors using enzymes in the pesticide detection process. Among these three types of biomolecules, aptamers display some advantages like prolonged shelf life, low cost and in some cases present strong affinity to their targets in comparison to antibodies. Those characteristics make aptamers good candidates for the analysis of pesticides in environmental waters. In this work, we aim at developing aptasensors for the detection of glyphosate and/or s-metolachlor herbicides extensively used in the Landes area in France[23]. Atrazine is also one of our targets since it is frequently found in France's surface water[24].

I. Pesticides

The term pesticides includes all chemical substances intended to repel, prevent or destroy undesirable species causing damage to agricultural products. According to the target to eliminate, pesticides are classified into different families (**Table 1**).

Table 1. Different families of pesticides according to the target to eliminate

PESTICIDE FAMILY	TARGET
HERBICIDES	Destroy weeds or unwanted plants
INSECTICIDES	Destroy or repel insects, ticks and mites
FUNGICIDES	Destroy mold, mildew and other fungi
RODENTICIDES	Used for rodents such as mice and rats
DISINFECTANTS	Used against bacteria, mold and mildew
PRESERVATION PRODUCTS OF WOOD	Protect wood from insects and fungi
BIOCIDES	Destroy all other living organisms

I.1. Classification of pesticides

Pesticides have been categorized into several classifications according to certain characteristics such as their use, general mode of action, chemical family and molecular structure. Each classification takes into consideration different aspects that help us to better understand their chemical and physical properties which allows the improvement of their efficiency on the exposed organisms. **Table 2** shows the main classes of pesticides and their characteristics.

Table 2. Main families of pesticides classified according to their chemical groups and their characteristics[25].

Classification	Characteristics
Organophosphates	- Usually derived from phosphoric acid. - Most organophosphates are insecticides. They control pests by acting on the nervous system. For example, the pesticide disrupts the transmission of nerve impulses by destabilizing the enzyme cholinesterase that regulates acetylcholine (a neurotransmitter). - With some exceptions, the majority of them are highly toxic. - The persistent (breaks down more quickly) in soil, food, or feed than other families of pesticides, such as organochlorines. However, many of them are being phased out or reserved for essential applications.
Organochlorines	- Control pests by disturbing the transmission of nerve impulses. - Generally, they are persistent in soil, food, and in the bodies of humans and animals. - They can accumulate in fatty tissue. - Traditionally, they are used to fight against insects and mites, but a lot of organochlorines are not used due to their persistence for a long time in the environment without decomposing
Carbamates and thiocarbamates	- They are derived from carbamic acid - They control pests by acting on the nervous system (they disturb the transmission of nervous impulses by disturbing the acetylcholinesterase enzyme which regulates the acetylcholine neurotransmitter). - Generally, they are less persistent in the environment than organochlorines.

	- They include insecticides, fungicides and herbicides. - The risks to human and animal health are moderate in the case of herbicides and fungicides in comparison to insecticides.
Synthetic pyrethroids	- They disturb the transmission of nervous impulses by increasing the flow of sodium ions in the axon, which leads finally to paralysis. - They are stable under solar rays.
Organo-nitrogens	- Identified by the suffix "zine". - They are mainly used as herbicides.

I.2. Utilisation of pesticides in France

According to the French Senate, France is the third-largest consumer of pesticides in the world, after the United States and Japan, using 110,000 tons per year, with 100,000 tons used in agriculture. France is also the largest phytosanitary products user, as it's the leading agricultural producer in the European Union, accounting for 21.7% of the total production. Additionally, France is the largest producer of corn in Europe, representing 42% of the total European production. Consequently, France is a significant consumer of herbicides, including glyphosate. According to new monitoring data from the Ecophyto plan, which is an initiative from the Ministry of Agriculture to reduce the use of plant protection products, glyphosate sales increased from 8,859 tons in 2017 to 9,732 tons in 2018. Glyphosate is particularly prevalent in some regions, such as in Alsace and in Les Landes, where corn production is high. (**Figure 2**).

Figure 2. Podium of glyphosate sales by department in France in 2018[26].

I.3. Pesticides effects on human health and environment

Although pesticides have provided significant economic benefits since their introduction and application in agriculture, their widespread use raises serious environmental and health concerns. Many studies have confirmed the association of pesticides with chronic diseases. Alavanja et al.[4] and Beane et al.[5] have confirmed the strong relationship between lung cancer and direct contact with some specific pesticides. The International Agency for Research on Cancer (IARC) has conducted evaluations of the potential health risks associated with pesticides. Their findings are essential references for identifying carcinogenic agents and aid governments in making decisions to safeguard the public against cancer-causing agents in food, the environment, and at workplace. IARC has classified several pesticides as probably carcinogenic, including captafol (a fungicide used for seed treatments on plants), chlordane, dichlorvos, and heptachlorophenol[27]. A cohort study of 57,311 licensed pesticide applicators in the U.S. has shown significant trends regarding the risk of bladder and colon cancer by increasing lifetime exposure to the imazethapyr pesticide[28]. Amr et al.[29] found that male agricultural workers in Egypt may be at higher risk than others for developing bladder cancer, a risk that is associated with pesticide exposure. According to a hospital-based, case-control study of brain cancer, the investigation on the 462 glioma and 195 meningioma sufferers in the United States showed that women who ever used herbicides had a significantly increased risk for meningioma in comparison to women who never used herbicides[30]. Besides, pesticides are also associated with various diseases such as diabetes[31–34], neurological[35–37], and Parkinson's disease[38–40]. Among pesticide substances, atrazine is classified as a priority substance due to its toxicity to the environment[41]. Gammon et al.[42] showed that lifetime exposure to atrazine may cause cancer. Besides, Araújo et al.[43] proved that exposure to atrazine can affect the spatial distribution of fish in freshwater by acting like a chemical barrier isolating fish populations. Furthermore, Cavas[44] has demonstrated the genotoxic potential of atrazine on fish and in which its exposure revealed significant increases in the frequencies of micronuclei and DNA strand breaks in erythrocytes of *Carrasius auratus*. Confirmed hazards of atrazine on human and environmental health led to its ban in 2003 in the European Union.

Pesticides are widely used in agriculture and have proven to be an effective tool for managing pests and increasing crop yields. However, the fate of pesticides is of major concern, as they can have adverse effects on the environment and human health. Once applied, pesticides can enter the soil and leach into groundwater or surface water, causing contamination that can persist for years (**Figure 3**). Pesticides can also be carried by wind or rain, leading to their

dispersal in nearby areas. Additionally, some pesticides can remain in soil and sediment, where they can accumulate and become more concentrated over time[45].

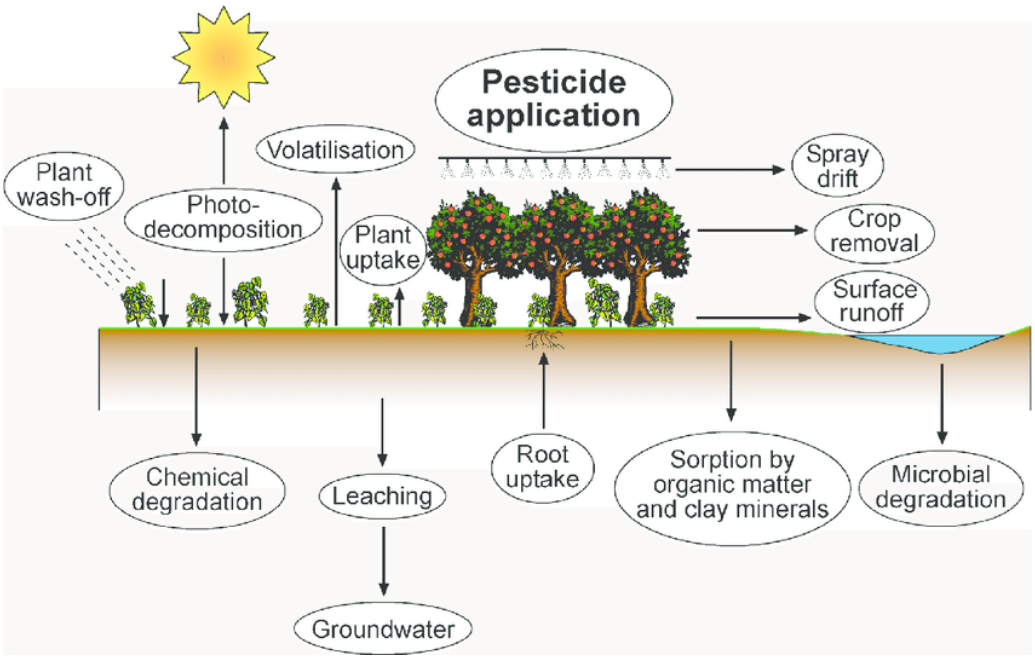

Figure 3. Processes responsible for the fate of applied pesticides in the environment[46].

I.3.1. Aquatic system deterioration

Pesticides are also significant contributors to the degradation of aquatic systems worldwide. Pesticides can enter waterways through runoff or leaching from agricultural and urban areas. Once in the water, pesticides can have adverse effects on aquatic organisms, disrupting their life cycles, growth, and reproductive success. In particular, pesticides can be highly toxic to fish and other aquatic animals, including insects and amphibians. Kole et al.[2] showed that more than 50% of 235 fish samples collected during the period between 1993-94 and 1997-98 contained endosulfan residues from 0.01 – 1.41 µg g^{-1}. Some pesticides, such as organophosphates and carbamates, can cause acute toxicity and death of aquatic organisms[47]. Other pesticides, such as herbicides, can have sub-lethal effects, affecting behaviour and physiology, and leading to long-term impacts on aquatic ecosystems. In France, quality reports of water in the region of Barbezieux-Saint-Hilare point regularly the presence of atrazine herbicide in drinking water[24] although atrazine has been banned since 2003.

I.4. Legislation

In the past two to three decades, public concern regarding the presence of pesticide residues in food and related commodities has risen significantly[48]. As a result, legislative authorities have

implemented strict regulations to monitor the quality of consumable products, including drinking water.

The contamination of water by pesticides is a major concern for the EU, particularly regarding the safety of drinking water. In response, Maximum Residue Levels (MRLs) have been set for each pesticide individually or by group, under the regulation of the European Directive 98/83/EC. This directive mandates continuous monitoring of water quality intended for human consumption, with a maximum concentration of 0.1 µg L^{-1} for each pesticide substance and 0.5 µg L^{-1} for total pesticides. However, to further reduce health and environmental risks, the 2009/128/EC directive requires each EU Member State to develop an action plan to reduce pesticide use. In France, the Ecophyto II^{+} project aims at the reduction of the use of phytosanitary products by 50% by 2025, through the development of less harmful alternatives and improved use techniques. The Labbe law, introduced in 2014, imposes restrictions on the use of plant protection products in private and non-agricultural activities on the French territory in response to this directive. Following the application of these measures, and since the 1st of January 2017, the following statements are noticeable:

- Prohibition for public persons to use or let use phytopharmaceutical products for the maintenance of green spaces, forests and promenades accessible to or open to the public.
- The ban of pesticide sales in self-service for individuals.

And since 1st January 2019:

- Interdiction of sale, utilization and detention of phytopharmaceutical products for non-professional usage.

II. Highlight: Glyphosate

Among all pesticides regulated by the EU directives, glyphosate (CAS number: 1071-83-6) is of special concern since its dangerousness for human health remains debated, and its analysis is challenging due to its specific properties.

Glyphosate (N-phosphonomethyl-glycine) is an organophosphorus pesticide and one of the most widely used pesticides worldwide due to its effectiveness in killing weeds at a moderate price. It was introduced by Monsanto in 1970 under the name of Roundup. Glyphosate inhibits the 5-enolpyruvylshikimate-3-phosphate synthase enzyme (EPSPS), which is responsible for the biosynthesis of aromatic amino acids, causing the cessation of growth and consequently the death of plants.

The carcinogenicity of glyphosate is also under discussion. The International Agency for Research on Cancer (IARC) established in 2015 a report classifying glyphosate in category 2A as "probably carcinogenic for humans"[49]. Two years after (2017), the European Food Safety Authority (EFSA) published a report concluding that glyphosate is not likely to be carcinogenic to humans[50]. These contradictions come from the difficulty of evaluating the real effects of this substance on the human body. The different forms of exposure, the combination with other pesticides or the time needed to carry out studies are parameters that shape the scientific outputs[51].

The massive utilization of glyphosate as a worldwide broad-spectrum herbicide, and the difficulties related to its analysis create the "glyphosate paradox" as it is the most used herbicide and one of the most hardly known[52].

III. Detection of pesticides

The low detection levels required by regulatory authorities and the complex nature of the matrices (food, vegetables, fruits, environmental waters…) in which pesticides are found render sample preparation crucial for pesticide analysis by analytical methods[53,54]. Despite the progress of analytical techniques, samples are too complex and cannot be directly analyzed without prior sample processing steps. Sample pre-treatment enhances both the concentration of analytes, which allows trace analysis and the purification of the matrix, minimizing the presence of interferents at final detection. Sample preparation contains generally three principal steps: extraction, concentration and purification (**Figure 4**).

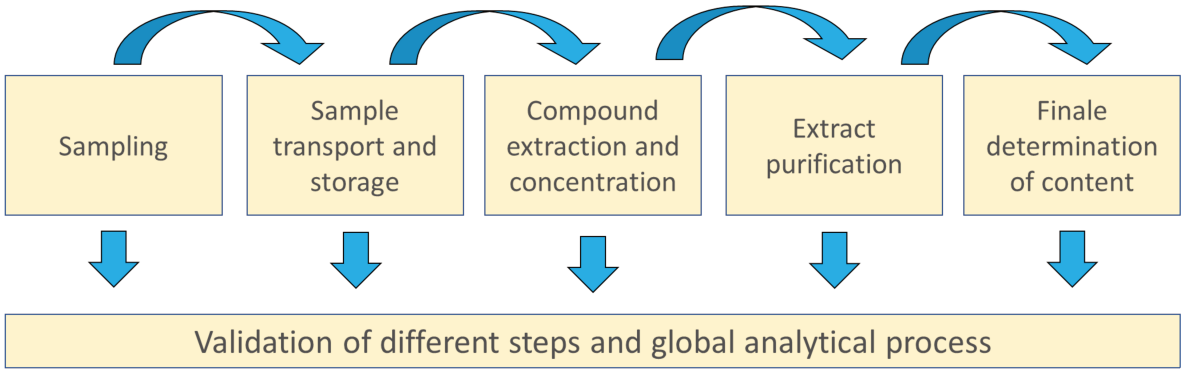

Figure 4. Principal steps for an analytical process used for the determination of pesticide residues in complex matrices.

Monitoring of pesticide residues for public health authorities requires the utilization of techniques that allow robust, sensitive and selective analysis. Two techniques are mainly used

for the separation of pesticides: gas chromatography (GC) and liquid chromatography (LC). The choice of the separation technique is generally based on the nature of the pesticides studied. The detection is ensured by the detectors coupled to these two techniques. They can be specific (UV absorption and fluorescence detectors) or universal (mass spectrometer MS). MS detectors coupled with these two techniques are widely used as it is considered a quasi-universal specific and sensitive analysis tool.

Before chromatographic analysis, pesticides generally need and require appropriate sample pretreatments to clean up or pre-concentrate the target species. Many techniques are used for this goal: liquid-liquid extraction (LLE)[55], solid-phase extraction (SPE)[55–57], for semi-volatile and nonvolatile compounds or headspace extraction[58] and purge-and trap (P and T)[59,60] for volatiles.

III.1. Gas chromatography

Gas chromatography (GC) is mainly applied to gaseous compounds or those that can be vaporized by heating without decomposition. It has been rapidly adopted for multi-residue analysis of pesticides since its introduction in the 1960s due to the high sensitivity and selectivity of analysis that it can provide. GC is compatible with many detectors: flame ionization detector (FID), the thermionic detector (TID), or the electron capture detector (ECD)[61]. Later, the coupling with mass spectrometry (MS) has allowed a gain in sensitivity with unambiguous pesticide analyses compared to the previously developed couplings with other detection systems. **Table 3** shows several examples of pesticide determinations by GC-MS[62].

Table 3. Examples of the application of GC-MS or GC-MS/MS in the analysis of pesticides in food matrices.

Pesticides		Matrices	Analytical methods	Limit of detection (mg kg^{-1})	References
Number	Chemical families				
90	Multi-classes	Apples, green beans and oranges	GC-MS	1.10^{-2} to 2.10^{-2}	Darinka Štajnbaher and Lucija Zupanciˇc-Kralj.
105	Multi-classes	Grapes, Lemons, Onions, and Tomatoes	GC-MS	4.10^{-4} to 5.10^{-2}	Lesueur et al.[63]

14	Organophosphates, organochlorines, carbamates, dicarboximides, and sulfanilamides	Apples, peaches, tomatoes, and potatoes	GC-MS	5.10^{-2} to 25.10^{-2}	Mattern et al.[64]
80	Organophosphates, organochlorines, organonitrates, and pyrethroids	Fruits and vegetables	GC-MS[2]	1.10^{-5} to 35.10^{-3}	Gamon et al.[65]

Nevertheless, the market for phytosanitary products is in constant evolution. New pesticide formulations are continuously introduced on the market both to meet the need for better selectivity depending on the crop and to reduce the persistence of compounds in the environment[66]. The advantage of these compounds is their high efficiency at low doses and their high degree of biodegradation. However, most of these compounds are not very volatile and/or thermolabile which makes them not suitable for direct analysis by GC-MS[7,67,68]. This limitation has led to a strong implementation of liquid chromatography (LC).

III.2. Liquid chromatography

Liquid chromatography is a technique that enables the separation of different compounds of a mixture in solution. The principle of separation is based on the differences in affinities and interactions of a substance for the mobile phase, in which compounds are soluble, and the stationary phase, which has a retarding effect. Reverse phase liquid chromatography (RPLC) is the most commonly used strategy for multi-residue analysis of pesticides[68,69]. Many pesticides with a variety of polarities can be analyzed efficiently by RPLC. Thus, since its introduction during the 1980s, LC coupled with ultraviolet (UV) or fluorescence detectors has been adopted as a complementary technique for GC pesticide analysis[70]. However, some pesticides like glyphosate, are not volatile (not suitable for GC analysis) and don't contain chromophore and/or fluorophore groups permitting their analysis by LC. In this case, derivative agents could be used to overcome this limitation. In the United States, the official method for the detection of glyphosate in drinking water involves liquid chromatography with post-column derivatization and fluorescence detection[71]. The most commonly used derivatization agent for glyphosate detection by LC is 9-fluorenylmethyloxycarbonyl chloride (FMOC-Cl)[72] which improves extraction and separation[19].

Liquid chromatography coupled with mass spectrometry (LC-MS) has also been widely used for the detection of pesticide residues. Due to the high sensitivity and selectivity of MS

detectors, LC-MS has become the reference method among all for pesticide analysis. **Table 4** shows some examples of pesticide detection by LC-MS.

Table 4. Examples of applications of LC-MS² in the analysis of pesticides.

Pesticides			Analytical methods	References
Number	Chemical families	Pesticides		
43	Carbamates, phenylamides, phenyl-ureas, spiracetalamines, phenylamino-pyrimidines, strobilurins, benzo-hydrazides, aryloxy-acids, oxadiazines, triazines, morpholines, pyridines	Aminocarbe, oxamyl, méthomyl, diméthoate, propoxur, carbofuran, carbaryl, isoproturon, diuron, atrazine....	LC-MS^2	Pang et al.[73]
74	Carbamates, conazole, pyrimidine, benzimidazoles	Acetamipride, aldicarbe, benfuracarbe, carbaryl, carbendazime, carbofuran, fenoxycarbe, imazalil...	LC-MS^2	Ortelli et al.[74]
108	Aryloxyacids, carbamates, sulfonylureas, triazines, strobilurins, benzonitriles, carbamates, benzimidazoles, cyclohexanones, phenylamino-pyrimidines, hydrazides, benzoylureas, phenyl-ureas, hydroxyanilides, morpholines, phenylpyrroles, organophosphates, imidazoles, oxadiazines, ureas, oxazoles, phenylamides, pyridazines, pyridines, spiroacetalamines,	2,4 D, aldicarb, carbendazim, carbofuran, dimethoate, diuron, fenoxycarb, ioxynil, linuron, methomyl, oxamyl, pirimicarb, pymetrozine, quinmerac, spiroxamine, vamidothion...	LC-MS^2	Klein et Alder[75]
144	Organophosphates and carbamides	methamidophos, acéphate, omethoate, asulam, tradimefon, tridemorphe....	LC-MS^2	Lehotay et al.[76]

III.3. Sensors

The objective of our work is to develop an analytical strategy to detect, in-situ and in real-time pesticide residues found essentially in environmental waters (tap water, drinking water, lakes, river water…). Chromatographic techniques (GC and LC) are both of high sensitivity and selectivity, however, they require highly qualified human resources to realize analysis and to interpret the obtained spectrum, thus samples need to be pre-treated and then analyzed in sophistical laboratories owning these expensive techniques which makes them unsuitable for the survey of running water that requires analysis at a suitable frequency to detect an eventual pollution peak in real-time and consequently take an action afterwards.

To meet these requirements, increasing efforts are invested to explore alternative measures to detect pesticides with selectivity and sensitivity. Sensors are interesting tools to replace conventional methods as they can detect analytes directly without passing through laborious and tedious sample pretreatment processes. Furthermore, they permit real-time analysis as they can be transported easily to the workplace. Research interests thus focus on the analysis of pesticide residues using sensors, especially in this last decade (**Figure 5**).

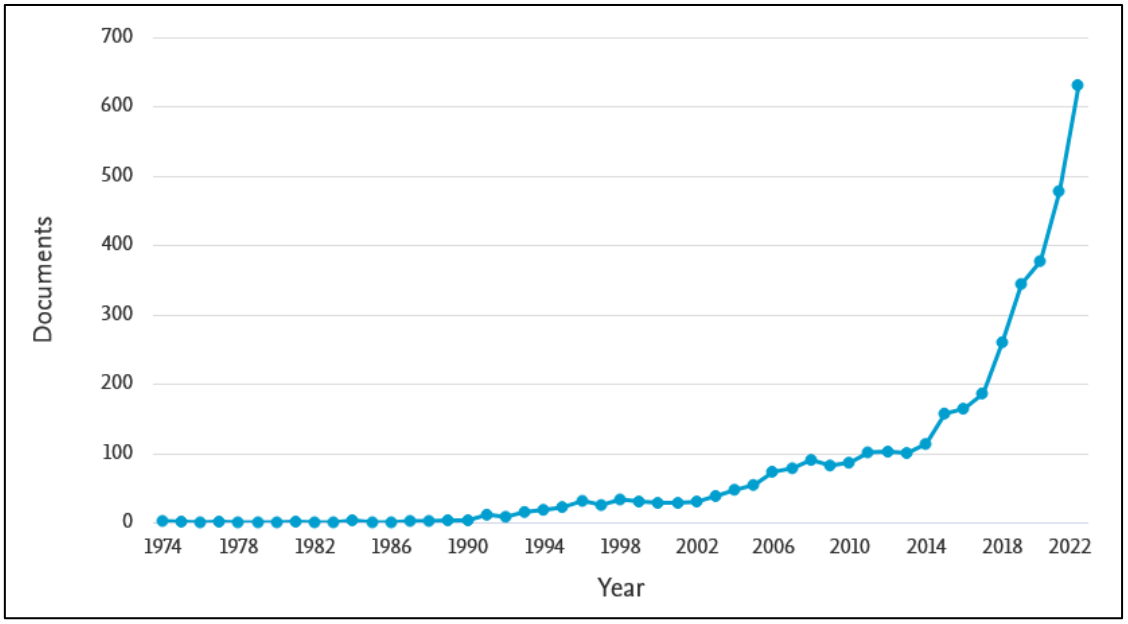

Figure 5. Evolution of the number of publications (a total of 3858 publications) reporting the uses of sensors for the detection of pesticides during the period between 1974 and 2021 according to the Scopus platform (Scopus)[77].

A sensor is a device that allows the transformation of an observed physicochemical phenomenon into a measurable signal through a platform of detection called a "transducer". We often confuse transducer and sensor. The sensor comprises at least one transducer. Sensors were

commonly used for the sensitive and selective detection of metallic compounds using electrochemical platforms as transducer elements as they are electroactive species capable of generating a selective signal leading to their identification and quantification[78–80]. **Figure 6** shows a schematic diagram explaining the operating principle of an electrochemical sensor for metal detection.

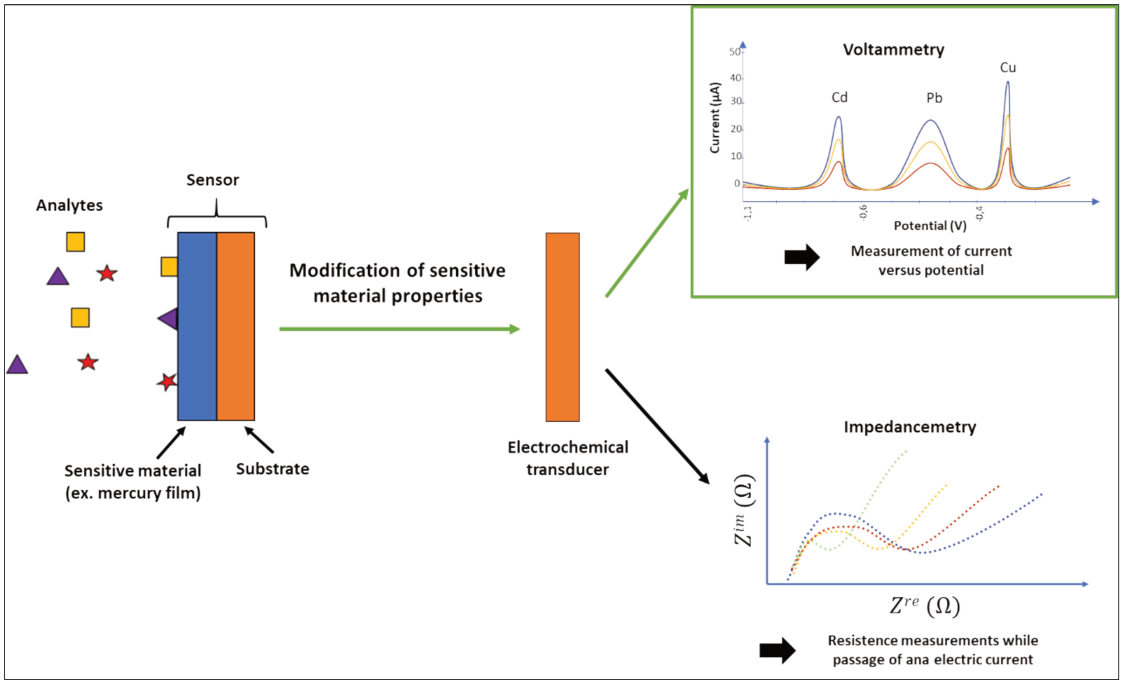

Figure 6. Operating principle of an electrochemical sensor for metal analysis.

However, pesticides are organic components that are not electroactive which makes them unsuitable for electrochemical detection. To overcome this problem related to pesticides, researchers have been focusing on the development of biosensors.

Thesis objective and research context

The techniques predominantly used for the analysis of pesticides in surface waters are liquid or gas chromatography coupled with mass spectrometry or other detectors. These methods are widely known for their high sensitivity and selectivity. However, due to the complexity of the samples under study, the analysis of pesticides using these techniques requires prior sample treatment to extract and purify them before analysis. Furthermore, the analyzed samples need to be collected and transported to analytical laboratories, thereby extending the analysis duration. All of this renders these techniques unsuitable for real-time pesticide analysis, despite the pressing need to quickly detect any pollution peak and take actions immediately to protect consumers.

The main objective of this thesis work is to study and develop a biosensor, considered as a promising solution to meet these urgent requirements. The potential of biosensors relies on their miniaturized design, enabling portability and, consequently, real-time analysis of pesticides. A biosensor is a combination of a recognition molecule, which can be an enzyme, an antibody, an aptamer, or even a whole cell, and a detection platform, which is typically electrochemical or optical. In this thesis work, we will thoroughly investigate the different types of existing biosensors to select the optimal design demonstrating the best performance for our specific application. The chosen biosensor will undergo further development.

IV. References

(1) *EU sales of pesticides rebounded in 2021 - Products Eurostat News - Eurostat*. https://ec.europa.eu/eurostat/web/products-eurostat-news/w/ddn-20230510-1 (accessed 2023-08-28).

(2) Kole, R. K.; Banerjee, H.; Bhattacharyya, A. Monitoring of Market Fish Samples for Endosulfan and Hexachlorocyclohexane Residues in and Around Calcutta. *Bull. Environ. Contam. Toxicol.* **2001**, *67* (4), 554–559. https://doi.org/10.1007/s001280159.

(3) *USGS Scientific Investigations Report 2009-5132: Trends in Pesticide Concentrations in Corn-Belt Streams, 1996–2006*. https://pubs.usgs.gov/sir/2009/5132/ (accessed 2021-10-22).

(4) Alavanja, M. C. R.; Dosemeci, M.; Samanic, C.; Lubin, J.; Lynch, C. F.; Knott, C.; Barker, J.; Hoppin, J. A.; Sandler, D. P.; Coble, J.; Thomas, K.; Blair, A. Pesticides and Lung Cancer Risk in the Agricultural Health Study Cohort. *American Journal of Epidemiology* **2004**, *160* (9), 876–885. https://doi.org/10.1093/aje/kwh290.

(5) Beane Freeman, L. E.; Bonner, M. R.; Blair, A.; Hoppin, J. A.; Sandler, D. P.; Lubin, J. H.; Dosemeci, M.; Lynch, C. F.; Knott, C.; Alavanja, M. C. R. Cancer Incidence among Male Pesticide Applicators in the Agricultural Health Study Cohort Exposed to Diazinon. *American Journal of Epidemiology* **2005**, *162* (11), 1070–1079. https://doi.org/10.1093/aje/kwi321.

(6) Solagro. *Une carte interactive sur l'utilisation des pesticides dans chaque commune*. Banque des Territoires. https://www.banquedesterritoires.fr/une-carte-interactive-sur-lutilisation-des-pesticides-dans-chaque-commune (accessed 2023-08-28).

(7) Núñez, O.; Moyano, E.; Galceran, M. T. LC–MS/MS Analysis of Organic Toxics in Food. *TrAC Trends in Analytical Chemistry* **2005**, *24* (7), 683–703. https://doi.org/10.1016/j.trac.2005.04.012.

(8) van der Hoff, G. R.; van Zoonen, P. Trace Analysis of Pesticides by Gas Chromatography. *Journal of Chromatography A* **1999**, *843* (1–2), 301–322. https://doi.org/10.1016/S0021-9673(99)00511-7.

(9) Anirudhan, T. S.; Alexander, S. Design and Fabrication of Molecularly Imprinted Polymer-Based Potentiometric Sensor from the Surface Modified Multiwalled Carbon Nanotube for the Determination of Lindane (γ-Hexachlorocyclohexane), an Organochlorine Pesticide. *Biosensors and Bioelectronics* **2015**, *64*, 586–593. https://doi.org/10.1016/j.bios.2014.09.074.

(10) Tan, X.; Liu, Y.; Zhang, T.; Luo, S.; Liu, X.; Tian, H.; Yang, Y.; Chen, C. Ultrasensitive Electrochemical Detection of Methyl Parathion Pesticide Based on Cationic Water-Soluble Pillar[5]Arene and Reduced Graphene Nanocomposite. *RSC Advances* **2019**, *9* (1), 345–353. https://doi.org/10.1039/C8RA08555B.

(11) Liu, B.; Zhou, P.; Liu, X.; Sun, X.; Li, H.; Lin, M. Detection of Pesticides in Fruits by Surface-Enhanced Raman Spectroscopy Coupled with Gold Nanostructures. *Food Bioprocess Technol* **2013**, *6* (3), 710–718. https://doi.org/10.1007/s11947-011-0774-5.

(12) Bolat, G.; Abaci, S.; Vural, T.; Bozdogan, B.; Denkbas, E. B. Sensitive Electrochemical Detection of Fenitrothion Pesticide Based on Self-Assembled Peptide-Nanotubes Modified Disposable Pencil Graphite Electrode. *Journal of Electroanalytical Chemistry* **2018**, *809*, 88–95. https://doi.org/10.1016/j.jelechem.2017.12.060.

(13) Tian, X.; Liu, L.; Li, Y.; Yang, C.; Zhou, Z.; Nie, Y.; Wang, Y. Nonenzymatic Electrochemical Sensor Based on CuO-TiO2 for Sensitive and Selective Detection of Methyl Parathion Pesticide in Ground Water. *Sensors and Actuators B: Chemical* **2018**, *256*, 135–142. https://doi.org/10.1016/j.snb.2017.10.066.

(14) Abnous, K.; Danesh, N. M.; Ramezani, M.; Alibolandi, M.; Emrani, A. S.; Lavaee, P.; Taghdisi, S. M. A Colorimetric Gold Nanoparticle Aggregation Assay for Malathion Based on Target-Induced Hairpin Structure Assembly of Complementary Strands of Aptamer. *Microchim Acta* **2018**, *185* (4), 216. https://doi.org/10.1007/s00604-018-2752-3.

(15) Abnous, K.; Danesh, N. M.; Ramezani, M.; Emrani, A. S.; Taghdisi, S. M. A Novel Colorimetric Sandwich Aptasensor Based on an Indirect Competitive Enzyme-Free Method for Ultrasensitive Detection of Chloramphenicol. *Biosensors and Bioelectronics* **2016**, *78*, 80–86. https://doi.org/10.1016/j.bios.2015.11.028.

(16) Chauhan, N.; Pundir, C. S. An Amperometric Biosensor Based on Acetylcholinesterase Immobilized onto Iron Oxide Nanoparticles/Multi-Walled Carbon Nanotubes Modified Gold Electrode for Measurement of Organophosphorus Insecticides. *Analytica Chimica Acta* **2011**, *701* (1), 66–74. https://doi.org/10.1016/j.aca.2011.06.014.

(17) González-Martínez, M. Á.; Brun, E. M.; Puchades, R.; Maquieira, Á.; Ramsey, K.; Rubio, F. Glyphosate Immunosensor. Application for Water and Soil Analysis. *Anal. Chem.* **2005**, *77* (13), 4219–4227. https://doi.org/10.1021/ac048431d.

(18) Lee, H. U.; Shin, H. Y.; Lee, J. Y.; Song, Y. S.; Park, C.; Kim, S. W. Quantitative Detection of Glyphosate by Simultaneous Analysis of UV Spectroscopy and Fluorescence Using DNA-Labeled Gold Nanoparticles. *J. Agric. Food Chem.* **2010**, *58* (23), 12096–12100. https://doi.org/10.1021/jf102784t.

(19) Bettazzi, F.; Romero Natale, A.; Torres, E.; Palchetti, I. Glyphosate Determination by Coupling an Immuno-Magnetic Assay with Electrochemical Sensors. *Sensors* **2018**, *18* (9), 2965. https://doi.org/10.3390/s18092965.

(20) Vaghela, C.; Kulkarni, M.; Haram, S.; Aiyer, R.; Karve, M. A Novel Inhibition Based Biosensor Using Urease Nanoconjugate Entrapped Biocomposite Membrane for Potentiometric Glyphosate Detection.

International Journal of Biological Macromolecules **2018**, *108*, 32–40. https://doi.org/10.1016/j.ijbiomac.2017.11.136.

(21) Xu, G.; Huo, D.; Hou, C.; Zhao, Y.; Bao, J.; Yang, M.; Fa, H. A Regenerative and Selective Electrochemical Aptasensor Based on Copper Oxide Nanoflowers-Single Walled Carbon Nanotubes Nanocomposite for Chlorpyrifos Detection. *Talanta* **2018**, *178*, 1046–1052. https://doi.org/10.1016/j.talanta.2017.08.086.

(22) Ma, L.; Zhou, L.; He, Y.; Wang, L.; Huang, Z.; Jiang, Y.; Gao, J. Mesoporous Bimetallic PtPd Nanoflowers as a Platform to Enhance Electrocatalytic Activity of Acetylcholinesterase for Organophosphate Pesticide Detection. *Electroanalysis* **2018**, *30* (8), 1801–1810. https://doi.org/10.1002/elan.201700845.

(23) *Dataviz - Les produits phytosanitaires en France*. Le portail technique de l'OFB. https://professionnels.ofb.fr/fr/doc-dataviz/dataviz-produits-phytosanitaires-en-france (accessed 2021-11-02).

(24) Lamy, D. Barbezieux-Saint-Hilaire : un chantier école pour prendre soin de l'eau potable. *Sud Ouest*. October 14, 2021. https://www.sudouest.fr/charente/barbezieux-saint-hilaire/barbezieux-saint-hilaire-un-chantier-ecole-pour-prendre-soin-de-l-eau-potable-6561742.php (accessed 2021-10-21).

(25) Gouvernement du Canada, C. canadien d'hygiène et de sécurité au travail. *Pesticides - Généralités : Réponses SST*. https://www.cchst.ca/oshanswers/chemicals/pesticides/general.html (accessed 2021-10-21).

(26) *Utilisation record de pesticides en France*. https://www.notre-planete.info/actualites/1398-record-utilisation-pesticides-France (accessed 2021-10-21).

(27) Cancer, I. A. for R. on; Cancer, I. A. for R. on. Occupational Exposures in Insecticide Application, and Some Pesticides. *IARC monographs on the evaluation of carcinogenic risks to humans* **1991**, *53*.

(28) Koutros, S.; Lynch, C. F.; Ma, X.; Lee, W. J.; Hoppin, J. A.; Christensen, C. H.; Andreotti, G.; Freeman, L. B.; Rusiecki, J. A.; Hou, L.; Sandler, D. P.; Alavanja, M. C. R. Heterocyclic Aromatic Amine Pesticide Use and Human Cancer Risk: Results from the U.S. Agricultural Health Study. *International Journal of Cancer* **2009**, *124* (5), 1206–1212. https://doi.org/10.1002/ijc.24020.

(29) Amr, S.; Dawson, R.; Saleh, D. A.; Magder, L. S.; St. George, D. M.; El-Daly, M.; Squibb, K.; Mikhail, N. N.; Abdel-Hamid, M.; Khaled, H.; Loffredo, C. A. Pesticides, Gene Polymorphisms, and Bladder Cancer Among Egyptian Agricultural Workers. *Archives of Environmental & Occupational Health* **2015**, *70* (1), 19–26. https://doi.org/10.1080/19338244.2013.853646.

(30) Samanic, C. M.; De Roos, A. J.; Stewart, P. A.; Rajaraman, P.; Waters, M. A.; Inskip, P. D. Occupational Exposure to Pesticides and Risk of Adult Brain Tumors. *American Journal of Epidemiology* **2008**, *167* (8), 976–985. https://doi.org/10.1093/aje/kwm401.

(31) Cox, S.; Niskar, A. S.; Narayan, K. M. V.; Marcus, M. Prevalence of Self-Reported Diabetes and Exposure to Organochlorine Pesticides among Mexican Americans: Hispanic Health and Nutrition Examination Survey, 1982–1984. *Environmental Health Perspectives* **2007**, *115* (12), 1747–1752. https://doi.org/10.1289/ehp.10258.

(32) Montgomery, M. P.; Kamel, F.; Saldana, T. M.; Alavanja, M. C. R.; Sandler, D. P. Incident Diabetes and Pesticide Exposure among Licensed Pesticide Applicators: Agricultural Health Study, 1993–2003. *American Journal of Epidemiology* **2008**, *167* (10), 1235–1246. https://doi.org/10.1093/aje/kwn028.

(33) Evangelou, E.; Ntritsos, G.; Chondrogiorgi, M.; Kavvoura, F. K.; Hernández, A. F.; Ntzani, E. E.; Tzoulaki, I. Exposure to Pesticides and Diabetes: A Systematic Review and Meta-Analysis. *Environment International* **2016**, *91*, 60–68. https://doi.org/10.1016/j.envint.2016.02.013.

(34) Velmurugan, G.; Ramprasath, T.; Swaminathan, K.; Mithieux, G.; Rajendhran, J.; Dhivakar, M.; Parthasarathy, A.; Babu, D. D. V.; Thumburaj, L. J.; Freddy, A. J.; Dinakaran, V.; Puhari, S. S. M.; Rekha, B.; Christy, Y. J.; Anusha, S.; Divya, G.; Suganya, K.; Meganathan, B.; Kalyanaraman, N.; Vasudevan, V.; Kamaraj, R.; Karthik, M.; Jeyakumar, B.; Abhishek, A.; Paul, E.; Pushpanathan, M.; Rajmohan, R. K.; Velayutham, K.; Lyon, A. R.; Ramasamy, S. Gut Microbial Degradation of Organophosphate Insecticides-Induces Glucose Intolerance via Gluconeogenesis. *Genome Biology* **2017**, *18* (1), 8. https://doi.org/10.1186/s13059-016-1134-6.

(35) Rastogi, S. K.; Tripathi, S.; Ravishanker, D. A Study of Neurologic Symptoms on Exposure to Organophosphate Pesticides in the Children of Agricultural Workers. *Indian Journal of Occupational and Environmental Medicine* **2010**, *14* (2), 54. https://doi.org/10.4103/0019-5278.72242.

(36) Faria, N. M. X.; Fassa, A. G.; Meucci, R. D.; Fiori, N. S.; Miranda, V. I. Occupational Exposure to Pesticides, Nicotine and Minor Psychiatric Disorders among Tobacco Farmers in Southern Brazil. *NeuroToxicology* **2014**, *45*, 347–354. https://doi.org/10.1016/j.neuro.2014.05.002.

(37) Khan, K.; Ismail, A. A.; Rasoul, G. A.; Bonner, M. R.; Lasarev, M. R.; Hendy, O.; Al-Batanony, M.; Crane, A. L.; Singleton, S. T.; Olson, J. R.; Rohlman, D. S. Longitudinal Assessment of Chlorpyrifos Exposure and Self-Reported Neurological Symptoms in Adolescent Pesticide Applicators. *BMJ Open* **2014**, *4* (3), e004177. https://doi.org/10.1136/bmjopen-2013-004177.

(38) Shimizu, K.; Matsubara, K.; Ohtaki, K.; Shiono, H. Paraquat Leads to Dopaminergic Neural Vulnerability in Organotypic Midbrain Culture. *Neuroscience Research* **2003**, *46* (4), 523–532. https://doi.org/10.1016/S0168-0102(03)00163-9.

(39) Tanner, C. M.; Kamel, F.; Ross, G. W.; Hoppin, J. A.; Goldman, S. M.; Korell, M.; Marras, C.; Bhudhikanok, G. S.; Kasten, M.; Chade, A. R.; Comyns, K.; Richards, M. B.; Meng, C.; Priestley, B.; Fernandez, H. H.; Cambi, F.; Umbach, D. M.; Blair, A.; Sandler, D. P.; Langston, J. W. Rotenone, Paraquat, and Parkinson's Disease. *Environmental Health Perspectives* **2011**, *119* (6), 866–872. https://doi.org/10.1289/ehp.1002839.

(40) Goldstein, D. S.; Sullivan, P.; Cooney, A.; Jinsmaa, Y.; Kopin, I. J.; Sharabi, Y. Rotenone Decreases Intracellular Aldehyde Dehydrogenase Activity: Implications for the Pathogenesis of Parkinson's Disease. *Journal of Neurochemistry* **2015**, *133* (1), 14–25. https://doi.org/10.1111/jnc.13042.

(41) No, D. 2455/2001/EC of the European Parliament and of the Council of 20 November 2001 Establishing the List of Priority Substances in the Field of Water Policy and Amending Directive 2000/60/EC. *Official Journal of the European Communities* **2001**, *15*, 1–5.

(42) Gammon, D. W.; Aldous, C. N.; Carr Jr, W. C.; Sanborn, J. R.; Pfeifer, K. F. A Risk Assessment of Atrazine Use in California: Human Health and Ecological Aspects. *Pest Management Science* **2005**, *61* (4), 331–355. https://doi.org/10.1002/ps.1000.

(43) Araújo, C. V. M.; Silva, D. C. V. R.; Gomes, L. E. T.; Acayaba, R. D.; Montagner, C. C.; Moreira-Santos, M.; Ribeiro, R.; Pompêo, M. L. M. Habitat Fragmentation Caused by Contaminants: Atrazine as a Chemical Barrier Isolating Fish Populations. *Chemosphere* **2018**, *193*, 24–31. https://doi.org/10.1016/j.chemosphere.2017.11.014.

(44) Cavas, T. In Vivo Genotoxicity Evaluation of Atrazine and Atrazine–Based Herbicide on Fish Carassius Auratus Using the Micronucleus Test and the Comet Assay. *Food and Chemical Toxicology* **2011**, *49* (6), 1431–1435. https://doi.org/10.1016/j.fct.2011.03.038.

(45) *Field Boundary Habitats: Implications for Weed, Insect and Disease Management*; Thomas, A. G., Canadian Weed Science Society, Eds.; Canadian Weed Science Society = Societe canadienne de malherbologie: Sainte-Anne-de-Bellevue, Quebec, 2005.

(46) *Fate and Behaviour of pesticides in agroecosystem-a review with a New Zealand perspective*. https://www.researchgate.net/publication/230794737_Fate_and_Behaviour_of_pesticides_in_agroecosystem-a_review_with_a_New_Zealand_perspective (accessed 2021-10-26).

(47) Kaymak, G.; Yön, N. D.; Kayhan, F. E. Insecticide Groups and Their Effects in Aquatic Environment. *MJS* **2013**, *4* (25), 167–167. https://doi.org/10.7240/MJS.2013254096.

(48) Haib, J.; Hofer, I.; Renaud, J.-M. Analysis of Multiple Pesticide Residues in Tobacco Using Pressurized Liquid Extraction, Automated Solid-Phase Extraction Clean-up and Gas Chromatography–Tandem Mass Spectrometry. *Journal of Chromatography A* **2003**, *1020* (2), 173–187. https://doi.org/10.1016/j.chroma.2003.08.049.

(49) Guyton, K. Z.; Loomis, D.; Grosse, Y.; El Ghissassi, F.; Benbrahim-Tallaa, L.; Guha, N.; Scoccianti, C.; Mattock, H.; Straif, K. Carcinogenicity of Tetrachlorvinphos, Parathion, Malathion, Diazinon, and Glyphosate. *The Lancet Oncology* **2015**, *16* (5), 490–491. https://doi.org/10.1016/S1470-2045(15)70134-8.

(50) Authority (EFSA), E. F. S. Peer Review of the Pesticide Risk Assessment of the Potential Endocrine Disrupting Properties of Glyphosate. *EFSA Journal* **2017**, *15* (9), e04979. https://doi.org/10.2903/j.efsa.2017.4979.

(51) Valle, A. L.; Mello, F. C. C.; Alves-Balvedi, R. P.; Rodrigues, L. P.; Goulart, L. R. Glyphosate Detection: Methods, Needs and Challenges. *Environ Chem Lett* **2019**, *17* (1), 291–317. https://doi.org/10.1007/s10311-018-0789-5.

(52) DGS_Anne.M; DGS_Anne.M. *Une réglementation stricte pour maîtriser les risques des pesticides*. Ministère des Solidarités et de la Santé. https://solidarites-sante.gouv.fr/sante-et-environnement/risques-microbiologiques-physiques-et-chimiques/pesticides/article/une-reglementation-stricte-pour-maitriser-les-risques-des-pesticides (accessed 2021-11-15).

(53) Liu, L.-B.; Hashi, Y.; Qin, Y.-P.; Zhou, H.-X.; Lin, J.-M. Development of Automated Online Gel Permeation Chromatography–Gas Chromatograph Mass Spectrometry for Measuring Multiresidual Pesticides in Agricultural Products. *Journal of Chromatography B* **2007**, *845* (1), 61–68. https://doi.org/10.1016/j.jchromb.2006.07.032.

(54) Wang, J.; Cheung, W.; Grant, D. Determination of Pesticides in Apple-Based Infant Foods Using Liquid Chromatography Electrospray Ionization Tandem Mass Spectrometry. *J. Agric. Food Chem.* **2005**, *53* (3), 528–537. https://doi.org/10.1021/jf048413x.

(55) Barceló, D. Environmental Protection Agency and Other Methods for the Determination of Priority Pesticides and Their Transformation Products in Water. *Journal of Chromatography A* **1993**, *643* (1–2), 117–143. https://doi.org/10.1016/0021-9673(93)80546-K.

(56) Masqué, N.; Marcé, R. M.; Borrull, F. Comparison of Different Sorbents for On-Line Solid-Phase Extraction of Pesticides and Phenolic Compounds from Natural Water Followed by Liquid Chromatography. *Journal of Chromatography A* **1998**, *793* (2), 257–263. https://doi.org/10.1016/S0021-9673(97)00936-9.

(57) Aguilar, C.; Borrull, F.; Marcé, R. M. Determination of Pesticides in Environmental Waters by Solid-Phase Extraction and Gas Chromatography with Electron-Capture and Mass Spectrometry Detection. *Journal of Chromatography A* **1997**, *771* (1), 221–231. https://doi.org/10.1016/S0021-9673(97)00091-5.

(58) Li, H.-P.; Li, G.-C.; Jen, J.-F. Determination of Organochlorine Pesticides in Water Using Microwave Assisted Headspace Solid-Phase Microextraction and Gas Chromatography. *Journal of Chromatography A* **2003**, *1012* (2), 129–137. https://doi.org/10.1016/S0021-9673(03)00916-6.

(59) Lee, M.-R.; Lee, J.-S.; Hsiang, W.-S.; Chen, C.-M. Purge-and-Trap Gas Chromatography–Mass Spectrometry in the Analysis of Volatile Organochlorine Compounds in Water. *Journal of Chromatography A* **1997**, *775* (1), 267–274. https://doi.org/10.1016/S0021-9673(97)00306-3.

(60) Zygmunt, B. Determination of Benzene Alkyl Derivatives in Heavily Loaded Environmental Aqueous Samples by Means of Combination of Distillation and Purge and Trap-Gas Chromatography-Mass Spectrometry. *Journal of High Resolution Chromatography* **1997**, *20* (9), 482–486. https://doi.org/10.1002/jhrc.1240200904.

(61) El Mrabet, K. Thèse : Développement d'une méthode d'analyse de résidus de pesticides par dilution isotopique associée à la chromatographie en phase liquide couplée à la spectrométrie de masse en tandem dans les matrices céréalières après extraction en solvant chaud pressurisé. 295.

(62) Di Corcia, A.; Crescenzi, C.; Guerriero, E.; Samperi, R. Ultratrace Determination of Atrazine and Its Six Major Degradation Products in Water by Solid-Phase Extraction and Liquid Chromatography−Electrospray/Mass Spectrometry. *Environ. Sci. Technol.* **1997**, *31* (6), 1658–1663. https://doi.org/10.1021/es960494t.

(63) Lesueur, C.; Knittl, P.; Gartner, M.; Mentler, A.; Fuerhacker, M. Analysis of 140 Pesticides from Conventional Farming Foodstuff Samples after Extraction with the Modified QuECheRS Method. *Food Control* **2008**, *19* (9), 906–914. https://doi.org/10.1016/j.foodcont.2007.09.002.

(64) Mattern, G. C.; Singer, G. M.; Louis, J.; Robson, M.; Rosen, J. D. Determination of Several Pesticides with a Chemical Ionization Ion Trap Detector. *J. Agric. Food Chem.* **1990**, *38* (2), 402–407. https://doi.org/10.1021/jf00092a013.

(65) Gamón, M.; Lleó, C.; Ten, A.; Mocholí, F. Multiresidue Determination of Pesticides in Fruit and Vegetables by Gas Chromatography/Tandem Mass Spectrometry. *Journal of AOAC INTERNATIONAL* **2001**, *84* (4), 1209–1216. https://doi.org/10.1093/jaoac/84.4.1209.

(66) Polati, S.; Bottaro, M.; Frascarolo, P.; Gosetti, F.; Gianotti, V.; Gennaro, M. C. HPLC-UV and HPLC-MSn Multiresidue Determination of Amidosulfuron, Azimsulfuron, Nicosulfuron, Rimsulfuron, Thifensulfuron Methyl, Tribenuron Methyl and Azoxystrobin in Surface Waters. *Analytica Chimica Acta* **2006**, *579* (2), 146–151. https://doi.org/10.1016/j.aca.2006.07.034.

(67) Garrido Frenich, A.; Martínez Vidal, J. L.; López López, T.; Cortés Aguado, S.; Martínez Salvador, I. Monitoring Multi-Class Pesticide Residues in Fresh Fruits and Vegetables by Liquid Chromatography with Tandem Mass Spectrometry. *Journal of Chromatography A* **2004**, *1048* (2), 199–206. https://doi.org/10.1016/j.chroma.2004.07.027.

(68) Hercegová, A.; Dömötörová, M.; Matisová, E. Sample Preparation Methods in the Analysis of Pesticide Residues in Baby Food with Subsequent Chromatographic Determination. *Journal of Chromatography A* **2007**, *1153* (1–2), 54–73. https://doi.org/10.1016/j.chroma.2007.01.008.

(69) Kovalczuk, T.; Jech, M.; Poustka, J.; Hajšlová, J. Ultra-Performance Liquid Chromatography–Tandem Mass Spectrometry: A Novel Challenge in Multiresidue Pesticide Analysis in Food. *Analytica Chimica Acta* **2006**, *577* (1), 8–17. https://doi.org/10.1016/j.aca.2006.06.023.

(70) Hogendoorn, E.; van Zoonen, P. Recent and Future Developments of Liquid Chromatography in Pesticide Trace Analysis. *Journal of Chromatography A* **2000**, *892* (1–2), 435–453. https://doi.org/10.1016/S0021-9673(00)00151-5.

(71) *Methods for the Determination of Organic Compounds in Drinking Water: Supplement I*; Environmental Monitoring Systems Laboratory, Office of Research and Development, U.S. Environmental Protection Agency, 1990.

(72) Gros, P.; Ahmed, A. A.; Kühn, O.; Leinweber, P. Influence of Metal Ions on Glyphosate Detection by FMOC-Cl. *Environ Monit Assess* **2019**, *191* (4), 244. https://doi.org/10.1007/s10661-019-7387-2.

(73) Pang, G.-F.; Liu, Y.-M.; Fan, C.-L.; Zhang, J.-J.; Cao, Y.-Z.; Li, X.-M.; Li, Z.-Y.; Wu, Y.-P.; Guo, T.-T. Simultaneous Determination of 405 Pesticide Residues in Grain by Accelerated Solvent Extraction Then Gas Chromatography-Mass Spectrometry or Liquid Chromatography-Tandem Mass Spectrometry. *Anal Bioanal Chem* **2006**, *384* (6), 1366–1408. https://doi.org/10.1007/s00216-005-0237-9.

(74) Ortelli, D.; Edder, P.; Corvi, C. Multiresidue Analysis of 74 Pesticides in Fruits and Vegetables by Liquid Chromatography–Electrospray–Tandem Mass Spectrometry. *Analytica Chimica Acta* **2004**, *520* (1–2), 33–45. https://doi.org/10.1016/j.aca.2004.03.037.

(75) Klein, J.; Alder, L. Applicability of Gradient Liquid Chromatography with Tandem Mass Spectrometry to the Simultaneous Screening for About 100 Pesticides in Crops. *Journal of AOAC INTERNATIONAL* **2003**, *86* (5), 1015–1037. https://doi.org/10.1093/jaoac/86.5.1015.

(76) Lehotay, S. J.; Kok, A. de; Hiemstra, M.; Bodegraven, P. van. Validation of a Fast and Easy Method for the Determination of Residues from 229 Pesticides in Fruits and Vegetables Using Gas and Liquid Chromatography and Mass Spectrometric Detection. *Journal of AOAC INTERNATIONAL* **2005**, *88* (2), 595–614. https://doi.org/10.1093/jaoac/88.2.595.

(77) *Scopus - Analyze search results*. https://www-scopus-com.inc.bib.cnrs.fr/term/analyzer.uri?sid=6aa6415f35d9a9bc4bc155fc9a41b87c&origin=resultslist&src=s&s=TITLE-ABS-KEY%28Pesticide+sensors%29&sort=plf-f&sdt=b&sot=b&sl=32&count=3116&analyzeResults=Analyze+results&txGid=1279ab55ba407fdbd4ca1f3150a8225f (accessed 2023-08-01).

(78) Brezonik, P. L.; Brauner, P. A.; Stumm, W. Trace Metal Analysis by Anodic Stripping Voltammetry: Effect of Sorption by Natural and Model Organic Compounds. *Water Research* **1976**, *10* (7), 605–612. https://doi.org/10.1016/0043-1354(76)90141-X.

(79) Buffle, J.; Tercier-Waeber, M.-L. Voltammetric Environmental Trace-Metal Analysis and Speciation: From Laboratory to in Situ Measurements. *TrAC Trends in Analytical Chemistry* **2005**, *24* (3), 172–191. https://doi.org/10.1016/j.trac.2004.11.013.

(80) Locatelli, C.; Torsi, G. Voltammetric Trace Metal Determinations by Cathodic and Anodic Stripping Voltammetry in Environmental Matrices in the Presence of Mutual Interference. *Journal of Electroanalytical Chemistry* **2001**, *509* (1), 80–89. https://doi.org/10.1016/S0022-0728(01)00422-3.

Chapter I. Pesticide biosensors: trends and progresses

Résumé

Un biocapteur est une combinaison entre une molécule de reconnaissance telle qu'une enzyme, un anticorps ou un aptamère (une séquence d'ADN simple brin), et une plateforme de détection qui peut être principalement électrochimique ou optique. L'élément de bio-reconnaissance interagit spécifiquement avec la cible étudiée. Cette interaction sera accompagnée par un changement des propriétés physico-chimiques à l'interface de la plateforme de détection qui, via un transducteur, traduit ces variations en un signal mesurable, optique ou électrochimique principalement. Les biocapteurs présentent plusieurs avantages par rapport aux techniques conventionnelles d'analyse des pesticides (chromatographie), y compris la simplicité d'utilisation, le coût d'analyse relativement faible, et la portabilité des biocapteurs qui permettent de réaliser des mesures in-situ afin de détecter des pics de pollution en temps réel et déclencher en conséquence des mesures immédiates afin de protéger le consommateur.

Dans ce chapitre, une étude approfondie des différents types de biocapteurs utilisés pour la détection des pesticides est réalisée, classés principalement selon la molécule de bio-reconnaissance employée. Les avantages et les inconvénients de chaque type de biocapteur sont également discutés dans ce chapitre.

Le travail présenté dans ce chapitre a été publié dans le journal *Analytical and Bioanalytical chemistry* le 05 septembre 2023 sous forme de revue critique.

Summary

A biosensor is a combination of a recognition molecule, such as an enzyme, antibody or aptamer (a single-stranded DNA sequence), and a detection platform, which may be primarily electrochemical or optical. The biorecognition element interacts specifically with the target under study. This interaction will be accompanied by a change in the physicochemical properties at the interface of the detection platform which, via a transducer, translates these variations into a measurable signal, mainly optical or electrochemical. Biosensors offer several advantages over conventional pesticide analysis techniques (chromatography), including ease of use, relatively low analysis costs, and the portability of biosensors, enabling them to perform in-situ measurements to detect pollution peaks in real-time and trigger immediate measures to protect consumers.

This chapter describes in-depth the different types of biosensors used to detect pesticides, classified mainly according to the biorecognition molecule used. The advantages and drawbacks of each type of biosensor are also discussed in this chapter.

The work presented in this chapter was published in the Journal of Analytical and Bioanalytical Chemistry on 05 September 2023 as a critical review.

Table of Contents

Chapter I. Pesticide biosensors: trends and progresses

Mohamed Amine Berkal[1] and Corinne Nardin[1*]

[1]M. A. Berkal, C. Nardin

Universite de Pau et des Pays de l'Adour, E2S UPPA, CNRS, IPREM, Pau, France.

[*]Corresponding author. E-mail: corinne.nardin@univ-pau.fr

Keywords: Pesticides, biosensors, enzyme inhibition-based biosensors, immunosensors, aptasensors.

Abstract

Pesticides, chemical substances extensively employed in agriculture to optimize crop yields, pose potential risks to human and environmental health. Consequently, regulatory frameworks are in place to restrict pesticide residue concentrations in water intended for human consumption. These regulations are implemented to safeguard consumer safety and mitigate any adverse effects on the environment and public health. Although Gas Chromatography- and Liquid Chromatography- Mass Spectrometry (GC-MS and LC-MS) are highly efficient techniques for pesticide quantification, their use is not suitable for real-time monitoring due to the need for sophisticated laboratory pretreatment of samples before analysis. Since they would enable analyte detection with selectivity and sensitivity without sample pretreatment, biosensors appear as a promising alternative. These consist of a bioreceptor allowing for specific recognition of the target and of a detection platform, which translates the biological interaction into a measurable signal. As early detection systems remain urgently needed to promptly alert and act in case of pollution, we review here the biosensors described in the literature for pesticide detection to advance their development for use in the field.

I. Introduction

Pesticides are essential for agriculture to increase crop yields and to provide suitable food production levels. Since their launch, they enabled substantial economic benefits and are thus widely utilized[1]. However, their widespread use concomitantly affects our health[2–5] and our environment[6,7]. The International Agency for Research on Cancer (IARC) plays a crucial role in assessing the impact of pesticides on human health. As a renowned authority in identifying carcinogenic agents, it provides valuable information to decision-making bodies responsible for alerting and safeguarding the public from cancer-causing agents found in food, the environment, and workplaces. Notably, the IARC has classified s-metolachlor, a pesticide of particular concern in France, as probably carcinogenic. In response, the French Agency for Food, Environmental and Occupational Health & Safety (ANSES) has taken steps to phase out its primary use in phytopharmaceuticals[8]. Additionally, the IARC has classified other pesticides, such as captafol (a fungicide used in seed treatments), chlordane, dichlorvos, and heptachlorophenol, as probably carcinogenic[9]. These assessments highlight the importance of rigorous monitoring and control measures to mitigate the potential health risks associated with these substances.

The use of pesticides also leads to the contamination of surface waters[6,7,10]. Over the last 20-25 years[11], public concerns about the presence of pesticide residues in food and drinking water have risen, leading to the implementation of strict regulations by legislative authorities control the quality of consumer products and especially of drinking water. According to the 98/83/EC EU Directive, specific regulations have been implemented regarding the quality limits of pesticide-active substances and their relevant metabolites in water. The general quality limit is set at 0.1 µg L^{-1} per individual substance for most pesticides. However, certain highly toxic substances such as aldrin, dieldrin, heptachlor, and heptachlor epoxide are currently banned, and their quality limit is set at a stricter level of 0.03 µg L^{-1}. Additionally, to address the potential simultaneous presence of multiple pesticides and relevant metabolites, a cumulative approach is adopted. The sum of concentrations of all pesticides and relevant metabolites in water should not exceed 0.5 µg L^{-1}, considering the combined effect of these substances. In parallel, EU Directive No 396/2005 ensures the quality of food products by setting Maximum Residue Limits (MRLs) for pesticides that may be present. These MRLs are continuously updated to accommodate the introduction of new pesticides in the market, reflecting the dynamic nature of agricultural practices.

These regulations are designed to ensure the safety and quality of food products and water resources, considering both individual substances and their potential cumulative impact on their quality.

To detect pesticides at the concentration limits set by the competent authorities, sophisticated techniques are required. Gas chromatography and liquid chromatography coupled with mass spectrometry (GC-MS and LC-MS) are classical techniques used for the sensitive, selective and reproducible analysis of pesticide residues in water[12–15]. Although these techniques are well suited for the quantification of pesticides, the samples studied must be pre-treated and then analyzed in sophisticated laboratories, which renders these techniques unsuitable for survey analyses of running water that require monitoring at a suitable frequency to detect an eventual pollution peak in real-time and to promptly take an action. In order to meet these requirements, increasing efforts are devoted to explore alternative measures to detect pesticides with selectivity and sensitivity. Biosensors appear as elegant tools to replace conventional methods as they could enable the detection of analytes in real-time, minimizing tedious sample pretreatments. **Table I-1** shows a detailed comparison of critical properties between classical techniques and biosensors employed for the detection of pesticides.

Table I-1. Comparison of characteristic parameters between traditional analytical techniques and biosensors employed for the detection of pesticides.

Parameters	Traditional Analytical Techniques	Biosensors
Analysis time	Collection of samples, storage, and transport	Limited sample preparation, Rapid real-time monitoring
Cost	Sophisticated laboratory detection, High-tech equipment, Trained laboratory personnel	Cost-effective, Portable and simple in-situ detection
Eco-friendly and reusability	More organic solvent consumption, Not reusable	No organic solvent is used, Reusable
Sensitivity and selectivity	Highly sensitive and selective	Sensitive and specific
Commercialization	/	Limited commercial applications

A biosensor is a combination of a bioreceptor and a detection platform (**Figure I-1**). The bioreceptor is a biological molecule that allows the specific recognition of the target, whereas the detection platform translates the biological interaction into a measurable, optical, magnetic or electrochemical signal[16–18].

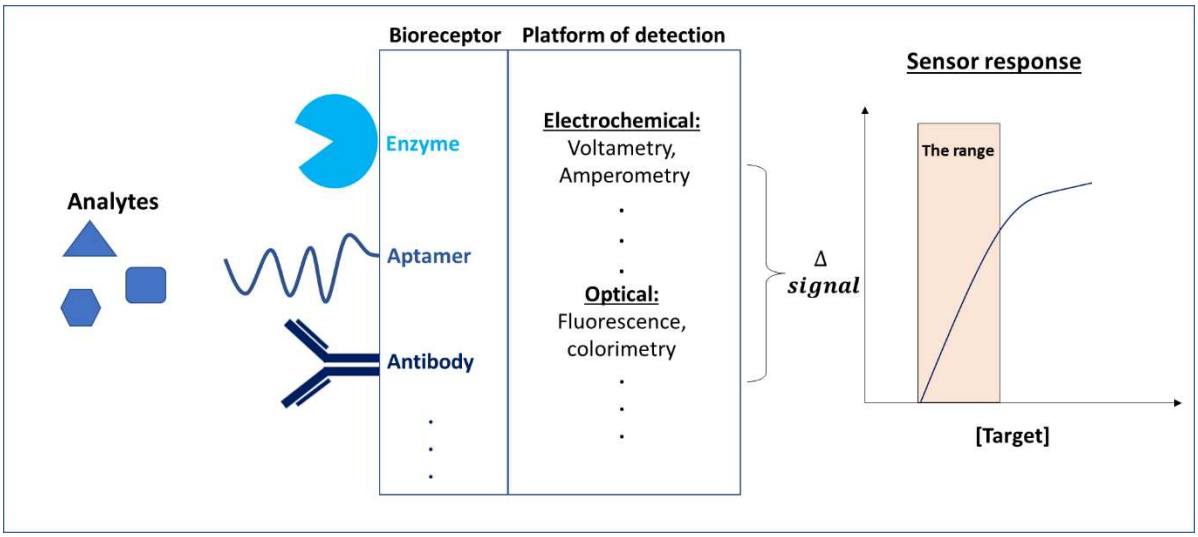

Figure I-1. Schematic illustration of the different types of bioreceptors and transducers used in a biosensor.

Due to their high sensitivity, electrochemical platforms are extensively used in pesticide biosensors[19–21]. In parallel, and due to their easiness of use, simple detection techniques, and satisfactory sensitivity, optical biosensors are also largely used for the detection of pesticides[20,22].

Different types of biomolecules have been employed in biosensors, mainly antibodies, enzymes and aptamers[23]. These biomolecules, due to their nature, undergo specific recognition with their target by different types of interaction, notably electrostatic interactions, hydrogen bonding, aromatic ring stacking and van der Waals interactions. The bioreceptor ensures the specificity of the analysis, whereas the sensitivity is ensured by the detection platform. Biosensors, as point-of-care devices, offer advantages such as rapid detection, user-friendliness, accuracy, portability, cost-effectiveness and easy on-site detection[24,25].

This review covers the bioreceptors the most used and investigated for biosensors development for on-site monitoring of pesticides, namely antibodies, enzymes and aptamers. All biosensors reported in this review are listed in **Table I-2**, where they are classified according to the targeted pesticide, the type of biomolecule employed, and the detection technique utilized. Aptamers, which can be considered chemical antibodies, are synthetic biological molecules that have been widely investigated in the last decade to develop biosensors for detecting pesticides. In this context, an in-depth description of the use of aptasensors as tools for pesticide detection is also reported here.

Table I-2. Comparison of the characteristic properties of different biosensors developed against pesticides.

Pesticide	Detection technique	Type of biomolecule	LOD	Reference
Malathion	Differential Pulse Voltammetry (DPV)	Acetylcholinesterase (AChE)	33 ng L^{-1}	Chauhan and Pundir (2011)[26]
	Cyclic Voltammetry (CV) and Electrochemical Impedance Spectroscopy (EIS)	AChE	0.39 µg L^{-1}	Li et al. (2020)[27]
	CV	AChE	0.31 pg L^{-1}	Jian et al. (2019)[28]
	Fluorescence	AChE and Choline Oxidase (ChOx)	76 µg L^{-1}	Korram et al. (2020)[29]
	DPV	Antibody	0.33 pg L^{-1}	Kaur et al. (2021)[30]
	Fluorescence	Aptamer	88.8 ng L^{-1}	Jiang et al. (2020)[31]
	Colorimetry	Aptamer	0.33 ng L^{-1}	Abnous et al. (2018)[32]
	Fluorescence	Aptamer	0.74 ng L^{-1}	Cheng et al. (2018)[33]
Chlorpyriphos	DPV	AChE	35 ng L^{-1}	Chauhan and Pundir (2011)[26]
	ChronoAmperometry (CA) and CV	Glutathione-S-transferase	60 µg L^{-1}	Borah et al. (2018)[34]
	High open circuit voltage (photoelectrochemical enzymatic fuel cell)	AChE	0.012 µg L^{-1}	Gai et al. (2018)[35]
	DPV	AChE	20 ng L^{-1}	Wang et al. (2016)[36]
	CV	AChE	50 ng L^{-1}	Chen et al. (2017)[37]
	DPV and CV	Antibody	3.5 pg L^{-1}	Talan et al. (2018)[38]

	White Light Reflectance Spectroscopy (WLRS)	Antibody	0.6 µg L^{-1}	Koukouvinos et al. (2017)[39]
	DPV	AChE	56 ng L^{-1}	Zhao et al. (2021)[40]
	EIS	Antibody	70 pg L^{-1}	Hou et al. (2020)[41]
	DPV	Aptamer	70 ng L^{-1}	Xu et al. (2018)[42]
	Colorimetry	Aptamer	11.3 mg L^{-1}	Weerathunge et al. (2019)[43]
	Fluorescence	Aptamer	0.73 ng L^{-1}	Cheng et al. (2018)[33]
Monocrotophos	DPV	AChE	223.2 ng L^{-1}	Chauhan et Pundir (2011)[26]
	Fluorescence	AChE	23 ng L^{-1}	Long et al. (2015) [44]
Endosulfan	DPV	AChE	4.06 µg L^{-1}	Chauhan et Pundir (2011)[26]
	Colorimetry and fluorescence	AChE	0.18 µg L^{-1}	Luo et al. (2018)[45]
	CV and Square Wave Voltammetry (SWV)	Antibody	0.05 µg L^{-1}	Liu et al. (2014)[46]
Glyphosate	Potentiometric assay	Urease	0.5 mg L^{-1}	Vaghela et al. (2018)[47]
	Fluorometric assay	Antibody	0.021 µg L^{-1}	Gonzalez-Martinez et al. (2005)[48]
	Fluorometric assay	Antibody	10 µg L^{-1}	Lee et al. (2010)[49]
	Chronoamperometric assay	Antibody	5 ng L^{-1}	Betazzi et al (2018)[50]
	SERS	Aptamer	0.34 ng L^{-1}	Liu et al (2021)[51]
	Luminescence	Aptamer	4.5 µg L^{-1}	Chen et al. (2020)[52]

	Fluorescence	Aptamer	72.2 ng L^{-1}	Jiang et al. (2020)[31]
	Fluorescence	Aptamer	10 µg L^{-1}	Lee et al. (2010)[49]
Carbendazim	CA and CV	Glutathione-S-transferase	2 µg L^{-1}	Borah et al. (2018)[34]
	Fluorescence	Aptamer	0.44 µg L^{-1}	Su et al. (2020)[53]
Omethoate	DPV	AChE	0.36 ng L^{-1}	Ma et al. (2018)[54]
	Colorimetry	Aptamer	0.35 µg L^{-1}	Liu et al. (2020)[55]
Paraoxon	CA	AChE	0.013 µg L^{-1}	Zhao et al. (2017)[56]
	CA	Butyrylcholinesterase (BChE)	2 µg L^{-1}	Arduini et al. (2019)[57]
	DPV	AChE	1.7 µg L^{-1}	Li et al. (2020)[58]
	Fluorescence	AChE	0.44 pg L^{-1}	Korram et al. (2020)[29]
	CV and SWV	Antibody	2 µg L^{-1}	Liu et al. (2014)[46]
2.4-dichloro-phenoxy-acetic acid	CA	Alkaline phosphatase	50 µg L^{-1}	Arduini et al. (2019)[57]
Phoxim	DPV	AChE	41 ng L^{-1}	Zhao et al. (2021)[40]
Atrazine	EIS	Aptamer	1.3 ng L^{-1}	Madianos et al. (2018)[59]
	CA	Tyrosinase	10 µg L^{-1}	Arduini et al. (2019)[57]
	EIS	Aptamer	2.1 ng L^{-1}	Madianos et al. (2018)[60]
	Photoelectrochemical assay	Aptamer	0.21 ng L^{-1}	Fan et al. (2021)[61]
	EIS	Aptamer	0.67 ng L^{-1}	Zhu et al. (2021)[62]
	Photoelectrochemical assay	Aptamer	2.6 pg L^{-1}	Sun et al. (2019)[63]

	DPV	Aptamer	21.5 pg L^{-1}	Fan et al. (2019)[64]
	LSV	Aptamer	1.6 µg L^{-1}	Wang et al. (2020)[65]
	Adsorption spectroscopy (ATR-SEIRAS)	Aptamer	0.23 µg L^{-1}	Sun et al. (2021)[66]
	Ultrafiltration system	Aptamer	ND	Romero-Reyes and Heemstra (2021)[67]
	Fluorescence	Aptamer	2 ng L^{-1}	Yao et al. (2021)[68]
	SERS	Aptamer	0.14 µg L^{-1}	Wei et al. (2020)[69]
Nitrofen	DPV	Candida Rugosa Lipase	7.38 µg L^{-1}	Cheng et al. (2021)[70]
Dinocap	CA and CV	Glutathione-S-transferase	50 µg L^{-1}	Borah et al. (2018)[34]
Ethyl paraoxon	CV	AChE-ChOx	0.46 ng L^{-1}	Yang et al. (2021)[71]
Dichlorvos	Fluorescence	AChE and ChOx	16.6 pg L^{-1}	Korram et al. (2020)[29]
	Fluorescence	AChE	10 µg L^{-1}	Apilux et al. (2017)[72]
	DPV	AChE	22 ng L^{-1}	Zhao et al. (2021)[40]
Methyl parathion	CV	AChE	0.19 pg L^{-1}	Jian et al. (2019)[28]
Fenthion	CV and EIS	AChE	0.100 mg L^{-1}	Cui et al. (2019)[73]
	DPV	AChE	43 ng L^{-1}	Zhao et al. (2021)[40]
Phosmet	CV and EIS	Tribolium castaneum acetylcholinesterase	1.14 µg L^{-1}	Bial et al. (2021)[74]
Triazophos	Fluorescence	AChE and ChOx	3 ng L^{-1}	Korram et al. (2020)[29]
Pirimicarb	Fluorescence	AChE	50 µg L^{-1}	Apilux et al. (2017)[72]

Carbaryl	Colorimetry and fluorescence	AChE	0.23 μg L^{-1}	Luo et al. (2018)[45]
	Fluorescence	AChE	10 μg L^{-1}	Apilux et al. (2017)[72]
Ethyl-parathion	Fluorescence	AChE	0.7 ng L^{-1}	Sharma et al. (2021)[75]
Parathionmethyl	Fluorescence	AChE	0.67 ng L^{-1}	Long et al. (2015)[44]
DDT	CA and CV	Glutathione-S-transferase	40 μg L^{-1}	Borah et al. (2018)[34]
Dimethoate	Fluorescence	AChE	67 ng L^{-1}	Long et al. (2015)[44]
	DPV	AChE	19 ng L^{-1}	Zhao et al. (2021)[40]
Ethodan	Colorimetry and fluorescence	AChE	0.32 μg L^{-1}	Luo et al. (2018)[45]
Chloramphenicol	Colorimetric assay	Antibody & aptamer	0.19 μg L^{-1} in milk 0.22 μg L^{-1} in serum	Abnous et al. (2016)[76]
Pirimiphos methyl	DPV	AChE	77 ng L^{-1}	Zhao et al. (2021)[40]
Fenitrothion	Enzyme-Linked ImmunoSorbantAssay (ELISA)	Antibody	5 μg L^{-1}	Jiao et al. (2018)[77]
Acetochlor	Colorimetry	Antibody	0.6 μg L^{-1}	Cheng et al. (2019)[78]
Acephate	Colorimetry and fluorescence	AChE	0.14 μg L^{-1}	Luo et al. (2018)[45]
Methamidophos	DPV	AChE	31 ng L^{-1}	Zhao et al. (2021)[40]
Fenpropathrin	Colorimetry	Antibody	0.24 μg L^{-1}	Cheng et al. (2019)[78]
Thiazophos	Surface Plasmon Resonance (SPR)	Antibody	96 ng L^{-1}	Guo et al. (2018)[79]
Amazalil	WLRS	Antibody	0.6 μg L^{-1}	Koukouvinos et al. (2017)[39]
Ethion	CA and CV	Glutathione-S-transferase	100 μg L^{-1}	Borah et al. (2018)[34]

Thiabendazol	WLRS	Antibody	0.8 µg L^{-1}	Koukouvinos et al. (2017)[39]
Paraquat	Amperometry	Antibody	1.4 µg L^{-1}	Valera et al. (2014)[80]
Parathion	EIS	Antibody	52 pg L^{-1}	Mehta et al. (2016)[81]
	ELISA	Antibody	2.5 µg L^{-1}	Jiao et al. (2018)[77]
	DPV	AChE	34 ng L^{-1}	Zhao et al. (2021)[40]
Acetamiprid	EIS	Aptamer	8.9 ng L^{-1}	Madianos et al. (2018)[59]
	EIS	Aptamer	0.2 ng L^{-1}	Madianos et al. (2018)[60]
Carbofuran	DPV	Aptamer	14.8 µg L^{-1}	Li et al. (2018)[82]
Methomyl	DPV	AChE	81 ng L^{-1}	Zhao et al. (2021)[40]
Diazinon	Fluorescence	Aptamer	6.7 ng L^{-1}	Cheng et al. (2018)[33]
	Fluorescence	Aptamer	23 ng L^{-1}	Ron et al. (2020)[83]
	DPV	AChE	55 ng L^{-1}	Zhao et al. (2021)[40]
Trichlorfon	Fluorescence	Aptamer	72.2 ng L^{-1}	Jiang et al. (2020)[31]
	DPV	AChE	21 ng L^{-1}	Zhao et al. (2021)[40]
Omethoate	Fluorescence	Aptamer	2.9 µg L^{-1}	Li et al. (2018)[84]
	Phosphorescence and colorimetric assays	Aptamer	Phosphorescence: 0.54 µg L^{-1} Colorimetry: 7.1 µg L^{-1}	Wang et al. (2019)[85]
	Colorimetry	Aptamer	0.47 µg L^{-1}	Liu et al. (2020)[55]
	DPV	AChE	30 ng L^{-1}	Zhao et al. (2021)[40]

II. Enzyme-based biosensors

Owing to their high selectivity for the substrates to which they bind and drive catalytic reactions, enzymes are of high potential for biosensors development. They are commonly used for the detection of organophosphate (OP) and carbamate pesticides that inhibit the activity of AChE, an essential enzyme for the functioning of the central nervous system[86]. The inhibition of AChE by OP and carbamate pesticides takes place via a phosphorylation mechanism, which blocks serine in the active site through a nucleophilic attack and the production of a serine phosphoester[87]. Based on this reaction scheme, the electrochemical and optical recording of the enzymatic activity reduction enables the detection of this particular type of pesticide in the matrices to be analyzed. Butyrylcholinesterase (BChE)[57], tyrosinase[88,89], alkaline phosphatase[90,91], peroxidase[92], acid phosphatase[93] urease[47] and exonuclease I[94] were also used in inhibition-based pesticide biosensors. As described below, several enzyme-based biosensors were reported for pesticide detection, based on electrochemical and optical transduction[26,35,54].

II.1. Enzymatic inhibition-based electrochemical biosensors

Electrochemical detection methods, including cyclic voltammetry, alternating current voltammetry (ACV), electrochemical impedance spectroscopy (EIS), square wave voltammetry (SWV), differential pulse voltammetry, photoelectrochemical, and electrochemiluminescence, enable the rapid and sensitive detection of redox-active target analytes without requiring complex sample pre-treatment[95]. These electrochemical techniques generate target-induced signals specifically triggered by the presence of the analyte, allowing for its accurate detection and quantification. In particular, enzyme inhibition-based electrochemical biosensors have emerged as a promising approach for pesticide detection (**Figure I-2(A)**), enabling real-time and on-site monitoring of pesticide residues. These biosensors utilize the inhibition of enzymatic activity to achieve precise and frequency-appropriate detection of pesticides, making them valuable tools in pesticide analysis and environmental monitoring.

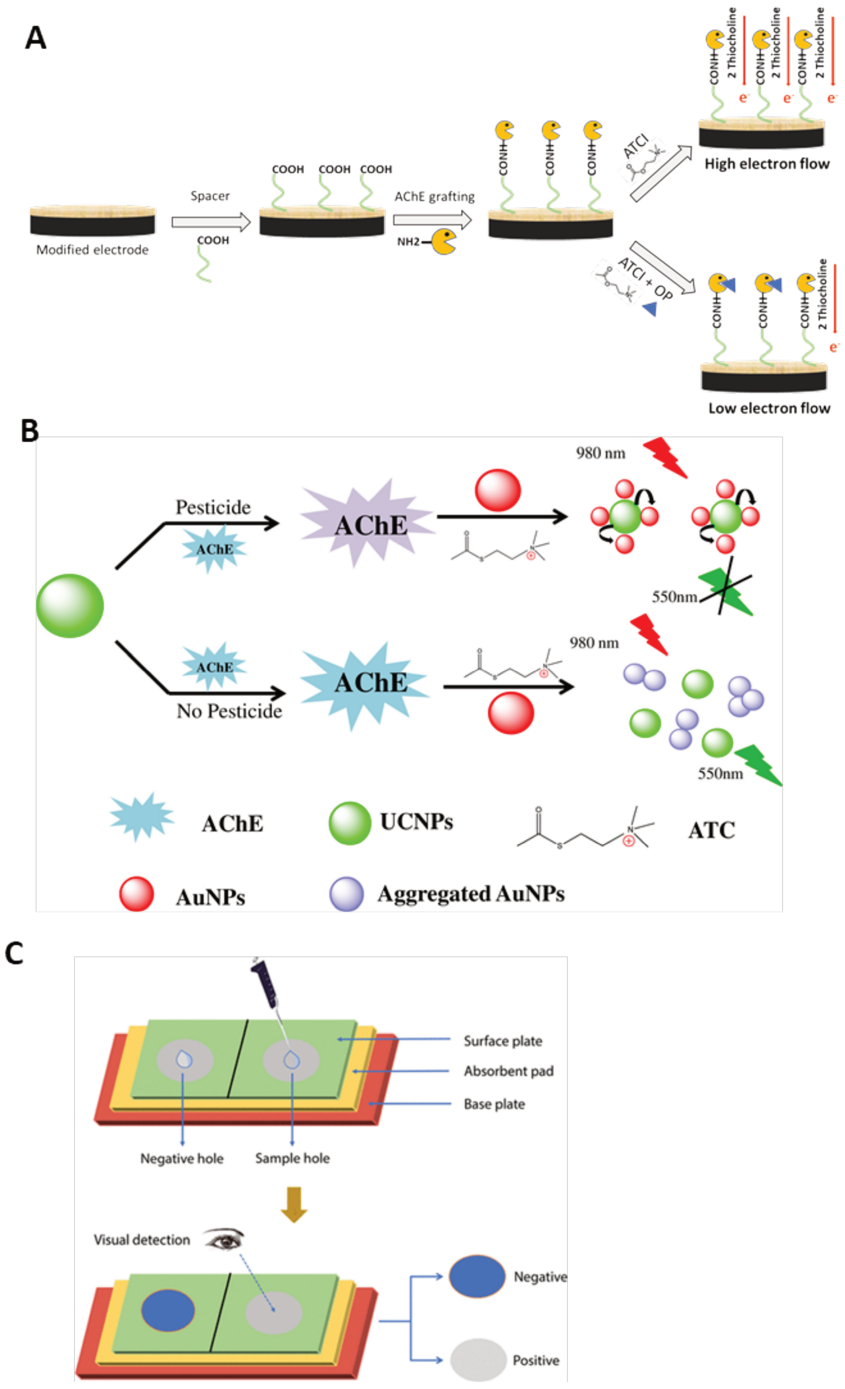

Figure I-2. Comparative schematic diagram of AChE inhibition-based: (A) electrochemical, (B) fluorometric, and (C) colorimetric biosensors for detection of organophosphorus compounds.
(B) Reprinted from [44], with permission from Elsevier. (C) Reprinted from [96], with permission from the American Chemical Society.

II.1.1. Differential pulse voltammetry

Chauhan et al.[26] have selectively detected several organophosphorus pesticides (malathion, chlorpyrifos, monocrotophos and endosulfan) with a high sensitivity by covalently

immobilizing AChE onto iron oxide nanoparticles (Fe_3O_4NPs) and carboxylated multiwalled carbon nanotubes (c-MWCNTs) modified Au electrodes. The acetylcholine (ATCI) is enzymatically hydrolyzed by AChE into thiocholine that undergoes electrocatalytic oxidative dimerization at +0.4 V vs. an Ag/AgCl reference electrode and produces a disulphide compound. The oxidation of thiocholine at the working electrode surface (**Equations I-1 and I-2**) is correlated to the activity of AChE.

ATCI + H_2O ➔ Thiocholine + CH_3COOH **Equation I-1**

2 Thiocholine ➔ $S(CH_2)_2N^+(CH_3)_3$ - $S(CH_2)_2N^+(CH_3)_3$ + $2H^+$ + $2e^-$ **Equation I-2**

In the presence of pesticides, AChE activity is reduced involving a decrease in thiocholine production, resulting in a decreased electrical signal which is proportional to pesticide concentration. Under optimal conditions, the degree of inhibition caused by those pesticides was found to be directly proportional to their concentrations, within the following ranges: 0.1-40 nM for malathion, 0.1-50 nM for chlorpyrifos, 1-50 nM for monocrotophos, and 10-100 nM for endosulfan. The detection limits were determined to be 0.1 nM for malathion and chlorpyrifos, 1 nM for monocrotophos, and 10 nM for endosulfan.

Ma et al.[97] have described the fabrication of PtPd@NCS core-shell structured nanocomposites consisting of a bimetal core (Pt and Pd) encased in an N-doped carbon shell (NCS). The nanocomposites were prepared using a simple one-pot approach, involving the reduction of metal salt precursors, self-polymerization of dopamine, and co-assembly of Pluronic F127. The nanocomposites were then used to prepare an AChE-inhibition-based biosensor for detecting the following organophosphate pesticides: malathion, chlorpyrifos and parathion methyl. The inhibition rate is defined following **Equation I-3** where I_0 represents the original signal recorded by DPV measurements with the as-prepared AChE/PtPd@NCS/graphene carbon electrode (GCE) biosensor in phosphate buffer saline (PBS, pH 7.5) containing ATCI (2.0 mM). I_1 represents the residual signal.

$$\boldsymbol{Inhibition}\ (\%) = \frac{\boldsymbol{I_0 - I_1}}{\boldsymbol{I_0}} \times \mathbf{100}\% \qquad \textbf{Equation I-3}$$

The biosensor functions in a linear detection range for each pesticide, at extremely low limits of detection in the range of femtomoles to attomoles (7.9×10^{-15} M, 7.1×10^{-14} M, and 8.6×10^{-15} M for malathion, chlorpyrifos, and parathion-methyl, respectively). These results underscore the exceptional sensitivity of the AChE biosensor prepared using PtPd@NCS nanocomposites. Recently, nanozyme-based biosensors also showed tremendous potential for pesticide detection[98]. In their study, Wu et al.[99] presented an innovative electrochemical biosensor for detecting

organophosphate pesticides using a two-dimensional MnO_2 nanozyme by DPV measurements. The researchers used manganese dioxide nanosheets (MnNS), more specifically two-dimensional (2D) MnO_2 sheets, in conjunction with AChE to create a homogeneous electrochemical biosensor. This novel biosensor demonstrated excellent performance, exhibiting a linear response for paraoxon in the 0.1 to 20 µg L^{-1} range, with an LOD of 0.025 µg L^{-1}. Importantly, these results align with the MRL requirements established by the European Union (EU).

II.1.2. Potentiometry

Vaghela et al.[47] have described a potentiometric electrochemical biosensor based on bio-nanoconjugate of urease with gold nanoparticles (AuNPs) entrapped in agarose-guar gum to detect glyphosate. The action of urease catalyzes the formation of ammonium ions (**Equation I-4**) that are measured by their selective electrode. In the presence of glyphosate, the urease activity is inhibited, leading to a decrease in ammonium ions formation. According to this inhibition mechanism, the decrease in potentiometric signal indicates the presence of glyphosate and can be used for its detection.

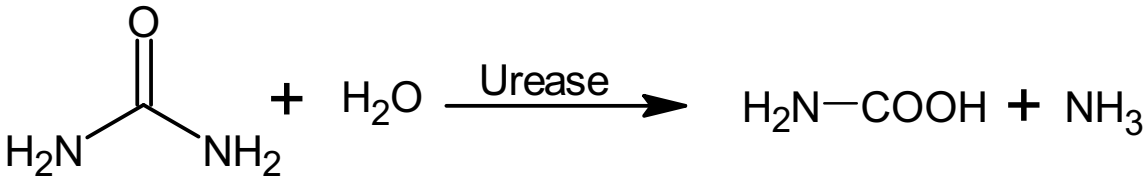

Equation I-4

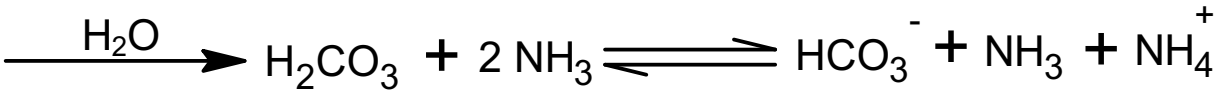

According to this mechanism of detection, a linear glyphosate concentration response is obtained in the range of 0.5 to 50 µg L^{-1}, which is within the MRL established by the World Health Organization (WHO).

II.1.3. Cyclic voltammetry

Five pesticides were detected by glutathione-S-transferase (GST) based electrochemical biosensing: carbendazim, chlorpyrifos, dichlorodiphenyltrichloroethane (DDT), dinocap and ethion[34]. Cyclic voltammetry was used to detect all five pesticides. GST was immobilized onto platinum electrodes using a graphene oxide-gelatin matrix. The immobilization of GST was confirmed through cyclic voltammetry, electrochemical impedance spectroscopy, scanning

electron microscopy and chronoamperometry. The developed GST biosensor has several advantages over other biosensors: it is cost-effective as it is reusable for 8-10 consecutive measurements, and real-time monitoring was demonstrated when using the chronoamperometric mode.

II.1.4. Chronoamperometry

BChE, alkaline phosphatase and tyrosinase were used to develop a novel three-dimensional origami paper-based device that utilizes enzyme inhibition to detect several pesticides: paraxon, 2,4-dichlorophenoxyacetic acid and atrazine[57]. This device combines two office paper-based screen-printed electrodes with multiple filter paper-based pads for loading enzymes and their substrates. By folding and unfolding the filter paper-based structure, the device can analyze pesticides without any need for reagents or sample treatment (**Figure I-3**).

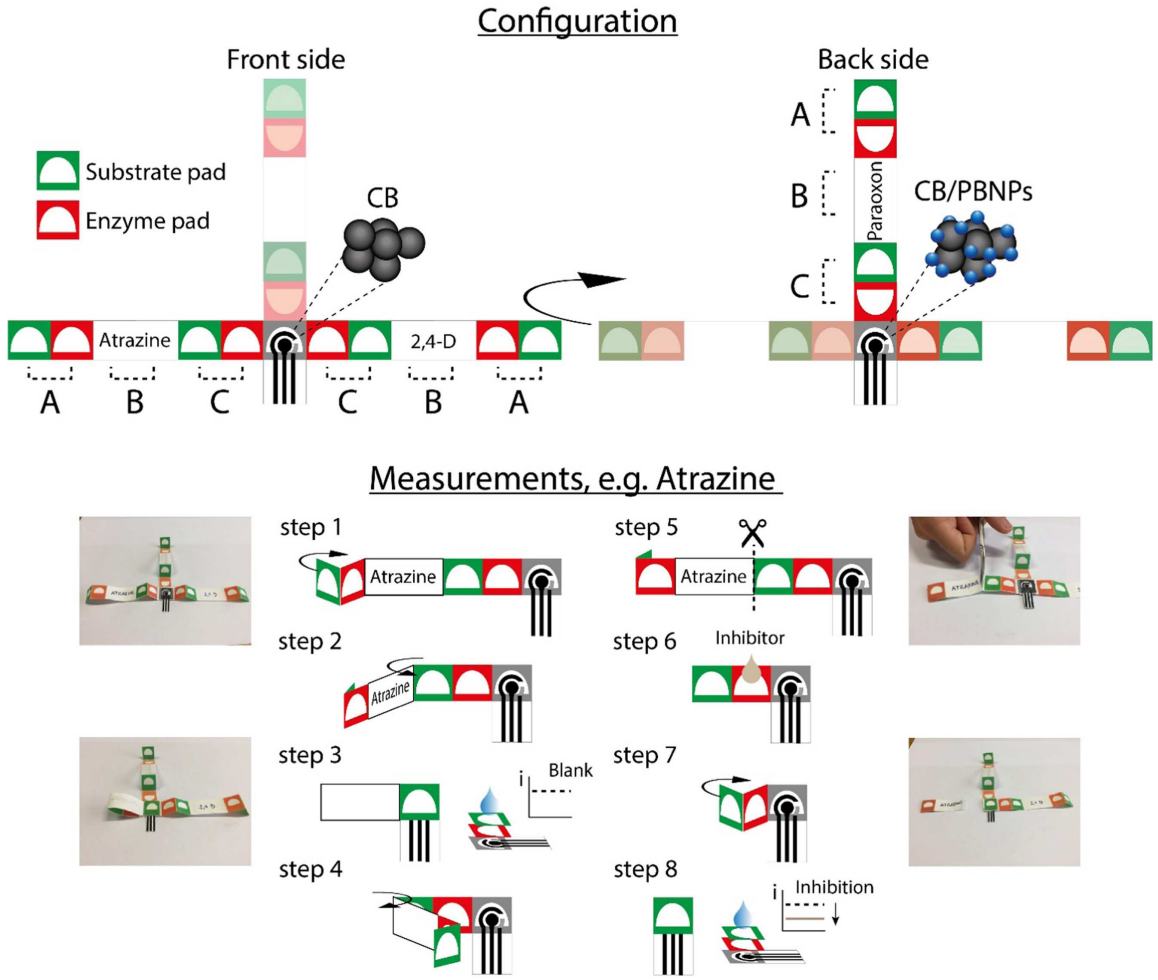

Figure I-3. Schematic illustration of configuration and measurement procedure of the paper-based platform. Reprinted from [57], with permission from Elsevier.

The paper-based platform is advantageous due to its low cost, portability, and ability to analyze multiple pesticides. However, it is based on enzyme inhibition and may not be suitable for

detecting certain types of pesticides. Zhao et al.[56] reported on an electrochemical sensor based on AChE inhibition to detect paraxon. The mentioned biosensor is composed of a screen-printed carbon electrode (SPCE) modified with electrodeposited AuNPs on which MoS_2 nanosheets were immobilized. AChE was immobilized in the last step onto MoS_2 via a glutaraldehyde crosslinker. Using amperometry under optimized conditions, paraxon could be detected at a very low LOD (0.013 µg L^{-1}).

II.2. Optical biosensors

Although enzyme-based biosensors relying on electrochemical detection are highly sensitive and could be used for real-time detection of pesticides, the immobilization of enzymes on the electrode surface is generally tedious and time-consuming. To overcome these difficulties, optical biosensors have been used as an alternative since they are reliable, easy to use, fast and reveal high sensitivity.

II.2.1. Fluorescence spectroscopy

A fluorometric AChE-based biosensor allowed the rapid, simple and sensitive detection of parathion-methyl (**Figure I-2(B)**)[44]. Gold nanoparticles immobilized on the surface of $NaYF_4$:Yb, Er up-conversion nanoparticles (UCNPs) enable fluorescence resonance energy transfer (FRET). Thiocholine present in the solution, after hydrolysis of acetylthiocholine by AChE, interacts with the AuNPs via electrostatic interactions preventing the formation of AuNPs-UCNP complexes, which leads to an increased fluorescence signal. In the presence of parathion-methyl, AChE activity is inhibited, thus preventing the production of thiocholine, which favors the FRET phenomenon, and thus the decrease of fluorescence. The biosensor developed in this study exhibited high sensitivity and stability, indicating its potential for detecting organophosphate pesticides in real samples. Moreover, the biosensor preparation process is less time-consuming compared to grafted enzyme biosensors as the enzyme is not immobilized onto the nanoparticle surfaces but only adsorbed. This advantageous feature makes the biosensor a promising tool for practical applications in detecting pesticides.

II.2.2. Colorimetric assay

The rapid and onsite detection of several pesticides remains challenging, like glyphosate, which is of high polarity, has metal-chelating properties and interferes with organic substances in the environment. Besides, its similarity with its by-products renders its detection difficult. Enzyme-based methods along with colorimetric detection reveal several advantages matching with

glyphosate analysis, i. e. simple preparation, rapid detection and ease of results acquisition[100,101]. Luo et al.[96] have reported a novel colorimetric nanozyme sheet for the rapid detection of glyphosate (**Figure I-2(C)**). Physically adsorbed peroxidase enzymes catalyze the oxidation of chromogenic substrates to produce a color change, the intensity of which is measured by UV-visible spectrophotometry. In the presence of glyphosate, peroxidase is inhibited which results in a decrease of the color intensity.

Targeting the same glyphosate analyte, Li Haiyin et al.[102] have reported a peroxidase-mimetic nanozyme to develop a portable Paper-based Analytical Device (PAD) allowing for its detection. In this article, the preparation of 2D nanosheet-like V_2O_5 (2D-VONz) with exclusive peroxidase-mimetic activity under optimal reaction conditions is described. Interestingly, the activity of 2D-VONz is inhibited by glyphosate, which was then exploited to develop a PAD, on which, glyphosate reduces the activity of 2D-VONz to prevent its catalytic oxidation of 3,3′,5,5′-tetramethylbenzidine, thus contributing to rapid, naked-eye and portable analysis of glyphosate using a smartphone. Another highly efficient biosensor, based on an enzyme-mediated dephosphorylation nanozyme, has been developed for the rapid, specific, and sensitive detection of paraoxon[103]. This biosensor utilizes a novel CeO_2@N-doped carbon (CeO_2@NC) nanozyme. The mechanism underlying the degradation of phosphotriesters, catalyzed by CeO_2@NC, involves the Ce(IV)/Ce(III) species acting as active sites for the polarization and hydrolysis of phosphoester bonds. Additionally, the N-doped carbon (NC) material acts as a synergistic site, facilitating the adsorption of the paraoxon substrate and promoting the hydrolysis process. The characteristic properties of this biosensor are presented in **Table I-3,** which shows different types of enzyme-based biosensors developed against pesticides.

II.2.3. Chemiluminescence assay

Chang et al.[104] introduced a highly sensitive nanozyme chemiluminescence-based (CL) biosensor for the specific detection of glyphosate. The biosensor utilizes a porous hydroxy zirconium oxide nanozyme (ZrO_X-OH) obtained through a straightforward alkali solution treatment of UIO_{66}.ZrO_X-OH which demonstrates remarkable phosphatase-like activity, enabling the dephosphorylation of 3-(2′-spiro-adamantyl)-4 methoxy-4-(3′-phosphoryloxyphenyl)-1,2-dioxetane (AMPPD), which results in the generation of an intense CL signals. Notably, the phosphatase-like ZrO_X-OH exhibited a distinctive response to glyphosate due to the unique interaction between the carboxyl group of glyphosate and the

surface hydroxyl group, leading to the development of a CL biosensor for the direct and selective detection of glyphosate without the need for bio-enzymes.

Table I-3. Enzyme-based biosensors developed for pesticide detection.

Pesticide	Detection technique	Enzyme used	LOD	Validation with real samples	Reference
Malathion, chlorpyrifos, monocrotophos and endosulfan	DPV	AChE	33 ng L^{-1}, 35 ng L^{-1} 223.2 ng L^{-1}, and 4 µg L^{-1}	Milk	Chauhan and Pundir (2011)[26]
Glyphosate	Potentiometric assay	Urease	0.5 mg L^{-1}	Tap water	Vaghela et al (2018)[47]
Carbendazim, chlorpyrifos, dichlorodiphenyltrichloroethane (DDT), dinocap, and ethion	CA and CV	Glutathione-S-transferase	2 µg L^{-1}, 60 µg L^{-1}, 40 µg L^{-1}, 50 µg L^{-1}, and 100 µg L^{-1}	Potatoes	Borah et al. (2018)[34]
Chlorpyrifos	High open circuit voltage (photoelectrochemical enzymatic fuel cell)	AChE	0.012 µg L^{-1}	Not mentioned (PB)	Gai et al. (2018)[35]
Omethoate	DPV	AChE	0.36 ng L^{-1}	Cabbage and cucumber	Ma et al. (2018)[54]
Paraoxon	CA	AChE	13 ng L^{-1}	Apple and pakchoi	Zhao et al. (2017)[56]
Paraoxon, 2.4-dichlorophenoxyacetic acid, and atrazine	CA	BChE, alkaline phosphatase, and tyrosinase	2 µg L^{-1}, 50 µg L^{-1}, and 10 µg L^{-1}	River water	Arduini et al. (2019)[57]
Malathion	CV and EIS	AChE	0.39 µg L^{-1}	Cabbage and carrots	Li et al. (2020)[27]
Nitrofen	DPV	Candida Rugosa Lipase	7.38 µg L^{-1}	Apricot	Cheng et al. (2021)[70]

Ethyl paraoxon	CV	AChE-ChOx	0.46 ng L^{-1}	Pakchoi, cabbage and lettuce	Yang et al. (2021)[71]
Paraoxon	DPV	AChE	1.7 µg L^{-1}	Apple and Eggplant	Li et al. (2020)[58]
Chlorpyrifos	DPV	AChE	20 ng L^{-1}	Cabbage and spinach	Wang et al. (2016)[36]
Chlorpyrifos	CV	AChE	50 ng L^{-1}	Cabbage, rape and lettuce	Chen et al. (2017)[37]
Malathion and methyl parathion	CV	AChE	0.31 pg L^{-1} and 0.188 pg L^{-1}	Tap water and Chinese cabbage	Jian et al. (2019)[28]
Fenthion	CV and EIS	AChE	100 µg L^{-1}	Cabbage juice	Cui et al. (2019)[73]
Phosmet	CV and EIS	Tribolium castaneum acetylcholinesterase	1.14 µg L^{-1}	Wheat flour	Bial et al. (2021)[74]
11 organophosphorus and methomyl	DPV and EIS	AChE	Organophosphorus: 19 – 77 ng L^{-1} Methomyl: 81 ng L^{-1}	Trichlorfon and dichlorvos: Apple and cabbage	Zhao et al. (2021)[40]
Paraoxon	CV	AChE	1.4 µg L^{-1}	Vegetable leaves	Jia et al. (2020)[105]
Paraoxon	CV	AChE	4 µg L^{-1}	Chinese chives and cabbage	Chen et al. (2020)[106]
Paraoxon, dichlorvos, malathion and triazophos	Fluorescence	AChE and ChOx	0.44 pg L^{-1}, 16.6 pg L^{-1}, 76 µg L^{-1} and 3 ng L^{-1}	ND	Korram et al. (2020)[29]
Pirimicarb, dichlorvos and carbaryl	Fluorescence	AChE	50 µg L^{-1}, 10 µg L^{-1} and 10 µg L^{-1}	Pirimicarb: Lettuce, choy and rice	Apilux et al. (2017)[72]

Ethylparathion	Fluorescence	AChE	0.7 ng L^{-1}	Tap water, soil water, apple and orange juice	Sharma et al. (2021)[75]
Parathionmethyl, monocrotophos and dimethoate	Fluorescence	AChE	0.67 ng L^{-1}, 23 ng L^{-1} and 67 ng L^{-1}	Apple, cucumber and capsicum	Long et al. (2015)[44]
Carbaryl, ethodan, endosulfan and acephate	Colorimetry and fluorescence	AChE	0.4 to 3 µg L^{-1}	River water	Luo et al. (2018)[45]
Glyphosate	Fluorescence	Exonuclease I	/	Drinking water	Berkal et al. (2023)[94]

Upon reviewing **Table I-3**, notable disparities in the LOD become evident among biosensors utilizing the same bioreceptor and targeting the identical pesticide. This variability predominantly stems from the choice of detection technique employed. Certain detection methods prove more adept at accurately detecting pesticides compared to others. Furthermore, additional factors, such as the composition of the analyzed matrix, whether it is a simple medium like water or a more complex one like food or vegetables, also contribute significantly to the observed variation in LOD values.

III. Immunosensors

Immunosensors are characterized by the directed and highly selective interaction between a ligand, or antigen (Ag), and its antibody (Ab), immobilized on the transducer surface[107–110]. Once the equilibrium is reached, the ratio of bound-to-free antigen is quantitatively related to the global amount of ligand. Unlike AChE-inhibition based biosensors, immunosensors have the advantage of being specific[111]. Several immunosensors have been developed for pesticide detection, based essentially on optical and electrochemical transduction methods.

Given the relatively small size of pesticides, competitive assay schemes are frequently utilized for analyzing pesticides with immunosensors[112]. Based on the detection principle, these immunosensors can be classified into two main categories, namely optical and electrochemical immunosensors. In contrast, electrochemical immunosensors utilize changes in current or

potential to detect pesticides, offering several advantages, such as rapid detection, portability, and low cost.

III.1. Optical immunosensors

Optical immunosensors rely on the specific binding interactions between an antibody or antigen and its corresponding analyte, resulting in a detectable signal change that can be measured using optical techniques such as absorbance, fluorescence, or surface plasmon resonance. These immunosensors offer several benefits, including high sensitivity, selectivity, real-time detection, and the ability to be easily miniaturized for use in portable devices.

III.1.1. Colorimetric immunosensors

Colorimetric immunoassays have several advantages over conventional methods for pesticide analysis, such as rapid detection, ease of use, and suitability for high-throughput analysis with limited technical requirements[113]. Liu and coworkers[114] have developed a colorimetric immunochromatographic strip (ICA) using a monoclonal antibody (mAb) for the detection of dicofol (**Figure I-4(A)**), an organo-insecticide widely spread on vegetables, fruits, teas, ornamental plants, and field crops[115]. The ICA displayed high sensitivity with an LOD of 50 µg L^{-1} with both apple and cucumber, and the cross-reactivity test revealed a good specificity for dicofol. These results were consistent with LC-MS and immunocapture ELISA, suggesting that the ICA method is reliable and practical for detecting dicofol in fruits and vegetables.

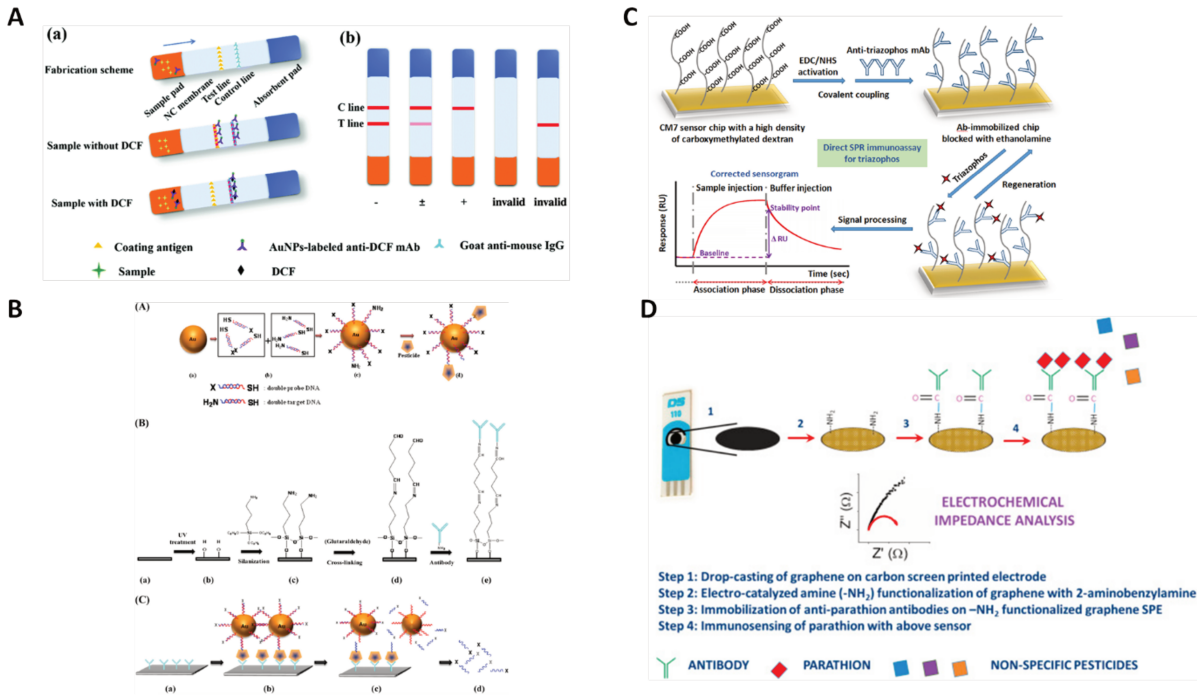

Figure I-4. (A) Schematic of the ICA strip (a) and interpretation of the test results (b). Reprinted from [114], with permission from the Royal Society of Chemistry. (B) Novel immunoassay containing glyphosate-double DNA-gold nanoparticles based on competitive inhibition reaction. Reprinted (adapted) from [49], with permission from the American Chemical Society. (C) Preparation of mAb-immobilized sensor chip for direct detection of triazophos and real-time SPR sensorgram for association and dissociation of the immunocomplex. Reprinted (adapted) from [79], with permission from Elsevier. (D) Schematic of the graphene-based screen-printed immunosensor for parathion. Reprinted (adapted) from [81], with permission from Elsevier.

III.1.2. Fluorescence-based immunosensors

Gonzalez-Martinez and coworkers[48] have developed a fluorescent immunosensor based on an immunocomplex capture assay protocol to detect glyphosate. The described immunosensor is fully automated and performs online analyte derivatization prior to the assay. It utilizes a highly selective anti-glyphosate serum, a glyphosate peroxidase enzyme tracer, and a fluorescent detection system for high sensitivity and accuracy. Its specific and sensitive detection reaches an LOD of 0.021 µg L^{-1}, which is lower than the concentration limit set by the European Council directive[116]. Lee et al.[49] have also described a new method for detecting glyphosate using Co–B/SiO_2/dye nanoparticles in a water-in-oil microemulsion (**Figure I-4(B)**). The nanoparticles have been surface-modified to enhance their detection limit. The approach utilized fluorescence

magnetic nanoparticles (FMP) and a glyphosate antibody. With this method, an LOD of 45.6 ng L^{-1} was reached, with a linear correlation in the range of 0.169 µg L^{-1} – 1.69 mg L^{-1}.

III.1.3. Reflectometric interference spectroscopy immunosensors

Reflectometric interference spectroscopy presents several advantages over classical optical techniques such as simple instrumentation, no need for optical alignment and low cost of the sensing element. Koukouvinos et al.[39] have developed a white light reflectance spectroscopy (WLRS) based immunosensor for the fast, real-time and label-free simultaneous detection of chlorpyrifos, imazalil and thiabendazole pesticides in drinking water and wine samples. The biosensor allowed the entire detection of those pesticides within 10 min. The accuracy of the measurements was evaluated through recovery experiments and comparison of the results with validated liquid chromatography coupled with tandem mass spectrometry (LC-MS/MS). Recovery values ranged from 86 to 116%, and the results were in good agreement with LC-MS/MS.

III.1.4. Surface Plasmon Resonance-(SPR) based immunosensors

SPR is an optical detection platform widely used for the detection of large molecules, with which the high mass of the analyte and the use of a sandwich immunoassay format provide a high signal and thus the desired sensitivity[117,118]. In contrast and due to the low change of refractive index induced by the binding of these analytes to the sensor surface, small molecular compounds such as pesticides present at low concentrations are very difficult to be directly detected by traditional SPR immunosensors[119]. Recent improvements in SPR devices, including lower-noise valves and improved microfluidics with more efficient vacuum pumps, have reduced the overall noise of these systems and thus improved sensitivity and reliability[120,121]. Owing to these improvements, SPR immunosensors could be employed for pesticide monitoring. Guo et al.[79] have described a SPR immunosensor for the detection of an organophosphate pesticide, triazophos (**Figure I-4(C)**). They immobilized two anti-triazophos monoclonal antibodies (mAbs) on the sensor chip and characterized them by SPR-based kinetic analysis. The mAb, characterized by a relatively slow dissociation rate, could be used for the development of a non-competitive SPR immunosensor for direct monitoring of triazophos residue in environmental and agricultural samples.

III.2. Electrochemical immunosensors:

Electrochemical immunosensors are interesting alternatives to classical chromatographic methods for pesticide analysis. Owing to their ability to detect specific targets with high sensitivity, they are promising tools for rapid and on-site analysis of pesticides[122–124].

III.2.1. Cyclic voltammetry

Talan et al.[38] have described a highly sensitive fluorine-doped tin oxide (FTO) based electrochemical immunosensor to detect chlorpyriphos using AuNPs and anti-chlorpyrifos antibodies (Chl-Ab). The developed biosensor allowed, via CV measurements, the successful detection of chlorpyrifos with very -high sensitivity ranging from 0.35 pg L^{-1} to 0.35 mg L^{-1} with an LOD of 3.5 pg L^{-1}.

III.2.2. Chronoamperometric assay

Bettazzi et al.[50] developed an electrochemical competitive immunoassay that utilizes antibody-modified magnetic particles. The assay works by employing a Horseradish Peroxidase (HRP)-conjugated glyphosate tracer and anti-glyphosate IgG-modified magnetic beads (MBs) for detection. A screen-printed electrochemical cell has been used to detect glyphosate. The calibration curve demonstrated a linear concentration range of 0 – 10000 ng L^{-1} with an LOD of 5 ng L^{-1} and LOQ of 30 ng L^{-1} which is well below the EU legislative recommendations. Furthermore, the developed biosensor showed good applicability for the analysis in real samples, namely spiked beer samples.

III.2.3. Impedance spectroscopy

A graphene-based immunosensor was developed and used to detect parathion[81] (**Figure I-4(D)**). The process involved modifying screen-printed carbon electrodes with graphene sheets and their functionalization with 2-aminobenzyl amine before bio-interfacing with anti-parathion antibodies. The biosensor demonstrated a broad linear range of detection (0.1–1000 ng L^{-1}) and a very low LOD (52 pg L^{-1}) with high selectivity towards parathion. The biosensor was also successfully used to detect parathion in real samples such as tomatoes and carrots and was cross-calibrated against high-performance liquid chromatography (HPLC) to confirm its viability. **Table I-4** provides a summary of the various types of immunosensors developed for the detection of pesticides.

Table I-4. Immunosensors developed against pesticides.

Pesticide	Detection technique	LOD	Validity for real samples	Reference
Parathion, methyl-parathion, and fenitrothion	ELISA	2.5 µg L^{-1} for parathion and methyl-parathion 5 µg L^{-1} for fenitrothion	Tap water	Jiao et al. (2018)[77]
Glyphosate	Fluorometric assay	0.021 µg L^{-1}	Water and soil	Gonzalez-Martinez et al. (2005[48]
Glyphosate	Fluorometric assay	10 µg L^{-1}	Not mentioned (PBS buffer)	Lee et al. (2010)[49]
Acetochlor and fenpropathrin	Colorimetry	0.6 µg L^{-1} and 0.24 µg L^{-1}	Corn, apple and cabbage	Cheng et al (2019)[78]
Glyphosate	Chronoamperometric assay	5 ng L^{-1}	Commercial beer	Betazzi et al. (2018)[50]
Chlorpyrifos	DPV and CV	3.5 pg L^{-1}	Apple, cabbage and pomegranate	Talan et al. (2018)[38]
Thiazophos	SPR	96 ng L^{-1}	Environmental water	Guo et al. (2018)[79]
Chlorpyrifos, amazalil, and thiabendazol	WLRS	0.6 µg L^{-1} for chlorpyrifos and imazalil 0.8 µg L^{-1} for thiabendazol	Drinking water and wine	Koukouvinos et al. (2017)[39]
Chlorpyrifos	EIS	70 pg L^{-1}	Chinese cabbage and lettuce	Hou et al (2020)[41]
Malathion	DPV	0.33 pg L^{-1}	Lettuce	Kaur et al (2021)[30]
Endosulfan and paraoxon	CV and SWV	0.05 µg L^{-1} and 2 µg L^{-1}	Environmental water	Liu et al (2014)[46]
Paraquat	Amperometry	1.4 µg L^{-1}	Potatoes	Valera et al (2014)[80]
Parathion	EIS	52 pg L^{-1}	Tomato and carrot	Mehta et al (2016)[81]

IV. Aptasensors

The development of the Systematic Evolution of Ligands by Exponential enrichment (SELEX) technique has led to the discovery of aptamers, oligonucleotide sequences composed of nucleotide bases (Adenine, Thymine, Cytosine, Guanine), capable of complexing a target with very high affinity and specificity. Aptamers offer many advantages over antibodies (**Table I-5**) and are specific to a wide variety of targets: ions[125–127], proteins[128], small molecules[129–131], and cells[132,133]. These characteristics make aptamers excellent candidates to replace antibodies in various fields, more particularly environmental analysis which requires stable and robust sensors.

Table I-5. Elevating the Distinctive Attributes of Aptamers over Antibodies: A Comparative Analysis [134].

Properties	Aptamers	Antibodies
Stability	Withstand repeated rounds of denaturation/renaturation. Temperature resistant: stable at room temperature. Long shelf life (several years). Can be lyophilized. Degradable by nucleases. Resistant to proteases.	Easily denatured. Temperature sensitive and require refrigeration to avoid denaturation. Limited shelf life. Must be refrigerated for storage and transport. Degradable by proteases. Resistant to nucleases.
Synthesis	In vitro SELEX takes only 2–8 weeks No batch-to-batch variation Cheap to synthesize	Produced in vivo More than 6 months Batch-to-batch variations Laborious and expensive
Target potential	From ions and small molecules to whole cells and live animals	Targets must cause a strong immune response for antibodies to be produced
Size	Small molecules	Relatively large by comparison
Modifiability	Aptamers can readily and easily be modified without affinity loss	Modifications often lead to reduced activity
Affinity	High and increased in multivalent aptamers	Dependent on the number of epitopes on the antigen.
Specificity	Single-point mutations identifiable	Different antibodies might bind to the same antigen
Tissue uptake/kidney filtration	Fast	Slow

Conventional SELEX methods are however not compatible with small molecules because of the immobilization step that is not only complicated[135] but leaves weak functional groups exposed to the oligonucleotides thus reducing the chance of selecting aptamers. In 2005, Stoltenburg et al. reported a method for selecting fluorophore-labelled aptamers that involves

the grafting of oligonucleotides onto magnetic beads (FluMag-SELEX)[136], which subsequently led to Capture-SELEX, a method suitable for small molecule aptamers selection. Unlike conventional SELEX, the immobilization in Capture-SELEX is done with the oligonucleotides and not with the target molecules, which allows the preservation of all functional groups of these molecules thus increasing the chance of selecting aptamers. The operating principle of the Capture-SELEX can be summarized in the following steps (**Figure I-5**):

1. Immobilization: the capture oligonucleotide (DNA complementary to the library) is immobilized on the solid matrix (magnetic beads for example).
2. Hybridization: the oligonucleotide library is hybridized with the immobilized capture oligonucleotides.
3. Incubation: the target is incubated with the oligonucleotide library.
4. Elution: the sequences with an affinity towards the target will detach from the capture oligonucleotide and go into solution.
5. Amplification: the recovered sequences are enriched by Polymerase Chain Reaction (PCR) for the next round.

Similar to conventional SELEX, candidate aptamers are sequenced and cloned at the end of the Capture-SELEX (6 to 20 rounds) to identify the aptamers that have the desired properties.

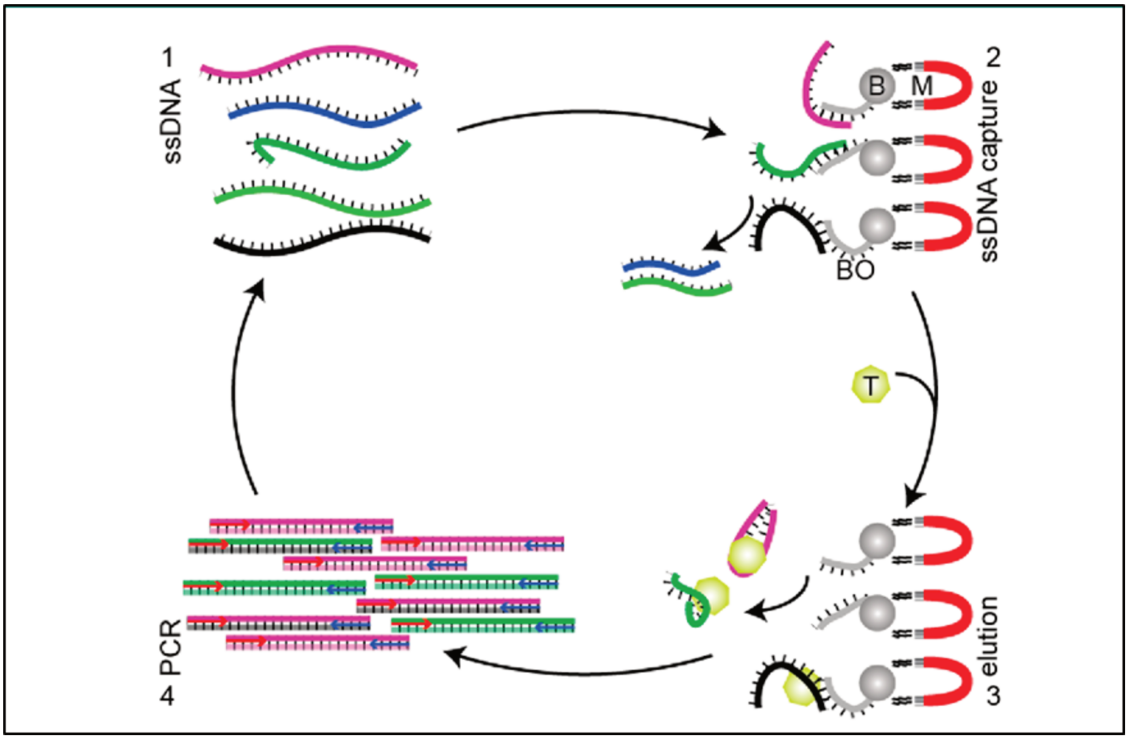

Figure I-5. Schematic illustration of Capture-SELEX using magnetic beads. Reprinted from [137], with permission from the American Chemical Society.

IV.1. Optical aptasensors

Optical aptasensors have become a well-established technology in the field of bioanalysis, utilizing aptamers as recognition elements to directly target and identify substances. These sensors utilize various light sources, including fluorescence, colorimetry, SERS, etc., and convert signals in the form of UV, visible, and IR radiation into different data formats. Compared to other detection methods, optical aptasensors offer several advantages, such as low cost, repeatable use, high specificity, simple sample preparation, minimal interference, and high accuracy. These characteristics make optical aptasensors particularly suitable for on-site detection applications[138].

IV.1.1. Colorimetric aptasensors

The primary benefit of colorimetric sensing is its straightforwardness and ease of implementation. Colorimetric aptasensors have been extensively employed for detecting pesticides in real samples due to the convenience of visual observation. However, a significant challenge in designing colorimetric aptasensors relies on converting the response change into a noticeable color change. Gold (Au) and silver (Ag) nanoparticles are the most commonly used probes in colorimetric assays, due to their ability to enhance surface plasmon resonance and thus produce robust signals as monitored by colorimetry (**Figure I-6(A)**)[139,140].

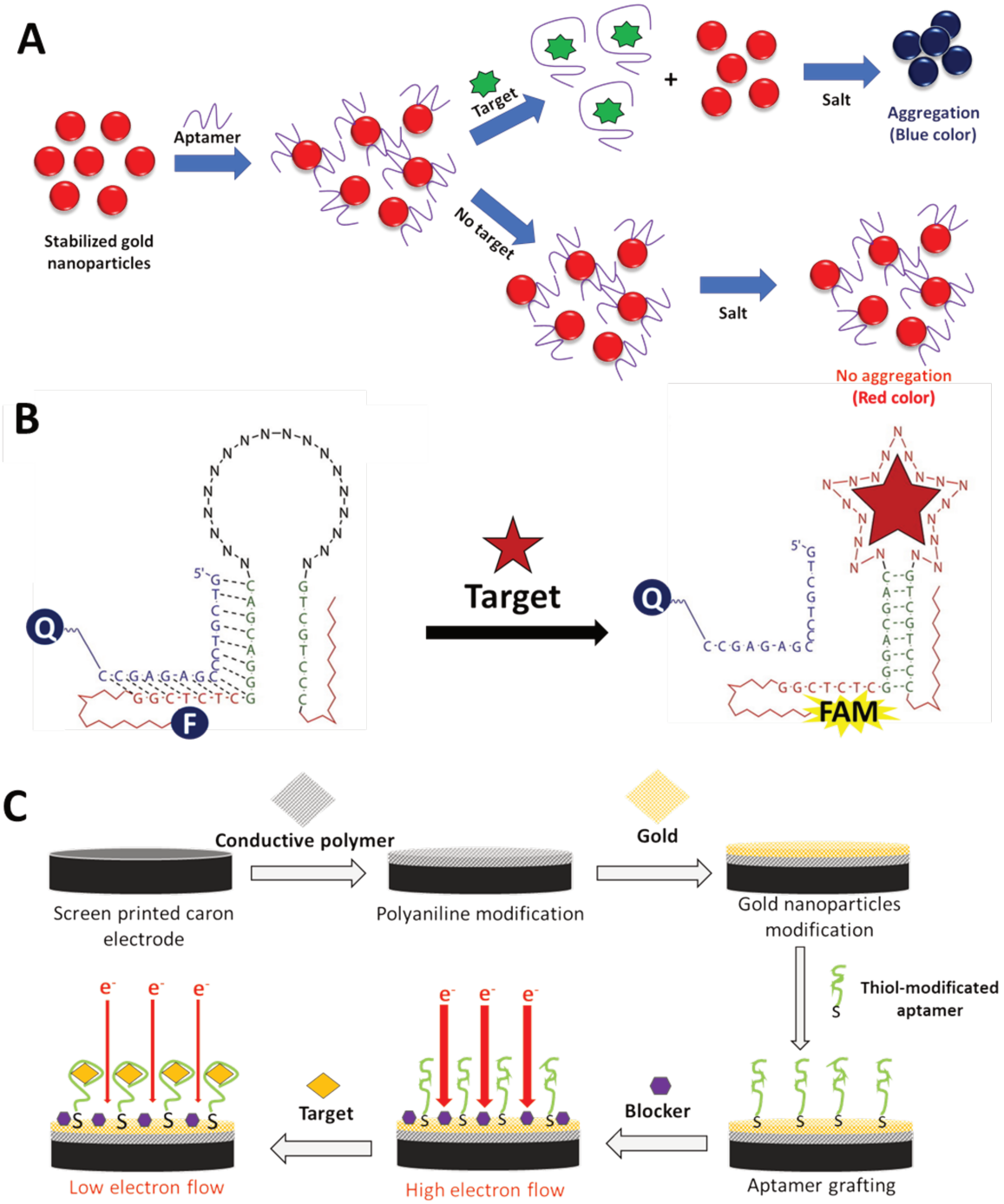

Figure I-6. Comparative schematic diagram of (A) colorimetric aptasensor, (B) FRET aptasensor and (C) electrochemical aptasensor. (B) Reprinted from [141], with permission from ScienceDirect.

IV.1.2. Fluorescence-based aptasensors

Fluorescence-based aptasensors rely on the correlation between changes in fluorescence intensity and the concentration of the target upon aptamer binding. Fluorescence changes are typically achieved through the introduction of a fluorescence quenching or FRET agent (**Figure**

I-6(B)). FRET occurs between two fluorophores at an appropriate distance and can utilize various materials as fluorescent donors, including dyes, quantum dots, metal nanoparticles, carbon dots, and carbon nanomaterials. Nanomaterials, such as graphene oxide, gold nanoparticles, carbon nanotubes, and nanocomposites, are also used as well-known fluorescence quenchers[142].

To create efficient aptasensors with high sensitivity, high throughput, and multiplexing capabilities, various combinations of nanomaterials are employed as fluorescent donors and receptors in sensing assays. Fluorescence detection relies on switching the fluorescence signals on and off to indicate the presence of analytes[143,144]. In most cases, fluorescence signals are in the "signal-off" state until the target is present and the blocking of signals is lifted, leading to a "signal-on" response. Fluorescence signals can be amplified using a variety of nanomaterials such as gold and silver nanoparticles, known for their superior performance[145,146]. Su et al. proposed a method for detecting carbendazim (CBZ) in water using a fluorescent aptasensor[53]. The aptasensor used a CBZ-specific aptamer as a sensing probe, and AuNPs and Rhodamine B (RhoB) as an indicator. In the absence of CBZ, the aptamer wrapped around the AuNPs and kept them dispersed in a solution. However, in the presence of CBZ, the aptamer forms a complex with CBZ, leaving the AuNPs which aggregate in a NaCl solution. The concentration of CBZ was determined by measuring the fluorescence intensity. The method had a wide linear range from 2.33 to 800 nM and an LOD of 2.33 nM. The fluorescent aptasensor showed potential for use in detecting CBZ in aquatic environments.

IV.1.3. Luminescence-based aptasensors

Common fluorescence techniques that rely on organic dyes are vulnerable to interference from naturally occurring fluorescent substances in the environment[147]. Time-resolved emission spectroscopy (TRES) is a useful method for discriminating between fluorophores with similar emission spectra but varying decay times. TRES records long-lived phosphorescence once the initial short-lived fluorescence background has faded[148–151]. Therefore, luminescent transition metal complexes, such as iridium(III) complexes, have become preferred for TRES due to their excellent optical characteristics and long-lived phosphorescence[152]. Chen et al.[52] have reported on a luminescent G-quadruplex-derived aptasensor for the monitoring of glyphosate using a phosphorescent iridium(III)-based probe. The developed platform displayed excellent sensitivity with good selectivity for glyphosate with an LOD of 4.46 µg L^{-1} in Tris-buffer, and 13.4 µg L^{-1} in Tris-buffer containing soybean extract to simulate a complex environment.

IV.1.4. Phosphorescence aptasensors

Persistent luminescence nanorods (PLNRs) have become the subject of extensive research owing to their unique afterglow or phosphorescence characteristics, which unlike fluorophores allow for reduced or even eliminated background luminescence. These nanorods exhibit persistent luminescence, which refers to the emission of light after the cessation of the excitation source. Wang et al. have developed an aptamer-based colorimetric-phosphorescence assay for the detection of isocarbophos[85]. The colorimetric assay used AuNPs that were aggregated by competitive binding of the aptamer between isocarbophos and AuNPs at high salt concentrations. The addition of persistent luminescence nanorods (PLNRs) to the system resulted in phosphorescence that was sensitive to the concentration of isocarbophos due to the inner filter effect between PLNRs and AuNPs. The assay showed good linearity within the range of 50-500 μg L^{-1} and 5-160 μg L^{-1}, with a limit of detection of 7.1 μg L^{-1} and 0.54 μg L^{-1} in colorimetry and phosphorescence mode, respectively. The method was successfully demonstrated for food analysis with the detection of isocarbophos residues in vegetables, showing both sensitivity and selectivity.

IV.1.5. SERS-based aptasensors

Surface-Enhanced Raman Spectroscopy (SERS) is a powerful spectroscopic technique that leverages plasmonic metal nanostructures for the detection of trace-level chemicals with high sensitivity and selectivity[153]. SERS has been widely adopted in analytical chemistry[154], biochemical analysis[155], and environmental sensing[156,157], including the detection of harmful agrochemicals, such as pesticides[158–160]. However, the lack of selectivity when the target molecule is mixed with other molecules in a complex matrix and susceptibility to interference from various ambient influences can limit SERS detection techniques. Therefore, sample pretreatment methods, such as purification and extraction, are critical for examining environmental samples. The use of aptamers, specific biomolecules that can enhance the selectivity of target analysis when combined with SERS, can address these limitations. Recently, Kamkrua et al.[161] developed a SERS aptasensor using gold nanoparticles to detect paraquat, a commonly used herbicide. The platform used AuNPs-SERS substrates modified with a thiol-aptamer as bioreceptors to selectively bind to paraquat molecules. The aptamer-modified SERS substrate showed improved sensitivity and selectivity compared to SERS substrates without aptamer modifications, with an LOD of 0.10 ± 0.03 μM. The platform was evaluated using natural water samples and demonstrated good stability against interferences from other similar herbicides and insecticides present along with paraquat in water.

IV.2. Electrochemical aptasensors

Electrochemical aptasensors produce an electrochemical signal upon the capture of a particular target substance, achieved through the use of aptamers. The design of electrochemical aptasensors involves three crucial steps, including the utilization of nanomaterials to amplify the signal, the binding of the aptamer to the sensor surface, and the detection process itself (**Figure I-6(C)**). Covalent bond formation is the most commonly employed method for aptamer immobilization onto the surface in these types of sensors[162]. Numerous electrochemical aptasensors have been reported for the identification of proteins, which are large molecules producing significant variations in electrochemical signals upon binding to the aptamer, thereby facilitating their detection. However, detecting pesticides which are small molecules requires a notable change in aptamer conformation to enable their detection by electrochemical platforms. To overcome this challenge, multiple approaches have been adopted, one of which is the use of oligonucleotide switching structures generated through the Capture-SELEX method that has proven to be more suitable for detecting pesticides due to the aptamers selection process: a significant conformational change occurs upon binding to the target[163]. This conformational change leads to an improved ability to detect and quantify small molecule pesticides using electrochemical aptasensors. In **Table I-6**, various aptasensors that were developed for the detection of pesticides have been listed.

Table I-6. Recent advances in aptasensors developed against pesticides.

Target	Detection technique	Aptamer sequence	LOD	Dynamic range	Validity for real samples	Reference
Acetamiprid Atrazine	EIS	Acetamiprid: 5'-(SH)-(CH_2)6-TGTAATTTGTCTGCAGCGGTTCTTGATCGCTGACACCATATTATGAAGA-[FITC]-3' Atrazine: 5'-(SH)-(CH_2)6-TACTGTTTGCACTGGCGGATTTAGCCAGTCAGTG-[FITC]-3'	Acetamiprid: 8.9 ng L^{-1} Atrazine: 1.3 ng L^{-1}	ND	Buffer	Madianos et al. (2018)[59]
Acetamiprid Atrazine	EIS	Acetamiprid: 5'-(SH)-(CH_2)6-TGTAATTTGTCTGCAGCGGTTCTTGATCGCTGACACCATATTATGAAGA-[Flc]−3' Atrazine: 5′-(SH)-(CH_2)6-TACTGTTTGCACTGGCGGATTTAGCCAGTCAGTG-[Flc]−3′	Acetamiprid: 0.2 ng L^{-1} Atrazine: 2.1 ng L^{-1}	Acetamiprid: 2.2 ng L^{-1}- 22.2 µg L^{-1} Atrazine: 21.5 ng L^{-1}– 215.7 µg L^{-1}	Tap water	Madianos et al. (2018)[60]
Atrazine	Photoelectrochemical assay	5’-SH-(CH_2)6-TGT-ACC-GTC-TGA-GCG-ATT-CGT-ACG-AAC-GGCTTT-GTA-CTG-TTT-GCA-CTG-GCG-GAT-TTA-GCC-AGT-CAG-TGT-TAA-GGA-GTG-C-3’	0.21 ng L^{-1}	0.5 ng L^{-1}– 0.11 µg L^{-1}	Lake water, agricultural	Fan et al. (2021)[61]

					wastewater and sewage water	
Carbofuran	DPV	5'-CACCTGGGGGAGTATTGCGGAGGAAAGAGAACACTGGGGCAGATATGGGCCAGCAGGTC-(CH_2)3-SH-3′	14.8 µg L^{-1}	44 ng L^{-1}-11 µg L^{-1}	Vegetables and fruits	Li et al. (2018)[82]
Chlorpyrifos	DPV	5′-CCTGCCACGCTCCGCAAGCTTAGGGTTACGCCTGCAGCGATTCTTGATCGCGCTGCTGGTAATCCTTCTTTAAGCTTGGCACCCGCATCGT-3′	70 ng L^{-1}	0.1-150 µg L^{-1}	Apple and celery cabbage	Xu et al. (2018)[42]
Atrazine	EIS	5' -TGT ACC GTC TGA GCG ATT CGT ACG AAC GGC TTT GTA CTG TTT GCA CTG GCG GAT TTA GCC AGT CAG TGT TAA GGA GTG C-3'	0.67 ng L^{-1}	1 ng L^{-1}-50 µg L^{-1}	River and tap water	Zhu et al. (2021)[62]
Atrazine	Photoelectrochemical assay	5′-TGT-ACC-GTC-TGA-GCG-ATT-CGT-ACG-AAC-GGC-TTT-GTA-CTG-TTT-GCA-CTG-GCG-GAT-TTA-GCC-AGT-CAG-TGT-TAA-GGA-GTG-C-3′	2.6 pg L^{-1}	10.7 pg L^{-1}–64.7 ng L^{-1}	Water	Sun et al. (2019)[63]
Atrazine	DPV	5'-SH-(CH_2)6-TGT-ACC-GTC-TGA-GCG-ATT-CGT-ACG-AAC-GGCTTT-GTA-CTG-TTT-GCA-CTG-GCG-GAT-TTA-GCC-AGT-CAG-TGT-TAAGGA-GTG-C-3'	21.5 pg L^{-1}	53.9 pg L^{-1}–53.7 ng L^{-1}	Lake and river water	Fan et al. (2019)[64]
Atrazine	Linear Sweep Voltametry (LSV)	5′-HS-(CH_2)6-TGT-ACC-GTC-TGA-GCG-ATT-CGT-ACG-AAC-GGCTTT-GTA-CTG-TTT-GCA-CTG-GCG-GAT-TTA-GCC-AGT-CAG-TGT-TAAGGA-GTG-C-3′	1.6 µg L^{-1}	ND	Environmental water	Wang et al. (2020)[65]

Atrazine	Adsorption spectroscopy (ATR-SEIRAS)	5′-HS-(CH_2)6-TGT-ACC-GTC-TGA-GCG-ATT-CGT-ACG-AAC-GGC-TTT-GTA-CTG-TTT-GCA-CTG-GCG-GAT-TTA-GCC-AGT-CAG-TGT-TAA-GGA-GT7G-C-3′	0.23 µg L^{-1}	ND	ND	Sun et al. (2021)[66]
Atrazine	Ultrafiltration system	5’-FAM-TACTGTTTGCACTGGCGGATTTAGCCAGTCAGTG-3’	ND	ND	ND	Romero-Reyes and Heemstra (2021)[67]
Atrazine	Fluorescence	5’-TTT-TTT-TTT-TTA-CTG-TTT-GCA-CTG-GCG-GAT-TTA-GCC-AGT-CAG-TG-3’	2 ng L^{-1}	ND	River simple	Yao et al. (2021)[68]
Atrazine	SERS	5′-(SH)-TACTG TTTGC ACTGG CGGAT TTAGC CAGTC AGTG-3′	0.14 µg L^{-1}	0.22 µg L^{-1}– 10.7 µg L^{-1}	Cherry tomato and grape	Wei et al. (2020)[69]
Carbendazim	Fluorescence	5′-CGACACAGCGGAGGCCACCCGCCCACCAGCCCCTGCAGCTCCTGTACCTGTGTGTGTG-3′	0.44 µg L^{-1}	0.44 µg L^{-1}– 0.15 mg L^{-1}	Water	Su et al. (2020)[53]
Chloramphenicol	Colorimetry	5′-ACTTCAGTGAGTTGTCCCACGGTCGGCGAGTCGGTGGTAG-Biotin-3′	0.19 µg L^{-1} in milk 0.23 µg L^{-1} in serum	ND	Milk and mouse serum	Abnous et al. (2016)[76]
Chlorpyrifos	Colorimetry	5'-CCTGCCACGCTCCGCAAGCTTAGGGTTACGCCTGCAGCGATTCTGATCGCGCTGCTGGTAATCCTTCTTTAAGCTTGGCACCCGCATCGT-3'	11.3 mg L^{-1}	10 mg L^{-1}- 200 mg L^{-1}	River water	Weerathunge et al. (2019)[43]

Chlorpyrifos and diazinon and	Fluorescence	Chlorpyrifos aptamer 5'-CCTGCCACGCTCCGCAAGCTTAGGGTTACGCCTGCAGCGATTCTTGATCGCGCTGCTGGTAATCCTTCTTTAAGCTTGGCACCCGCATCGT-3'	0.73 ng L^{-1} and 6.7 ng L^{-1}	ND	12 vegetables and fruits	Cheng et al. (2018)[33]
Diazinon	Fluorescence	5′-NH_2-(CH_2)6-ATCCGTCACACCTGCTCTAATATAGAGGTATTGCTCTTGGACAAGGTACAGGGATGGTGTTGGCTCCCGTAT-3′	23 ng L^{-1}	0.05 µg L^{-1}-500 µg L^{-1}	Tea, apple and tap water	Ron et al. (2020)[83]
Glyphosate	Fluorescence	5'-CGC ATT CAG GAT TGC ATG ATT GCC AAA AAA AAA A-NH_2-3'	10 µg L^{-1}	10 µg L^{-1}-100 mg L^{-1}	PBS buffer	Lee et al. (2010)[49]
Glyphosate	SERS	5′-TGC TAG ACG ATA TTC GTC CAT CCG AGC CCG TGG CGG GTC TTA GGA CTC TGC GGG CTT CGC GGC GCT GTC AGA CTG AAT ATG TCA-3′	0.34 ng L^{-1}	0.51 ng L^{-1}–11.8 ng L^{-1}	Soil	Liu et al. (2021)[51]
Glyphosate	Luminiscence	5′-TGCTAGACGATATTCGTCCATCCGAGCCCGTGGCGGGCTTTAGGACTCTGCGGGCTTCGCGGCGCTGTCAGACTGAATATGTCA-3′	4.5 µg L^{-1} in buffer 13.4 µg L^{-1} in buffer containing soybean extract	8.5 µg L^{-1}–50.7 µg L^{-1}	Buffer containing soybean extract	Chen et al. (2020)[52]

Glyphosate, malathion and trichlorfon	Fluorescence	5′-6 FAM-AGCTTGCTGCAGCGATTCTTGATCGCCACAGAGCT-3′	88.8 ng L^{-1}, 195.37 ng L^{-1} and 72.2 ng L^{-1},	0.1 μg L^{-1}-10 mg L^{-1}	Lettuce and carrot	Jiang et al. (2020)[31]
Isocarbophos	Fluorescence	5′-ATTCTTGATCGCCACGGTCTGGAAAAAGAGAAGTGGGTAGGGCGGGTTGG–3′	2.9 μg L^{-1}	2.9 μg L^{-1}– 0.14 mg L^{-1}	Chinese cabbage and apple	Li et al. (2018)[84]
Isocarbophos	Phosphorescence and colorimetric assays	5′-AGCTTGCTGCAGCGATTCTTGATCGCCACAGAGCT-3′	Phosphorescence: 0.54 μg L^{-1} Colorimetry: 7.1 μg L^{-1}	Phosphorescence: 5-160 μg L^{-1} Colorimetry: 50-500 μg L^{-1}	Chinese cabbage, brassica rape and lettuce	Wang et al. (2019)[85]
Isocarbophos and omethoate	Colorimetry	5'-AAG CTT TTT TGA CTG ACT GCA GCG ATT CTT GAT CGC CAC GGT CTG GAA AAA GAG-3'	0.47 μg L^{-1} and 0.35 μg L^{-1}	50-1000 μg L^{-1} and 100-500 μg L^{-1}	Buffer	Liu et al. (2020)[55]
Malathion	Colorimetry	5′-ATCCGTCACACCTGCTCTTATACACAATTGTTTTTCTCTTAACTTCTTGACTGCTGGTGTTGGCTCCCGTAT-3′	0.33 ng L^{-1}	1.65 ng L^{-1}– 3.3 μg L^{-1}	Human serum	Abnous et al. (2018)[32]
Malathion	Fluorescence	5′-ATCCGTCACACCTGCTCTTATACACAATTGTTTTTCTCTTAACTTCTTGACTGCTGGTGTTGGCTCCCGTAT-3′	0.74 ng L^{-1}	ND	12 vegetables and fruits	Cheng et al. (2018)[33]

V. Conclusion and perspectives

Biosensors have emerged as a promising technology for the detection of pesticides, offering rapid, sensitive, and reliable results. Recent advances in biosensor design, and especially the use of biorecognition elements such as antibodies, enzymes and recently aptamers, have enabled the development of highly sensitive and specific biosensors that can detect a wide range of pesticides with high accuracy.

Despite the numerous advantages of biosensors, several challenges must be addressed to unlock their full potential. One key challenge lies in the selectivity of immunosensors and enzyme-based biosensors, which often encounter issues such as cross-interactions among antibodies and a lack of specificity of many enzymes employed in biosensors which are inhibited by organophosphate pesticides, limiting their effectiveness.

Furthermore, biosensors deployed in complex sample matrices face hurdles due to interference from various substances. Mitigating these effects requires the development of effective strategies. Moreover, the limited commercial applications of biosensors call for efforts to scale up production, reduce costs, and comply with regulatory requirements.

To foster wider adoption and successful integration of biosensor technologies, standardized protocols for their development, validation, and manufacturing are essential. Establishing these protocols will ensure consistent performance and facilitate comparability of results across different platforms and laboratories.

Looking to the future, biosensors are expected to play an increasingly important role in the detection and monitoring of pesticides, particularly in the context of environmental and food safety. The integration of biosensors with other technologies, such as smartphone apps and cloud computing, is also expected to further enhance the capabilities of biosensors and expand their applications.

In conclusion, biosensors represent a promising technology for the detection of pesticides, and further research and development in this area is essential to address the challenges and unlock the full potential of this technology for environmental and food safety.

VI. References

(1) Cooper, J.; Dobson, H. The Benefits of Pesticides to Mankind and the Environment. *Crop Protection* **2007**, *26* (9), 1337–1348. https://doi.org/10.1016/j.cropro.2007.03.022.

(2) Koutros, S.; Lynch, C. F.; Ma, X.; Lee, W. J.; Hoppin, J. A.; Christensen, C. H.; Andreotti, G.; Freeman, L. B.; Rusiecki, J. A.; Hou, L.; Sandler, D. P.; Alavanja, M. C. R. Heterocyclic Aromatic Amine Pesticide Use and Human Cancer Risk: Results from the U.S. Agricultural Health Study. *International Journal of Cancer* **2009**, *124* (5), 1206–1212. https://doi.org/10.1002/ijc.24020.

(3) Amr, S.; Dawson, R.; Saleh, D. A.; Magder, L. S.; St. George, D. M.; El-Daly, M.; Squibb, K.; Mikhail, N. N.; Abdel-Hamid, M.; Khaled, H.; Loffredo, C. A. Pesticides, Gene Polymorphisms, and Bladder Cancer Among Egyptian Agricultural Workers. *Archives of Environmental & Occupational Health* **2015**, *70* (1), 19–26. https://doi.org/10.1080/19338244.2013.853646.

(4) Alavanja, M. C. R.; Dosemeci, M.; Samanic, C.; Lubin, J.; Lynch, C. F.; Knott, C.; Barker, J.; Hoppin, J. A.; Sandler, D. P.; Coble, J.; Thomas, K.; Blair, A. Pesticides and Lung Cancer Risk in the Agricultural Health Study Cohort. *American Journal of Epidemiology* **2004**, *160* (9), 876–885. https://doi.org/10.1093/aje/kwh290.

(5) Beane Freeman, L. E.; Bonner, M. R.; Blair, A.; Hoppin, J. A.; Sandler, D. P.; Lubin, J. H.; Dosemeci, M.; Lynch, C. F.; Knott, C.; Alavanja, M. C. R. Cancer Incidence among Male Pesticide Applicators in the Agricultural Health Study Cohort Exposed to Diazinon. *American Journal of Epidemiology* **2005**, *162* (11), 1070–1079. https://doi.org/10.1093/aje/kwi321.

(6) Kole, R. K.; Banerjee, H.; Bhattacharyya, A. Monitoring of Market Fish Samples for Endosulfan and Hexachlorocyclohexane Residues in and Around Calcutta. *Bull. Environ. Contam. Toxicol.* **2001**, *67* (4), 554–559. https://doi.org/10.1007/s001280159.

(7) *USGS Scientific Investigations Report 2009-5132: Trends in Pesticide Concentrations in Corn-Belt Streams, 1996–2006*. https://pubs.usgs.gov/sir/2009/5132/ (accessed 2021-10-22).

(8) *S-métolachlore : vers l'interdiction des principaux usages pour préserver la qualité des eaux souterraines*. Anses - Agence nationale de sécurité sanitaire de l'alimentation, de l'environnement et du travail. https://www.anses.fr/fr/content/s-metolachlor-preserver-qualite-eaux (accessed 2023-04-18).

(9) Vainio, H.; Heseltine, E.; Shuker, L.; McGregor, D.; Partensky, C. Meeting Report: Occupational Exposures in Insecticide Application and Some Pesticides. *European Journal of Cancer and Clinical Oncology* **1991**, *27* (3), 284–289. https://doi.org/10.1016/0277-5379(91)90517-H.

(10) Lamy, D. Barbezieux-Saint-Hilaire : un chantier école pour prendre soin de l'eau potable. *Sud Ouest* **2021**.

(11) Haib, J.; Hofer, I.; Renaud, J.-M. Analysis of Multiple Pesticide Residues in Tobacco Using Pressurized Liquid Extraction, Automated Solid-Phase Extraction Clean-up and Gas Chromatography–Tandem Mass Spectrometry. *Journal of Chromatography A* **2003**, *1020* (2), 173–187. https://doi.org/10.1016/j.chroma.2003.08.049.

(12) Lesueur, C.; Knittl, P.; Gartner, M.; Mentler, A.; Fuerhacker, M. Analysis of 140 Pesticides from Conventional Farming Foodstuff Samples after Extraction with the Modified QuECheRS Method. *Food Control* **2008**, *19* (9), 906–914. https://doi.org/10.1016/j.foodcont.2007.09.002.

(13) Gamón, M.; Lleó, C.; Ten, A.; Mocholí, F. Multiresidue Determination of Pesticides in Fruit and Vegetables by Gas Chromatography/Tandem Mass Spectrometry. *Journal of AOAC INTERNATIONAL* **2001**, *84* (4), 1209–1216. https://doi.org/10.1093/jaoac/84.4.1209.

(14) Pang, G.-F.; Liu, Y.-M.; Fan, C.-L.; Zhang, J.-J.; Cao, Y.-Z.; Li, X.-M.; Li, Z.-Y.; Wu, Y.-P.; Guo, T.-T. Simultaneous Determination of 405 Pesticide Residues in Grain by Accelerated Solvent Extraction Then Gas Chromatography-Mass Spectrometry or Liquid Chromatography-Tandem Mass Spectrometry. *Anal Bioanal Chem* **2006**, *384* (6), 1366–1408. https://doi.org/10.1007/s00216-005-0237-9.

(15) Lehotay, S. J.; Kok, A. de; Hiemstra, M.; Bodegraven, P. van. Validation of a Fast and Easy Method for the Determination of Residues from 229 Pesticides in Fruits and Vegetables Using Gas and Liquid Chromatography and Mass Spectrometric Detection. *Journal of AOAC INTERNATIONAL* **2005**, *88* (2), 595–614. https://doi.org/10.1093/jaoac/88.2.595.

(16) Baruah, S.; Dutta, J. Nanotechnology Applications in Pollution Sensing and Degradation in Agriculture: A Review. *Environ Chem Lett* **2009**, *7* (3), 191–204. https://doi.org/10.1007/s10311-009-0228-8.

(17) Verma, M. L. Nanobiotechnology Advances in Enzymatic Biosensors for the Agri-Food Industry. *Environ Chem Lett* **2017**, *15* (4), 555–560. https://doi.org/10.1007/s10311-017-0640-4.

(18) Verdian, A. Apta-Nanosensors for Detection and Quantitative Determination of Acetamiprid – A Pesticide Residue in Food and Environment. *Talanta* **2018**, *176*, 456–464. https://doi.org/10.1016/j.talanta.2017.08.070.

(19) Hara, T. O.; Singh, B. Electrochemical Biosensors for Detection of Pesticides and Heavy Metal Toxicants in Water: Recent Trends and Progress. *ACS EST Water* **2021**, *1* (3), 462–478. https://doi.org/10.1021/acsestwater.0c00125.

(20) Gong, Z.; Huang, Y.; Hu, X.; Zhang, J.; Chen, Q.; Chen, H. Recent Progress in Electrochemical Nano-Biosensors for Detection of Pesticides and Mycotoxins in Foods. *Biosensors* **2023**, *13* (1), 140. https://doi.org/10.3390/bios13010140.

(21) *Electrochemical Biosensors for Detection of Pesticides and Heavy Metal Toxicants in Water: Recent Trends and Progress*. https://doi.org/10.1021/acsestwater.0c00125.

(22) Ba Hashwan, S. S.; Khir, M. H. B. M.; Al-Douri, Y.; Ahmed, A. Y. Recent Progress in the Development of Biosensors for Chemicals and Pesticides Detection. *IEEE Access* **2020**, *8*, 82514–82527. https://doi.org/10.1109/ACCESS.2020.2991380.

(23) Sharma, S. K.; Sehgal, N.; Kumar, A. Biomolecules for Development of Biosensors and Their Applications. *Current Applied Physics* **2003**, *3* (2–3), 307–316. https://doi.org/10.1016/S1567-1739(02)00219-5.

(24) Patel, H.; Rawtani, D.; Agrawal, Y. K. A Newly Emerging Trend of Chitosan-Based Sensing Platform for the Organophosphate Pesticide Detection Using Acetylcholinesterase- a Review. *Trends in Food Science & Technology* **2019**, *85*, 78–91. https://doi.org/10.1016/j.tifs.2019.01.007.

(25) Yan, X.; Li, H.; Su, X. Review of Optical Sensors for Pesticides. *TrAC Trends in Analytical Chemistry* **2018**, *103*, 1–20. https://doi.org/10.1016/j.trac.2018.03.004.

(26) Chauhan, N.; Pundir, C. S. An Amperometric Biosensor Based on Acetylcholinesterase Immobilized onto Iron Oxide Nanoparticles/Multi-Walled Carbon Nanotubes Modified Gold Electrode for Measurement of Organophosphorus Insecticides. *Analytica Chimica Acta* **2011**, *701* (1), 66–74. https://doi.org/10.1016/j.aca.2011.06.014.

(27) Li, S.; Li, M. Q.; Jia Fu, W.; Xue Qin, R.; Xi, N. Acetylcholinesterase Based RGO-TEPA-Copper Nanowires Biosensor for Detecting Malathion. *Int. J. Electrochem. Sci.* **2020**, 505–514. https://doi.org/10.20964/2020.01.75.

(28) Jiang, B.; Lu, M.; Xu, M. Amperometric Sensing of Organophosphorus Pesticides Based on Covalently Attached Multilayer Assemblies of Diazo-Resin, Prussian Blue Single-Walled Carbon Nanotubes, and Acetylcholinesterase. *Rev.Roum.Chim.* **2019**, *64* (9), 763–774. https://doi.org/10.33224/rrch/2019.64.9.3.

(29) Korram, J.; Dewangan, L.; Karbhal, I.; Nagwanshi, R.; Vaishanav, S. K.; Ghosh, K. K.; Satnami, M. L. CdTe QD-Based Inhibition and Reactivation Assay of Acetylcholinesterase for the Detection of Organophosphorus Pesticides. *RSC Adv* **2020**, *10* (41), 24190–24202. https://doi.org/10.1039/d0ra03055d.

(30) Kaur, N.; Bhatnagar, A.; Bhalla, A.; Prabhakar, N. Determination of an Organophosphate Pesticide Using Antibody Immobilised Hybrid Nanocomposites. *International Journal of Environmental Analytical Chemistry* **2021**, *101* (11), 1485–1498. https://doi.org/10.1080/03067319.2019.1685665.

(31) Jiang, M.; Chen, C.; He, J.; Zhang, H.; Xu, Z. Fluorescence Assay for Three Organophosphorus Pesticides in Agricultural Products Based on Magnetic-Assisted Fluorescence Labeling Aptamer Probe. *Food chemistry* **2020**, *307*, 125534-.

(32) Abnous, K.; Danesh, N. M.; Ramezani, M.; Alibolandi, M.; Emrani, A. S.; Lavaee, P.; Taghdisi, S. M. A Colorimetric Gold Nanoparticle Aggregation Assay for Malathion Based on Target-Induced Hairpin Structure Assembly of Complementary Strands of Aptamer. *Microchim Acta* **2018**, *185* (4), 216. https://doi.org/10.1007/s00604-018-2752-3.

(33) Cheng, N.; Song, Y.; Fu, Q.; Du, D.; Luo, Y.; Wang, Y.; Xu, W.; Lin, Y. Aptasensor Based on Fluorophore-Quencher Nano-Pair and Smartphone Spectrum Reader for on-Site Quantification of Multi-Pesticides. *Biosensors and Bioelectronics* **2018**, *117*, 75–83. https://doi.org/10.1016/j.bios.2018.06.002.

(34) Borah, H.; Gogoi, S.; Kalita, S.; Puzari, P. A Broad Spectrum Amperometric Pesticide Biosensor Based on Glutathione S-Transferase Immobilized on Graphene Oxide-Gelatin Matrix. *Journal of Electroanalytical Chemistry* **2018**, *828*, 116–123. https://doi.org/10.1016/j.jelechem.2018.09.047.

(35) Gai, P.; Zhang, S.; Yu, W.; Li, H.; Li, F. Light-Driven Self-Powered Biosensor for Ultrasensitive Organophosphate Pesticide Detection via Integration of the Conjugated Polymer-Sensitized CdS and Enzyme Inhibition Strategy. *J. Mater. Chem. B* **2018**, *6* (42), 6842–6847. https://doi.org/10.1039/C8TB02286K.

(36) Key Lab of Modern Precision Agriculture System Integration Research and Key Lab of Agricultural Information Acquisition Technology Ministry of Education, China Agricultural University, Beijing 100083 P.R. China; Wang, H. A Sensitive Acetylcholinesterase Biosensor Based on Screen Printed Electrode Modified with Fe3O4 Nanoparticle and Graphene for Chlorpyrifos Determination. *Int. J. Electrochem. Sci.* **2016**, 10906–10918. https://doi.org/10.20964/2016.12.90.

(37) Chen, D.; Jiayun, F.; Zengning, L.; Yemin, G.; Xia, S.; Xiangyou, W.; Zhiqiang, W. A Simple Acetylcholinesterase Biosensor Based on Ionic Liquid/Multiwalled Carbon Nanotubes-Modified Screen-Printed Electrode for Rapid Detecting Chlorpyrifos. *Int. J. Electrochem. Sci.* **2017**, 9465–9477. https://doi.org/10.20964/2017.10.12.

(38) Talan, A.; Mishra, A.; Eremin, S. A.; Narang, J.; Kumar, A.; Gandhi, S. Ultrasensitive Electrochemical Immuno-Sensing Platform Based on Gold Nanoparticles Triggering Chlorpyrifos Detection in Fruits and Vegetables. *Biosensors and Bioelectronics* **2018**, *105*, 14–21. https://doi.org/10.1016/j.bios.2018.01.013.

(39) Koukouvinos, G.; Tsialla, Z.; Petrou, P. S.; Misiakos, K.; Goustouridis, D.; Ucles Moreno, A.; Fernandez-Alba, A. R.; Raptis, I.; Kakabakos, S. E. Fast Simultaneous Detection of Three Pesticides by a White Light Reflectance Spectroscopy Sensing Platform. *Sensors and Actuators B: Chemical* **2017**, *238*, 1214–1223. https://doi.org/10.1016/j.snb.2016.09.035.

(40) Zhao, G.; Zhou, B.; Wang, X.; Shen, J.; Zhao, B. Detection of Organophosphorus Pesticides by Nanogold/Mercaptomethamidophos Multi-Residue Electrochemical Biosensor. *Food Chem* **2021**, *354*, 129511. https://doi.org/10.1016/j.foodchem.2021.129511.

(41) Hou, L.; Zhang, X.; Kong, M.; Jiang, G.; Sun, Y.; Mo, W.; Lin, T.; Ye, F.; Zhao, S. A Competitive Immunoassay for Electrochemical Impedimetric Determination of Chlorpyrifos Using a Nanogold-Modified Glassy Carbon Electrode Based on Enzymatic Biocatalytic Precipitation. *Mikrochim Acta* **2020**, *187* (4), 204. https://doi.org/10.1007/s00604-020-4175-1.

(42) Xu, G.; Huo, D.; Hou, C.; Zhao, Y.; Bao, J.; Yang, M.; Fa, H. A Regenerative and Selective Electrochemical Aptasensor Based on Copper Oxide Nanoflowers-Single Walled Carbon Nanotubes Nanocomposite for Chlorpyrifos Detection. *Talanta* **2018**, *178*, 1046–1052. https://doi.org/10.1016/j.talanta.2017.08.086.

(43) Weerathunge, P.; Behera, B. K.; Zihara, S.; Singh, M.; Prasad, S. N.; Hashmi, S.; Mariathomas, P. R. D.; Bansal, V.; Ramanathan, R. Dynamic Interactions between Peroxidase-Mimic Silver NanoZymes and Chlorpyrifos-Specific Aptamers Enable Highly-Specific Pesticide Sensing in River Water. *Analytica Chimica Acta* **2019**, *1083*, 157–165. https://doi.org/10.1016/j.aca.2019.07.066.

(44) Long, Q.; Li, H.; Zhang, Y.; Yao, S. Upconversion Nanoparticle-Based Fluorescence Resonance Energy Transfer Assay for Organophosphorus Pesticides. *Biosensors and Bioelectronics* **2015**, *68*, 168–174. https://doi.org/10.1016/j.bios.2014.12.046.

(45) Luo, Q.; Yu, F.; Yang, F.; Yang, C.; Qiu, P.; Wang, X. A 3D-Printed Self-Propelled, Highly Sensitive Mini-Motor for Underwater Pesticide Detection. *Talanta* **2018**, *183*, 297–303. https://doi.org/10.1016/j.talanta.2018.02.059.

(46) Liu, G.; Guo, W.; Song, D. A Multianalyte Electrochemical Immunosensor Based on Patterned Carbon Nanotubes Modified Substrates for Detection of Pesticides. *Biosensors and Bioelectronics* **2014**, *52*, 360–366. https://doi.org/10.1016/j.bios.2013.09.009.

(47) Vaghela, C.; Kulkarni, M.; Haram, S.; Aiyer, R.; Karve, M. A Novel Inhibition Based Biosensor Using Urease Nanoconjugate Entrapped Biocomposite Membrane for Potentiometric Glyphosate Detection. *International Journal of Biological Macromolecules* **2018**, *108*, 32–40. https://doi.org/10.1016/j.ijbiomac.2017.11.136.

(48) González-Martínez, M. Á.; Brun, E. M.; Puchades, R.; Maquieira, Á.; Ramsey, K.; Rubio, F. Glyphosate Immunosensor. Application for Water and Soil Analysis. *Anal. Chem.* **2005**, *77* (13), 4219–4227. https://doi.org/10.1021/ac048431d.

(49) Lee, H. U.; Shin, H. Y.; Lee, J. Y.; Song, Y. S.; Park, C.; Kim, S. W. Quantitative Detection of Glyphosate by Simultaneous Analysis of UV Spectroscopy and Fluorescence Using DNA-Labeled Gold Nanoparticles. *J. Agric. Food Chem.* **2010**, *58* (23), 12096–12100. https://doi.org/10.1021/jf102784t.

(50) Bettazzi, F.; Romero Natale, A.; Torres, E.; Palchetti, I. Glyphosate Determination by Coupling an Immuno-Magnetic Assay with Electrochemical Sensors. *Sensors* **2018**, *18* (9), 2965. https://doi.org/10.3390/s18092965.

(51) Liu, Q.; Zhang, R.; Yu, B.; Liang, A.; Jiang, Z. A Highly Sensitive Gold Nanosol SERS Aptamer Assay for Glyphosate with a New COF Nanocatalytic Reaction of Glycol-Au(III). *Sensors and Actuators B: Chemical* **2021**, *344*, 130288. https://doi.org/10.1016/j.snb.2021.130288.

(52) Chen, F.; Li, G.; Liu, H.; Leung, C.-H.; Ma, D.-L. G-Quadruplex-Based Detection of Glyphosate in Complex Biological Systems by a Time-Resolved Luminescent Assay. *Sensors and Actuators B: Chemical* **2020**, *320*, 128393. https://doi.org/10.1016/j.snb.2020.128393.

(53) Su, L.; Wang, S.; Wang, L.; Yan, Z.; Yi, H.; Zhang, D.; Shen, G.; Ma, Y. Fluorescent Aptasensor for Carbendazim Detection in Aqueous Samples Based on Gold Nanoparticles Quenching Rhodamine B. *Spectrochimica Acta Part A: Molecular and Biomolecular Spectroscopy* **2020**, *225*, 117511. https://doi.org/10.1016/j.saa.2019.117511.

(54) Ma, L.; Zhou, L.; He, Y.; Wang, L.; Huang, Z.; Jiang, Y.; Gao, J. Mesoporous Bimetallic PtPd Nanoflowers as a Platform to Enhance Electrocatalytic Activity of Acetylcholinesterase for Organophosphate Pesticide Detection. *Electroanalysis* **2018**, *30* (8), 1801–1810. https://doi.org/10.1002/elan.201700845.

(55) Liu, D.-L.; Li, Y.; Sun, R.; Xu, J.-Y.; Chen, Y.; Sun, C.-Y. Colorimetric Detection of Organophosphorus Pesticides Based on the Broad-Spectrum Aptamer. *Journal of Nanoscience and Nanotechnology* **2020**, *20* (4), 2114–2121. https://doi.org/10.1166/jnn.2020.17358.

(56) Zhao, F.; Yao, Y.; Li, X.; Lan, L.; Jiang, C.; Ping, J. Metallic Transition Metal Dichalcogenide Nanosheets as an Effective and Biocompatible Transducer for Electrochemical Detection of Pesticide. *Anal. Chem.* **2018**, *90* (19), 11658–11664. https://doi.org/10.1021/acs.analchem.8b03250.

(57) Arduini, F.; Cinti, S.; Caratelli, V.; Amendola, L.; Palleschi, G.; Moscone, D. Origami Multiple Paper-Based Electrochemical Biosensors for Pesticide Detection. *Biosensors and Bioelectronics* **2019**, *126*, 346–354. https://doi.org/10.1016/j.bios.2018.10.014.

(58) Li, X.; Gao, X.; Gai, P.; Liu, X.; Li, F. Degradable Metal-Organic Framework/Methylene Blue Composites-Based Homogeneous Electrochemical Strategy for Pesticide Assay. *Sensors and Actuators B: Chemical* **2020**, *323*, 128701. https://doi.org/10.1016/j.snb.2020.128701.

(59) Madianos, L.; Skotadis, E.; Tsekenis, G.; Patsiouras, L.; Tsigkourakos, M.; Tsoukalas, D. Impedimetric Nanoparticle Aptasensor for Selective and Label Free Pesticide Detection. *Microelectronic Engineering* **2017**, *189*, 39–45. https://doi.org/10.1016/j.mee.2017.12.016.

(60) Madianos, L.; Tsekenis, G.; Skotadis, E.; Patsiouras, L.; Tsoukalas, D. A Highly Sensitive Impedimetric Aptasensor for the Selective Detection of Acetamiprid and Atrazine Based on Microwires Formed by Platinum Nanoparticles. *Biosensors and Bioelectronics* **03/2018b**, *101*, 268–274. https://doi.org/10.1016/j.bios.2017.10.034.

(61) Fan, L.; Zhang, C.; Liang, G.; Yan, W.; Guo, Y.; Bi, Y.; Dong, C. Highly Sensitive Photoelectrochemical Aptasensor Based on MoS2 Quantum Dots/TiO2 Nanotubes for Detection of Atrazine. *Sensors and Actuators B: Chemical* **2021**, *334*, 129652. https://doi.org/10.1016/j.snb.2021.129652.

(62) Zhu, Q.-Q.; Li, H.-K.; Sun, X.-L.; Han, Z.-Y.; Sun, J.; He, H. Rational Incorporation of Covalent Organic Framework/Carbon Nanotube (COF/CNT) Composites for Electrochemical Aptasensing of Ultra-Trace Atrazine. *J. Mater. Chem. C* **2021**, *9* (25), 8043–8050. https://doi.org/10.1039/D1TC01506K.

(63) Sun, C.; Liu, M.; Sun, H.; Lu, H.; Zhao, G. Immobilization-Free Photoelectrochemical Aptasensor for Environmental Pollutants: Design, Fabrication and Mechanism. *Biosensors and Bioelectronics* **2019**, *140*, 111352. https://doi.org/10.1016/j.bios.2019.111352.

(64) Fan, L.; Zhang, C.; Yan, W.; Guo, Y.; Shuang, S.; Dong, C.; Bi, Y. Design of a Facile and Label-Free Electrochemical Aptasensor for Detection of Atrazine. *Talanta* **2019**, *201*, 156–164. https://doi.org/10.1016/j.talanta.2019.03.114.

(65) Wang, Y.; Sun, H.; Liu, M.; Lu, H.; Zhao, G. A Novel Self-Powered Aptasensor for Environmental Pollutants Detection Based on Simple and Efficient Enzymatic Biofuel Cell. *Sensors and Actuators B: Chemical* **2020**, *305*, 127468. https://doi.org/10.1016/j.snb.2019.127468.

(66) Sun, H.; Sun, C.; Ding, X.; Lu, H.; Liu, M.; Zhao, G. In Situ Monitoring of the Selective Adsorption Mechanism of Small Environmental Pollutant Molecules on Aptasensor Interface by Attenuated Total Reflection Surface Enhanced Infrared Absorption Spectroscopy (ATR–SEIRAS). *Journal of Hazardous Materials* **2021**, *403*, 123953. https://doi.org/10.1016/j.jhazmat.2020.123953.

(67) Romero-Reyes, M. A.; Heemstra, J. M. Sequestration and Removal of Multiple Small-Molecule Contaminants Using an Optimized Aptamer-Based Ultrafiltration System. *Bioconjugate Chem.* **2021**, *32* (9), 2043–2051. https://doi.org/10.1021/acs.bioconjchem.1c00344.

(68) Yao, Z.; Yao, Z.; Jia, X.; Ren, S.; Yang, S.; Gao, Z. *Suspension Array Platform Based on Aptamer for High-Throughput Detection of Five Environmental Hormones*; preprint; In Review, 2021. https://doi.org/10.21203/rs.3.rs-1089406/v1.

(69) Wei, X.; Sun, Y.; Liu, C.; Li, Z.; Zou, X.; Zhang, D.; Zhang, W.; Shi, J.; Huang, X.; Li, Y. A Nitrile-Mediated SERS Aptasensor Coupled with Magnetic Separation for Optical Interference-Free Detection of Atrazine. *Sensors and Actuators B: Chemical* **2021**, *329*, 129075. https://doi.org/10.1016/j.snb.2020.129075.

(70) Cheng, Y.; Lai, O.-M.; Tan, C.-P.; Panpipat, W.; Cheong, L.-Z.; Shen, C. Proline-Modified UIO-66 as Nanocarriers to Enhance Candida Rugosa Lipase Catalytic Activity and Stability for Electrochemical Detection of Nitrofen. *ACS Appl. Mater. Interfaces* **2021**, *13* (3), 4146–4155. https://doi.org/10.1021/acsami.0c17134.

(71) Yang, G.; He, Y.; Zhao, J.; Chen, S.; Yuan, R. Ratiometric Electrochemiluminescence Biosensor Based on Ir Nanorods and CdS Quantum Dots for the Detection of Organophosphorus Pesticides. *Sensors and Actuators B: Chemical* **2021**, *341*, 130008. https://doi.org/10.1016/j.snb.2021.130008.

(72) Apilux, A.; Siangproh, W.; Insin, N.; Chailapakul, O.; Prachayasittikul, V. Paper-Based Thioglycolic Acid (TGA)-Capped CdTe QD Device for Rapid Screening of Organophosphorus and Carbamate Insecticides. *Anal. Methods* **2017**, *9* (3), 519–527. https://doi.org/10.1039/C6AY02883G.

(73) Cui, H.-F.; Zhang, T.-T.; Lv, Q.-Y.; Song, X.; Zhai, X.-J.; Wang, G.-G. An Acetylcholinesterase Biosensor Based on Doping Au Nanorod@SiO2 Nanoparticles into TiO2-Chitosan Hydrogel for Detection of Organophosphate Pesticides. *Biosens Bioelectron* **2019**, *141*, 111452. https://doi.org/10.1016/j.bios.2019.111452.

(74) Bilal, S.; Mudassir Hassan, M.; Fayyaz ur Rehman, M.; Nasir, M.; Jamil Sami, A.; Hayat, A. An Insect Acetylcholinesterase Biosensor Utilizing WO3/g-C3N4 Nanocomposite Modified Pencil Graphite Electrode for Phosmet Detection in Stored Grains. *Food Chemistry* **2021**, *346*, 128894. https://doi.org/10.1016/j.foodchem.2020.128894.

(75) Sharma, D.; Wangoo, N.; Sharma, R. K. Sensing Platform for Pico-Molar Level Detection of Ethyl Parathion Using Au–Ag Nanoclusters Based Enzymatic Strategy. *Talanta* **2021**, *221*, 121267. https://doi.org/10.1016/j.talanta.2020.121267.

(76) Abnous, K.; Danesh, N. M.; Ramezani, M.; Emrani, A. S.; Taghdisi, S. M. A Novel Colorimetric Sandwich Aptasensor Based on an Indirect Competitive Enzyme-Free Method for Ultrasensitive Detection of Chloramphenicol. *Biosensors and Bioelectronics* **2016**, *78*, 80–86. https://doi.org/10.1016/j.bios.2015.11.028.

(77) Jiao, S.; Liu, P.; Liu, Y.; Zou, R.; Zhao, Y.; Liu, Y.; Zhu, G.; Guo, Y. Binding Properties of Broad-Specific Monoclonal Antibodies against Three Organophosphorus Pesticides by a Direct Surface Plasmon Resonance Immunosensor. *Anal Bioanal Chem* **2018**, *410* (28), 7263–7273. https://doi.org/10.1007/s00216-018-1337-7.

(78) Cheng, N.; Shi, Q.; Zhu, C.; Li, S.; Lin, Y.; Du, D. Pt-Ni(OH)2 Nanosheets Amplified Two-Way Lateral Flow Immunoassays with Smartphone Readout for Quantification of Pesticides. *Biosens Bioelectron* **2019**, *142*, 111498. https://doi.org/10.1016/j.bios.2019.111498.

(79) Guo, Y.; Liu, R.; Liu, Y.; Xiang, D.; Liu, Y.; Gui, W.; Li, M.; Zhu, G. A Non-Competitive Surface Plasmon Resonance Immunosensor for Rapid Detection of Triazophos Residue in Environmental and Agricultural Samples. *Science of The Total Environment* **2018**, *613–614*, 783–791. https://doi.org/10.1016/j.scitotenv.2017.09.157.

(80) Valera, E.; García-Febrero, R.; Pividori, I.; Sánchez-Baeza, F.; Marco, M.-P. Coulombimetric Immunosensor for Paraquat Based on Electrochemical Nanoprobes. *Sensors and Actuators B: Chemical* **2014**, *194*, 353–360. https://doi.org/10.1016/j.snb.2013.12.029.

(81) Mehta, J.; Vinayak, P.; Tuteja, S. K.; Chhabra, V. A.; Bhardwaj, N.; Paul, A. K.; Kim, K.-H.; Deep, A. Graphene Modified Screen Printed Immunosensor for Highly Sensitive Detection of Parathion. *Biosensors and Bioelectronics* **2016**, *83*, 339–346. https://doi.org/10.1016/j.bios.2016.04.058.

(82) Li, S.; Li, J.; Luo, J.; Xu, Z.; Ma, X. A Microfluidic Chip Containing a Molecularly Imprinted Polymer and a DNA Aptamer for Voltammetric Determination of Carbofuran. *Microchim Acta* **2018**, *185* (6), 295. https://doi.org/10.1007/s00604-018-2835-1.

(83) Rong, Y.; Li, H.; Ouyang, Q.; Ali, S.; Chen, Q. Rapid and Sensitive Detection of Diazinon in Food Based on the FRET between Rare-Earth Doped Upconversion Nanoparticles and Graphene Oxide. *Spectrochimica Acta Part A: Molecular and Biomolecular Spectroscopy* **2020**, *239*, 118500. https://doi.org/10.1016/j.saa.2020.118500.

(84) Li, X.; Tang, X.; Chen, X.; Qu, B.; Lu, L. Label-Free and Enzyme-Free Fluorescent Isocarbophos Aptasensor Based on MWCNTs and G-Quadruplex. *Talanta* **2018**, *188*, 232–237. https://doi.org/10.1016/j.talanta.2018.05.092.

(85) Wang, R.-H.; Zhu, C.-L.; Wang, L.-L.; Xu, L.-Z.; Wang, W.-L.; Yang, C.; Zhang, Y. Dual-Modal Aptasensor for the Detection of Isocarbophos in Vegetables. *Talanta* **2019**, *205*, 120094. https://doi.org/10.1016/j.talanta.2019.06.094.

(86) Dalefield, R. *Veterinary Toxicology for Australia and New Zealand*; Elsevier: Masterton, New Zealand, 2017.

(87) Simonian, A. L.; Efremenko, E. N.; Wild, J. R. Discriminative Detection of Neurotoxins in Multi-Component Samples. *Analytica Chimica Acta* **2001**, *444* (2), 179–186. https://doi.org/10.1016/S0003-2670(01)01099-6.

(88) de Lima, F.; Lucca, B. G.; Barbosa, A. M. J.; Ferreira, V. S.; Moccelini, S. K.; Franzoi, A. C.; Vieira, I. C. Biosensor Based on Pequi Polyphenol Oxidase Immobilized on Chitosan Crosslinked with Cyanuric Chloride for Thiodicarb Determination. *Enzyme and Microbial Technology* **2010**, *47* (4), 153–158. https://doi.org/10.1016/j.enzmictec.2010.05.006.

(89) Kim, G.-Y.; Kang, M.-S.; Shim, J.; Moon, S.-H. Substrate-Bound Tyrosinase Electrode Using Gold Nanoparticles Anchored to Pyrroloquinoline Quinone for a Pesticide Biosensor. *Sensors and Actuators B: Chemical* **2008**, *133* (1), 1–4. https://doi.org/10.1016/j.snb.2008.01.055.

(90) García Sánchez, F.; Navas Díaz, A.; Ramos Peinado, M. C.; Belledone, C. Free and Sol–Gel Immobilized Alkaline Phosphatase-Based Biosensor for the Determination of Pesticides and Inorganic Compounds. *Analytica Chimica Acta* **2003**, *484* (1), 45–51. https://doi.org/10.1016/S0003-2670(03)00310-6.

(91) Mazzei, F.; Botrè, F.; Montilla, S.; Pilloton, R.; Podestà, E.; Botrè, C. Alkaline Phosphatase Inhibition Based Electrochemical Sensors for the Detection of Pesticides. *Journal of Electroanalytical Chemistry* **2004**, *574* (1), 95–100. https://doi.org/10.1016/j.jelechem.2004.08.004.

(92) Moccelini, S. K.; Vieira, I. C.; de Lima, F.; Lucca, B. G.; Barbosa, A. M. J.; Ferreira, V. S. Determination of Thiodicarb Using a Biosensor Based on Alfalfa Sprout Peroxidase Immobilized in Self-Assembled Monolayers. *Talanta* **2010**, *82* (1), 164–170. https://doi.org/10.1016/j.talanta.2010.04.015.

(93) Mazzei, F.; Botrè, F.; Botrè, C. Acid Phosphatase/Glucose Oxidase-Based Biosensors for the Determination of Pesticides. *Analytica Chimica Acta* **1996**, *336* (1), 67–75. https://doi.org/10.1016/S0003-2670(96)00378-9.

(94) Berkal, M. A.; Palas, Q.; Ricard, E.; Lartigau-Dagron, C.; Ronga, L.; Toulmé, J.-J.; Parat, C.; Nardin, C. Glyphosate-Exonuclease Interactions: Reduced Enzymatic Activity as a Route to Glyphosate Biosensing. *Macromol Biosci* **2023**, e2200508. https://doi.org/10.1002/mabi.202200508.

(95) El-Moghazy, A. Y.; Amaly, N.; Istamboulie, G.; Nitin, N.; Sun, G. A Signal-on Electrochemical Aptasensor Based on Silanized Cellulose Nanofibers for Rapid Point-of-Use Detection of Ochratoxin A. *Microchim Acta* **2020**, *187* (9), 535. https://doi.org/10.1007/s00604-020-04509-y.

(96) Luo, D.; Huang, X.; Liu, B.; Zou, W.; Wu, Y. Facile Colorimetric Nanozyme Sheet for the Rapid Detection of Glyphosate in Agricultural Products Based on Inhibiting Peroxidase-Like Catalytic Activity of Porous Co_3O_4 Nanoplates. *J. Agric. Food Chem.* **2021**, *69* (11), 3537–3547. https://doi.org/10.1021/acs.jafc.0c08208.

(97) Ma, L.; Zhou, L.; He, Y.; Wang, L.; Huang, Z.; Jiang, Y.; Gao, J. Hierarchical Nanocomposites with an N-Doped Carbon Shell and Bimetal Core: Novel Enzyme Nanocarriers for Electrochemical Pesticide Detection. *Biosensors and Bioelectronics* **2018**, *121*, 166–173. https://doi.org/10.1016/j.bios.2018.08.038.

(98) Goyal, M. R.; Malik, J. A.; Pandiselvam, R. *Enzyme Inactivation in Food Processing: Technologies, Materials, and Applications*; CRC Press, 2023.

(99) Wu, J.; Yang, Q.; Li, Q.; Li, H.; Li, F. Two-Dimensional MnO2 Nanozyme-Mediated Homogeneous Electrochemical Detection of Organophosphate Pesticides without the Interference of H2O2 and Color. *Anal. Chem.* **2021**, *93* (8), 4084–4091. https://doi.org/10.1021/acs.analchem.0c05257.

(100) Han, Z.; Chi, C.; Bai, B.; Liu, G.; Rao, Q.; Peng, S.; Liu, H.; Zhao, Z.; Zhang, D.; Wu, A. Chromogenic Platform Based on Recombinant Drosophila Melanogaster Acetylcholinesterase for Visible Unidirectional Assay of Organophosphate and Carbamate Insecticide Residues. *Analytica Chimica Acta* **2012**, *720*, 126–133. https://doi.org/10.1016/j.aca.2012.01.041.

(101) Matějovský, L.; Pitschmann, V. New Carrier Made from Glass Nanofibres for the Colorimetric Biosensor of Cholinesterase Inhibitors. *Biosensors* **2018**, *8* (2), 51. https://doi.org/10.3390/bios8020051.

(102) Li, H.; Zhao, S.; Wang, Z.; Li, F. Controllable Preparation of 2D V2O5 Peroxidase-Mimetic Nanozyme to Develop Portable Paper-Based Analytical Device for Intelligent Pesticide Assay. *Small* **2023**, *19* (14), 2206465. https://doi.org/10.1002/smll.202206465.

(103) Gai, P.; Pu, L.; Wang, C.; Zhu, D.; Li, F. CeO2@NC Nanozyme with Robust Dephosphorylation Ability of Phosphotriester: A Simple Colorimetric Assay for Rapid and Selective Detection of Paraoxon. *Biosensors and Bioelectronics* **2023**, *220*, 114841. https://doi.org/10.1016/j.bios.2022.114841.

(104) Chang, J.; Yu, L.; Hou, T.; Hu, R.; Li, F. Direct and Specific Detection of Glyphosate Using a Phosphatase-like Nanozyme-Mediated Chemiluminescence Strategy. *Anal. Chem.* **2023**, *95* (9), 4479–4485. https://doi.org/10.1021/acs.analchem.2c05198.

(105) Jia, L.; Zhou, Y.; Wu, K.; Feng, Q.; Wang, C.; He, P. Acetylcholinesterase Modified AuNPs-MoS2-RGO/PI Flexible Film Biosensor: Towards Efficient Fabrication and Application in Paraoxon Detection. *Bioelectrochemistry* **2020**, *131*, 107392. https://doi.org/10.1016/j.bioelechem.2019.107392.

(106) Chen, G.; Jin, M.; Ma, J.; Yan, M.; Cui, X.; Wang, Y.; Zhang, X.; Li, H.; Zheng, W.; Zhang, Y.; Abd El-Aty, A. M.; Hacımüftüoğlu, A.; Wang, J. Competitive Bio-Barcode Immunoassay for Highly Sensitive Detection of Parathion Based on Bimetallic Nanozyme Catalysis. *J. Agric. Food Chem.* **2020**, *68* (2), 660–668. https://doi.org/10.1021/acs.jafc.9b06125.

(107) Kröger, S.; Setford, S. J.; Turner, A. P. F. Immunosensor for 2,4-Dichlorophenoxyacetic Acid in Aqueous/Organic Solvent Soil Extracts. *Anal. Chem.* **1998**, *70* (23), 5047–5053. https://doi.org/10.1021/ac9805100.

(108) Skládal, P.; Kaláb, T. A Multichannel Immunochemical Sensor for Determination of 2,4-Dichlorophenoxyacetic Acid. *Analytica Chimica Acta* **1995**, *316* (1), 73–78. https://doi.org/10.1016/0003-2670(95)00342-W.

(109) Kaláb, T.; Skládal, P. A Disposable Amperometric Immunosensor for 2,4-Dichlorophenoxyacetic Acid. *Analytica Chimica Acta* **1995**, *304* (3), 361–368. https://doi.org/10.1016/0003-2670(94)00641-X.

(110) Bier, F. F.; Ehrentreich-Förster, E.; Dölling, R.; Eremenko, A. V.; Scheller, F. W. A Redox-Label Immunosensor on Basis of a Bi-Enzyme Electrode. *Analytica Chimica Acta* **1997**, *344* (1), 119–124. https://doi.org/10.1016/S0003-2670(97)00050-0.

(111) Audrey, S.; Beatriz, P.-S.; Jean-Louis, M. Biosensors for Pesticide Detection: New Trends. *American Journal of Analytical Chemistry* **2012**, *2012*. https://doi.org/10.4236/ajac.2012.33030.

(112) Reynoso, E. C.; Torres, E.; Bettazzi, F.; Palchetti, I. Trends and Perspectives in Immunosensors for Determination of Currently-Used Pesticides: The Case of Glyphosate, Organophosphates, and Neonicotinoids. *Biosensors* **2019**, *9* (1), 20. https://doi.org/10.3390/bios9010020.

(113) Hongsibsong, S.; Wipasa, J.; Pattarawarapan, M.; Chantara, S.; Stuetz, W.; Nosten, F.; Prapamontol, T. Development and Application of an Indirect Competitive Enzyme-Linked Immunosorbent Assay for the Detection of *p* , *p* ’-DDE in Human Milk and Comparison of the Results against GC-ECD. *J. Agric. Food Chem.* **2012**, *60* (1), 16–22. https://doi.org/10.1021/jf203440b.

(114) Liu, J.; Song, S.; Wu, A.; Kuang, H.; Liu, L.; Xiao, J.; Xu, C. Development of Immunochromatographic Strips for the Detection of Dicofol. *Analyst* **2021**, *146* (7), 2240–2247. https://doi.org/10.1039/D0AN02238A.

(115) Qiu, X.; Zhu, T.; Yao, B.; Hu, J.; Hu, S. Contribution of Dicofol to the Current DDT Pollution in China. *Environ. Sci. Technol.* **2005**, *39* (12), 4385–4390. https://doi.org/10.1021/es050342a.

(116) European Parliament COUNCIL DIRECTIVE 98/83/EC, Official Journal. *Council Directive 98/83/EC on the quality of water intended for human consumption.* https://eur-lex.europa.eu/legal-content/EN/TXT/PDF/?uri=CELEX:01998L0083-20151027&from=EN (accessed 2022-11-14).

(117) Riedel, T.; Majek, P.; Rodriguez-Emmenegger, C.; Brynda, E. Surface Plasmon Resonance: Advances of Label-Free Approaches in the Analysis of Biological Samples. *Bioanalysis* **2014**, *6* (24), 3325–3336. https://doi.org/10.4155/bio.14.246.

(118) Scarano, S.; Mascini, M.; Turner, A. P. F.; Minunni, M. Surface Plasmon Resonance Imaging for Affinity-Based Biosensors. *Biosensors and Bioelectronics* **2010**, *25* (5), 957–966. https://doi.org/10.1016/j.bios.2009.08.039.

(119) Gouzy, M.-F.; Keß, M.; Krämer, P. M. A SPR-Based Immunosensor for the Detection of Isoproturon. *Biosensors and Bioelectronics* **2009**, *24* (6), 1563–1568. https://doi.org/10.1016/j.bios.2008.08.005.

(120) Yakes, B. J.; Kanyuck, K. M.; DeGrasse, S. L. First Report of a Direct Surface Plasmon Resonance Immunosensor for a Small Molecule Seafood Toxin. *Anal. Chem.* **2014**, *86* (18), 9251–9255. https://doi.org/10.1021/ac502271y.

(121) Munoz, E. M.; Lorenzo-Abalde, S.; González-Fernández, Á.; Quintela, O.; Lopez-Rivadulla, M.; Riguera, R. Direct Surface Plasmon Resonance Immunosensor for in Situ Detection of Benzoylecgonine, the Major Cocaine Metabolite. *Biosensors and Bioelectronics* **2011**, *26* (11), 4423–4428. https://doi.org/10.1016/j.bios.2011.04.056.

(122) Wijaya, I. P. M.; Ju Nie, T.; Gandhi, S.; Boro, R.; Palaniappan, A.; Wei Hau, G.; Rodriguez, I.; Raman Suri, C.; G. Mhaisalkar, S. Femtomolar Detection of 2,4-Dichlorophenoxyacetic Acid Herbicides via Competitive Immunoassays Using Microfluidic Based Carbon Nanotube Liquid Gated Transistor. *Lab on a Chip* **2010**, *10* (5), 634–638. https://doi.org/10.1039/B918566F.

(123) Sharma, P.; Gandhi, S.; Chopra, A.; Sekar, N.; Raman Suri, C. Fluoroimmunoassay Based on Suppression of Fluorescence Self-Quenching for Ultra-Sensitive Detection of Herbicide Diuron. *Analytica Chimica Acta* **2010**, *676* (1), 87–92. https://doi.org/10.1016/j.aca.2010.07.042.

(124) Jiao, Y.; Jia, H.; Guo, Y.; Zhang, H.; Wang, Z.; Sun, X.; Zhao, J. An Ultrasensitive Aptasensor for Chlorpyrifos Based on Ordered Mesoporous Carbon/Ferrocene Hybrid Multiwalled Carbon Nanotubes. *RSC Advances* **2016**, *6* (63), 58541–58548. https://doi.org/10.1039/c6ra07735h.

(125) Cui, L.; Wu, J.; Ju, H. Label-Free Signal-on Aptasensor for Sensitive Electrochemical Detection of Arsenite. *Biosensors and Bioelectronics* **2016**, *79*, 861–865. https://doi.org/10.1016/j.bios.2016.01.010.

(126) Verdian-Doghaei, A.; Housaindokht, M. R.; Abnous, Kh. A Fluorescent Aptasensor for Potassium Ion Detection-Based Triple-Helix Molecular Switch. *Analytical Biochemistry* **2014**, *466*, 72–75. https://doi.org/10.1016/j.ab.2014.08.014.

(127) Ran, G.; Wu, F.; Ni, X.; Li, X.; Li, X.; Liu, D.; Sun, J.; Xie, C.; Yao, D.; Bai, W. A Novel Label-Free Electrochemical Aptasensor with One-Step Assembly Process for Rapid Detection of Lead (II) Ions. *Sensors and Actuators B: Chemical* **2020**, *320*, 128326. https://doi.org/10.1016/j.snb.2020.128326.

(128) Xiao, Y.; Lubin, A. A.; Heeger, A. J.; Plaxco, K. W. Label-Free Electronic Detection of Thrombin in Blood Serum by Using an Aptamer-Based Sensor. *Angewandte Chemie* **2005**, *117* (34), 5592–5595. https://doi.org/10.1002/ange.200500989.

(129) Huizenga, D. E.; Szostak, J. W. A DNA Aptamer That Binds Adenosine and ATP. *Biochemistry* **1995**, *34* (2), 656–665.

(130) Qi, X.; Yan, X.; Zhao, L.; Huang, Y.; Wang, S.; Liang, X. A Facile Label-Free Electrochemical Aptasensor Constructed with Nanotetrahedron and Aptamer-Triplex for Sensitive Detection of Small Molecule: Saxitoxin. *Journal of Electroanalytical Chemistry* **2020**, *858*, 113805. https://doi.org/10.1016/j.jelechem.2019.113805.

(131) Li, W.; Luo, Y.; Gao, T.; Yang, L.; Wang, J.; Pei, R. In Vitro Selection of DNA Aptamers for a Small-Molecule Porphyrin by Gold Nanoparticle-Based SELEX. *J Mol Evol* **2019**, *87* (7), 231–239. https://doi.org/10.1007/s00239-019-09905-4.

(132) Kaur, H. Aptamer Conjugated Quantum Dots for Imaging Cellular Uptake in Cancer Cells. *j nanosci nanotechnol* **2019**, *19* (7), 3798–3803. https://doi.org/10.1166/jnn.2019.16735.

(133) Wang, Q.; Luo, B.; Yang, X.; Wang, K.; Liu, L.; Du, S.; Li, Z. Elucidation of the Effect of Aptamer Immobilization Strategies on the Interaction between Cell and Its Aptamer Using Atomic Force Spectroscopy. *Journal of Molecular Recognition* **2016**, *29* (4), 151–158. https://doi.org/10.1002/jmr.2514.

(134) Zhang, Y.; Lai, B. S.; Juhas, M. Recent Advances in Aptamer Discovery and Applications. *Molecules* **2019**, *24* (5), 941. https://doi.org/10.3390/molecules24050941.

(135) McKeague, M.; DeRosa, M. C. Challenges and Opportunities for Small Molecule Aptamer Development. *Journal of Nucleic Acids* **2012**, *2012*, e748913. https://doi.org/10.1155/2012/748913.

(136) Stoltenburg, R.; Reinemann, C.; Strehlitz, B. FluMag-SELEX as an Advantageous Method for DNA Aptamer Selection. *Anal Bioanal Chem* **2005**, *383* (1), 83–91. https://doi.org/10.1007/s00216-005-3388-9.

(137) Spiga, F. M.; Maietta, P.; Guiducci, C. More DNA–Aptamers for Small Drugs: A Capture–SELEX Coupled with Surface Plasmon Resonance and High-Throughput Sequencing. *ACS Comb. Sci.* **2015**, *17* (5), 326–333. https://doi.org/10.1021/acscombsci.5b00023.

(138) Xie, M.; Zhao, F.; Zhang, Y.; Xiong, Y.; Han, S. Recent Advances in Aptamer-Based Optical and Electrochemical Biosensors for Detection of Pesticides and Veterinary Drugs. *Food Control* **2022**, *131*, 108399. https://doi.org/10.1016/j.foodcont.2021.108399.

(139) Bala, R.; Kumar, M.; Bansal, K.; Sharma, R. K.; Wangoo, N. Ultrasensitive Aptamer Biosensor for Malathion Detection Based on Cationic Polymer and Gold Nanoparticles. *Biosensors and Bioelectronics* **2016**, *85*, 445–449. https://doi.org/10.1016/j.bios.2016.05.042.

(140) Bai, W.; Zhu, C.; Liu, J.; Yan, M.; Yang, S.; Chen, A. Gold Nanoparticle–Based Colorimetric Aptasensor for Rapid Detection of Six Organophosphorous Pesticides. *Environmental Toxicology and Chemistry* **2015**, *34* (10), 2244–2249. https://doi.org/10.1002/etc.3088.

(141) Yang, K.-A.; Pei, R.; Stojanovic, M. N. In Vitro Selection and Amplification Protocols for Isolation of Aptameric Sensors for Small Molecules. *Methods* **2016**, *106*, 58–65. https://doi.org/10.1016/j.ymeth.2016.04.032.

(142) Wang, H.-B.; Li, Y.; Bai, H.-Y.; Liu, Y.-M. DNA-Templated Au Nanoclusters and MnO2 Sheets: A Label-Free and Universal Fluorescence Biosensing Platform. *Sensors and Actuators B: Chemical* **2018**, *259*, 204–210. https://doi.org/10.1016/j.snb.2017.12.048.

(143) Xiong, Z.; Wang, Q.; Xie, Y.; Li, N.; Yun, W.; Yang, L. Simultaneous Detection of Aflatoxin B1 and Ochratoxin A in Food Samples by Dual DNA Tweezers Nanomachine. *Food Chemistry* **2021**, *338*, 128122. https://doi.org/10.1016/j.foodchem.2020.128122.

(144) Li, Y.; Zhang, N.; Wang, H.; Zhao, Q. Fluorescence Anisotropy-Based Signal-Off and Signal-On Aptamer Assays Using Lissamine Rhodamine B as a Label for Ochratoxin A. *J. Agric. Food Chem.* **2020**, *68* (14), 4277–4283. https://doi.org/10.1021/acs.jafc.0c00549.

(145) Zhu, X.; Xu, H.; Li, W.; Dong, Y.; Chi, Y. A Novel Hybrid Platform of G-C3N4 Nanosheets /Nucleic-Acid-Stabilized Silver Nanoclusters for Sensing Protein. *Analytica Chimica Acta* **2019**, *1091*, 112–118. https://doi.org/10.1016/j.aca.2019.09.030.

(146) Yin, N.; Yuan, S.; Zhang, M.; Wang, J.; Li, Y.; Peng, Y.; Bai, J.; Ning, B.; Liang, J.; Gao, Z. An Aptamer-Based Fluorometric Zearalenone Assay Using a Lighting-up Silver Nanocluster Probe and Catalyzed by a Hairpin Assembly. *Microchim Acta* **2019**, *186* (12), 765. https://doi.org/10.1007/s00604-019-3984-6.

(147) Zhu, K.; Lv, T.; Qin, T.; Huang, Y.; Wang, L.; Liu, B. A Flavonoid-Based Fluorescent Probe Enables the Accurate Quantification of Human Serum Albumin by Minimizing the Interference from Blood Lipids. *Chemical Communications* **2019**, *55* (93), 13983–13986. https://doi.org/10.1039/C9CC08015E.

(148) Wang, W.; Vellaisamy, K.; Li, G.; Wu, C.; Ko, C.-N.; Leung, C.-H.; Ma, D.-L. Development of a Long-Lived Luminescence Probe for Visualizing β-Galactosidase in Ovarian Carcinoma Cells. *Anal. Chem.* **2017**, *89* (21), 11679–11684. https://doi.org/10.1021/acs.analchem.7b03114.

(149) Ko, C.-N.; Yang, C.; Lin, S.; Li, S.; Dong, Z.; Liu, J.; Lee, S. M.-Y.; Leung, C.-H.; Ma, D.-L. A Long-Lived Phosphorescence Iridium(III) Complex as a Switch on-off-on Probe for Live Zebrafish Monitoring of Endogenous Sulfide Generation. *Biosensors and Bioelectronics* **2017**, *94*, 575–583. https://doi.org/10.1016/j.bios.2017.03.050.

(150) Li, G.; Adam Henry, S.; Liu, H.; Kang, T.-S.; Nao, S.-C.; Zhao, Y.; Wu, C.; Jin, J.; Zhang, J.-T.; Leung, C.-H.; Chan, P. W. H.; Ma, D.-L. A Robust Photoluminescence Screening Assay Identifies Uracil-DNA Glycosylase Inhibitors against Prostate Cancer. *Chemical Science* **2020**, *11* (7), 1750–1760. https://doi.org/10.1039/C9SC05623H.

(151) Lagarto, J.; Dyer, B. T.; Talbot, C.; Sikkel, M. B.; Peters, N. S.; French, P. M. W.; Lyon, A. R.; Dunsby, C. Application of Time-Resolved Autofluorescence to Label-Free in Vivo Optical Mapping of Changes in Tissue Matrix and Metabolism Associated with Myocardial Infarction and Heart Failure. *Biomed. Opt. Express, BOE* **2015**, *6* (2), 324–346. https://doi.org/10.1364/BOE.6.000324.

(152) Ma, D.-L.; Wang, M.; He, B.; Yang, C.; Wang, W.; Leung, C.-H. A Luminescent Cocaine Detection Platform Using a Split G-Quadruplex-Selective Iridium(III) Complex and a Three-Way DNA Junction Architecture. *ACS Appl. Mater. Interfaces* **2015**, *7* (34), 19060–19067. https://doi.org/10.1021/acsami.5b05861.

(153) Hossain, M. K.; Kitahama, Y.; Huang, G. G.; Han, X.; Ozaki, Y. Surface-Enhanced Raman Scattering: Realization of Localized Surface Plasmon Resonance Using Unique Substrates and Methods. *Anal Bioanal Chem* **2009**, *394* (7), 1747–1760. https://doi.org/10.1007/s00216-009-2762-4.

(154) Yu, J.; Ma, Y.; Yang, C.; Zhang, H.; Liu, L.; Su, J.; Gao, Y. SERS-Active Composite Based on RGO and Au/Ag Core-Shell Nanorods for Analytical Applications. *Sensors and Actuators B: Chemical* **2018**, *254*, 182–188. https://doi.org/10.1016/j.snb.2017.07.034.

(155) Liu, Y.; Li, R.; Zhou, N.; Li, M.; Huang, C.; Mao, H. Recyclable 3D SERS Devices Based on ZnO Nanorod-Grafted Nanowire Forests for Biochemical Sensing. *Applied Surface Science* **2022**, *582*, 152336. https://doi.org/10.1016/j.apsusc.2021.152336.

(156) Song, D.; Yang, R.; Long, F.; Zhu, A. Applications of Magnetic Nanoparticles in Surface-Enhanced Raman Scattering (SERS) Detection of Environmental Pollutants. *Journal of Environmental Sciences* **2019**, *80*, 14–34. https://doi.org/10.1016/j.jes.2018.07.004.

(157) Botta, R.; Eiamchai, P.; Horprathum, M.; Limwichean, S.; Chananonnawathorn, C.; Patthanasettakul, V.; Maezono, R.; Jomphoak, A.; Nuntawong, N. 3D Structured Laser Engraves Decorated with Gold Nanoparticle SERS Chips for Paraquat Herbicide Detection in Environments. *Sensors and Actuators B: Chemical* **2020**, *304*, 127327. https://doi.org/10.1016/j.snb.2019.127327.

(158) Pang, S.; Yang, T.; He, L. Review of Surface Enhanced Raman Spectroscopic (SERS) Detection of Synthetic Chemical Pesticides. *TrAC Trends in Analytical Chemistry* **2016**, *85*, 73–82. https://doi.org/10.1016/j.trac.2016.06.017.

(159) Bernat, A.; Samiwala, M.; Albo, J.; Jiang, X.; Rao, Q. Challenges in SERS-Based Pesticide Detection and Plausible Solutions. *J. Agric. Food Chem.* **2019**, *67* (45), 12341–12347. https://doi.org/10.1021/acs.jafc.9b05077.

(160) Albarghouthi, N.; Eisnor, M. M.; Pye, C. C.; Brosseau, C. L. Electrochemical Surface-Enhanced Raman Spectroscopy (EC-SERS) and Computational Study of Atrazine: Toward Point-of-Need Detection of Prevalent Herbicides. *J. Phys. Chem. C* **2022**, *126* (23), 9836–9842. https://doi.org/10.1021/acs.jpcc.2c02337.

(161) Kamkrua, N.; Ngernsutivorakul, T.; Limwichean, S.; Eiamchai, P.; Chananonnawathorn, C.; Pattanasetthakul, V.; Ricco, R.; Choowongkomon, K.; Horprathum, M.; Nuntawong, N.; Bora, T.; Botta, R. Au Nanoparticle-Based Surface-Enhanced Raman Spectroscopy Aptasensors for Paraquat Herbicide Detection. *ACS Appl. Nano Mater.* **2023**, *6* (2), 1072–1082. https://doi.org/10.1021/acsanm.2c04556.

(162) Yuan, R.; Li, H.-K.; He, H. Recent Advances in Metal/Covalent Organic Framework-Based Electrochemical Aptasensors for Biosensing Applications. *Dalton Transactions* **2021**, *50* (40), 14091–14104. https://doi.org/10.1039/D1DT02360H.

(163) Nutiu, R.; Li, Y. In Vitro Selection of Structure-Switching Signaling Aptamers. *Angewandte Chemie International Edition* **2005**, *44* (7), 1061–1065.

(164) Guyton, K. Z.; Loomis, D.; Grosse, Y.; El Ghissassi, F.; Benbrahim-Tallaa, L.; Guha, N.; Scoccianti, C.; Mattock, H.; Straif, K. Carcinogenicity of Tetrachlorvinphos, Parathion, Malathion, Diazinon, and Glyphosate. *The Lancet Oncology* **2015**, *16* (5), 490–491. https://doi.org/10.1016/S1470-2045(15)70134-8.

Chapter II. Glyphosate-exonuclease interactions: reduced enzymatic activity as a route to glyphosate biosensing

Résumé

Ce chapitre présente une étude approfondie réalisée dans le but d'identifier un aptamer montrant une interaction spécifique contre le glyphosate afin de pouvoir l'utiliser sur la plateforme électrochimique pour détecter ce pesticide. Dans cette optique, 3 aptamères candidats, GLY1, GLY2 et GLY3 ont été identifiés dans la littérature. Leur interaction avec le glyphosate a été évaluée via une méthode de digestion enzymatique suivie par spectroscopie de fluorescence. Cette méthode, décrite dans la littérature, utilise l'exonucléase I, une enzyme digérant les oligonucléotides simple brin dans le sens 3' vers 5'. En utilisant une sonde de fluorescence, le SYBR Gold, le pourcentage de digestion est quantitativement mesuré. En présence de la cible, un complexe aptamère/cible est formé retardant ainsi la digestion de l'Exo I. Cependant, en l'absence de la cible, l'Exo I réalise une digestion quasi-totale dans les conditions optimisées. La réalisation des tests d'interaction a montré une baisse de la digestion enzymatique pour l'aptamère GLY3, supposant ainsi sa potentielle interaction avec le glyphosate. Après avoir réalisé plusieurs études de vérification et d'avoir répondu à plusieurs hypothèses, il s'est avéré que le glyphosate inhibe potentiellement l'activité de l'Exo I dans des conditions bien particulières, et aucun des trois aptamères n'a montré une interaction envers le glyphosate. Les résultats d'inhibition d'Exo I, suggérés par nos résultats, ont été exploités afin de développer un biocapteur de fluorescence basé sur l'inhibition enzymatique. Ce dernier a permis une détection simple, rapide et spécifique du glyphosate dans une gamme linéaire entre 16,9 et 84,5 mg L^{-1}.

Ce travail a été publié sur le journal *Macromolecular Bioscience* (21 février 2023).

Summary

This chapter presents an in-depth study conducted to identify an aptamer exhibiting specific interaction with glyphosate for potential use on an electrochemical platform for this pesticide detection. In this context, three candidate aptamers, GLY1, GLY2, and GLY3, were identified in the literature. Their interaction with glyphosate was evaluated using an enzymatic digestion method followed by fluorescence spectroscopy. This method, as described in the literature, employs exonuclease I, an enzyme that digests single-stranded oligonucleotides in the 3' to 5' direction. Using a fluorescence probe, SYBR Gold, the percentage of digestion is quantitatively measured. In the presence of the target, an aptamer/target complex is formed, thus retarding the digestion of Exo I. However, in the absence of the target, Exo I undergoes nearly complete digestion under optimized conditions. Interaction tests revealed a reduced enzymatic digestion with the GLY3 aptamer candidate, suggesting its potential interaction with glyphosate. After conducting multiple verification studies and addressing several hypotheses, it was found that glyphosate potentially inhibits the activity of Exo I under particular conditions, and none of the three aptamers exhibited interaction with glyphosate. The results of Exo I inhibition, as obtained with our research, were then exploited to develop a fluorescence biosensor based on enzymatic inhibition. This biosensor enabled simple, rapid, and specific detection of glyphosate in water within a linear range of 16,9 to 84,5 mg L^{-1}.

This work was published in the journal of Macromolecular Bioscience (21 February 2023).

Table of Contents

Chapter II. Glyphosate-exonuclease interactions: reduced enzymatic activity as a route to glyphosate biosensing

*Mohamed Amine Berkal, Quentin Palas, Estelle Ricard, Christine Lartigau-Dagron, Luisa Ronga, Jean-Jacques Toulmé, Corinne Parat, Corinne Nardin**

M. A. Berkal, Q. Palas, E. Ricard, C. Lartigau-Dagron, L. Ronga, C. Parat, C. Nardin
Université de Pau et des Pays de l'Adour, E2S UPPA, CNRS, IPREM, Pau, France

E-mail: corinne.nardin@univ-pau.fr

J. J. Toulmé
ARNA Laboratory, Inserm U1212, CNRS UMR5320, University of Bordeaux, 33076 Bordeaux, France
Novaptech, 146 rue Léo Saignat, 33076 Bordeaux, France

Keywords: Glyphosate, oligonucleotide switching structures, enzymatic inhibition, fluorescence spectroscopy, biosensing

ABSTRACT: N-phosphonomethyle-glycine (glyphosate) is the most widely used pesticide worldwide due to its effectiveness in killing weeds at a moderate cost, bringing significant economic benefits. However, owing to its massive use, glyphosate and its residues contaminate surface waters. On-site, fast monitoring of contamination is therefore urgently needed to alert local authorities and raise population awareness. We report here the hindrance of the activity of two enzymes, the exonuclease I (Exo I) and the T5 exonuclease (T5 Exo) by glyphosate. These two enzymes digest oligonucleotides into shorter sequences, down to single nucleotides. The presence of glyphosate in the reaction medium hampers the activity of both enzymes, slowing down enzymatic digestion. We show by fluorescence spectroscopy that the inhibition of Exo I enzymatic activity is specific to glyphosate, paving the way for the development of a biosensor to detect this pollutant in drinking water at suitable detection limits, i.e. 0.1 µg L^{-1}.

I. INTRODUCTION

Pesticides and herbicides are essential to agriculture to increase crop yields and to provide sufficient food. Since their launch in the last century, they enabled substantial economic benefits and are thus widely used[1]. Organophosphates are particularly used worldwide since they target a wide variety of pests and weeds, enhancing agricultural production[2]. N-phosphonomethyle-glycine (glyphosate) is the most widely used organophosphorus pesticide due to its efficiency in killing weeds. It was introduced by Monsanto in 1970 under the name Roundup[3]. Glyphosate inhibits the 5-enolpyruvylshikimate-3-phosphate synthase enzyme (EPSPS), which is responsible for the biosynthesis of aromatic amino acids, causing cessation of growth and plant death[4]. Due to its high solubility in water, glyphosate residues accumulate in surface waters causing serious problems in the environment and human health, e. g. the irreversible inhibition of the activity of the acetylcholinesterase enzyme has detrimental effects on the central nervous system[5]. Besides, several studies demonstrated that glyphosate could affect cell cycle regulation, inhibit steroid hormone secretion in men, and also cause effects adverse to animals and aquatic vegetation[6,7]. The carcinogenicity of glyphosate remains however under debate. An International Agency for Research on Cancer (IARC) report in 2015 classified glyphosate in category 2A, i.e. "probably carcinogenic for humans"[8]. Two years later (2017), the European Food Safety Authority (EFSA) published a report concluding that glyphosate is not likely to be carcinogenic to humans[9]. Since glyphosate carcinogenicity remains to be confirmed, it is therefore regularly evaluated by national and international regulatory agencies. European Directive 98/83/EC set a maximum residue limit (MRL) for each pesticide in drinking water, including glyphosate, at 0.1 µg L^{-1} [10]. Furthermore, the tolerable daily intake (TDI) of glyphosate under chronic oral exposure and the acute reference dose is estimated at 0.5 mg kg^{-1} body weight per day[11]. Although the presence of glyphosate in different waters is already regulated, its low molecular weight, high polarity, and lack of fluorophore or chromophore groups rendered its detection difficult up to now[12,13].

The main means of analysis of glyphosate are therefore chromatographic methods coupled with mass spectrometry (MS), including high-pressure liquid chromatography (HPLC), ion exchange chromatography (IEC), ion chromatography (IC) and gas chromatography (GC)[14–16]. These conventional techniques are sensitive and highly specific, allowing trace analysis of pesticides in environmental samples. However, they require highly qualified operators. Besides that, samples need to be pre-treated and then analyzed in sophisticated off-site laboratories

offering these expensive techniques. This mode of detection is thus unsuitable for the survey of flowing waters. They require on-site analysis at a suitable frequency to detect a possible pollution peak to rapidly alert the authorities and population. Most of the technologies used for the detection of glyphosate require high-end throughput equipment and resources. None of them are adequate for field detection[12]. Increasing efforts are thus devoted to finding sensitive and selective alternative ways to detect glyphosate on-site. Biosensors, combining a biological sensing element and a transducer, are an appealing alternative to conventional laboratory-based methods. Specificity and selectivity are ensured by the biological sensing elements, which could be antibodies, enzymes, aptamers or even cells[17], while sensitivity is provided by the transducer, which converts the biological interaction into an electrical signal allowing detection of the analyte.

The potential selectivity and sensitivity of optical and electrochemical-based biosensors make them attractive for the detection of pesticides[18–21]. Methods include absorption (UV-Vis) spectroscopy[22,23], fluorescence spectroscopy[24,25], photoluminescence assay[26,27] chemiluminescence assay[2829], surface-enhanced Raman scattering (SERS)[30,31], potentiometric sensing[32], impedence sensing[3334], and amperometry[3521]. Only a few of these biosensors developed to detect pesticides, have been applied to glyphosate (**Table II-S1**)[36–40]. Moreover, none had sensing elements suitable for the in-situ detection of glyphosate.

Our main objective is thus the identification of a suitable sensing element to develop in the future an electrochemical aptasensor.[41]. This biosensor would thus be composed of an aptamer sensing element and an electrochemical detection platform. Aptamers are oligonucleotide switching structures that form a complex with the target, e.g. small organic molecules, proteins or even cells, with very high affinity and specificity[42,43]. The interaction between glyphosate and its aptamers described in the literature[39,44,45] was thus tested using enzymatic digestion by the T5 exonuclease (T5 Exo) and exonuclease I (Exo I)[46]. The activity of these enzymes is widely used to demonstrate the specific interaction between a ligand and an oligonucleotide switching structure[47–51]. The enzymes digest the aptamer into shorter oligonucleotides and/or mononucleotides. In the presence of the target, an aptamer/target complex is formed which leads to a decrease in enzymatic activity allowing detection of the interaction.

As reported below, we demonstrate the specific inhibition of Exo I and T5 Exo enzymatic activity in a specific buffer by glyphosate, with high potential for the development of an efficient and specific biosensor of glyphosate in the future.

II. Experimental Section

II.1. Chemicals and Reagents

All the chemicals and reagents were of analytical grade (> 99%) and used without further purification. Tris(hydroxymethyl)aminomethane (Tris-HCl), sodium chloride (NaCl), potassium chloride (KCl), hydrochloric acid (HCl), sodium hydroxide (NaOH), magnesium chloride hexahydrate ($MgCl_26H_2O$), calcium chloride tetrahydrate ($CaCl_24H_2O$), formamide, ethylenediaminetetraacetic acid (EDTA), glycerol and sodium dodecyl sulfate 4X (SDS) were purchased from Euromedex (Strasbourg, France). Ethanol (EtOH), magnesium acetate, sodium acetate, potassium acetate, tris(hydroxymethyl)aminomethane, boric acid, EDTA, tris(hydroxymethyl)aminomethane and boric acid (TBE), urea and tetramethyl ethylenediamine (TEMED) were purchased from VWR Chemicals (Radnor, Pennsylvania, USA). Glyphosate, aminomethylphosphonic acid (AMPA), atrazine, xylene cyanol and ammonium persulfate (APS) were purchased from Sigma Aldrich (St. Louis, MO, USA). SYBR Gold was purchased from Invitrogen (Thermo Fischer Scientific, Waltham, Massachusetts, USA). 4-(2-hydroxyethyl)-1-piperazine ethane sulfonic acid (HEPES) was purchased from Pan Reac Application (ITW Reagents, Castellar del Vallès, Spain). Exo I (20000 U mL^{-1}) and T5 Exo (10000 U mL^{-1}) were purchased from New England Biolabs (Ipswich, Massachusetts, USA).

II.2. Oligonucleotides

All oligonucleotides used in this work were synthesized by Eurogentec (Seraing, Belgium) with polyacrylamide gel electrophoresis (PAGE) purification grade. The oligonucleotides were dissolved in MilliQ water and the concentrations were measured by UV-Vis spectroscopy using the Nanodrop 2000 spectrometer (Mettler Toledo, Columbus, Ohio, USA). The sequences of the glyphosate aptamer candidates are listed in **Table II-1**.

Table II-1. Sequences of glyphosate aptamer candidates.

Aptamer name	Sequence
GLY1 aptamer[39]	5'-AGC-TTG-CTG-CAG-CGA-TTC-TTG-ATC-GCC-ACA-GAG-CT-3'
GLY2 aptamer[44]	5'-CGT-ACG-GAA-TTC-GCT-AGC-AGA-GGG-ATG-GTG-TGG-GTG-GCT-GCG-GCT-ATA-GGA-GCG-TAC-CGGATC-CGA-GCT-CCA-CGT-G-3'
GLY3 aptamer[45]	5'-TGC-TAG-ACG-ATA-TTC-GTC-CAT-CCG-AGC-CCG-TGG-CGG-GCT-TTA-GGA-CTC-TGC-GGG-CTT-CGCGGC-GCT-GTC-AGA-CTG-AAT-ATG-TCA-3'

II.3. Design of Negative Controls (DNA Oligonucleotides)

To assess the specificity of interaction of the GLY2 and GLY3 aptamer candidates towards glyphosate, two DNA oligonucleotide negative controls, scrambled GLY2 and scramble GLY3 (SCR GLY2, SCR GLY3), were designed and used with the same buffers as GLY2 and GLY3. Two aptamers developed against atrazine, ATZ1[52] and ATZ2[53], the thrombin aptamer[54], the arsenic aptamer[55], ssDNA, and the AA40 library sequences (which contains about 10^{15} unique sequences) were also used as negative controls (**Table II-S2**).

II.4. Experimental Conditions

All incubations between glyphosate and its aptamer candidates, as well as enzymatic digestion, were performed using a thermomixer (Eppendorf, Hamburg, Germany).

Enzymatic digestion was performed at room temperature (~20 °C) and at 37 °C with stirring (240 rpm). In each experiment, the buffers described in **Table II-S3** were used with their corresponding aptamer. All experiments were done in duplicate or triplicate. The standard deviations are presented in the form of error bars. The pH of all buffers was measured with a Seveneasy pH meter (Mettler Toledo, Columbus, Ohio, USA) and was adjusted using either a 1 M NaOH solution or a 0.1 M HCl solution.

II.5. T5 Exonuclease Digestion and Gel Electrophoresis

The interaction between glyphosate and its aptamer candidates described in the literature was done by T5 Exo digestion prior to PAGE[46]. The T5 Exo enzyme digests double-stranded and single-stranded DNA sequences in the 5' to 3' direction, down to single nucleotides (**Figure II-S10**). The working principle of this method is described in **Figure II-S11**. Interaction

between the aptamer and its target results in delayed digestion of the oligonucleotide due to the formation of an aptamer/target complex impeding the enzymatic digestion[47–51].

For all digestion assays, 1 µL of a 25 µM aptamer solution is added to 22 µL of interaction buffer containing glyphosate at a final concentration of 0.169 g L^{-1}. After incubation between glyphosate and their aptamer candidates in the appropriate conditions (**Table II-S4**), 0.5 µL of the T5 Exo enzyme at 10 U μL^{-1} is added to the reaction mixture (at a final concentration of 0.2 U μL^{-1}), and the digestion is started at room temperature under gentle stirring. After each digestion period, 5 µL of the reaction mixture are drawn off and added to 15 µL of loading buffer (75% formamide (v/v), 10% glycerol (v/v), 0. 125% SDS (v/v), 10 mM EDTA and a pinch of xylene cyanol) and then loaded into the wells of a previously prepared denaturing polyacrylamide gel plate (final gel concentration = 15%, see preparation in electronic supplementary information ESI). The samples are separated by gel migration using an EPS-300X electric generator (CBS, Paris, France), under the following conditions: applied voltage U = 750 V, intensity I = 300 mA, power P = 20 W and 1 h10 min of migration time.

The gel plate is dismantled and the polyacrylamide gel is immersed in 100 mL of 0.5X TBE containing 1X SYBR Gold, which is an intercalator binding to DNA by insertion between the DNA bases[56] (the absorption spectrum of SYBR Gold as well as calculations of its molar concentration are shown in **Figure II-S12** and **Table II-S5** respectively). The whole set is incubated for 25 min in the dark under gentle stirring (18 rpm) on a horizontal incubator (See-saw rocker, Stuart-equipment, Waltham, Massachusetts, USA). After incubation, the gel fluorescence is visualized with G-Box (SYNGENE, Synoptics, Cambridge, UK).

II.6. Fluorescence Spectroscopy

To achieve a fast, quantitative analysis of the interaction between potential aptamer candidates and glyphosate, a second enzyme, exonuclease I, is combined with T5 Exo, and the analysis is done by measuring the fluorescence intensity of SYBR Gold. The activity of Exo I is indeed complementary to that of the T5 Exo as it digests single-stranded DNA into mononucleotides in the opposite direction to T5 Exo (from 3' to 5', **Figure II-S13**). In addition, it digests the products of T5 Exo enzymatic digestion, which accelerates the process. Protection of the aptamer by its target thus translates into a higher fluorescence intensity of SYBR gold than without. Fluorescence intensity is converted to the digestion yield via **Equation II-1**. The yield of digestion is lower when the target protects its aptamer (**Figure II-1**).

$$\%\ of\ digestion = \frac{(F_0 - F)}{F_0} \times 100 \qquad \textbf{Equation II-1}$$

F_0: Fluorescence signal before digestion

F: Fluorescence signal after digestion

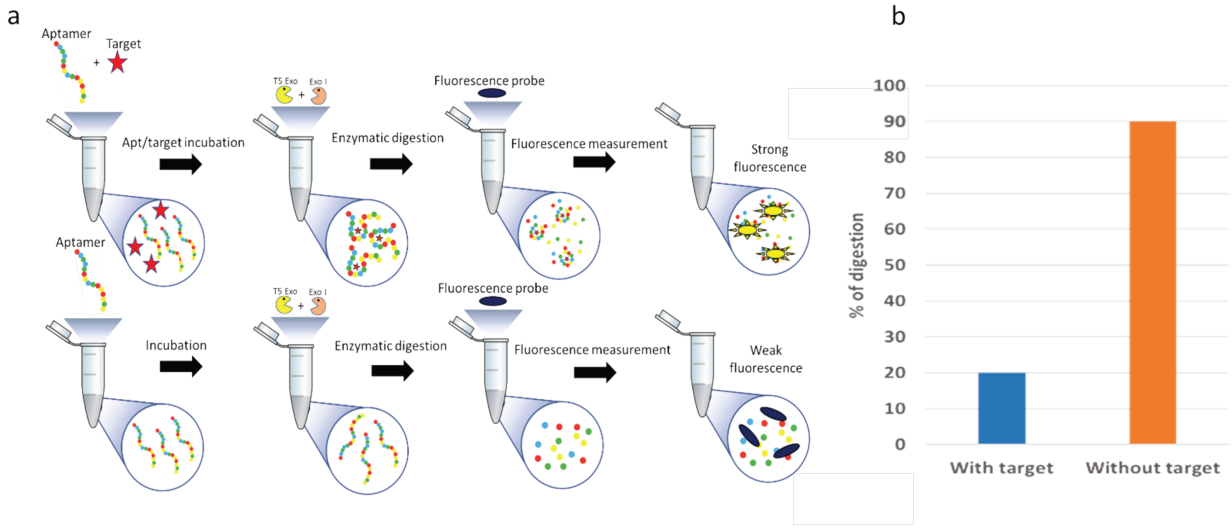

Figure II-1. (a) Principle of analyzing aptamer/target interaction by T5 Exo and Exo I digestion, followed by fluorescence spectroscopy. (b) The expected percentage of enzymatic digestion in the presence and the absence of the target.

We followed the protocol reported previously[46]. 1 µL of a 25 µM aptamer solution is added to 22 µL of interaction buffer containing glyphosate at a final concentration of 1 mM. After incubation between glyphosate and aptamer candidates in the appropriate conditions (**Table II-S4**), 1.5 µL of both T5 Exo and Exo I at a final concentration of 0.2 U μL^{-1} and 3.75 U μL^{-1} respectively were added to the reaction mixture, and the digestion started at 37 °C under gentle stirring. After each incubation period, 5 µL of the reaction mixture was drawn off and loaded into the wells of a black 384-well microplate (Corning black, Thermo Fischer Scientific) containing 25 µL of stop solution (1.2X SYBR Gold, 12 mM Tris-HCl pH = 7.4, 48% formamide (v/v), 3.75 mM EDTA). Fluorescence was measured at 545 nm (excitation at 495 nm) (Tecan Infinite M1000 Pro, Männedorf, Suisse).

III. Results and Discussion

III.1. Interaction of Aptamer Candidates with Glyphosate as Assessed by T5 Exo Enzymatic Digestion followed by Polyacrylamide Gel Electrophoresis (PAGE)

Conventional PAGE[46] subsequent to T5 Exo digestion was used to assess the interaction between glyphosate and its aptamer candidates. The interaction between glyphosate and potential aptamer candidates reported in the literature, GLY1[39], GLY2[44] and GLY3[45], was first tested. In parallel to the use of GLY2 and GLY3 glyphosate-specific aptamer candidates, two negative controls, SCR GLY2 and SCR GLY3, were designed in order to further validate the specificity of GLY2 and GLY3 against glyphosate. The main conformations of the aptamers and negative controls are shown in **Figure II-S1**. No negative control was designed for the GLY1 aptamer since it is specific not to glyphosate but to two other pesticides, i.e. trichlorfon and malathion[39]. The negative control sequences have the same number of nucleic acid bases and the same GC content as GLY2 and GLY3 but were designed with a random nucleic acid order resulting in a new conformation that prevents target recognition.

Reduced enzymatic activity in the presence of glyphosate was observed with the GLY1 and GLY3 candidates, as well as for the SCR GLY3 negative control (**Figure II-2**).

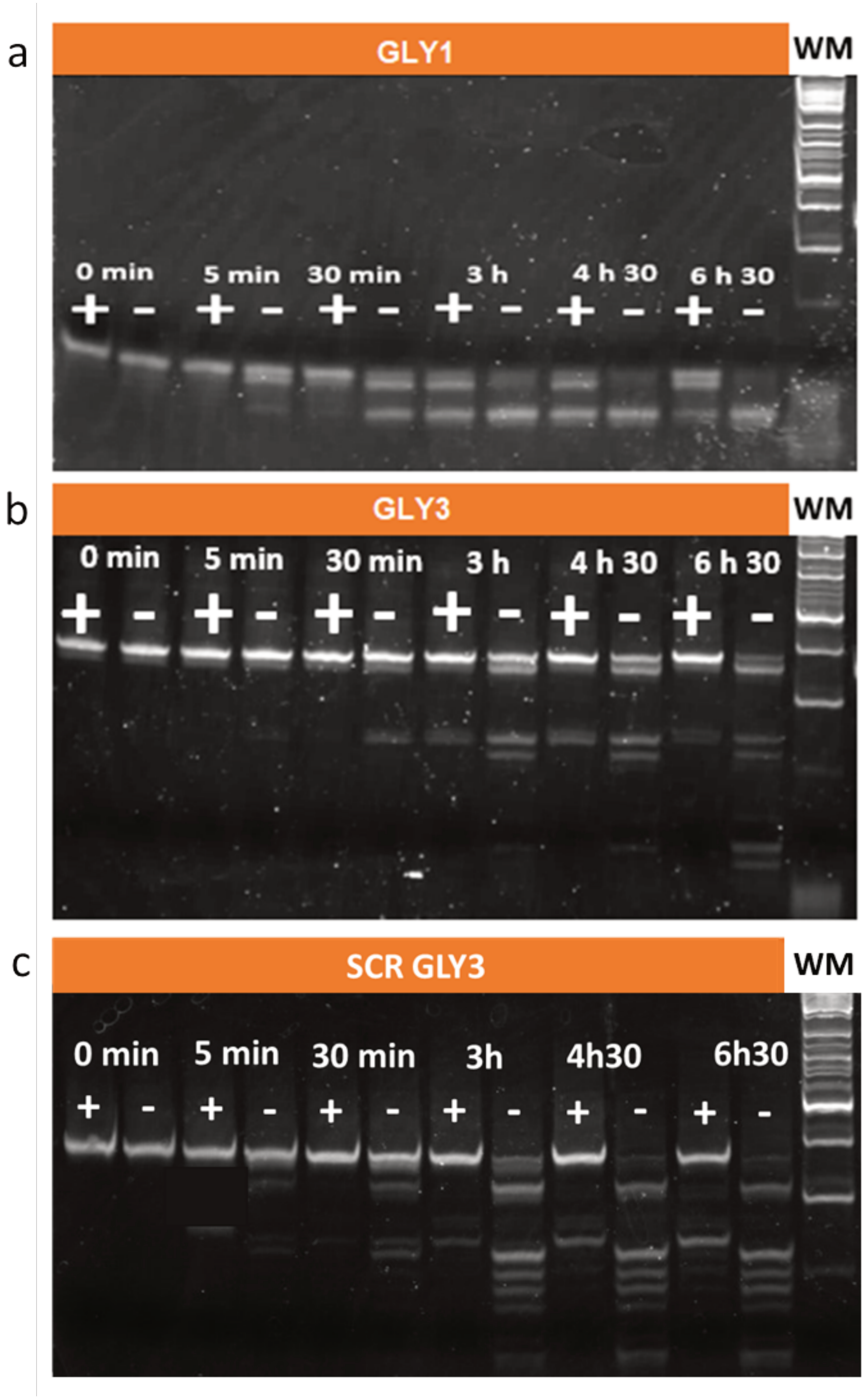

Figure II-2. Digestion of the GLY1 candidate (a), GLY3 candidate (b) and SCR GLY3 (c) at 1 µM each by T5 Exo (0.2 U/µL) at room temperature in GLY1 and GLY3 buffers, respectively, after 2 h incubation at 37°C with (+) or without (-) glyphosate (0.169 mg L^{-1}).

GLY2 and SCR GLY2 (**Figure II-S2**) yielded no reduction in enzymatic activity in the presence of glyphosate, throughout the digestion time tested. These results suggest that GLY1 and GLY3 are probably aptamers of glyphosate since a reduction in enzymatic activity is observed, potentially due to the formation of a complex between the aptamer and glyphosate,

whereas with this method GLY2 showed no interaction with glyphosate. As expected the SCR GLY2 negative control showed no interaction with glyphosate. However, the negative control SCR GLY3, which should not interact with glyphosate, showed the opposite. To conclude on a potential interaction between glyphosate and SCR GLY3, a rapid detection approach was thus needed to replace PAGE which is a tedious method as it requires several cumbersome steps, namely the preparation of the gel plate, the migration step, the disassembly of the gel plate, the staining step and finally reading of the fluorescence. In addition, enzymatic digestion by T5 Exo is relatively slow (complete digestion of SCR GLY3 is achieved in about ten hours or more, **Figure II-S3**) and doesn't allow quantification.

III.2. Quantitative Analysis of the Interaction between Glyphosate and its Aptamer Candidates as Assessed by Fluorescence Spectroscopy

In order to quantify the percentage of digestion and to shorten the analysis time, we resorted to fluorescence spectroscopy. Assays were carried out first with both GLY3 and SCR GLY3 which demonstrated a decrease in T5 Exo activity in the presence of glyphosate by PAGE. Different conditions of incubation and digestion were tested using both enzymes, T5 Exo and Exo I (**Figure II-S4**). The reduction of the enzymatic activity was confirmed with both GLY3 and SCR GLY3 regardless of the incubation time or the temperature of incubation and/or digestion tested. As expected, digestion at 37 °C is more efficient than digestion at room temperature[46,47,50,57]. Digestion at 37 °C with two hours of incubation between GLY3 or SCR GLY3 and glyphosate at 37 °C was thus selected as the reference condition for subsequent studies of interaction specificity as it provides the best digestion efficiency while enabling differentiation between the two conditions, i.e. with or without glyphosate.

In order to shorten the digestion time needed to exhibit enzymatic activity, the digestion kinetics of GLY1, GLY3 and SCR GLY3 were measured (**Figure II-S5**). Near-total digestion (in the absence of glyphosate) was achieved with all candidates in only 30 min, demonstrating the acceleration of enzymatic digestion when combining both enzymes. In what follows, we fix the digestion time to 30 min.

Figure II-3 shows the percentage of digestion obtained with GLY1, GLY3 and SCR GLY3, measured by fluorescence spectroscopy, in the presence or absence of glyphosate.

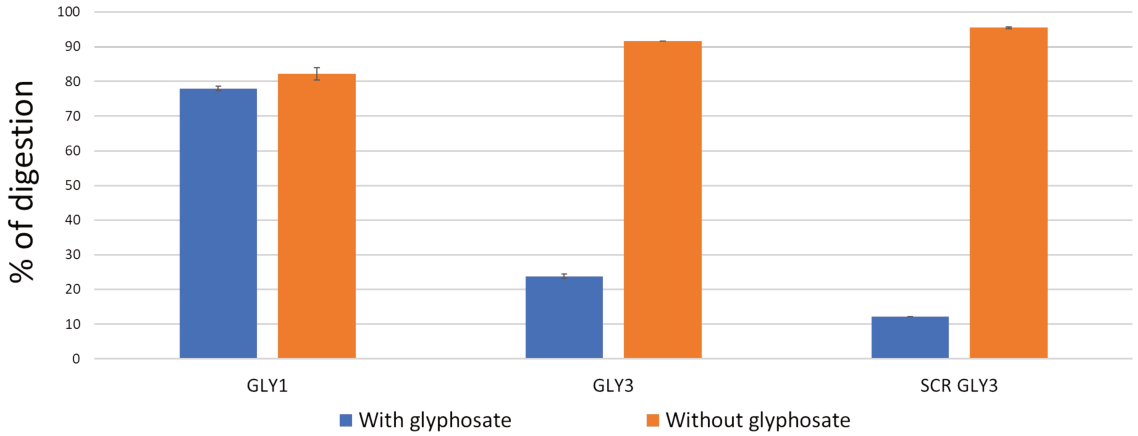

Figure II-3. Digestion of GLY1, GLY3 and SCR GLY3 at 1 µM by both enzymes, T5 Exo and Exo I, at 37 °C for 30 min, after 2 hours of incubation at 37 °C with or without glyphosate (0.169 mg L^{-1}) in GLY3 buffer.

Contrary to when PAGE was used, no decrease in the enzymatic activity of GLY1 was observed in the presence of glyphosate. This is explained by the fact that fluorescence spectroscopy measures the total fluorescence in a sample. However, it is the shortest sequence hence low fluorescence. GLY1 led to the same low fluorescence signal and thus to the same percentage of digestion even in the presence of glyphosate (78% and 82% of digestion, **Figure II-3**). On the contrary, with GLY3 and SCR GLY3, the fluorescence intensity after digestion in the presence of glyphosate is higher (24% vs. 12% digestion) than in its absence (92% vs. 95% digestion, **Figure II-3**) because they are protected against digestion.

As observed in **Figure II-3**, for both GLY3 and SCR GLY3 candidates, decreased enzymatic activity in the presence of glyphosate is observed. Similar to PAGE, fluorescence spectroscopy shows reduced activity of the negative control SCR GLY3 in the presence of glyphosate.

Glyphosate inhibits the activity of the enzyme 5-enolpyruvylshikimate-3-phosphate synthase (EPSPS),[4] and inhibition of both Exo I and T5 Exo enzymes activity cannot be ruled out. EPSPS synthase catalyzes the transfer of the carboxyvinyl portion of phosphoenolpyruvate (PEP) regiospecifically to the 5-OH of shikimate 3-phosphate (S3P), forming 5-enolpyruvoylshikimate 3-phosphate (EPSP) and inorganic phosphate[58] (**Figure II-S6a**). Glyphosate however mimics the PEP substrate of the enzyme (**Figure II-S6b**) which results in a stable complex of EPSPS.S3P.glyphosate leading to the inhibition of EPSPS[59–63]. A similar mechanism could be proposed to understand the inhibition of Exo I by glyphosate. ExoI breaks PEP phosphodiester bonds (**Figure II-S6c**)[64]. In the presence of glyphosate, a more stable complex of the enzyme with glyphosate instead of one with its substrate, i. e. oligonucleotides, might preferentially form leading to enzymatic inhibition.

Before concluding on the interaction between glyphosate and SCR GLY3, we however investigated the role of sequence composition and the buffer on the reduction of enzymatic activity by glyphosate.

I.1. Sequence Composition and Reduction of Enzymatic Activity in the Presence of Glyphosate

By definition, an aptamer is a unique sequence that recognizes a specific target. If SCR GLY3 is an aptamer specific to glyphosate, it must be unique and none of the sequences selected for this assay should interact with glyphosate.

Several oligonucleotides were therefore tested in the same conditions of digestion as GLY3 and SCR GLY3, namely GLY1 and GLY2, the AA40 library (which contains about 10^{15} unique sequences), and ATZ1[52], ATZ2[53] which are aptamers developed against atrazine (**Figure II-4**).

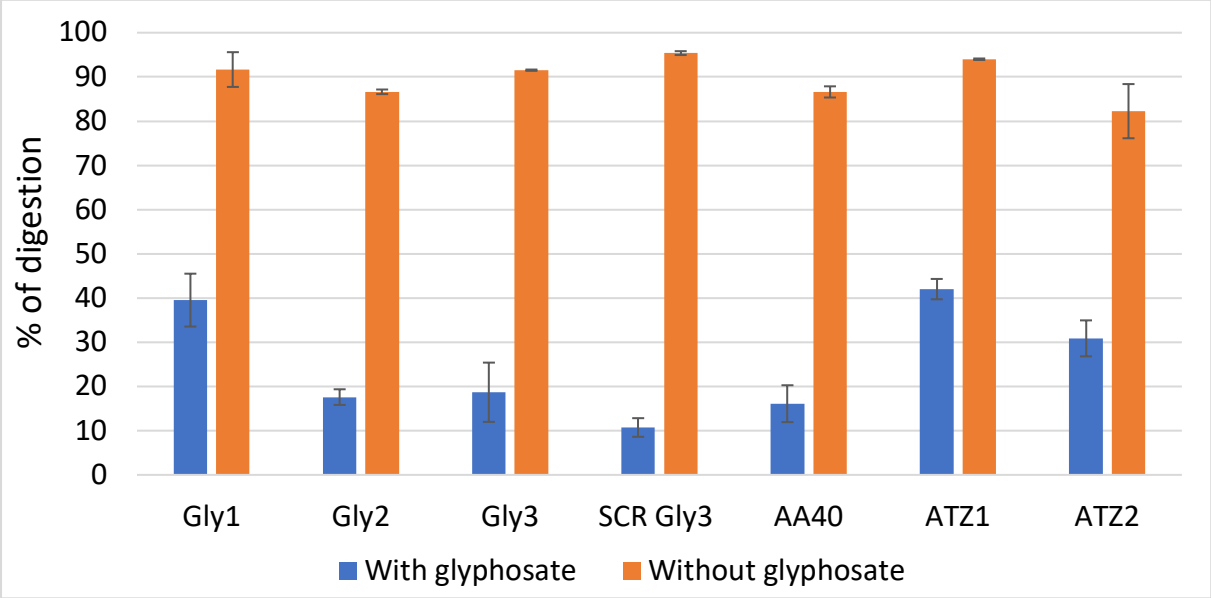

Figure II-4. Digestion of different oligonucleotides at 1 µM by both enzymes, T5 Exo and Exo I, at 37 °C for 30 min after 2 hours of incubation at 37 °C with or without glyphosate (0.169 mg L^{-1}) in GLY3 buffer.

Decreased enzymatic activity in the presence of glyphosate is found with all these oligonucleotides tested but before concluding non-specificity, we should check if reduced activity is related to the GLY3 buffer or to enzyme inhibition by glyphosate.

I.2. Role of the GLY3 Interaction Buffer in the Reduction of Enzymatic Activity

We, therefore, assessed the role of the GLY3 interaction buffer in enzymatic inhibition by the digestion of both the GLY3 and the AA40 library sequences in the HEPES buffer, which is used frequently in the development of aptamers at Novaptech (**Figure II-S7**).

Neither showed a reduction of enzymatic activity in the presence of glyphosate, and both enzymes are active in the HEPES buffer (90 % digestion). These results clearly confirm that the GLY3 interaction buffer is crucial to the reduction of enzymatic activity.

Although it contains few divalent cations (1 mM of Mg^{2+}) it is essential to enzymatic activity. Indeed, as reported earlier, Mg^{2+} concentrations as low as 10^{-2} to 10^{-3} mM reduce the activity of Exo I by 10 to 20%[65]. Besides, according to the literature, glyphosate has a chelating effect strongly complexing divalent cations, including Mg^{2+}[66]. Thus 1 mM of Mg^{2+} could be complexed by 1 mM of glyphosate and reduce enzymatic activity. To rule out this effect, GLY3 was digested in its buffer with or without glyphosate, but with an excess of Mg^{2+} cations, i.e. 5 mM (instead of 1 mM) (**Figure II-S8**). Enzymatic activity was nevertheless reduced implying that enzymatic inhibition is not related to the cation concentration.

To rule out the effect of monovalent cations (K^+ and Na^+) on enzymatic activity, different concentration ratios were tested in the GLY3 buffer in the same conditions of digestion (**Figure II-S9a**). The first is the same as in which enzymatic activity is not reduced. The same test was performed with the HEPES buffer (**Figure II-S9b**).

Thus, monovalent cations do not significantly affect enzymatic digestion. It is rather the Tris buffer component, contrary to HEPES, which plays the main role in the reduction of enzymatic activity.

I.3. Glyphosate as an Inhibitor of Enzymatic Activity

We probed separately the inhibition of either Exo I and T5 Exo by the digestion of a random sequence, SUP000, of comparable length to GLY3 (81 nucleotides *vs.* 84 nucleotides), in GLY3 and HEPES buffers, but without the incubation step of SUP000 with glyphosate. The enzymes were tested separately in order to evaluate their individual behavior in the two buffers.

Being a random sequence, SUP000 is not expected to interact with glyphosate. Therefore, each enzyme solution was prepared with and without glyphosate and the SUP000 sequence was added at the last stage. The whole set was incubated for 30 min at 37 °C.

As observed in **Figure II-5**, and in the HEPES buffer, neither enzyme reduces activity in the HEPES buffer, with or without glyphosate. In the GLY3 buffer, T5 Exo is already inhibited (20% digestion without glyphosate) compared to the HEPES buffer (90% digestion without glyphosate). Exo I is active in both buffers. However, this test clearly shows that the presence of glyphosate in the GLY3 buffer potentially inhibits the activity of Exo I.

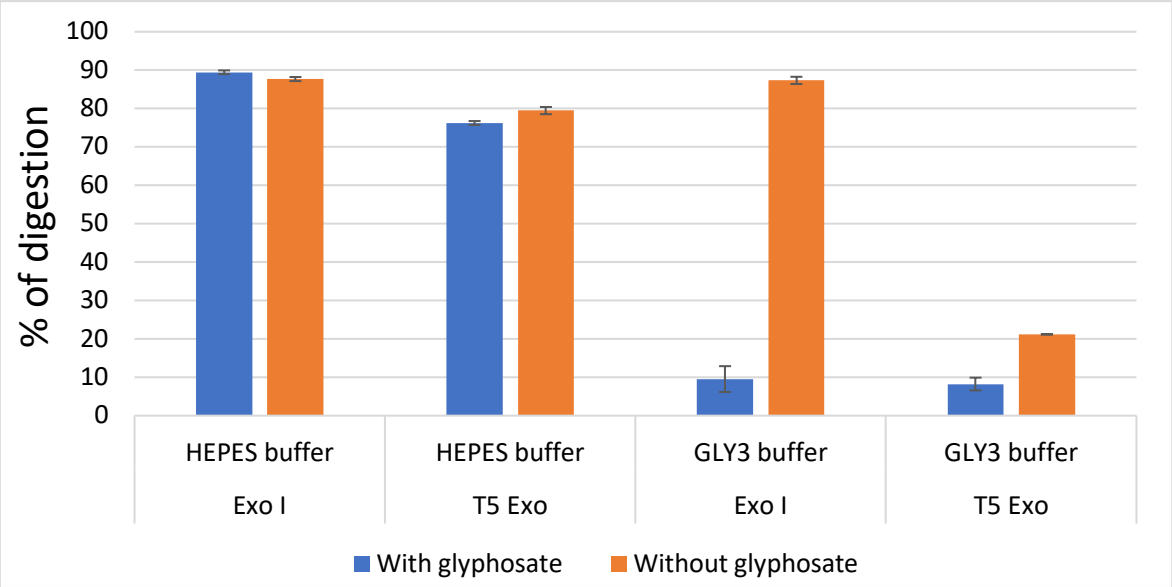

Figure II-5. Digestion of SUP000 (1 µM) by Exo I and T5 Exo, for 30 min at 37 °C in HEPES and GLY3 buffers with and without glyphosate (0.169 mg L^{-1}).

I.4. Specificity of the Reduction of the Enzymatic Activity

Since its activity is inhibited in the GLY3 buffer, the expected enhancement of digestion by T5 Exo is ruled out and therefore its use is discarded from studies reported below. Is the reduction of enzymatic activity specific to glyphosate? Other pesticide molecules having similar weight and structure, especially the main metabolite of glyphosate, AMPA, were tested using SUP000 as the substrate for Exo I: simazine, alachlor, atrazine, isoproturon, and atrazine-desethyl (**Figure II-6**).

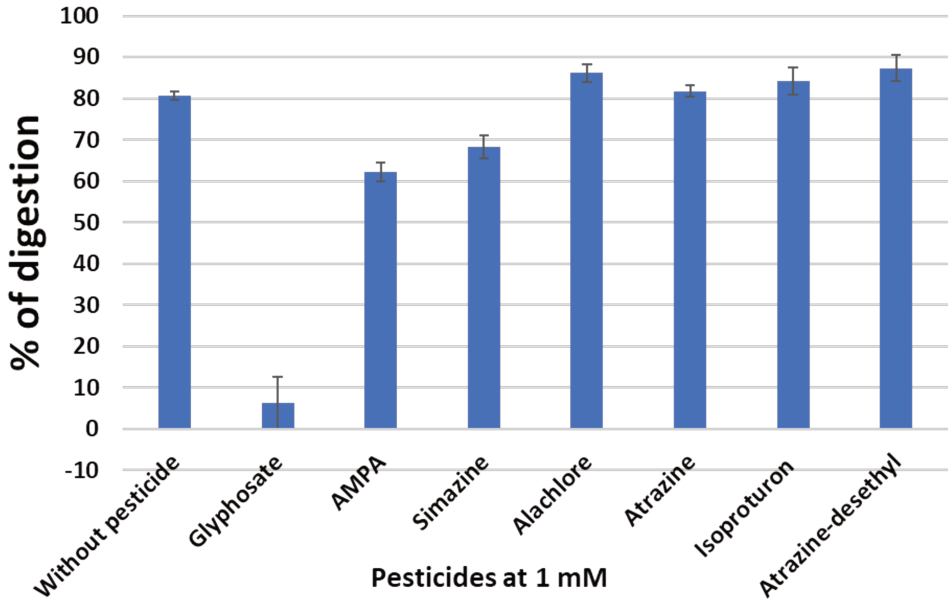

Figure II-6. Digestion of SUP000 at 1 µM by Exo I (0.15 U µL-1) at 37 °C for 30 min in GLY3 buffer in the absence or the presence of different pesticide molecules at 1 mM.

Slight inhibition is observed in the presence of AMPA and simazine, (62% and 68% digestion compared to 80% without pesticide). But only glyphosate induces strong inhibition (≈ 6% of digestion), which means that inhibition is specific to glyphosate.

II. Conclusion

Here we show that glyphosate inhibits the T5 Exo and Exo I, as quantified by fluorescence spectroscopy. Identification of this oligonucleotide digesting enzyme sensing element paves the way to the future development of a biosensor since the activity is specifically inhibited by glyphosate. The outcomes of this study are of high relevance since exonucleases are human enzymes, especially the Exo I enzyme that is required for 5' and 3' mismatch repair in human[67], further demonstrating that the mechanisms, consequences and danger to human health of this pesticide should be urgently elucidated.

In conclusion, the culmination of this study brings to light a strategic shift driven by the unavailability of an aptamer showcasing a specific interaction with glyphosate. This redirection led us to an alternative pesticide target, namely thiabendazole, for which a dedicated aptamer known as BOL009 has been meticulously developed. Sourced from Novaptech, an esteemed company in aptamer development, BOL009 serves as a molecular recognition element having the capacity to interact specifically with thiabendazole.

This transition opens new avenues, guiding our focus towards a goal of profound significance: the integration of BOL009 onto an engineered electrochemical platform. By seamlessly merging this aptamer with cutting-edge electrochemical technology, we aim to develop an innovative electrochemical aptasensor – a powerful analytical instrument designed for the specific and, if attainable, sensitive detection of thiabendazole within water matrices.

The subsequent chapter provides a comprehensive depiction of the distinct procedural phases employed to construct the electrochemical aptasensor. This includes the fabrication and validation of the electrochemical platform, the BOL009 grafting process, and finally the detection tests of thiabendazole.

Acknowledgements:

We acknowledge grants from the Université de Pau et de Pays de l'Adour through its project Energy and Environment Solutions supported by the Agence National pour la recherche (ANR OPE-2018-0020) and the Communauté d'agglomération de Pau Béarn Pyrénées (CDAPBP, OPE-2020-0032) and from the Région Nouvelle Aquitaine (CONV-2019-0227). R. Brown kindly read the revised manuscript.

III. References

(1) Cooper, J.; Dobson, H. The Benefits of Pesticides to Mankind and the Environment. *Crop Protection* **2007**, *26* (9), 1337–1348. https://doi.org/10.1016/j.cropro.2007.03.022.

(2) Kwong, T. C. Organophosphate Pesticides: Biochemistry and Clinical Toxicology. *Therapeutic Drug Monitoring* **2002**, *24* (1), 144–149.

(3) Benbrook, C. M. Trends in Glyphosate Herbicide Use in the United States and Globally. *Environmental Sciences Europe* **2016**, *28* (1), 3. https://doi.org/10.1186/s12302-016-0070-0.

(4) AMRHEIN, N.; J, S.; HC, S. THE MODE OF ACTION OF THE HERBICIDE GLYPHOSATE. *THE MODE OF ACTION OF THE HERBICIDE GLYPHOSATE* **1980**.

(5) Bera, M. K.; Mohapatra, S. Ultrasensitive Detection of Glyphosate through Effective Photoelectron Transfer between CdTe and Chitosan Derived Carbon Dot. *Colloids and Surfaces A: Physicochemical and Engineering Aspects* **2020**, *596*, 124710. https://doi.org/10.1016/j.colsurfa.2020.124710.

(6) Smith, N. J.; Martin, R. C.; St. Croix, R. G. Levels of the Herbicide Glyphosate in Well Water. *Bull. Environ. Contam. Toxicol.* **1996**, *57* (5), 759–765. https://doi.org/10.1007/s001289900254.

(7) Acquavella, J. F.; Alexander, B. H.; Mandel, J. S.; Gustin, C.; Baker, B.; Chapman, P.; Bleeke, M. Glyphosate Biomonitoring for Farmers and Their Families: Results from the Farm Family Exposure Study. *Environmental Health Perspectives* **2004**, *112* (3), 321–326. https://doi.org/10.1289/ehp.6667.

(8) Guyton, K. Z.; Loomis, D.; Grosse, Y.; El Ghissassi, F.; Benbrahim-Tallaa, L.; Guha, N.; Scoccianti, C.; Mattock, H.; Straif, K. Carcinogenicity of Tetrachlorvinphos, Parathion, Malathion, Diazinon, and Glyphosate. *The Lancet Oncology* **2015**, *16* (5), 490–491. https://doi.org/10.1016/S1470-2045(15)70134-8.

(9) Authority (EFSA), E. F. S. Peer Review of the Pesticide Risk Assessment of the Potential Endocrine Disrupting Properties of Glyphosate. *EFSA Journal* **2017**, *15* (9), e04979. https://doi.org/10.2903/j.efsa.2017.4979.

(10) European Parliament COUNCIL DIRECTIVE 98/83/EC, Official Journal. *Council Directive 98/83/EC on the quality of water intended for human consumption.* https://eur-lex.europa.eu/legal-content/EN/TXT/PDF/?uri=CELEX:01998L0083-20151027&from=EN (accessed 2022-11-14).

(11) Glyphosate : l'Anses fait le point sur les données de surveillance, ANSES Journal. *Glyphosate : l'Anses fait le point sur les données de surveillance | Anses - Agence nationale de sécurité sanitaire de l'alimentation, de l'environnement et du travail*.

(12) Valle, A. L.; Mello, F. C. C.; Alves-Balvedi, R. P.; Rodrigues, L. P.; Goulart, L. R. Glyphosate Detection: Methods, Needs and Challenges. *Environ Chem Lett* **2019**, *17* (1), 291–317. https://doi.org/10.1007/s10311-018-0789-5.

(13) Raina-Fulton, R. A Review of Methods for the Analysis of Orphan and Difficult Pesticides: Glyphosate, Glufosinate, Quaternary Ammonium and Phenoxy Acid Herbicides, and Dithiocarbamate and Phthalimide Fungicides. *Journal of AOAC INTERNATIONAL* **2014**, *97* (4), 965–977. https://doi.org/10.5740/jaoacint.SGERaina-Fulton.

(14) Marc, J.; Mulner-Lorillon, O.; Bellé, R. Glyphosate-Based Pesticides Affect Cell Cycle Regulation. *Biology of the Cell* **2004**, *96* (3), 245–249. https://doi.org/10.1016/j.biolcel.2003.11.010.

(15) Schönherr, J.; Schreiber, L. Interactions of Calcium Ions with Weakly Acidic Active Ingredients Slow Cuticular Penetration: A Case Study with Glyphosate. *J. Agric. Food Chem.* **2004**, *52* (21), 6546–6551. https://doi.org/10.1021/jf049500s.

(16) Arregui, M. C.; Lenardón, A.; Sanchez, D.; Maitre, M. I.; Scotta, R.; Enrique, S. Monitoring Glyphosate Residues in Transgenic Glyphosate-Resistant Soybean. *Pest Management Science* **2004**, *60* (2), 163–166. https://doi.org/10.1002/ps.775.

(17) Sharma, S. K.; Sehgal, N.; Kumar, A. Biomolecules for Development of Biosensors and Their Applications. *Current Applied Physics* **2003**, *3* (2–3), 307–316. https://doi.org/10.1016/S1567-1739(02)00219-5.

(18) Pang, S.; Yang, T.; He, L. Review of Surface Enhanced Raman Spectroscopic (SERS) Detection of Synthetic Chemical Pesticides. *TrAC Trends in Analytical Chemistry* **2016**, *85*, 73–82. https://doi.org/10.1016/j.trac.2016.06.017.

(19) Chen, N.; Liu, H.; Zhang, Y.; Zhou, Z.; Fan, W.; Yu, G.; Shen, Z.; Wu, A. A Colorimetric Sensor Based on Citrate-Stabilized AuNPs for Rapid Pesticide Residue Detection of Terbuthylazine and Dimethoate. *Sensors and Actuators B: Chemical* **2018**, *255*, 3093–3101. https://doi.org/10.1016/j.snb.2017.09.134.

(20) Luo, Q.; Yu, F.; Yang, F.; Yang, C.; Qiu, P.; Wang, X. A 3D-Printed Self-Propelled, Highly Sensitive Mini-Motor for Underwater Pesticide Detection. *Talanta* **2018**, *183*, 297–303. https://doi.org/10.1016/j.talanta.2018.02.059.

(21) Vinoth Kumar, J.; Karthik, R.; Chen, S.-M.; Natarajan, K.; Karuppiah, C.; Yang, C.-C.; Muthuraj, V. 3D Flower-Like Gadolinium Molybdate Catalyst for Efficient Detection and Degradation of Organophosphate Pesticide (Fenitrothion). *ACS Appl. Mater. Interfaces* **2018**, *10* (18), 15652–15664. https://doi.org/10.1021/acsami.8b00625.

(22) Abnous, K.; Danesh, N. M.; Ramezani, M.; Alibolandi, M.; Emrani, A. S.; Lavaee, P.; Taghdisi, S. M. A Colorimetric Gold Nanoparticle Aggregation Assay for Malathion Based on Target-Induced Hairpin Structure Assembly of Complementary Strands of Aptamer. *Microchim Acta* **2018**, *185* (4), 216. https://doi.org/10.1007/s00604-018-2752-3.

(23) Palanivelu, J.; Chidambaram, R. Acetylcholinesterase with Mesoporous Silica: Covalent Immobilization, Physiochemical Characterization, and Its Application in Food for Pesticide Detection. *Journal of Cellular Biochemistry* **2019**, *120* (6), 10777–10786. https://doi.org/10.1002/jcb.28369.

(24) Long, Q.; Li, H.; Zhang, Y.; Yao, S. Upconversion Nanoparticle-Based Fluorescence Resonance Energy Transfer Assay for Organophosphorus Pesticides. *Biosensors and Bioelectronics* **2015**, *68*, 168–174. https://doi.org/10.1016/j.bios.2014.12.046.

(25) Lin, B.; Yu, Y.; Li, R.; Cao, Y.; Guo, M. Turn-on Sensor for Quantification and Imaging of Acetamiprid Residues Based on Quantum Dots Functionalized with Aptamer. *Sensors and Actuators B: Chemical* **2016**, *229*, 100–109. https://doi.org/10.1016/j.snb.2016.01.114.

(26) Sahub, C.; Tuntulani, T.; Nhujak, T.; Tomapatanaget, B. Effective Biosensor Based on Graphene Quantum Dots via Enzymatic Reaction for Directly Photoluminescence Detection of Organophosphate Pesticide. *Sensors and Actuators B: Chemical* **2018**, *258*, 88–97. https://doi.org/10.1016/j.snb.2017.11.072.

(27) Zor, E.; Morales-Narváez, E.; Zamora-Gálvez, A.; Bingol, H.; Ersoz, M.; Merkoçi, A. Graphene Quantum Dots-Based Photoluminescent Sensor: A Multifunctional Composite for Pesticide Detection. *ACS Appl. Mater. Interfaces* **2015**, *7* (36), 20272–20279. https://doi.org/10.1021/acsami.5b05838.

(28) He, L.; Jiang, Z. W.; Li, W.; Li, C. M.; Huang, C. Z.; Li, Y. F. In Situ Synthesis of Gold Nanoparticles/Metal–Organic Gels Hybrids with Excellent Peroxidase-Like Activity for Sensitive Chemiluminescence Detection of Organophosphorus Pesticides. *ACS Appl. Mater. Interfaces* **2018**, *10* (34), 28868–28876. https://doi.org/10.1021/acsami.8b08768.

(29) Ouyang, H.; Tu, X.; Fu, Z.; Wang, W.; Fu, S.; Zhu, C.; Du, D.; Lin, Y. Colorimetric and Chemiluminescent Dual-Readout Immunochromatographic Assay for Detection of Pesticide Residues Utilizing g-C3N4/BiFeO3 Nanocomposites. *Biosensors and Bioelectronics* **2018**, *106*, 43–49. https://doi.org/10.1016/j.bios.2018.01.033.

(30) Liu, B.; Zhou, P.; Liu, X.; Sun, X.; Li, H.; Lin, M. Detection of Pesticides in Fruits by Surface-Enhanced Raman Spectroscopy Coupled with Gold Nanostructures. *Food Bioprocess Technol* **2013**, *6* (3), 710–718. https://doi.org/10.1007/s11947-011-0774-5.

(31) Mu, T.; Wang, S.; Li, T.; Wang, B.; Ma, X.; Huang, B.; Zhu, L.; Guo, J. Detection of Pesticide Residues Using Nano-SERS Chip and a Smartphone-Based Raman Sensor. *IEEE J. Select. Topics Quantum Electron.* **2019**, *25* (2), 1–6. https://doi.org/10.1109/JSTQE.2018.2869638.

(32) Anirudhan, T. S.; Alexander, S. Design and Fabrication of Molecularly Imprinted Polymer-Based Potentiometric Sensor from the Surface Modified Multiwalled Carbon Nanotube for the Determination of Lindane (γ-Hexachlorocyclohexane), an Organochlorine Pesticide. *Biosensors and Bioelectronics* **2015**, *64*, 586–593. https://doi.org/10.1016/j.bios.2014.09.074.

(33) Li, H.; Wang, Z.; Wu, B.; Liu, X.; Xue, Z.; Lu, X. Rapid and Sensitive Detection of Methyl-Parathion Pesticide with an Electropolymerized, Molecularly Imprinted Polymer Capacitive Sensor. *Electrochimica Acta* **2012**, *62*, 319–326. https://doi.org/10.1016/j.electacta.2011.12.035.

(34) Madianos, L.; Skotadis, E.; Tsekenis, G.; Patsiouras, L.; Tsigkourakos, M.; Tsoukalas, D. Impedimetric Nanoparticle Aptasensor for Selective and Label Free Pesticide Detection. *Microelectronic Engineering* **2017**, *189*, 39–45. https://doi.org/10.1016/j.mee.2017.12.016.

(35) Fan, L.; Zhang, C.; Yan, W.; Guo, Y.; Shuang, S.; Dong, C.; Bi, Y. Design of a Facile and Label-Free Electrochemical Aptasensor for Detection of Atrazine. *Talanta* **2019**, *201*, 156–164. https://doi.org/10.1016/j.talanta.2019.03.114.

(36) Vaghela, C.; Kulkarni, M.; Haram, S.; Aiyer, R.; Karve, M. A Novel Inhibition Based Biosensor Using Urease Nanoconjugate Entrapped Biocomposite Membrane for Potentiometric Glyphosate Detection. *International Journal of Biological Macromolecules* **2018**, *108*, 32–40. https://doi.org/10.1016/j.ijbiomac.2017.11.136.

(37) Bettazzi, F.; Romero Natale, A.; Torres, E.; Palchetti, I. Glyphosate Determination by Coupling an Immuno-Magnetic Assay with Electrochemical Sensors. *Sensors* **2018**, *18* (9), 2965. https://doi.org/10.3390/s18092965.

(38) Chen, F.; Li, G.; Liu, H.; Leung, C.-H.; Ma, D.-L. G-Quadruplex-Based Detection of Glyphosate in Complex Biological Systems by a Time-Resolved Luminescent Assay. *Sensors and Actuators B: Chemical* **2020**, *320*, 128393. https://doi.org/10.1016/j.snb.2020.128393.

(39) Jiang, M.; Chen, C.; He, J.; Zhang, H.; Xu, Z. Fluorescence Assay for Three Organophosphorus Pesticides in Agricultural Products Based on Magnetic-Assisted Fluorescence Labeling Aptamer Probe. *Food chemistry* **2020**, *307*, 125534-.

(40) Liu, D.-L.; Li, Y.; Sun, R.; Xu, J.-Y.; Chen, Y.; Sun, C.-Y. Colorimetric Detection of Organophosphorus Pesticides Based on the Broad-Spectrum Aptamer. *Journal of Nanoscience and Nanotechnology* **2020**, *20* (4), 2114–2121. https://doi.org/10.1166/jnn.2020.17358.

(41) Akki, S. U.; Werth, C. J. Critical Review: DNA Aptasensors, Are They Ready for Monitoring Organic Pollutants in Natural and Treated Water Sources? *Environ. Sci. Technol.* **2018**, *52* (16), 8989–9007. https://doi.org/10.1021/acs.est.8b00558.

(42) Ruscito, A.; McConnell, E. M.; Koudrina, A.; Velu, R.; Mattice, C.; Hunt, V.; McKeague, M.; DeRosa, M. C. In Vitro Selection and Characterization of DNA Aptamers to a Small Molecule Target. *Current Protocols in Chemical Biology* **2017**, *9* (4), 233–268. https://doi.org/10.1002/cpch.28.

(43) Wang, H.; Cheng, H.; Wang, J.; Xu, L.; Chen, H.; Pei, R. Selection and Characterization of DNA Aptamers for the Development of Light-up Biosensor to Detect Cd(II). *Talanta* **2016**, *154*, 498–503. https://doi.org/10.1016/j.talanta.2016.04.005.

(44) Dna aptamer binding to glyphosate with Specificity. Dna Aptamer Binding to Glyphosate with Specificity. 2011.

(45) Aptamer specifically bound with glyphosate and application. Aptamer Specifically Bound with Glyphosate and Application. 2015.

(46) Alkhamis, O.; Yang, W.; Farhana, R.; Yu, H.; Xiao, Y. Label-Free Profiling of DNA Aptamer-Small Molecule Binding Using T5 Exonuclease. *Nucleic Acids Research* **2020**, *48* (20), e120. https://doi.org/10.1093/nar/gkaa849.

(47) Zheng, D.; Zou, R.; Lou, X. Label-Free Fluorescent Detection of Ions, Proteins, and Small Molecules Using Structure-Switching Aptamers, SYBR Gold, and Exonuclease I. *Anal. Chem.* **2012**, *84* (8), 3554–3560. https://doi.org/10.1021/ac300690r.

(48) Lv, L.; Li, D.; Liu, R.; Cui, C.; Guo, Z. Label-Free Aptasensor for Ochratoxin A Detection Using SYBR Gold as a Probe. *Sensors and Actuators B: Chemical* **2017**, *246*, 647–652. https://doi.org/10.1016/j.snb.2017.02.143.

(49) Gao, X.; Qi, L.; Liu, K.; Meng, C.; Li, Y.; Yu, H.-Z. Exonuclease I-Assisted General Strategy to Convert Aptamer-Based Electrochemical Biosensors from "Signal-Off" to "Signal-On." *Anal. Chem.* **2020**, *92* (9), 6229–6234. https://doi.org/10.1021/acs.analchem.0c00005.

(50) Li, H.; Song, S.; Wen, M.; Bao, T.; Wu, Z.; Xiong, H.; Zhang, X.; Wen, W.; Wang, S. A Novel Label-Free Electrochemical Impedance Aptasensor for Highly Sensitive Detection of Human Interferon-Gamma Based on Target-Induced Exonuclease Inhibition. *Biosensors and Bioelectronics* **2019**, *142*, 111532. https://doi.org/10.1016/j.bios.2019.111532.

(51) Guo, Z.; Lv, L.; Cui, C.; Wang, Y.; Ji, S.; Fang, J.; Yuan, M.; Yu, H. Detection of Aflatoxin B 1 with a New Label-Free Fluorescent Aptasensor Based on Exonuclease I and SYBR Gold. *Analytical Methods* **2020**, *12* (22), 2928–2933. https://doi.org/10.1039/D0AY00967A.

(52) Williams, R. M.; Crihfield, C. L.; Gattu, S.; Holland, L. A.; Sooter, L. J. In Vitro Selection of a Single-Stranded DNA Molecular Recognition Element against Atrazine. *International Journal of Molecular Sciences* **2014**, *15* (8), 14332–14347. https://doi.org/10.3390/ijms150814332.

(53) Roueinfar, M.; Abraham, K. M.; Hong, K. L. In-Solution Molecular Recognition Comparison of Aptamers against the Herbicide Atrazine. *ACS Omega* **2019**, *4* (14), 16201–16208. https://doi.org/10.1021/acsomega.9b02414.

(54) Bock, L. C.; Griffin, L. C.; Latham, J. A.; Vermaas, E. H.; Toole, J. J. Selection of Single-Stranded DNA Molecules That Bind and Inhibit Human Thrombin. *Nature* **1992**, *355* (6360), 564–566. https://doi.org/10.1038/355564a0.

(55) Kim, M.; Um, H.-J.; Bang, S.; Lee, S.-H.; Oh, S.-J.; Han, J.-H.; Kim, K.-W.; Min, J.; Kim, Y.-H. Arsenic Removal from Vietnamese Groundwater Using the Arsenic-Binding DNA Aptamer. *Environ. Sci. Technol.* **2009**, *43* (24), 9335–9340. https://doi.org/10.1021/es902407g.

(56) Kolbeck, P. J.; Vanderlinden, W.; Gemmecker, G.; Gebhardt, C.; Lehmann, M.; Lak, A.; Nicolaus, T.; Cordes, T.; Lipfert, J. Molecular Structure, DNA Binding Mode, Photophysical Properties and Recommendations for Use of SYBR Gold. *Nucleic Acids Research* **2021**, *49* (9), 5143–5158. https://doi.org/10.1093/nar/gkab265.

(57) Canoura, J.; Yu, H.; Alkhamis, O.; Roncancio, D.; Farhana, R.; Xiao, Y. Accelerating Post-SELEX Aptamer Engineering Using Exonuclease Digestion. *J. Am. Chem. Soc.* **2021**, *143* (2), 805–816. https://doi.org/10.1021/jacs.0c09559.

(58) Sikorski, J. A.; Gruys, K. J. Understanding Glyphosate's Molecular Mode of Action with EPSP Synthase: Evidence Favoring an Allosteric Inhibitor Model. *Acc. Chem. Res.* **1997**, *30* (1), 2–8. https://doi.org/10.1021/ar950122.

(59) Boocock, M. R.; Coggins, J. R. Kinetics of 5-Enolpyruvylshikimate-3-Phosphate Synthase Inhibition by Glyphosate. *FEBS Letters* **1983**, *154* (1), 127–133. https://doi.org/10.1016/0014-5793(83)80888-6.

(60) Anderson, K. S.; Sikorski, J. A.; Johnson, K. A. *Evaluation of 5-enolpyruvoylshikimate-3-phosphate synthase substrate and inhibitor binding by stopped-flow and equilibrium fluorescence measurements*. ACS Publications. https://doi.org/10.1021/bi00405a032.

(61) Castellino, S.; Leo, G. C.; Sammons, R. D.; Sikorski, J. A. *Phosphorus-31, nitrogen-15, and carbon-13 and NMR of glyphosate: comparison of pH titrations to the herbicidal dead-end complex with 5-enolpyruvoylshikimate-3-phosphate synthase*. ACS Publications. https://doi.org/10.1021/bi00435a035.

(62) McDowell, L. M.; Klug, C. A.; Beusen, D. D.; Schaefer, J. Ligand Geometry of the Ternary Complex of 5-Enolpyruvylshikimate-3-Phosphate Synthase from Rotational-Echo Double-Resonance NMR. *Biochemistry* **1996**, *35* (17), 5395–5403. https://doi.org/10.1021/bi9529059.

(63) Ream, J. E.; Yuen, H. K.; Frazier, R. B.; Sikorski, J. A. *EPSP synthase: binding studies using isothermal titration microcalorimetry and equilibrium dialysis and their implications for ligand recognition and kinetic mechanism*. ACS Publications. https://doi.org/10.1021/bi00139a015.

(64) Lehman, I. R.; Nussbaum, A. L. The Deoxyribonucleases of Escherichia Coli: V. ON THE SPECIFICITY OF EXONUCLEASE I (PHOSPHODIESTERASE). *Journal of Biological Chemistry* **1964**, *239* (8), 2628–2636. https://doi.org/10.1016/S0021-9258(18)93898-6.

(65) Kushner, S. R.; Nagaishi, H.; Templin, A.; Clark, A. J. Genetic Recombination in Escherichia Coli: The Role of Exonuclease I. *PNAS* **1971**, *68* (4), 824–827. https://doi.org/10.1073/pnas.68.4.824.

(66) Mertens, M.; Höss, S.; Neumann, G.; Afzal, J.; Reichenbecher, W. Glyphosate, a Chelating Agent—Relevant for Ecological Risk Assessment? *Environ Sci Pollut Res Int* **2018**, *25* (6), 5298–5317. https://doi.org/10.1007/s11356-017-1080-1.

(67) Genschel, J.; Bazemore, L. R.; Modrich, P. Human Exonuclease I Is Required for 5′ and 3′ Mismatch Repair ∗. *Journal of Biological Chemistry* **2002**, *277* (15), 13302–13311. https://doi.org/10.1074/jbc.M111854200.

(68) Lee, H. U.; Shin, H. Y.; Lee, J. Y.; Song, Y. S.; Park, C.; Kim, S. W. Quantitative Detection of Glyphosate by Simultaneous Analysis of UV Spectroscopy and Fluorescence Using DNA-Labeled Gold Nanoparticles. *J. Agric. Food Chem.* **2010**, *58* (23), 12096–12100. https://doi.org/10.1021/jf102784t.

(69) Jiang, M.; Chen, C.; He, J.; Zhang, H.; Xu, Z. Fluorescence Assay for Three Organophosphorus Pesticides in Agricultural Products Based on Magnetic-Assisted Fluorescence Labeling Aptamer Probe. *Food Chemistry* **2020**, *307*, 125534. https://doi.org/10.1016/j.foodchem.2019.125534.

(70) Liu, Q.; Zhang, R.; Yu, B.; Liang, A.; Jiang, Z. A Highly Sensitive Gold Nanosol SERS Aptamer Assay for Glyphosate with a New COF Nanocatalytic Reaction of Glycol-

Au(III). *Sensors and Actuators B: Chemical* **2021**, *344*, 130288. https://doi.org/10.1016/j.snb.2021.130288.

(71) González-Martínez, M. Á.; Brun, E. M.; Puchades, R.; Maquieira, Á.; Ramsey, K.; Rubio, F. Glyphosate Immunosensor. Application for Water and Soil Analysis. *Anal. Chem.* **2005**, *77* (13), 4219–4227. https://doi.org/10.1021/ac048431d.

(72) Mir, M.; Vreeke, M.; Katakis, I. Different Strategies to Develop an Electrochemical Thrombin Aptasensor. *Electrochemistry Communications* **2006**, *8* (3), 505–511. https://doi.org/10.1016/j.elecom.2005.12.022.

Supporting Informations

Glyphosate -exonuclease interactions: reduced enzymatic activity as a route to glyphosate biosensing

Mohamed Amine Berkal[*]*, Quentin Palas, Estelle Ricard, Christine Lartigau-Dagron, Luisa Ronga, Jean-Jacques Toulmé, Corinne Parat, Corinne Nardin*[*]

M. A. Berkal, Q. Palas, E. Ricard, C. Lartigau-Dagron, L. Ronga, C. Parat, C. Nardin
Université de Pau et des Pays de l'Adour, E2S UPPA, CNRS, IPREM, Pau, France

E-mail: corinne.nardin@univ-pau.fr

J. J. Toulmé
ARNA Laboratory, Inserm U1212, CNRS UMR5320, University of Bordeaux, 33076 Bordeaux, France
Novaptech, 146 rue Léo Saignat, 33076 Bordeaux, France

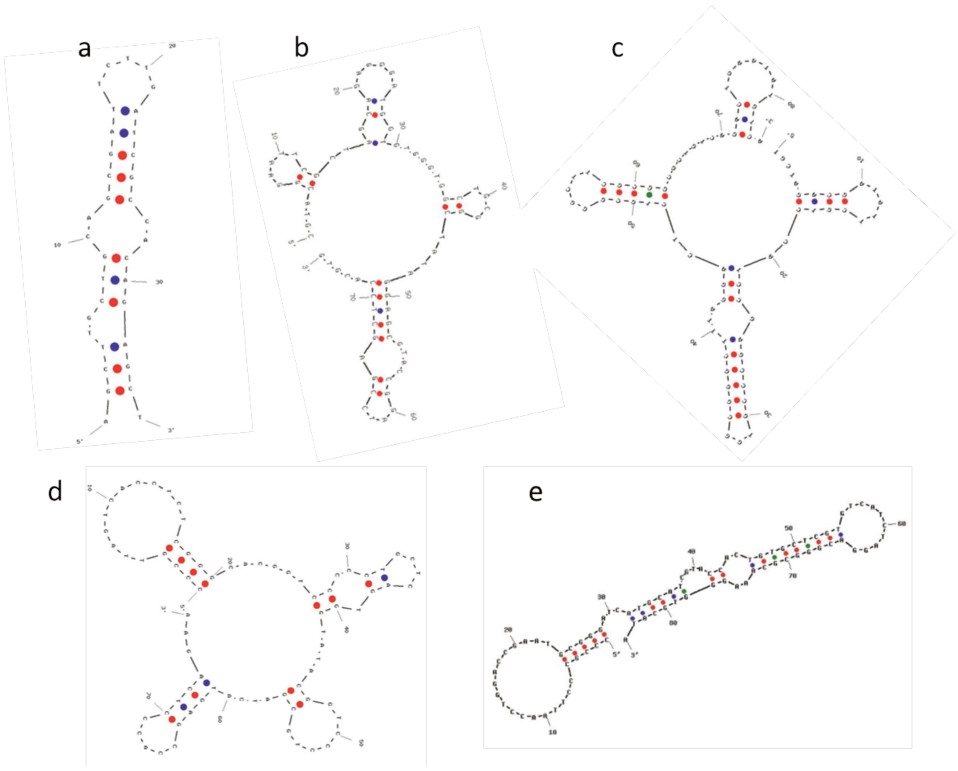

Figure II-S1. Conformations of (a) GLY1, (b) GLY2, (c) GLY3, (d) SCR GLY2 and (e) SCR GLY3 in their specific interaction buffer (Integrated DNA Technologies website).

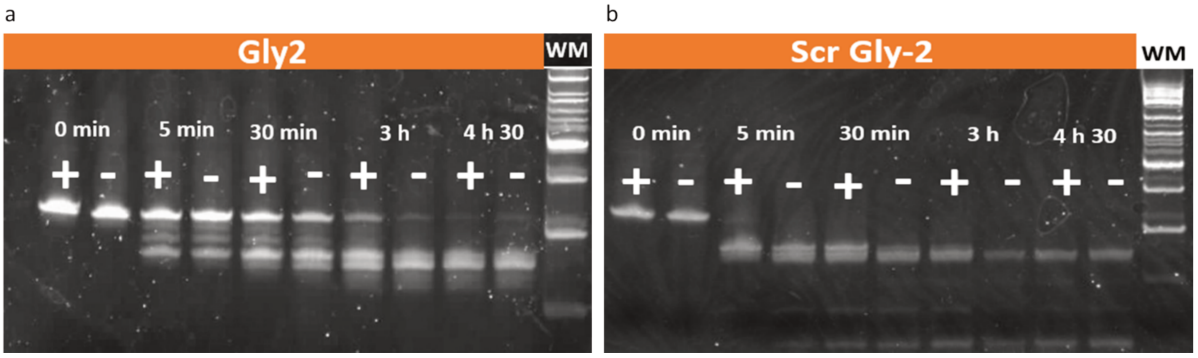

Figure II-S2. Digestion of (a) candidate GLY2 and (b) SCR GLY2 at 1 µM by T5 Exo (0.2 U µL^{-1}) at room temperature in GLY2 buffer after incubation for 30 min at room temperature with (+) or without (-) glyphosate (0.169 mg L^{-1}).

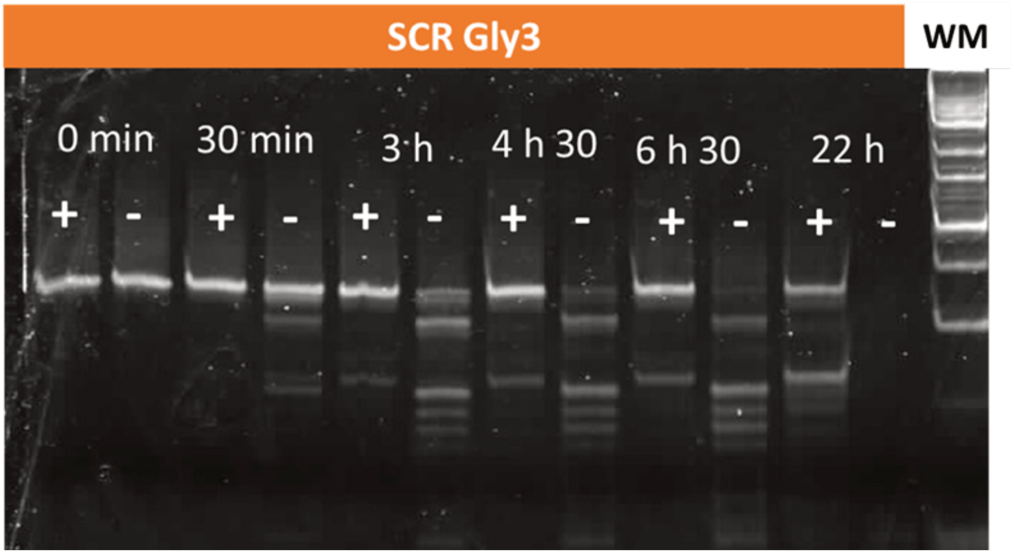

Figure II-S3. Digestion of SCR GLY3 at 1 µM by T5 Exo (0.2 U µL^{-1}) at room temperature in GLY3 buffer after incubation for 2 hours at 37 °C at room temperature with (+) or without (-) glyphosate (0.169 mg L^{-1}).

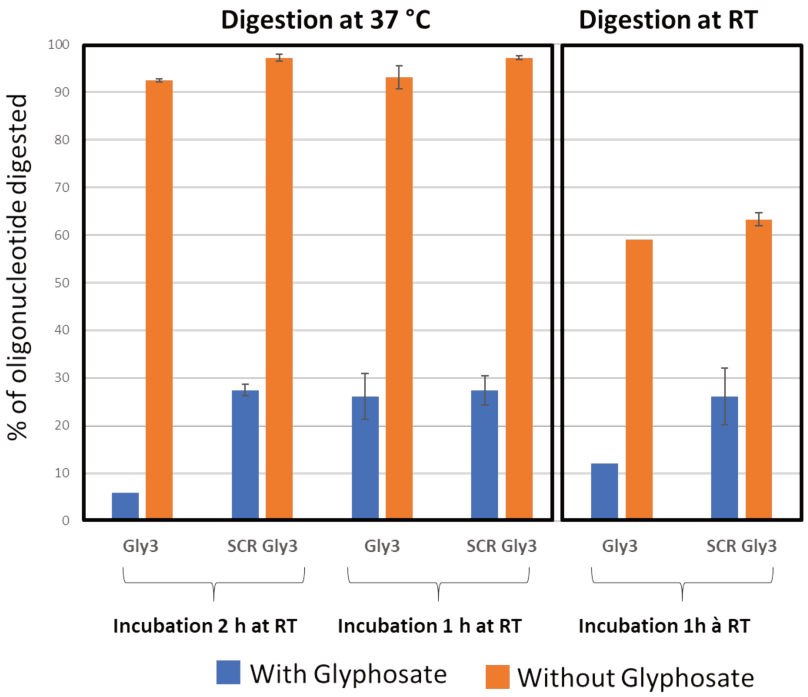

Figure II-S4. Digestion of GLY3 and SCR GLY3 (1 µM each) by both enzymes, T5 Exo and Exo I, in GLY3 buffer with or without glyphosate (0.169 mg L^{-1}) and at different conditions of incubation and digestion.

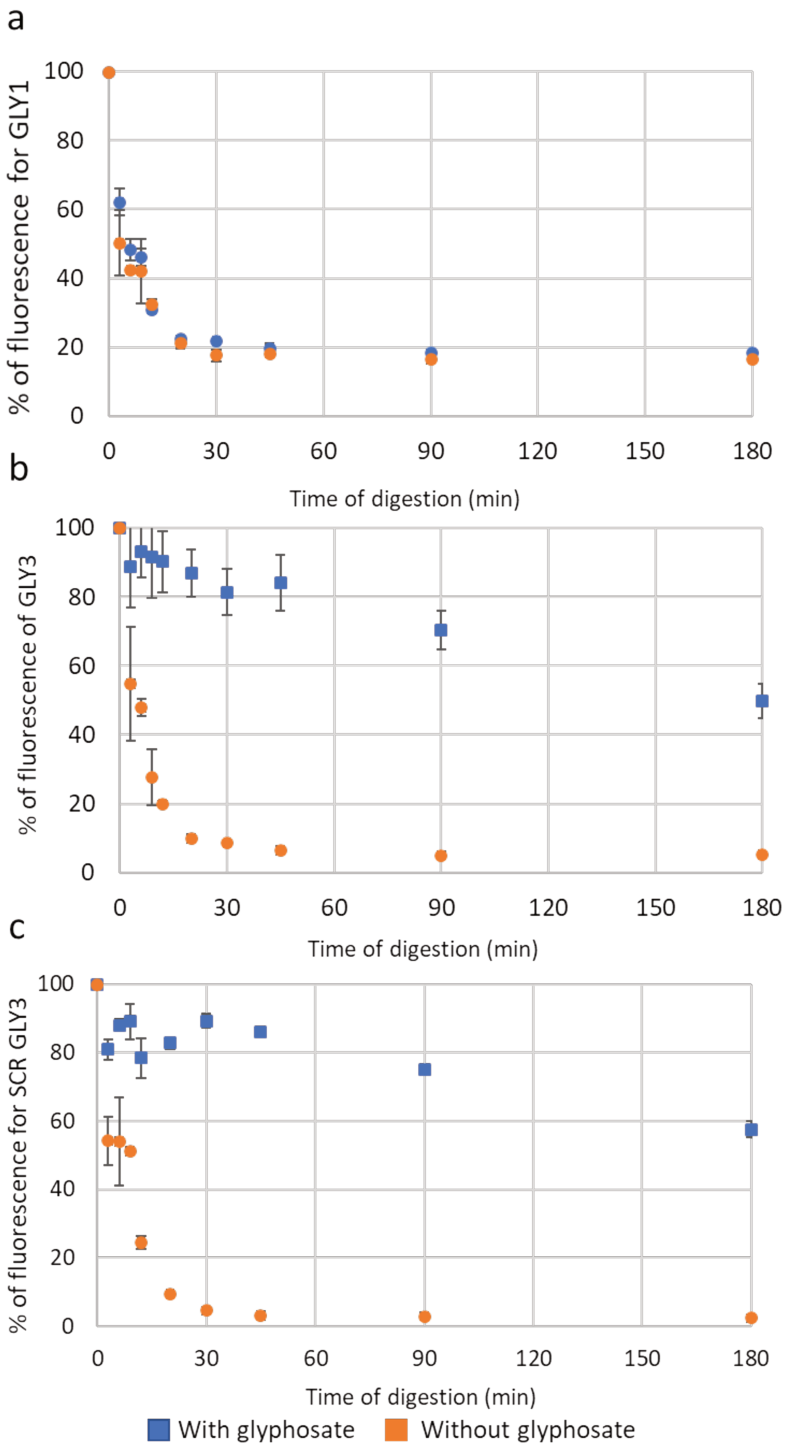

Figure II-S5. Digestion kinetics of GLY1 candidate (a), GLY3 candidate (b), and the SCR GLY3 (c), at 1 µM each by the two enzymes, T5 Exo and Exo I, at 37 °C in GLY1 and GLY3 buffers successively after 2 hours of incubation at 37 °C with or without glyphosate (0.169 mg L^{-1}).

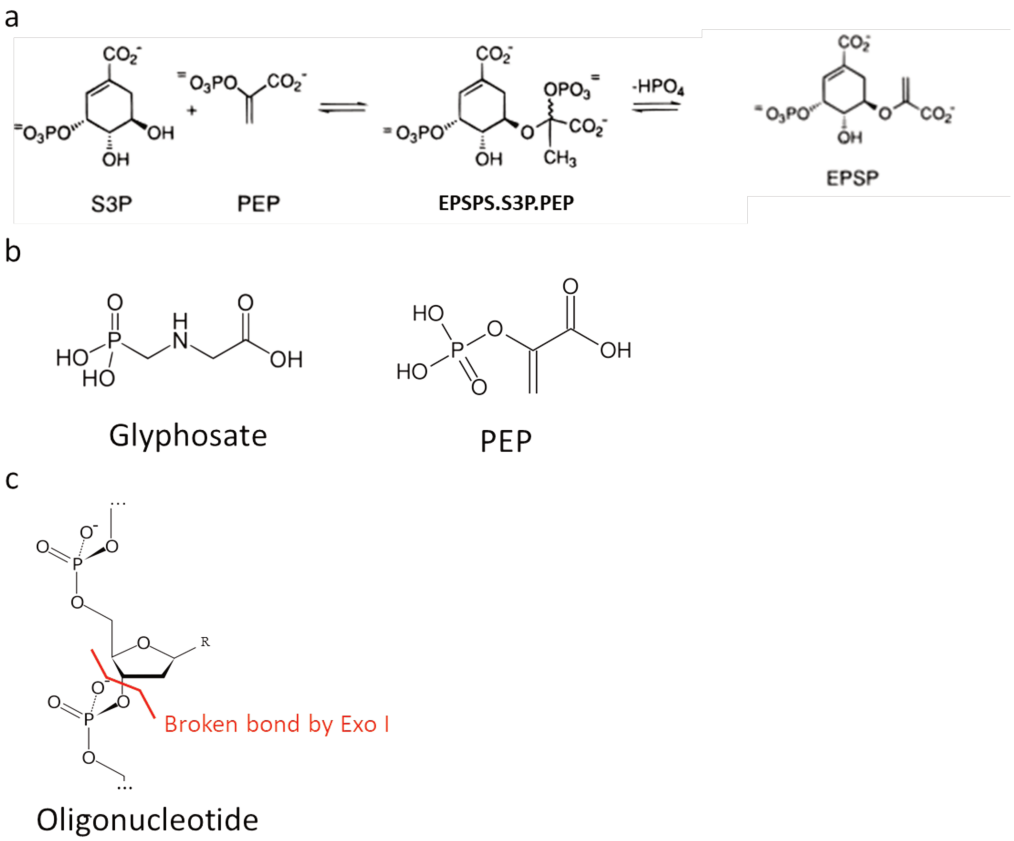

Figure II-S6. (a) Reaction catalyzed by EPSP synthase (EPSPS). (b) Structural similarity between glyphosate and PEP involved in the EPSPS inhibition mechanism. (c) Exo I activity: phosphodiester bond breakage [64].

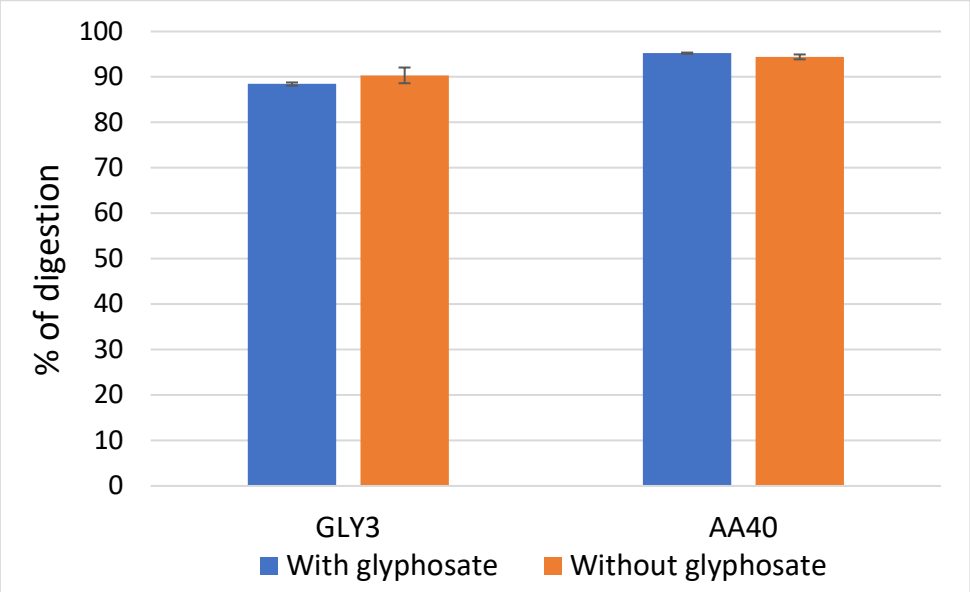

Figure II-S7. Digestion of GLY3 and AA40 library sequences at 1 µM by both enzymes, T5 Exo and Exo I, at 37 °C for 30 min after 2 hours of incubation at 37 °C with or without glyphosate (0.169 mg L^{-1}) in HEPES buffer.

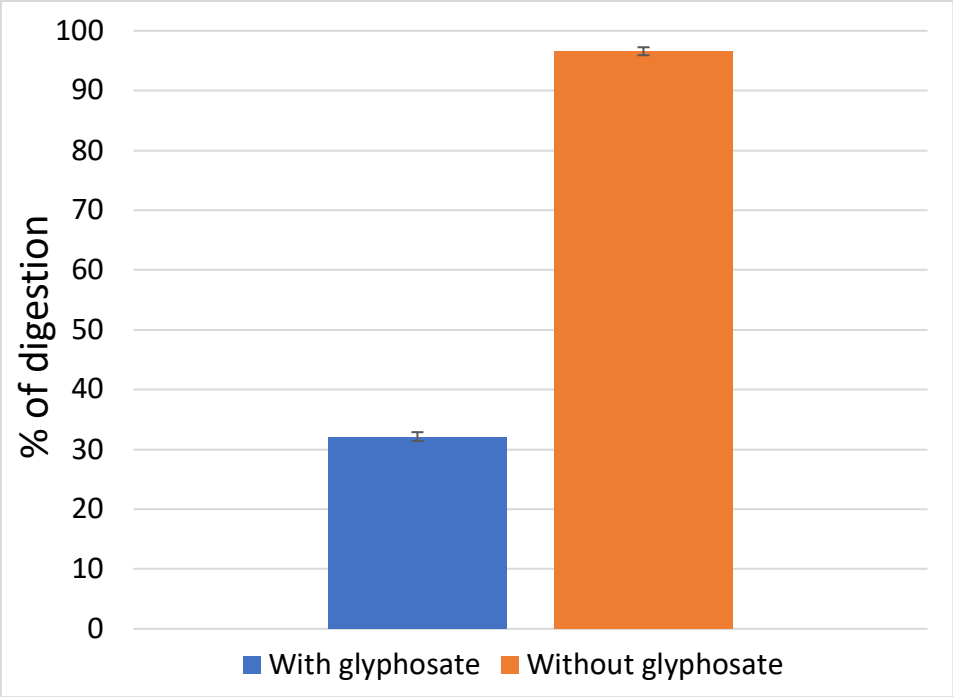

Figure II-S8. Digestion of GLY3 (1 µM) by both enzymes, T5 Exo and Exo I, at 37 °C for 30 min after 2 hours of incubation at 37 °C with or without glyphosate (0.169 mg L^{-1}) in GLY3 buffer containing 5 mM Mg^{2+} cations.

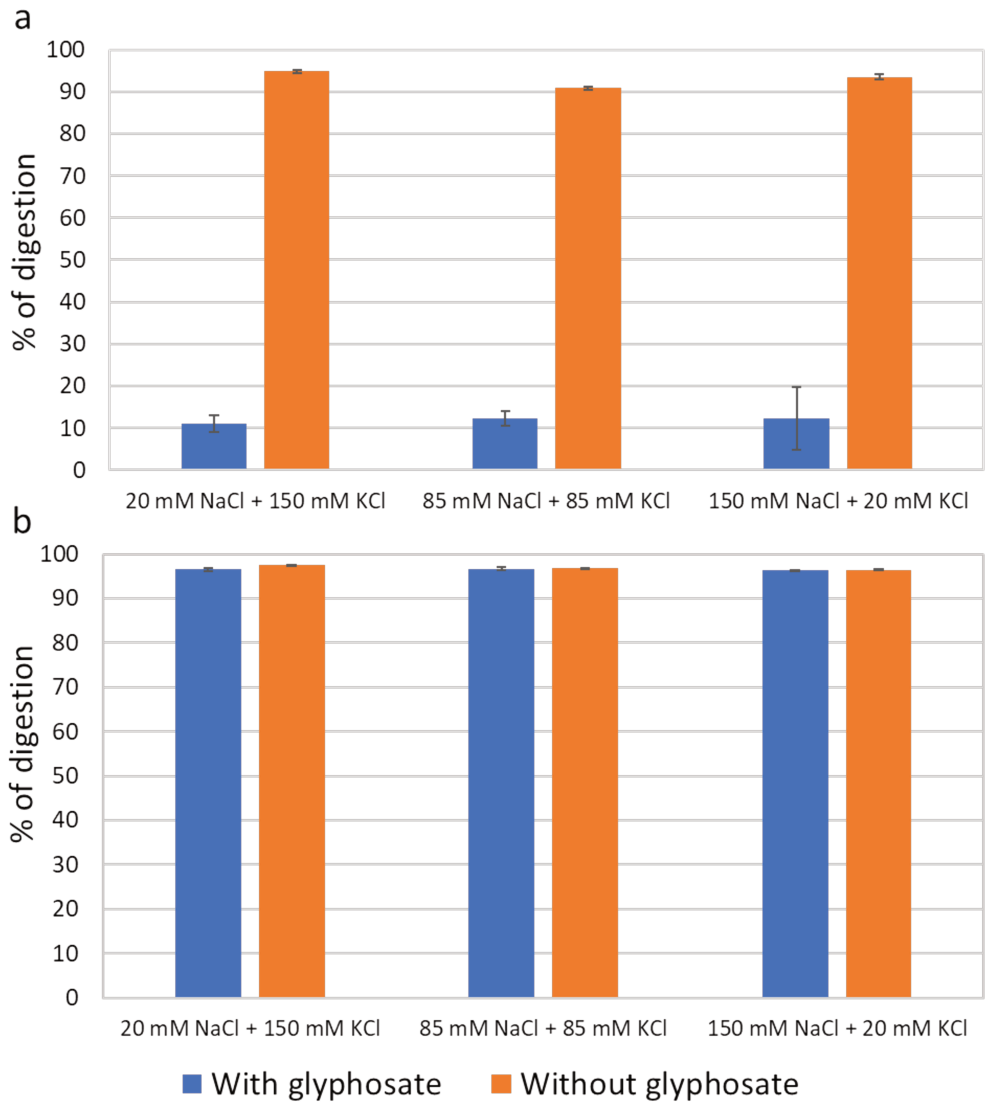

Figure II-S9. Digestion of GLY3 (1 µM) by both enzymes, T5 Exo and Exo I, for 30 min at 37 °C after 2 hours of incubation at 37 °C with or without glyphosate (0.169 mg L^{-1}) in (a) GLY3 buffer, and (b) HEPES buffer with different $[K^+]/[Na^+]$ ratios.

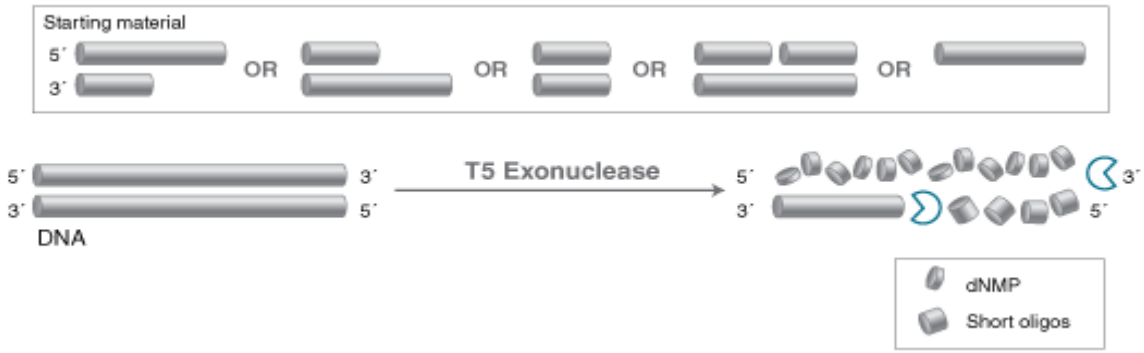

Figure II-S10. Mechanism of operation of the T5 Exo enzyme (England Biolabs).

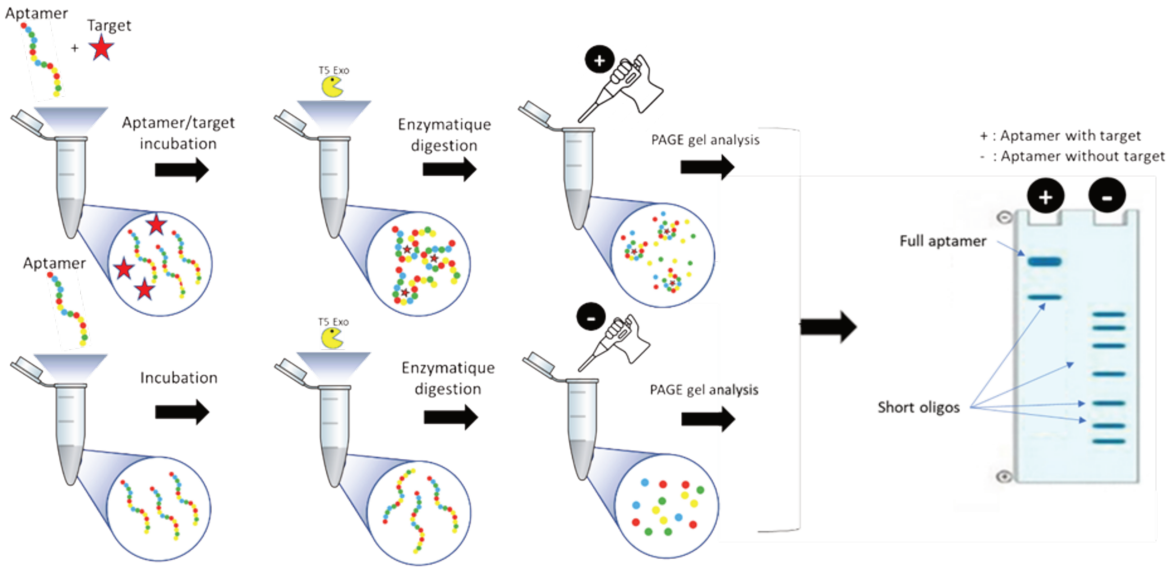

Figure II-S11. Principle of T5 Exo digestion followed by PAGE to assess an aptamer's interaction with its target.

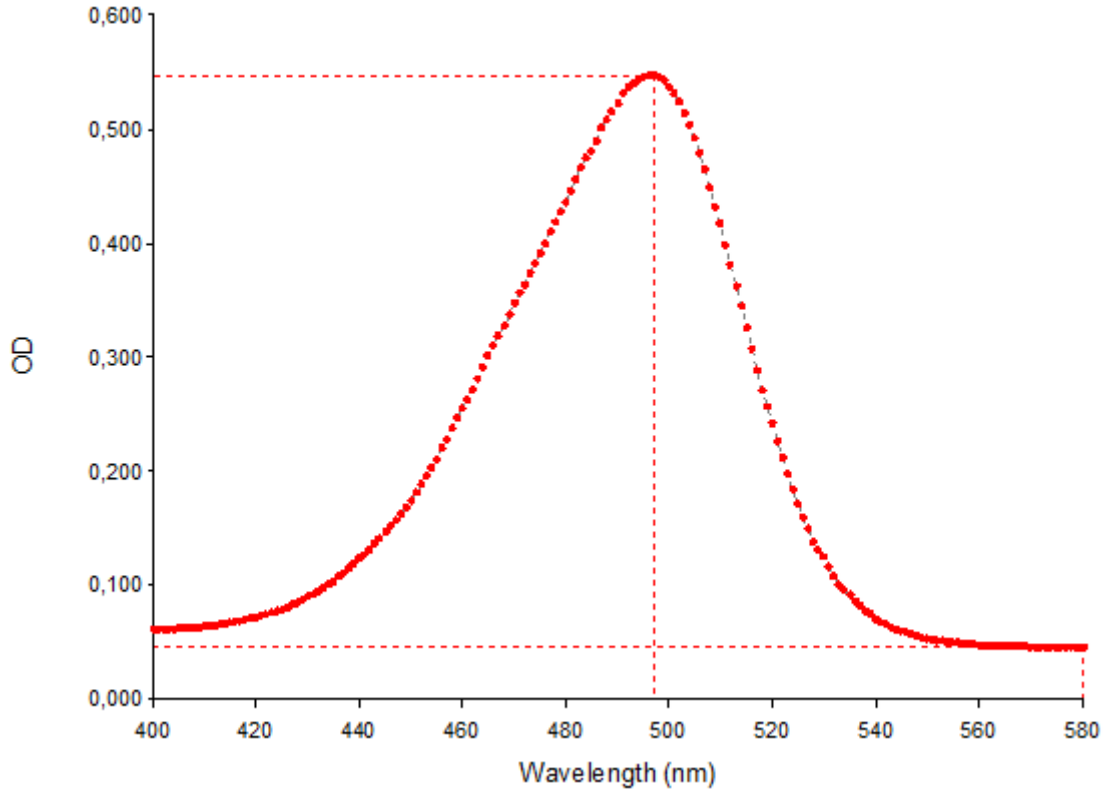

Figure II-S12. Absorbance spectrum of 10X SYBR Gold (λ_{max} = 497 nm).

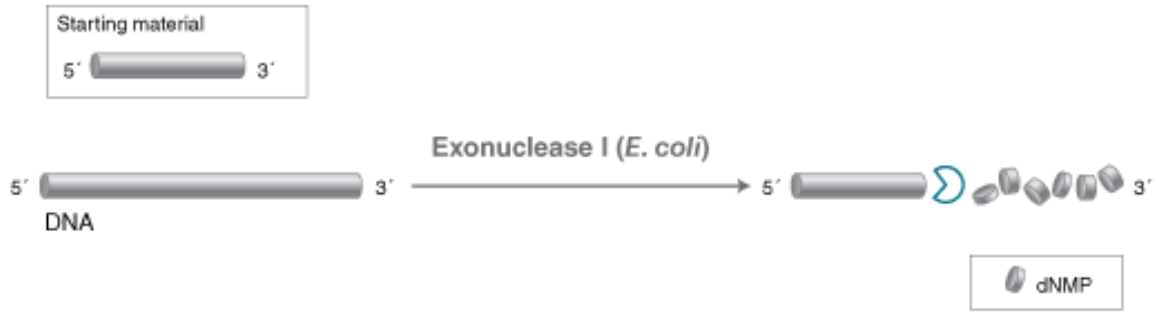

Figure II-S13. Mechanism of operation of the Exo I enzyme (New England Biolabs).

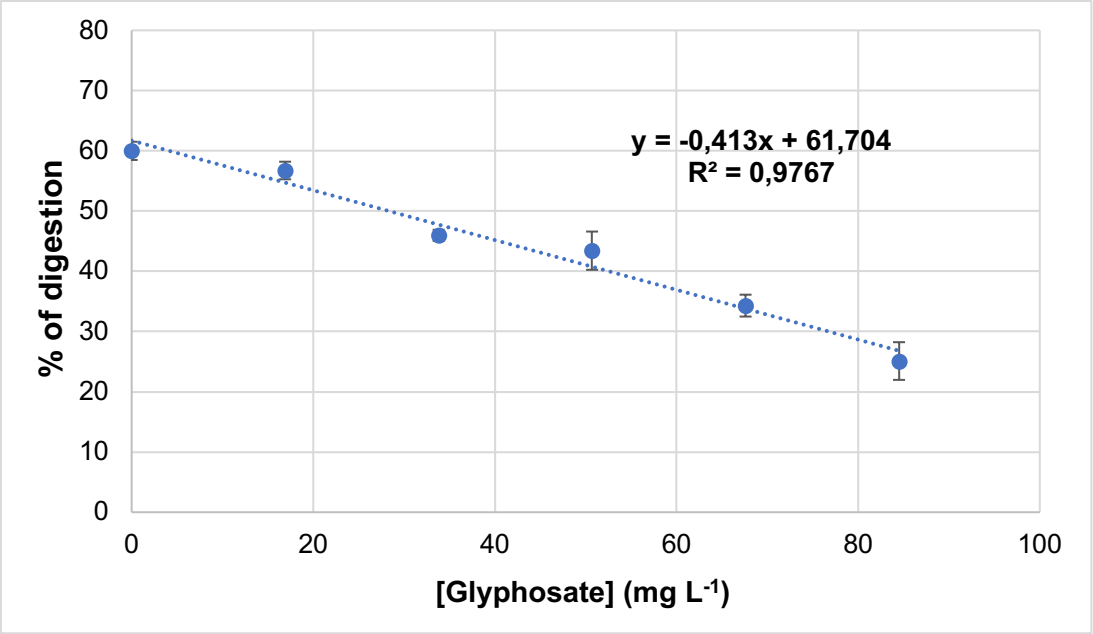

Figure II-S14. Enzymatic digestion of SUP000 at 1 µM by Exo I (0.15 U μL^{-1}) in GLY3 buffer in absence and presence of different concentrations of glyphosate (16,9 – 84,5 mg L^{-1}).

Denaturing PAGE preparation:

Polyacrylamide 20%, TBE 0.5X, 7 M urea:

- 1 liter acrylamide/bisacrylamide 40%, 19/1 (v/v) [20% final]
- 200 mL TBE 10X [0.5X final]
- 840.84 g urea (MW = 60.06 g/mol) [7 M final]
- Mix in a 2 L beaker with a stirrer and heat to facilitate dissolution (caution: do not exceed 55 °C!)
- Once the solution is clear, adjust the volume to 2 L with H_2O

Cut a Whatman paper of the same diameter as the sinter, then filter the solution on the sinter + the Whatman paper thanks to the spouted flask and the vacuum pump. Then pour the solution into 2 brown bottles and store at 4 °C.

PAGE plate (15%):

- 15 mL of 0.5X TBE is added to 49 mL of 20% acrylamide (in 0.5X TBE and 7 M Urea), the whole is mixed.
- 650 µL of 10% APS are added to the reaction volume.
- The whole is mixed in a 50 mL tube then 65 µL of TEMED is added to the volume reaction.
- The whole is mixed and poured directly into the gel plates.

Table II-S1. Different biosensors developed against glyphosate pesticide.

Pesticide	Detection technique	Biomolecule or nanocomposite	LOD	Validity for real samples	References
Glyphosate	Fluorometric assay	Aptamer & antibody	0.01 mg L^{-1}	Phosphate-buffered saline (PBS)	Lee et al. (2010)[68]
Trichlorfon, glyphosate and malathion	Fluorometric assay	MNPs/complementary DNA/FAM-aptamer	72.2 ng L^{-1}, 88.8 ng L^{-1} and 195.37 ng L^{-1}	Lettuce and carrot	Jiang et al., (2020)[69]
Glyphosate	SERS	Aptamer	0.338 ng L^{-1}	Soil	Liu et al., (2021)[70]
Glyphosate	Luminescent assay	Aptamer	72.2 ng L^{-1}	Lettuce and carrot	Chen et al., (2020)[38]
Isocarbophos, omethoate and glyphosate	Colorimetric assay	Aptamer	Isocarbophos: 0.47 µg L^{-1} Omethoate: 0.35 µg L^{-1}	Buffer	Liu et al., (2020)[40]
Glyphosate	Potentiometric assay	Urease	0.5 mg L^{-1}	Tap water	Vaghela et al. (2018)[36]
Glyphosate	Fluorometric assay	Antibody	0.021 µg L^{-1}	Water and soil	Gonzalez-Martinez et al. (2005)[71]
Glyphosate	Chronoamperometric assay	Antibody	5 ng L^{-1}	Commercial beer	Betazzi et al. (2018)[37]
Glyphosate	Fluorometric assay	Enzyme	16.9 mg L^{-1}	Drinking water	The present work

Table II-S2. DNA oligonucleotide sequences used in this work as negative controls.

Oligonucleotide	Sequence
SCR GLY2	5'-CCC-GTT-AGT-CAC-CTC-TCG-GGC-ACG-GTC-CCC-CTG-CTC-AGT-GGT-ATA-CGG-TCC-CTG-CGA-TCATGA-GCC-ACC-CTC-AGA-A-3'
SCR GLY3	5'-TGC-TAG-ACG-ATA-TTC-GTC-CAT-CCG-AGC-CCG-TGG-CGG-GCT-TTA-GGA-CTC-TGC-GGG-CTT-CGCGGC-GCT-GTC-AGA-CTG-AAT-ATG-TCA-3'
ATZ1[52]	5'-TGT-ACC-GTC-TGA-GCG-ATT-CGT-ACG-AAC-GGC-TTT-GTA-CTG-TTT-GCA-CTG-GCG-GAT-TTA-GCCAGT-CAG-TGT-TAA-GGA-GTG-C-3'
ATZ2[53]	5'-TAC-TGT-TTG-CAC-TGG-CGG-ATT-TAG-CCA-GTC-AGT-G-3'
AA40 library	5'-AGC-CTG-TTG-TGA-GCC-TCC-TGT-CGA-ANN-NNN-NNN-NNN-NNN-NNN-NNN-NNN-NNN-NNN-NNN-NNN-NNN-NNN-NNT-TGA-GCG-TTT-ATT-CTT-GTC-TCC-C-3'
Arsenic aptamer[55]	5'-GGTAATACGACTCACTATAGGGAGATACCAGCTTATTCAATTTTACAGAACAACCAACGTCGCTCCGGGTACTTCTTCATCGAGATAGTAAGTGCAATCT-3'
Thrombin aptamer[72]	5'-CCAACGGTTGGTGTGGTTGG-3'
ssDNA	5'CGGAATCAGTGAATGCTTATACATCCG-3'

Table II-S3. Composition of the interaction buffers used with their corresponding aptamer.

Aptamer	Interaction buffer composition
GLY1	10 mM Tris-HCl, pH 7.2, 150 mM NaCl, 122.5 mM $MgCl_2(6H_2O)$, and 10 mM KCl
GLY2	20 mM Tris-HCl, pH 7.6, 100 mM NaCl, 2 mM $MgCl_2(6H_2O)$, 5 mM KCl, and 1 mM $CaCl_2(4H_2O)$
GLY3	20 mM Tris-HCl, pH 7.2, 150 mM NaCl, 1 mM $MgCl_2(6H_2O)$, and 20 mM KCl

Table II-S4. Incubation conditions of glyphosate with aptamers.

Aptamer	Target	Incubation conditions with the target
GLY1	Glyphosate	2 hours at 37 °C under gentle stirring in GLY1 buffer
GLY2	Glyphosate	30 minutes at room temperature under gentle stirring in GLY2 buffer
GLY3	Glyphosate	2 hours at 37 °C under slight gentle in GLY3 buffer

Table II-S5. Calculation of the molar concentration of 10X SYBR Gold

λ_{max} (nm)	Absorbance (n = 3)	Optical path (cm)	Extinction coefficient (M^{-1} cm^{-1})	[SYBR Gold] (µM)
497	0.494 +/- 0.008	0.7	57000[56]	12.38

Chapter III. Development of an electrochemical aptasensor: detection of Macromolecules (thrombin) vs. Small Molecules (thiabendazole)

Résumé

L'étude menée pour analyser l'interaction entre le glyphosate et les aptamères candidats identifiés dans la littérature en utilisant la méthode de digestion enzymatique n'a pas confirmé d'interaction entre eux. Par conséquent, aucun des trois aptamères ne pouvait être utilisé sur la plateforme électrochimique développée par l'équipe du projet Captain Ad Hoc pour la détection du glyphosate. Pour surmonter cette limitation, une nouvelle cible, dont l'aptamère fonctionnel est fourni par l'entreprise Novaptech, a été étudiée. Cet aptamère est connu sous le nom de BOL009. Il a ensuite été greffé sur la plateforme électrochimique développée pour détecter le thiabendazole. De plus, une étude de validation du fonctionnement de la plateforme électrochimique a été réalisée en examinant la détection de la thrombine, une molécule de grande taille (37 000 daltons) dont l'aptamère fonctionnel est bien décrit dans la littérature. Ce chapitre décrit les étapes de préparation de la plateforme électrochimique, les étapes de greffage du BOL009 et de l'aptamère de thrombine, ainsi que la détection du thiabendazole et de la thrombine. En conclusion de ce chapitre, nous présentons les résultats de la détection obtenus pour la thrombine (une grosse molécule) et le thiabendazole (une petite molécule).

Summary

The study conducted to analyze the interaction between glyphosate and the candidate aptamers identified in the literature using the enzymatic digestion method did not confirm any interaction between them. Consequently, none of the three aptamers could be used on the electrochemical platform developed by the Captain Ad Hoc project team for glyphosate detection. To overcome this limitation, a new target, with its functional aptamer provided by the company Novaptech, was investigated. This aptamer is known as BOL009. It was subsequently grafted onto the electrochemical platform developed for the detection of thiabendazole. Additionally, a validation study of the electrochemical platform's performance was conducted by examining the detection of thrombin, a large molecule (37,000 daltons) whose functional aptamer is well-described in the literature. This chapter describes the steps involved in preparing the electrochemical platform, the grafting of BOL009 and the thrombin aptamer, as well as the detection of thiabendazole and thrombin. In conclusion of this chapter, we present the detection results obtained for thrombin (a large molecule) and thiabendazole (a small molecule).

Table of Contents

Chapter III. Development of an electrochemical aptasensor: detection of Macromolecules (thrombin) vs. Small Molecules (thiabendazole)

I. Introduction

The reliable detection of pesticides is of utmost importance for ensuring food safety and environmental protection. Electrochemical aptasensors have emerged as powerful analytical devices due to their high sensitivity, selectivity, portability, and simplicity of operation. These aptasensors harness the unique properties of aptamers, which are single-stranded nucleic acid molecules (ssDNA) selected for their high affinity towards specific targets including pesticides. When integrated with electrochemical transducers, aptamers allow the conversion of molecular recognition events into measurable electrical signals, facilitating thus sensitive pesticide detection.

I.1. Screen Printed Carbon Electrode (SPCE)

One commonly used electrochemical platform is based on Screen Printed Carbon Electrodes (SPCEs)[1]. The SPCE consists of a carbon working electrode printed on a disposable substrate, typically made of a polymer material. The carbon working electrode serves as the sensing element in the aptasensor, on which the aptamer is immobilized. The SPCE offers several advantages in the development of electrochemical aptasensors. Firstly, its small size and low-cost nature make it practical and disposable. It allows for mass production, making it suitable for point-of-care and field applications. The simplicity of the design also facilitates miniaturization and integration with portable devices. The carbon material of the working electrode provides good electrical conductivity and a large surface area, which enhances the electrochemical performance of the aptasensor. This allows for efficient electron transfer reactions at the electrode surface, leading to sensitive and rapid detection of target molecules. The SPCE platform offers compatibility with various electrochemical techniques, such as cyclic voltammetry, chronoamperometry, and impedance spectroscopy. These techniques can be employed to monitor changes in current, potential, or impedance resulting from the interaction between the immobilized aptamer and the target molecule. By measuring these electrochemical signals, quantitative and selective detection of the target analyte can be achieved. Furthermore, the SPCE platform can be modified to enhance the sensitivity and selectivity of the aptasensor[2].

In summary, SPCE is widely used in the development of electrochemical aptasensors. Its simplicity, disposability, and compatibility with various electrochemical techniques make it an attractive tool. With the integration of aptamers, SPCE-based aptasensors offer great potential for applications in clinical diagnostics, environmental monitoring, and food safety, providing rapid, sensitive, and selective detection of target molecules[3].

I.2. Improvement of the conductivity parameters of SPCE by its modification with a conductive polymer and gold nanoparticles

SPCEs have gained significant attention as versatile electrodes due to their small size, low cost, and ease of use. However, their inherent conductivity may limit their sensitivity and detection capabilities. To overcome this limitation, various strategies have been employed to enhance the conductivity parameters of SPCEs. We focused on the modification of SPCEs using a conductive polymer and gold nanoparticles to improve their electrochemical performance[4]. The conductivity parameters of SPCEs can be significantly improved through the deposition of a conductive polymer onto the carbon working electrode surface. Conductive polymers, such as polyaniline (PANI), polypyrrole, or poly(3,4-ethylenedioxythiophene) (PEDOT), are commonly employed due to their excellent electrical conductivity, stability, and ease of synthesis[4–6]. The conductive polymer modification process involves electrochemical polymerization of the monomers onto the surface of the carbon working electrode. This can be achieved by cyclic voltammetry or chronoamperometry. During the polymerization process, the monomers undergo oxidation and reduction cycles, leading to the formation of a conductive polymer layer. The thickness of the conductive polymer layer can be controlled by adjusting the deposition parameters, such as the polymerization potential, the number of cycles, and the monomer concentration. The conductive polymer-modified SPCEs offer several advantages. They provide an increased surface area for redox probe interaction, enhancing sensitivity. The conductive polymer layer also promotes electron transfer between the redox probe and the electrode surface, resulting in enhanced electrochemical response. Additionally, the conductive polymer acts as a protective barrier, preventing direct contact between the redox probe and the carbon electrode, which can reduce unwanted electrochemical reactions or fouling. The conductivity enhancement achieved through conductive polymer modification enables more efficient electron transfer kinetics and improves the overall electrochemical performance of SPCEs[4–6]. This makes them highly suitable for applications such as electrochemical sensing, biosensing, and electroanalytical techniques. In summary, conductive polymer modification of

SPCEs involves electrochemically depositing a conductive polymer layer onto the carbon working electrode surface. The choice of the conductive polymer depends on the specific requirements of the application. PANI, with its pronounced conductivity and environmental resilience, emerges as an ideal candidate for our electrochemical application. Consequently, it is the chosen material for the development of our electrochemical aptasensor. **Figure III-1** shows the mechanism of electropolymerization of aniline.

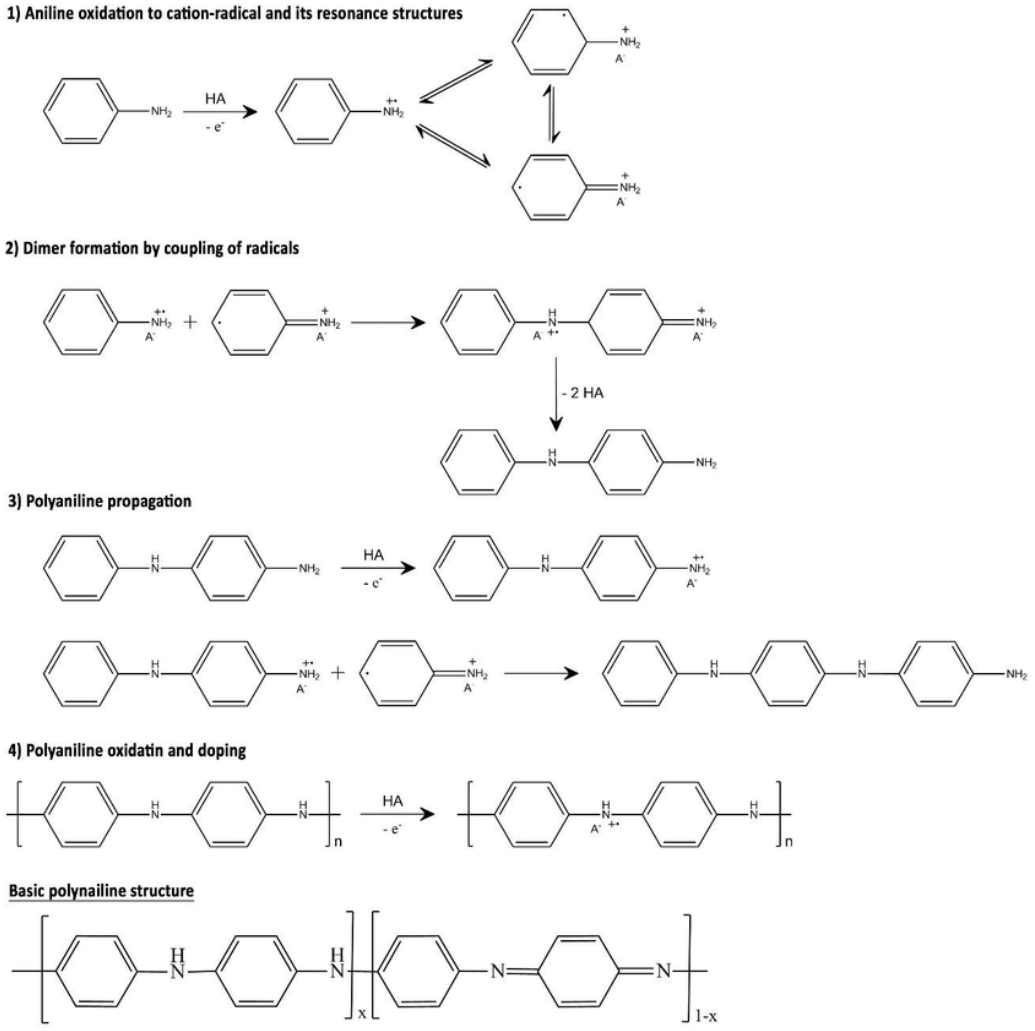

Figure III-1. Mechanism of electropolymerization of PANI[7].

The process of electrochemical synthesis involving the electropolymerization of PANI can be elucidated through a series of four distinct steps[7]:

- Step 1: Initiation begins with the creation of a primary cation radical, achieved through the oxidation of the monomer at the anode.
- Step 2: Subsequent to initiation, dimers are formed through a process of deprotonation and re-aromatization.

- Step 3: Progressive growth and chain development, accompanied by oxidation, transpires in the third step. This involves the conversion of dimers into cation radicals, followed by their interaction with monomer cation radicals.
- Step 4: The final step involves an inherent doping of the resultant polymeric chain, resulting in the attainment of the polymer in a doped configuration. Notably, this particular doping phenomenon is exclusive to the electrochemical methodology.

The ultimate structure of the PANI polymeric chain encompasses a fusion of two recurring components: oxidized elements (quinoid rings) and reduced counterparts (benzene rings). Depending on the ratio between these components and their respective oxidation states, PANI assumes three distinctive and stable oxidation forms: x = 1, corresponding to the leucoemeraldine configuration (completely reduced); x = 0.5, manifesting as emeraldine (partially oxidized); and x = 0, indicative of pernigraniline fully oxidized (as illustrated in **Figure III-1**)[7].

In the present study, the surface of SPCE was subject to modification through electrodeposition of PANI, and its characterization was undertaken utilizing CV as outlined in the Materials and Methods section. The obtained outcomes are illustrated in **Figure III-2**.

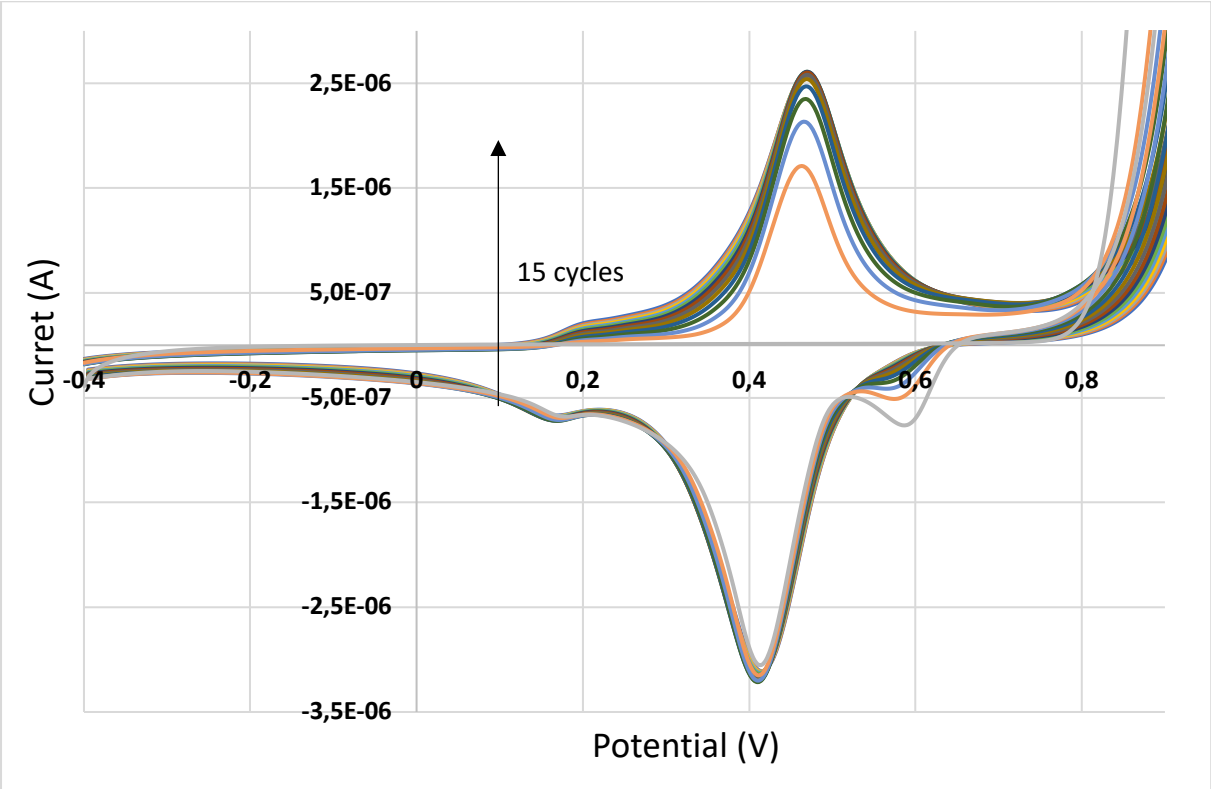

Figure III-2. Electrodeposition of PANI using 15 cycles of CV in the range between 0 and 1 V, with a speed of 0.1 V s^{-1}.

Various discernible peaks confirming the deposition of PANI are evident:

- Anodic peak (0.2 V) and cathodic peak (0.16 V): These peaks correspond to the oxidation and reduction processes of p-benzoquinone into hydroquinone, an intermediary degradation product, along with its subsequent reduction.
- Anodic peak (0.47 V) and cathodic peaks (0.41 V and 0.59 V): These peaks are associated with the oxidation of emeraldine into pernigraniline, as well as the corresponding reduction reactions[7].

In addition to PANI modification, the incorporation of AuNPs further enhances the conductivity parameters of SPCEs. AuNPs are widely utilized in the modification of SPCEs due to their exceptional conductivity, high surface area, and easy modification properties when using thiol-modified materials[4]. The incorporation of AuNPs/PANI-modified SPCEs further improves the conductivity and electrochemical performance of the electrodes. There are two common methods for incorporating AuNPs onto the SPCE surface: physical adsorption and covalent attachment. In physical adsorption, the AuNPs are immobilized onto the conductive polymer layer through non-covalent interactions, such as electrostatic forces, hydrogen bonding, or van der Waals interactions. This method is relatively simple, allowing for easy modification of the SPCEs. Covalent attachment involves functionalizing the surface of AuNPs and the conductive polymer layer with complementary reactive groups. These groups can then form strong chemical bonds, such as thiol-gold bonds, to link the AuNPs to the conductive polymer layer. The incorporation of AuNPs onto PANI-modified SPCEs results in the formation of a conductive nanocomposite layer. This layer combines the conductivity of the AuNPs with the electrochemical properties of PANI and SPCEs. The AuNPs not only improve the electron transfer kinetics but allow for easy grafting of thiol-modified aptamer via robust covalent thiol-gold bounds, which is an essential step for the fabrication of our electrochemical aptasensor[4]. Furthermore, the conductive nanocomposite layer enhances the stability and robustness of the modified SPCEs, enabling long-term and reliable electrochemical measurements.

In this work, AuNPs were physically adsorbed onto PANI/SPCE using chronoamperometry (refer to MM section for details). The curve depicting the relationship between the number of charges (C) obtained during AuNPs electrodeposition is shown in **Figure III-3**.

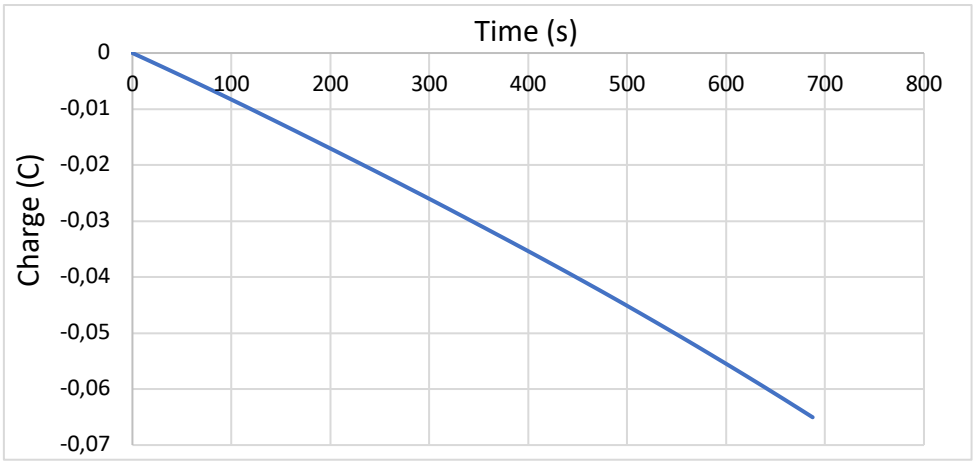

Figure III-3. Electrodeposition of $HAuCl_4$ onto PANI/SPCE in H_2SO_4 (0.5 M) using CA with a -0.065 C cut-off under continuous stirring.

The plot illustrates the relationship between the number of charges (C) and the electrodeposition time, demonstrating the successful adsorption of AuNPs onto the PANI/SPCE surface. A visual assessment of the deposition was also performed to confirm the uniform distribution of the AuNPs layer and to identify any potential deposition defects (**Figure III-4**).

Figure III-4. Images of (a) well-homogenized deposition of gold nanoparticles, yielding a soft yellow surface, and (b) poor deposition resulting in black surfaces.

I.3. Aptamer grafting onto AuNPs/PANI/SPCE

Thiol modification involves the attachment of a thiol group (-SH) to the aptamer molecule, typically at the 5'- or 3'-end, to facilitate covalent bonding with AuNPs. The immobilization of thiol-modified aptamers onto AuNPs/PANI-modified electrodes is a crucial step in the development of highly sensitive and specific biosensors. The thiol-modified aptamers,

synthesized or modified to contain generally a C_6-thiol group at their ends, serve as the molecular recognition elements for the target analyte. The C_6 is used as a spacer in order to preserve the recognition properties of the aptamer. The first stage involves incubating the C6-thiol-modified aptamers with SPCE/PANI/AuNPs, where the thiol groups covalently bind to the AuNPs surface through Au-S bonding. This step ensures the stable and oriented immobilization of the aptamers on the AuNPs, preserving their inherent binding affinity and selectivity. To minimize non-specific interactions, the non-specific binding sites on the electrode are often blocked with a suitable blocking agent such as bovine serum albumin (BSA) or 6-mercaptohexanol (MCH). In this project, MCH has been chosen as it shows good properties that allow a better orientation of ssDNA onto the surface of the electrode preventing thus their inclination and ensuring their interaction with the target [8–10].

In summary, the modified electrode developed in this study consisted of a substrate of screen-printed carbon electrode (SPCE) coated with PANI, followed by the immobilization of gold nanoparticles (AuNPs) functionalized with C_6-thiol-modified aptamers and MCH as a stabilizing agent (SPCE/PANI/AuNPs/Aptamer/MCH). The schematic illustration of the steps involved in the modified electrode fabrication is presented in **Scheme 1**.

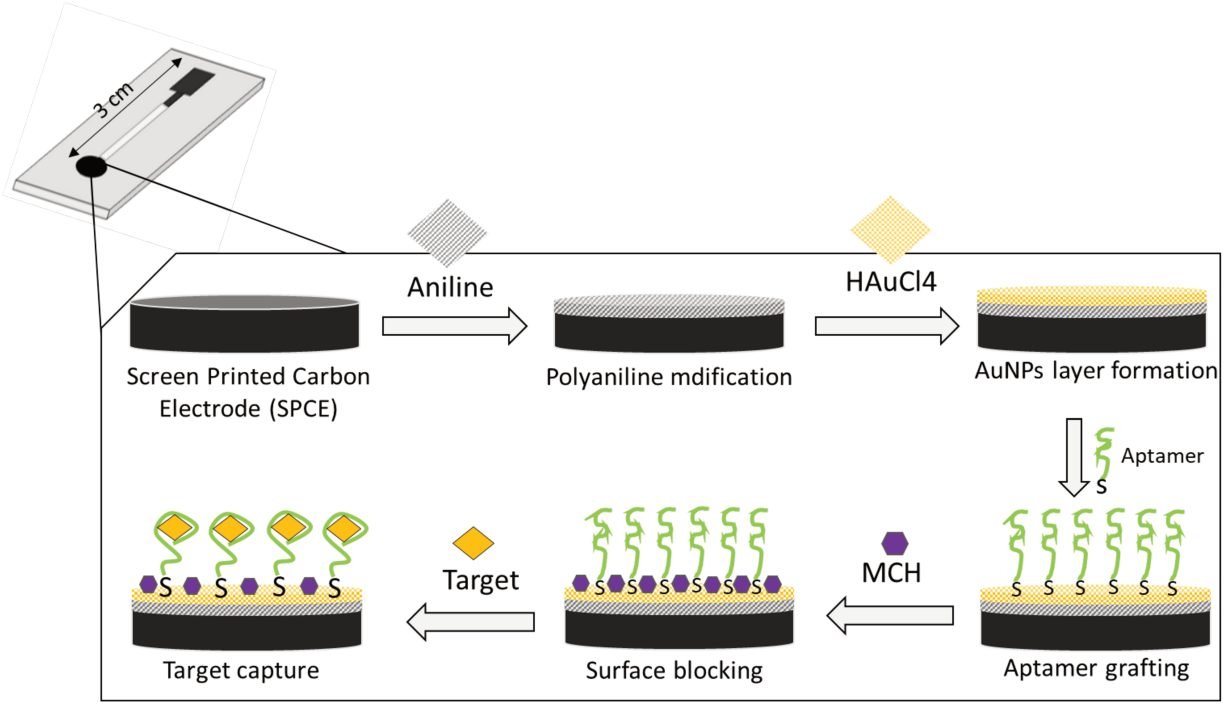

Scheme 1. Schematic illustration of the fabricated SPCE/PANI/AuNPs/thrombin Apt/MCH.

II. Experimental section

II.1. Fabrication of modified screen-printed carbon electrode (SPCE)

The electrode manufacturing process begins by positioning the anchor on a mold with ten designated electrode locations, ensuring even distribution along the mold surface. Next, a narrow board is used to guide the carbon anchor through the carbon mold, allowing the electrodes to be printed on plastic plates. After the electrodes are formed, a drying period of one hour at room temperature is required, followed by an additional hour at 60°C to ensure complete drying. To conclude the manufacturing process, an insulator is applied to insulate the part of the electrode that is not involved in the electrochemical measurements. Finally, the electrodes are left for two days at room temperature to dry completely before use.

II.2. Modification of SPCE with PANI and gold nanoparticles (PANI/AuNPs)

In order to enhance the conductivity of SPCE, and as discussed above, a modification with PANI and gold nanoparticles is realized. First, the electrodes are cleaned in 0.5 M H_2SO_4 using CV at the following conditions: 5 scans at 100 mV s^{-1}, from -0.5 V until 1.5 V. After the cleaning step, the PANI layer is formed in 50 mM $HClO_4$ solution containing 2.5 mM aniline using CV at following conditions: 15 scans of CV at 50 mV s^{-1} from -0.4 until 1 V. Once the electropolymerization of aniline is finished, 0.6 mM of $HAuCl_4$ prepared in 0.5 M H_2SO_4 gold nanoparticles are directly electrodeposited on the surface of SPCE/PANI using chronoamperometry (CM) with the following conditions: -0.6 V until -0.065 C with constant stirring in order to homogenize constantly the solution for homogenous modification.

II.3. Immobilization of 38mer-BOL009 and thrombin aptamer on the modified SPCE/PANI/AuNPs:

38mer-BOL009 or thrombin aptamer are covalently bound to the modified electrode by incubating SPCE/PANI/AuNPs for 1 hour in HEPES or Tris buffers containing an optimized concentration of 5'-C_6-thiol modified BOL009 or thrombin aptamer, respectively. The immobilization is performed via thiol function and AuNPs, as well described in literature[11].

II.4. Blocking free sites of modified SPCE using 6-mercaptohexanol

Once 38mer-BOL009 or thrombin aptamer grafting is performed, a blocking step is done to block free sites on SPCE/PANI/AuNPs/38mer-BOL009 or thrombin aptamer that could potentially interact with the redox probe. The covalent bonding procedure used for BOL009 grafting is also employed to form a covalent bond between 6-Mercaptohexanol (MCH) and AuNPs via its thiol function.

II.5. Detection of thiabendazole or thrombin molecules

The detection of thiabendazole and thrombin is performed using DPV and Fe^{3+}/Fe^{2+} as a redox probe. SPCE/PANI/AuNPs/38mer-BOL009 or thrombin aptamer/MCH is fooled for 1 hour in HEPES or Tris buffers containing an excess of thiabendazole or thrombin respectively, and DPV is employed to measure current signal as a function of the applied potential. All detection measurements are performed in duplicate or triplicate.

II.6. Detection of thiabendazole using 38mer-BOL009 and complementary oligonucleotides (CO)

The following steps are executed in order to perform this experiment test:

First, a water solution containing 1 µM final concentration of 38mer-BOL009 and 5 µM final concentration of CO11 or CO13 was prepared. The whole set was then heated for 3 min at 95 °C and then cooled on ice for 3 min, and finally was incubated in 1X HEPES buffer containing 17% MeOH for 30 min to respectively denature and structure the 38mer-BOL009/CO11 or CO13 complex. Next, SPCE/PANI/AuNPs was incubated into 80 µL of the hybridized complex solution for 1 hour in order to accomplish the grafting via the covalent bonds formed between the thiol group and AuNPs. Once the grafting is finished, the MCH is added as described in the section materials and methods. All detection measurements are performed in duplicate or triplicate.

III. Results and Discussion

III.1. Detection of thrombin by the developed electrochemical aptasensor (Captain Ad Hoc project)

To validate the functionality of the modified SPCE, the thrombin molecule is employed as a target analyte. The selection of thrombin is based on the fact that its aptamer is well described in the literature, and the interaction between thrombin and its aptamer has been extensively demonstrated[12–14]. This well-established knowledge makes thrombin an ideal choice for evaluating the performance of the modified electrode. The fabricated electrode is then immersed in a 50 µM thrombin solution prepared in thrombin's interaction buffer (see composition in MM), and the resulting current is measured after each incubation period, as shown in **Figure III-5**. A detailed description of the experimental protocol can be found in the Materials and Methods section.

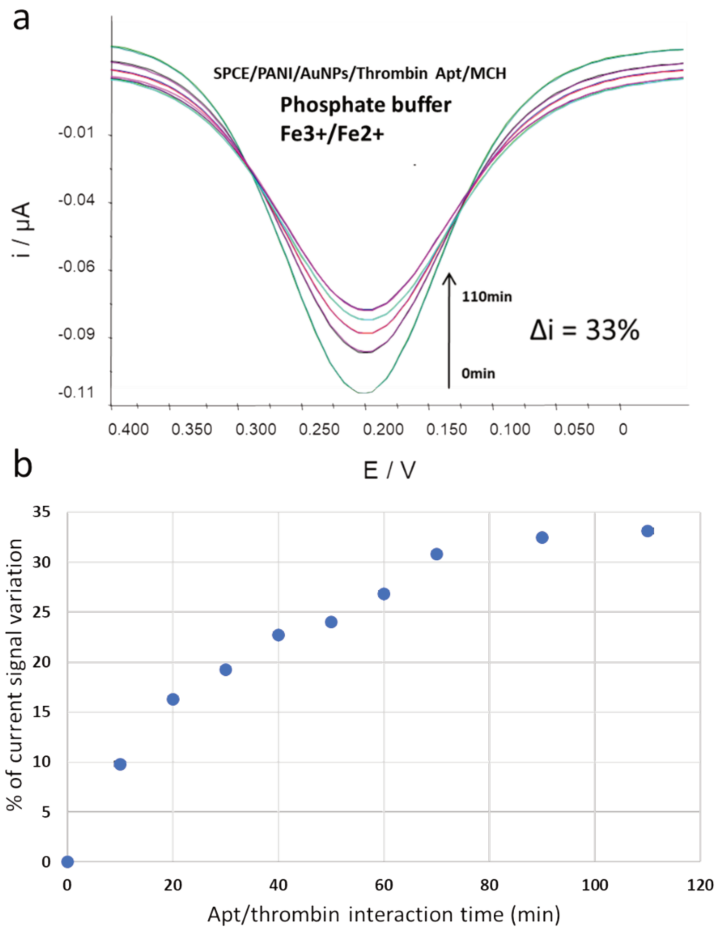

Figure III-5. (a) Current measurement in phosphate buffer solution after immersing the modified SPCE into a solution containing 50 µM thrombin in the thrombin's aptamer interaction buffer. (b) The percentage corresponding to the variation of current.

Figure III-5a illustrates a gradual decrease in the current signal of the modified electrode as the contact time with the thrombin solution increases. Notably, a maximal current variation of 33% is observed after 110 minutes of electrode contact (**Figure III-5b**). This reduction in the current signal confirms the formation of a specific complex between thrombin and its corresponding aptamer on the electrode surface. The binding of thrombin to the aptamer obstructs available binding sites, hindering the electron transfer process and resulting in the observed decrease in current signal. The formation of the thrombin-aptamer complex modifies the local electrochemical environment and disrupts the electron flow at the electrode interface. These findings demonstrate the high specificity of the thiol-modified aptamer for thrombin and the successful detection and interaction of thrombin by the modified electrode.

III.2. Development of an electrochemical aptasensor for the detection of thiabendazole using 38mer-BOL009

Following the successful validation of the developed platform for the detection of thrombin, we conducted a preliminary study to explore the possibility of using this electrochemical platform for detecting thiabendazole, using its specific optimized aptamer, 38mer-BOL009. It is important to note that although 38-BOL009 aptamer differs from the thrombin aptamer in length, with 38 nucleotides compared to the 15 nucleotides of the thrombin aptamer[15], and that thrombin is a biomacromolecule (33701 daltons) whereas thiabendazole is a small molecule (201.25 g mol^{-1}), we aimed at the investigation of the suitability of the thrombin electrochemical platform for thiabendazole detection. The results obtained from this investigation are presented in **Figure III-6**.

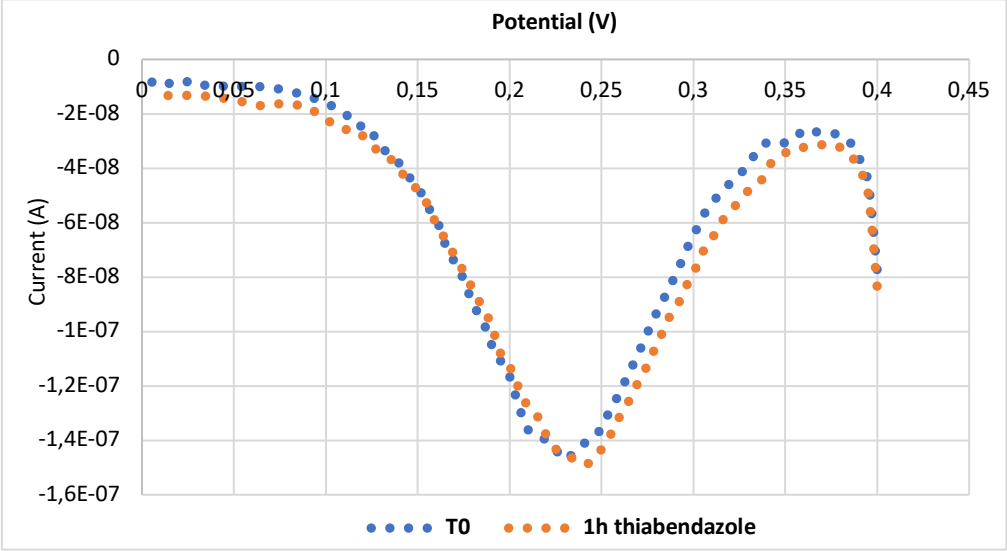

Figure III-6. DPV measurement in HEPES buffer after immersing the modified SPCE into HEPES buffer containing 17% MeOH and 80.4 mg L^{-1} thiabendazole.

Upon incubating the modified SPCE with thiabendazole, the current signal remained stable even after 1 hour of interaction. Two hypotheses can be proposed to explain this observation. The first hypothesis is that 38mer-BOL009, upon immobilization, may have undergone changes in its recognizing conformation, resulting in its inability to interact with thiabendazole. This could explain the lack of significant change in the current signal. The second hypothesis could be that the interaction between 38mer-BOL009 and thiabendazole did occur on the electrode surface, but it did not significantly affect the electron flow, as thiabendazole is a small molecule that does not lead to surface obstruction. Consequently, the absence of a notable current change may be attributed to the relatively small size of thiabendazole and its limited impact on the properties of the electrode surface. Further investigations are needed to differentiate the precise mechanism underlying the observed stable current signal and to elucidate the interaction dynamics between 38mer-BOL009 and thiabendazole on the electrode surface.

Another approach using complementary strands (CO11 having 11 mer and CO13 having 13 mer) was also considered in order to try to enhance the signal variation leading to thiabendazole detection. In fact, complementary oligonucleotides are used to hybridize and immobilize 38mer-BOL009 during its development with Capture SELEX. The idea behind this approach is to hybridize 38mer-BOL009 with either CO11 or CO13 and then graft the complex on the surface of the modified electrode (**Figure III-7**). When thiabendazole is in solution, it forms a complex with 38mer-BOL009 and CO11 or CO13 will switch into solution due to the competitive interactions of thiabendazole.

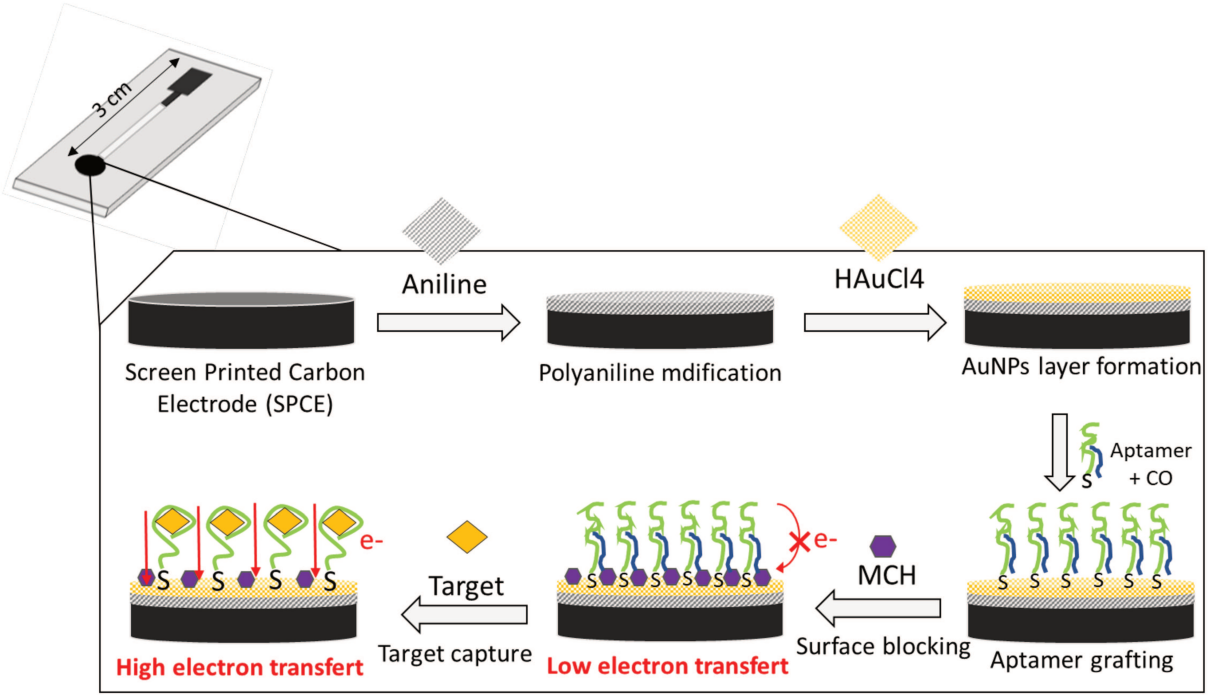

Figure III-7. Schematic representation of the proposed approach for detecting thiabendazole using complementary oligonucleotides and a modified SPCE/PANI/AuNP/BOL009/MCH.

The detailed protocol followed for the construction of this modified SPCE/PANI/AuNPs/BOL009/MCH is described in the MM section. The stability of these prepared electrodes was studied using the phosphate buffer for the electrochemical measurements (**Figure III-8**).

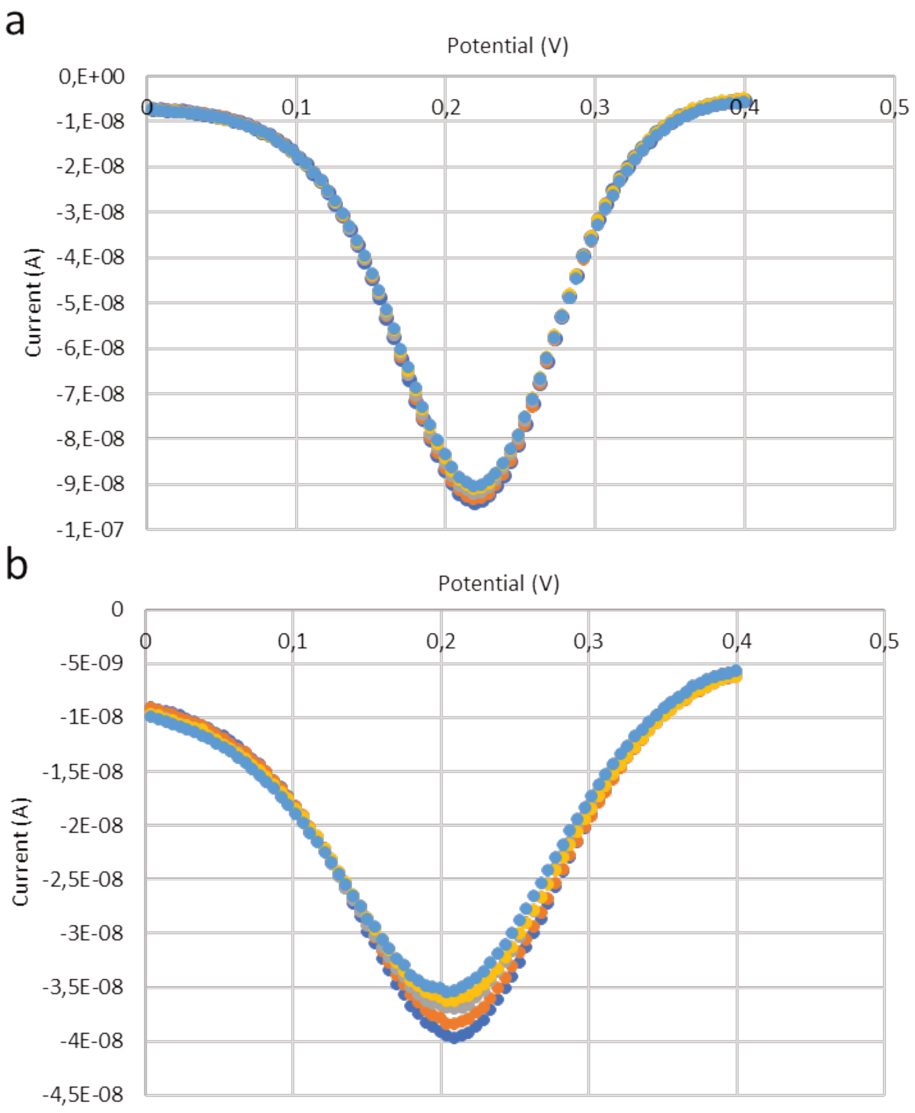

Figure III-8. DPV measurements of (a) SPCE/PANI/AuNPs/38mer-BOL009/CO11/MCH, and (b) SPCE/PANI/AuNPs/38mer-BOL009/CO13/MCH using 40 µM of Fe^{3+}/Fe^{2+} probe in phosphate buffer.

The CO11 showed a little variation in DPV measurements during 5 successive measurements, meanwhile, CO13 showed an instability of signal. This instability could be attributed to the

switch to phosphate buffer during electrochemical measurements. Indeed, the electrodes manufactured are stored in HEPES buffer, and switching to phosphate buffer during electrochemical measurements is potentially responsible for a conformational change of the 38mer-BOL009 and CO, leading to instability of the electrochemical signal. In order to confirm this hypothesis, the HEPES buffer was further used for electrochemical measurements (**Figure III-9**).

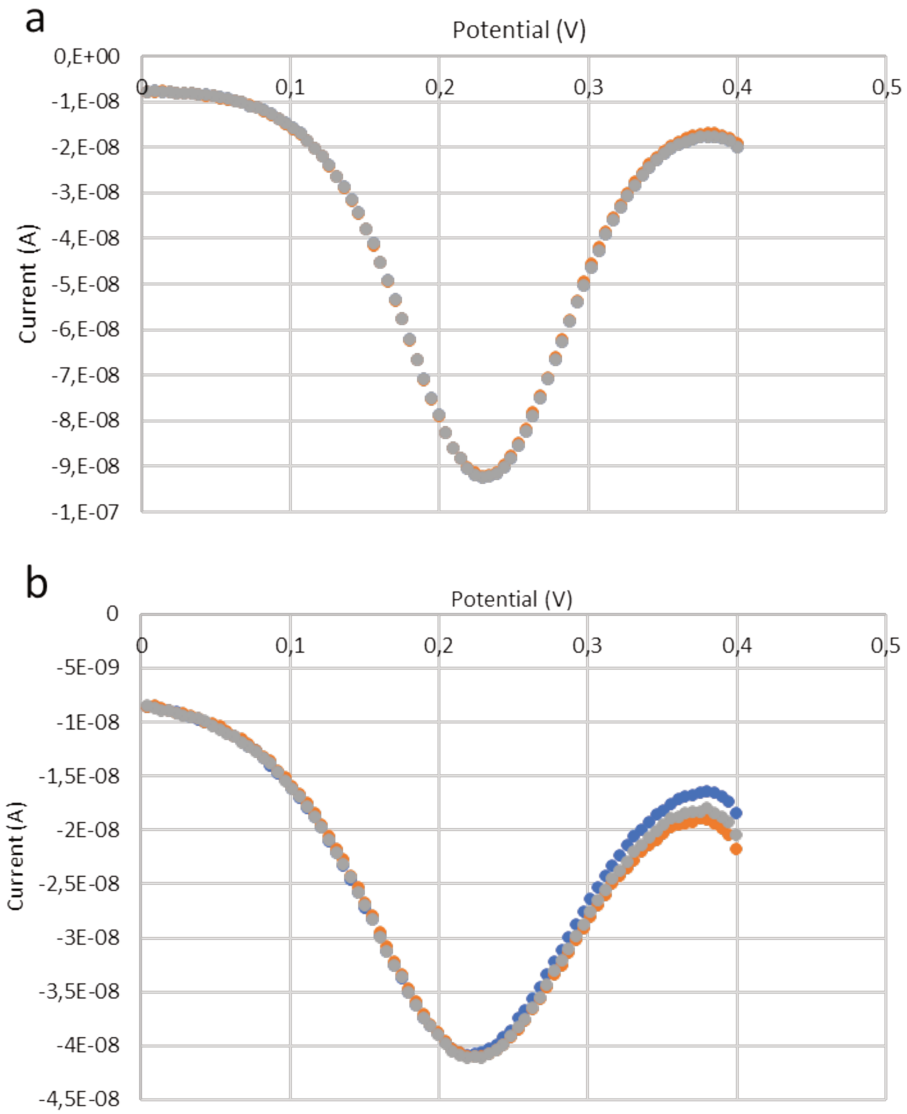

Figure III-9. DPV measurements of (a) SPCE/PANI/AuNPs/38mer-BOL009/CO11/MCH, and (b) SPCE/PANI/AuNPs/38mer-BOL009/CO13/MCH using 40 µM of Fe^{3+}/Fe^{2+} probe in HEPES buffer.

Both modified electrodes exhibited identical current values as in phosphate buffer, and the signal was stable Consequently, HEPES buffer was chosen for subsequent investigations. After those optimizations, the detection test of thiabendazole could be tempted.

The modified electrodes were first incubated for 1 hour in HEPES buffer in order to confirm their stability and then incubated for 1 hour in HEPES buffer containing 17% MeOH and 80.4 mg L^{-1} thiabendazole (**Figure III-10**).

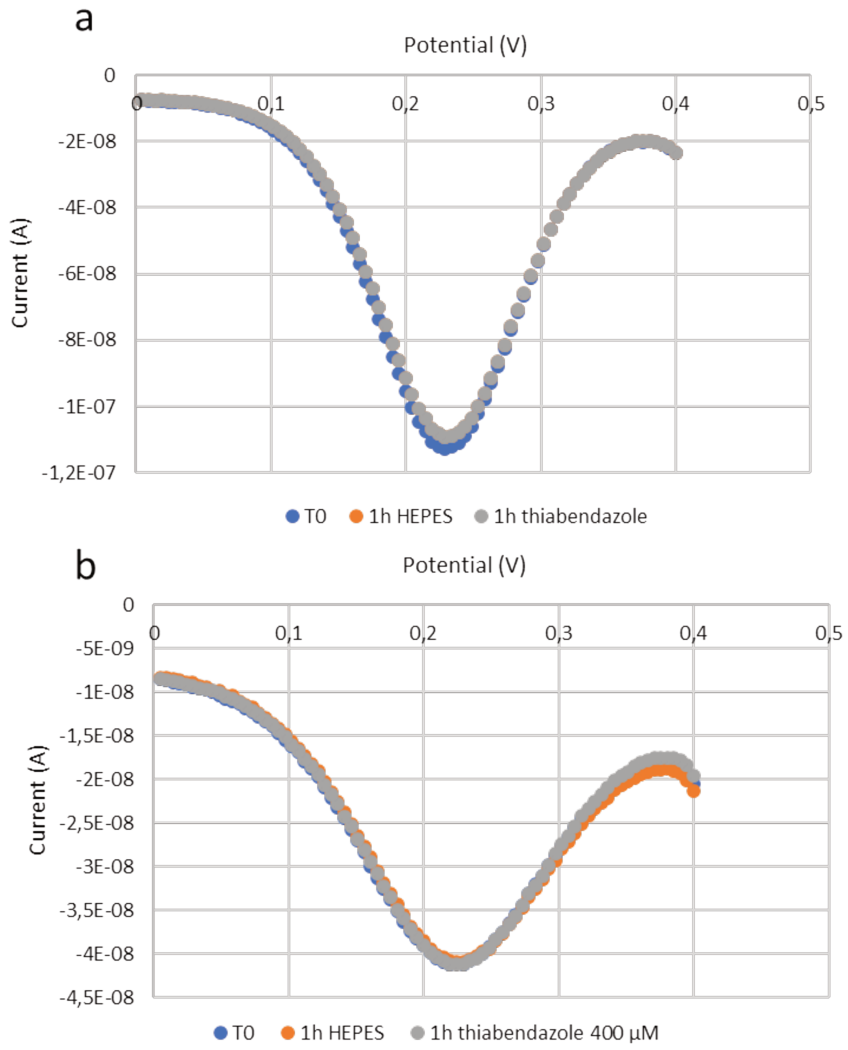

Figure III-10. DPV measurements of (a) SPCE/PANI/AuNPs/38mer-BOL009/CO11/MCH, and (b) SPCE/PANI/AuNPs/38mer-BOL009/CO13/MCH after incubating 1 hour in HEPES buffer then 1 hour in HEPES buffer containing 17% MeOH and 80.4 mg L^{-1} thiabendazole. Signals are obtained using 40 µM of Fe^{3+}/Fe^{2+} probe.

After 1-hour incubation in HEPES buffer, the current signal was shown to be stable confirming thus the stability of the fabricated electrodes. However, after incubation with thiabendazole, no decrease in the current signal was observed. These findings provide evidence that no interaction has occurred between the 38mer-BOL009/CO11-13 complexes and thiabendazole. This result could be explained by the grafting process of the hybridized complex, 38mer-BOL009/CO11-13, during which the aptamer might undergo a conformational change. This could lead to the

dissociation of complementary sequences even before conducting the interaction test with thiabendazole and generating a measurable signal.

Considering that 38mer-BOL009 is a short sequence, it is plausible that its binding to thiabendazole may not elicit a substantial change in the current signal. To investigate this hypothesis, we employed the complete 82mer-BOL009 aptamer instead of the optimized sequence. The rationale behind this choice is that the longer aptamer sequence could potentially induce a more pronounced conformational change upon interaction with thiabendazole, resulting in a more significant alteration in electron flow and, consequently, the current signal. A SPCE/PANI/AuNPs/82mer-BOL009/MCH was fabricated and was dedicated for the interaction test with thiabendazole. The results obtained from this experiment are presented in **Figure III-11a**, providing insights into the effectiveness of the 82mer-BOL009 in capturing thiabendazole and its impact on the electrochemical response.

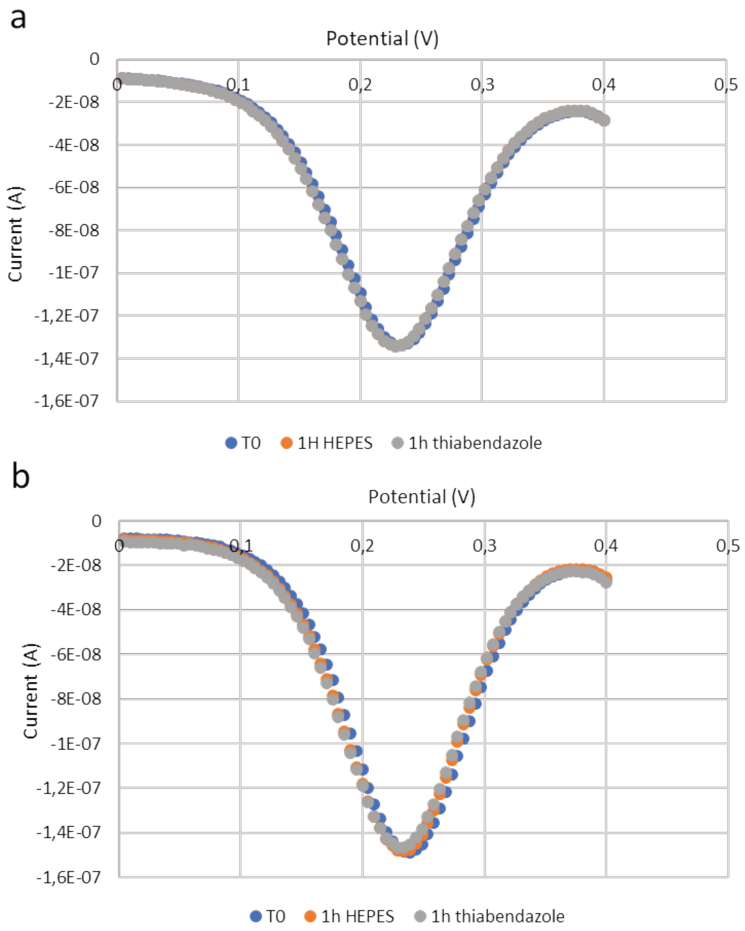

Figure III-11. DPV measurement of SPCE/PANI/AuNPs/82mer-BOL009/MCH immersed 1 hour in HEPES buffer containing 17% MeOH and 80,4 mg L^{-1} thiabendazole. The 82mer-BOL009 was grafted onto AuNPs over (a) 1 hour, and (b) 15 hours.

These findings contribute to our understanding of the role of aptamer length and conformational dynamics in modulating the current signal and have implications for the design and optimization of aptamer-based sensing platforms. As observed in **Figure III-11a**, no interaction of 82mer-BOL009 with thiabendazole occurred as the DPV signal was stable after 1 hour of incubation with thiabendazole. It was found in the literature that aptamers grafted onto AuNPs during the whole night (15 hours) reveal recognition properties[16]. For this purpose, 82mer-BOL009 was grafted over 15 hours onto AuNPs and then used for the interaction test, but similarly to the precedent test, no interaction occurred (**Figure III-11b**).

A last approach consisting in using another redox probe, Ruthenium Hexanol (RuHex) was considered. The fabricated electrode used in this approach is the same as the previous one but without grafted aptamer: SPCE/PANI/AuNPs/MCH (**Figure III-12a)**. RuHex is positively charged, while 82mer-BOL009 is negatively charged due to the phosphate groups. The hypothesis stipulates that RuHex positively charged is attracted by 82mer-BOL009 via electrostatic forces[17], which renders RuHex not available for redox activity, reducing thus the DPV signal after measurements. The last step will be the addition of thiabendazole that interacts with 82mer-BOL009 allowing the switching of RuHex molecules into measurement solution increasing thus DPV signals, and confirming thus the interaction or the detection of thiabendazole (**Figure III-12b).**

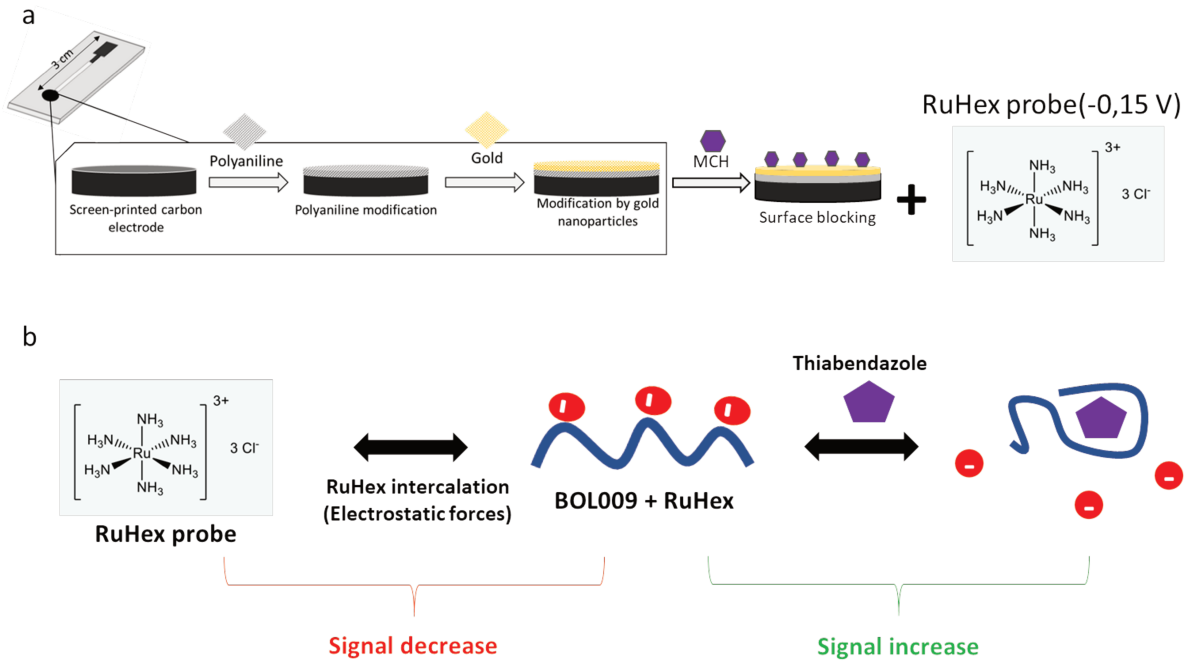

Figure III-12. Schematic illustration of (a) the different steps of fabrication of SPCE/PANI/AuNPs/MCH, and (b) the principle of work of the proposed approach for the detection of thiabendazole.

The appropriate RuHex concentration selection corresponds to the minimum amount of RuHex necessary to achieve a notable signal peak. This peak enables the straightforward identification of signal decrease upon the introduction of the 82-mer BOL009 aptamer into the electrochemical measurement cell, as well as signal increase upon the addition of thiabendazole at the last step (**Figure III-13a**).

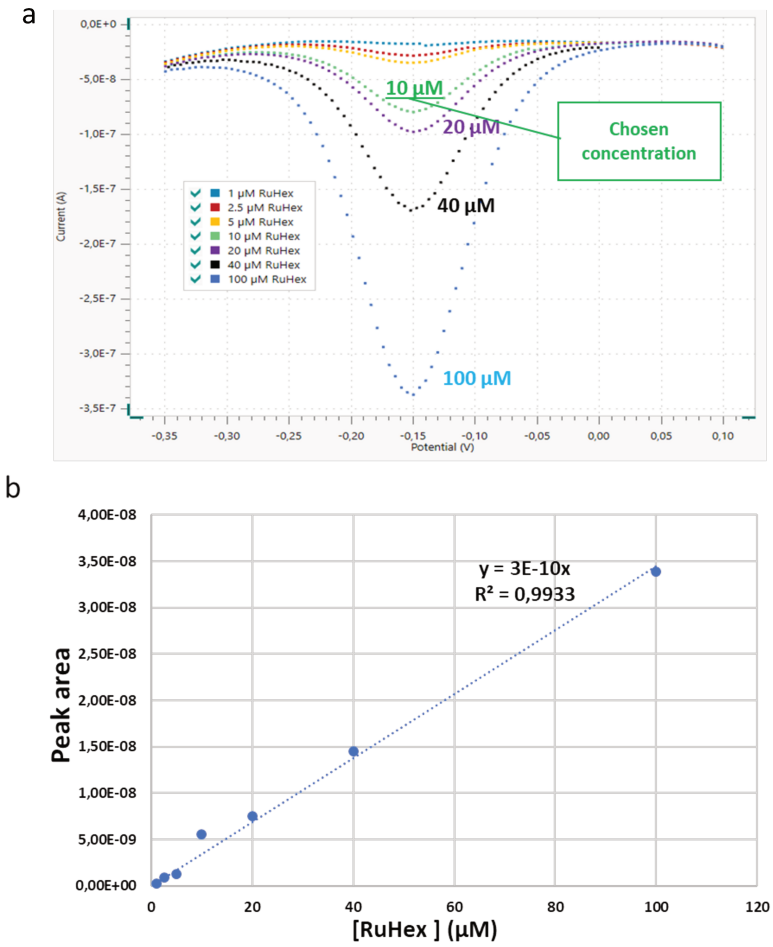

Figure III-13. (a) Differential Pulse Voltammetry (DPV) measurements of RuHex at various concentrations in HEPES buffer, conducted using Nova software. (b) Display of the reduction peaks corresponding to the distinct RuHex concentrations.

As can be observed in **Figure III-13a**, we opted for 10 µM RuHex for the upcoming study due to its optimal sensitivity and clear signal peaks. To verify the link between the current signal and reduction peak area – crucial for confirming that signal reduction indeed relates to the 82-mer BOL009 aptamer and RuHex interaction – we constructed a corresponding curve (**Figure III-13b**). The appearance of a linear relationship here is pivotal, as it allows us to confidently progress. With this validation in hand, we moved forward to the next phase, with which we evaluated the presence of the 82-mer BOL009 aptamer (**Figure III-14**).

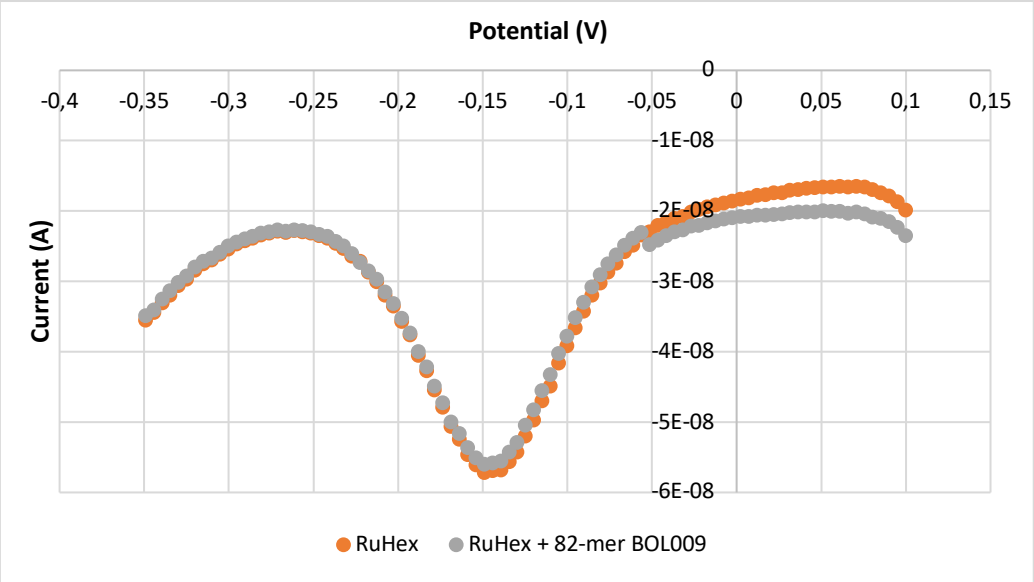

Figure III-14. DPV measurement of SPCE/PANI/AuNPs/MCH immersed 30 min in HEPES buffer containing 10 µM RuHex probe (orange curve), and then immersed for 30 min in the same solution after the addition of 1 µM 82-mer BOL009.

The addition of the BOL009 aptamer didn't lead to any signal decrease, which can be explained by the fact that the RuHex probe can always be functional and transport current either after its attraction by the 82-mer BOL009.

IV. Conclusion

In conclusion, the developed electrochemical aptasensor demonstrated effective detection of thrombin, yet proved less responsive to thiabendazole. The marked difference in molecular size plays a pivotal role in this outcome. The substantial size of thrombin engenders a significant alteration at the electrode surface upon interaction with its aptamer, hindering electron transfer and ultimately resulting in a discernible decrease in the DPV signal. Conversely, thiabendazole's petite molecular dimensions might lead to minimal shifts in the electrode surface properties, potentially caused by only a limited section of the aptamer participating in the interaction. As a result, negligible signal variation was observed. In summary of the electrochemical findings, while electrochemical aptasensors effectively detect larger molecules like thrombin, their efficacy may be limited in detecting smaller compounds such as pesticides due to their distinct molecular sizes.

The limitations of electrochemical aptasensors in detecting thiabendazole underscore the necessity for alternative approaches. In this context, the utilization of an enzymatic digestion

method followed by fluorescence spectroscopy emerges as a promising avenue for enhancing thiabendazole detection.

V. References

(1) Smart, A.; Crew, A.; Pemberton, R.; Hughes, G.; Doran, O.; Hart, J. P. Screen-Printed Carbon Based Biosensors and Their Applications in Agri-Food Safety. *TrAC Trends in Analytical Chemistry* **2020**, *127*, 115898. https://doi.org/10.1016/j.trac.2020.115898.

(2) Wahyuni, W. T.; Putra, B. R.; Fauzi, A.; Ramadhanti, D.; Rohaeti, E.; Heryanto, R. A Brief Review on Fabrication of Screen-Printed Carbon Electrode: Materials and Techniques. *Indonesian Journal of Chemical Research* **2021**, *8* (3), 210–218. https://doi.org/10.30598//ijcr.2021.7-wul.

(3) Taleat, Z.; Khoshroo, A.; Mazloum-Ardakani, M. Screen-Printed Electrodes for Biosensing: A Review (2008–2013). *Microchim Acta* **2014**, *181* (9), 865–891. https://doi.org/10.1007/s00604-014-1181-1.

(4) Shoaie, N.; Daneshpour, M.; Azimzadeh, M.; Mahshid, S.; Khoshfetrat, S. M.; Jahanpeyma, F.; Gholaminejad, A.; Omidfar, K.; Foruzandeh, M. Electrochemical Sensors and Biosensors Based on the Use of Polyaniline and Its Nanocomposites: A Review on Recent Advances. *Microchim Acta* **2019**, *186* (7), 465. https://doi.org/10.1007/s00604-019-3588-1.

(5) Wang, Y. Research Progress on a Novel Conductive Polymer–Poly(3,4-Ethylenedioxythiophene) (PEDOT). *J. Phys.: Conf. Ser.* **2009**, *152* (1), 012023. https://doi.org/10.1088/1742-6596/152/1/012023.

(6) Ramanavičius, A.; Ramanavičienė, A.; Malinauskas, A. Electrochemical Sensors Based on Conducting Polymer—Polypyrrole. *Electrochimica Acta* **2006**, *51* (27), 6025–6037. https://doi.org/10.1016/j.electacta.2005.11.052.

(7) Korent, A.; Soderžnik, K. Ž.; Šturm, S.; Rožman, K. Ž. A Correlative Study of Polyaniline Electropolymerization and Its Electrochromic Behavior. *J. Electrochem. Soc.* **2020**, *167* (10), 106504. https://doi.org/10.1149/1945-7111/ab9929.

(8) Li, B.; Wang, Y.; Wei, H.; Dong, S. Amplified Electrochemical Aptasensor Taking AuNPs Based Sandwich Sensing Platform as a Model. *Biosensors and Bioelectronics* **2008**, *23* (7), 965–970. https://doi.org/10.1016/j.bios.2007.09.019.

(9) Pavlov, V.; Shlyahovsky, B.; Willner, I. Fluorescence Detection of DNA by the Catalytic Activation of an Aptamer/Thrombin Complex. *J. Am. Chem. Soc.* **2005**, *127* (18), 6522–6523. https://doi.org/10.1021/ja050678k.

(10) Radi, A.-E.; Acero Sánchez, J. L.; Baldrich, E.; O'Sullivan, C. K. Reusable Impedimetric Aptasensor. *Anal. Chem.* **2005**, *77* (19), 6320–6323. https://doi.org/10.1021/ac0505775.

(11) Choi, D. Y.; Kim, S.; Oh, J.-W.; Nam, J.-M. Conjugation Strategies of DNA to Gold Nanoparticles. *Bulletin of the Korean Chemical Society* **2022**, *43* (12), 1298–1306. https://doi.org/10.1002/bkcs.12621.

(12) Sosic, A.; Meneghello, A.; Cretaio, E.; Gatto, B. Human Thrombin Detection Through a Sandwich Aptamer Microarray: Interaction Analysis in Solution and in Solid Phase. *Sensors* **2011**, *11* (10), 9426–9441. https://doi.org/10.3390/s111009426.

(13) Liu, Y.; Liu, N.; Ma, X.; Li, X.; Ma, J.; Li, Y.; Zhou, Z.; Gao, Z. Highly Specific Detection of Thrombin Using an Aptamer-Based Suspension Array and the Interaction Analysis via Microscale Thermophoresis. *Analyst* **2015**, *140* (8), 2762–2770. https://doi.org/10.1039/C5AN00081E.

(14) Bai, Y.; Feng, F.; Zhao, L.; Wang, C.; Wang, H.; Tian, M.; Qin, J.; Duan, Y.; He, X. Aptamer/Thrombin/Aptamer-AuNPs Sandwich Enhanced Surface Plasmon Resonance Sensor for the Detection of Subnanomolar Thrombin. *Biosensors and Bioelectronics* **2013**, *47*, 265–270. https://doi.org/10.1016/j.bios.2013.02.004.

(15) Bock, L. C.; Griffin, L. C.; Latham, J. A.; Vermaas, E. H.; Toole, J. J. Selection of Single-Stranded DNA Molecules That Bind and Inhibit Human Thrombin. *Nature* **1992**, *355* (6360), 564–566. https://doi.org/10.1038/355564a0.

(16) Liu, J.; Lu, Y. Preparation of Aptamer-Linked Gold Nanoparticle Purple Aggregates for Colorimetric Sensing of Analytes. *Nat Protoc* **2006**, *1* (1), 246–252. https://doi.org/10.1038/nprot.2006.38.

(17) Grubb, M.; Wackerbarth, H.; Wengel, J.; Ulstrup, J. Direct Imaging of Hexaamine-Ruthenium(III) in Domain Boundaries in Monolayers of Single-Stranded DNA. *Langmuir* **2007**, *23* (3), 1410–1413. https://doi.org/10.1021/la062555z.

Chapter IV. Rapid and specific detection of thiabendazole: Enzymatic digestion-enabled fluorescent aptasensor

Résumé

D'après les résultats obtenus au cours de nos recherche, l'aptacapteur électrochimique s'est révélé inadapté à la détection du thiabendazole, considéré comme une petite molécule, comme détaillé dans les hypothèses du chapitre précédent. Pour explorer une méthode de détection alternative du thiabendazole, nous avons étudié la digestion enzymatique suivie par spectroscopie de fluorescence. Nous avons suivi un protocole similaire à celui décrit dans le premier chapitre, à l'exception de l'utilisation du mélange Exo I et T5 Exo qui a été remplacé par l'Exo I seule vu qu'elle est plus performante et a fourni des résultats plus homogènes grâce à sa capacité à digérer complètement les oligonucléotides en mononucléotides non fluorescents.

Dans ce chapitre, nous avons d'abord entrepris une évaluation de l'impact du thiabendazole sur l'activité de l'Exo I avant de nous plonger dans l'analyse de l'interaction entre le BOL009 et le thiabendazole. Une fois l'intégrité de l'activité de l'Exo I confirmée en présence du thiabendazole, nous avons approfondi notre étude de l'interaction entre le thiabendazole et le BOL009. En conclusion de cette étude, nous avons soigneusement évalué la spécificité de la réduction de l'activité enzymatique attribuable au thiabendazole, tout en déterminant la plage de linéarité permettant la détection précise du thiabendazole.

Ce travail représente une avancée significative dans le domaine de la détection des pesticides en utilisant la digestion enzymatique et la spectroscopie de fluorescence. En conséquence, nous envisageons de soumettre ce travail à la revue "*Chemical Communications*" pour publication.

Summary

According to the outcomes of our research activities, the electrochemical aptasensor has proven to be unsuitable for detecting thiabendazole, considering its small size, as detailed in the hypotheses of the previous chapter. To explore an alternative method for thiabendazole detection, we investigated enzymatic digestion detected by fluorescence spectroscopy. We followed a protocol similar to that described in the first chapter, with the exception of using Exo I alone instead of the Exo I and T5 Exo mixture, as it demonstrated better performance and provided more consistent results by fully digesting oligonucleotides into non-fluorescent mononucleotides in presence of SYBR Gold.

In this chapter, we initially assessed the impact of thiabendazole on the activity of Exo I before delving into the analysis of the interaction between BOL009 and thiabendazole. Once we confirmed the integrity of Exo I's activity in the presence of thiabendazole, we deeply studied the interaction between thiabendazole and BOL009. Overall, we carefully evaluated the specificity of the reduction in enzymatic activity attributed to thiabendazole, while determining the linear range for precise thiabendazole detection.

This work represents a significant advancement in the field of pesticide detection using enzymatic digestion and fluorescence spectroscopy. As a result, we intend to submit this work to the journal "Chemical Communications" for publication.

Table of Contents

Chapter IV. Rapid and specific detection of thiabendazole: Enzymatic digestion-enabled fluorescent aptasensor

*Mohamed Amine Berkal, Jean-Jacques Toulmé, Corinne Nardin**

M. A. Berkal, C. Nardin

Universite de Pau et des Pays de l'Adour, E2S UPPA, CNRS, IPREM, Pau, France

E-mail: corinne.nardin@univ-pau.fr

J. J. Toulmé

ARNA Laboratory, Inserm U1212, CNRS UMR5320, University of Bordeaux, 33076 Bordeaux, France

Novaptech, 146 rue Léo Saignat, 33076 Bordeaux, France

Keywords: Thiabendazole, oligonucleotide switching structures, enzymatic digestion, fluorescence spectroscopy, biosensing

ABSTRACT**:** Thiabendazole, a broad-spectrum fungicide extensively employed in agriculture across various species ranging from tropical crops to cereals, poses a potential risk to human health due to its residual presence. To monitor the presence of thiabendazole in water, we propose a fluorescent aptasensor based on exonuclease I (Exo I) activity, which combines an aptamer and a fluorescence detection platform. The outcomes of our study show a linear correlation between thiabendazole concentrations and Exo I digestion percentage with a limit LOD exceeding 0.2 mg L^{-1} and a determination coefficient (R^2) of 0.959. The developed aptasensor has also been shown to be specific to thiabendazole among other pesticides with similar properties. This detection system, by combining aptamer and fluorescence spectroscopy, allows for rapid, specific and sensitive detection of thiabendazole, and of the potential to analyze other contaminants in food matrices.

I. INTRODUCTION

Pesticides play a crucial role in agriculture by enhancing crop yields and ensuring adequate food production levels. Since their introduction, they have yielded significant economic advantages and are thus extensively utilized[1]. Nevertheless, their extensive utilization has an impact on both our well-being[2–5] and on our environment[6,7]. Thiabendazole is a widely used fungicide to prevent fruits, such as citrus, apples, and pears, from being affected by mold, rot, and blight, thus keeping them fresh before the waxing stage for storage[8]. Even though thiabendazole is of low toxicity in comparison to other pesticides, it has been associated with a range of harmful effects, including nephrotoxicity, hepatotoxicity, carcinogenicity, and teratogenicity[9]. As a result, the U.S. Environmental Protection Agency (EPA) has classified thiabendazole as potentially carcinogenic, particularly at doses that disrupt the balance of thyroid hormones[10]. Consequently, there is a need to develop rapid and sensitive methods for detecting thiabendazole in agricultural and food products to safeguard the health of consumers. Generally, identification and quantification of pesticides, including thiabendazole, are based on chromatographic methods, such as high-performance liquid chromatography (HPLC) and gas chromatography (GC) coupled with mass spectrometry (MS)[11–13]. These techniques are highly sensitive and specific. However, they do not allow real-time analysis as they require lengthy sample preparation steps, in addition to highly skilled technical labor, which makes the analysis expensive.

To meet the requirements of selectivity and sensitivity for thiabendazole detection, there have been increasing efforts to explore alternative measures. Biosensors are promising tools that could potentially replace conventional methods, as they enable the real-time detection of analytes while minimizing the need for tedious sample pretreatments.

Biosensors, which combine a biological sensing element and a transducer, are a promising alternative to traditional laboratory-based methods. Biological sensing elements such as antibodies, enzymes, aptamers, or cells ensure specificity and selectivity[14], whereas the transducer provides sensitivity by converting the biological interaction into an electrical signal for analyte detection. Optical and electrochemical-based biosensors are particularly attractive for pesticide detection due to their potential selectivity and sensitivity[15–18]. These biosensors employ various methods including absorption (UV-Vis) spectroscopy[19,20], fluorescence spectroscopy[21,22], photoluminescence assay[23,24], chemiluminescence assay[25,26], surface-enhanced Raman scattering (SERS)[27,28], potentiometric sensing[29], impedance sensing[30,31], and

amperometry[32,18]. However, only a few biosensors developed for pesticide detection have been applied to thiabendazole[33–36] (**Table IV-1)**, and none of them are currently suitable for in situ detection.

Table IV-1. Biosensor developed against thiabendazole.

Transduction	Sensing element	LOD	Validity for real samples	References
White light Reflectance Spectroscopy (WLRS)	Antibody	0.8 µg L^{-1}	Wine	Koukouvinos et al. (2017)[33]
Surface Plasmon Resonance (SPR)	Antibody	0.05 mg L^{-1}	Phosphate-Buffered Saline (PBS)	Belenguer et al. (2010)[34]
SPR	Antibody	0.13 µg L^{-1}	Orange	Estevez et al. (2012)[35]
Strip-based assay (colorimetry)	Antibody	0.08 µg L^{-1}	Fruit juices	Blazková et al. (2010)[36]
Fluorescence spectroscopy	Aptamer	0.2 mg L^{-1}	Buffer	This work

We present here a novel approach for the specific detection of thiabendazole using a fluorometric aptasensor based on the exonuclease I (Exo I) enzymatic digestion. The biosensor is composed of an aptamer sensing element and a fluorescence detection platform, offering high specificity and sensitivity. Aptamers, which are oligonucleotide switching structures, form a complex with the target with high affinity and specificity[37,38]. In our study, we tested the interaction between thiabendazole and its aptamer (BOL009), developed by Novaptech, using enzymatic digestion by Exo I. The activity of Exo I is commonly used to demonstrate the specific interaction between a ligand and an oligonucleotide switching structure[39–43]. We observed that Exo I digests the aptamer into mononucleotides, and in the presence of thiabendazole, a BOL009/thiabendazole complex is formed, leading to a decrease in Exo I activity, thereby allowing the detection of thiabendazole. The whole analysis process of thiabendazole using the developed fluorescence aptasensor requires 2 hours, and the detection showed to be specific to thiabendazole. Thrombin target was also studied in order to test the application of this fluorescence aptasensor for the detection of other targets against which an aptamer exists. The results obtained showed the suitability of this system to detect thrombin. These findings demonstrate the potential of our biosensor for the simple, rapid and specific detection of various targets using their respective aptamers.

II. Experimental Section

II.1. Chemicals and Reagents

All the chemicals and reagents were of analytical grade (> 99%) and used without further purification. Tris(hydroxymethyl)aminomethane (Tris-HCl), sodium chloride (NaCl), sodium acetate (CH_3CO_2Na), potassium chloride (KCl), potassium acetate (CH_3CO_2K), magnesium acetate tetrahydrate ($CH_3CO_22Mg4H_2O$), hydrochloric acid (HCl), sodium hydroxide (NaOH), magnesium chloride hexahydrate ($MgCl_26H_2O$), ethylenediaminetetraacetic acid (EDTA), and sodium dodecyl sulfate 4X (SDS) were purchased from Euromedex (Strasbourg, France). Ethanol (EtOH) and methanol (MeOH), were purchased from VWR Chemicals (Radnor, Pennsylvania, USA). Thiabendazole, glyphosate, aminomethylphosphonic acid (AMPA) and atrazine were purchased from Sigma Aldrich (St. Louis, MO, USA). SYBR Gold was purchased from Invitrogen (Thermo Fischer Scientific, Waltham, Massachusetts, USA). 4-(2-hydroxyethyl)-1-piperazine ethane sulfonic acid (HEPES) was purchased from Pan Reac Application (ITW Reagents, Castellar del Vallès, Spain). Exo I (20000 U mL^{-1}) was purchased from New England Biolabs (Ipswich, Massachusetts, USA).

II.2. Oligonucleotides

All oligonucleotides used in this work were synthesized by Eurogentec (Seraing, Belgium) with polyacrylamide gel electrophoresis (PAGE) purification grade. The oligonucleotides were dissolved in MilliQ water and the concentrations were measured by UV-Vis spectroscopy using the Nanodrop 2000 spectrometer (Mettler Toledo, Columbus, Ohio, USA).

II.3. Inhibition control test

Exo I is inhibited by glyphosate in particular conditions as described by Berkal et al.[44]. In order to assess whether thiabendazole inhibits the activity of Exo I, a verification test was performed using the glyphosate aptamer[45] (GLY3, **Table IV-2**).

Table IV-2. The sequence of glyphosate aptamer used to study the inhibition of Exo I activity by thiabendazole.

Aptamer name	Sequence
GLY3 aptamer[45]	5'-TGC-TAG-ACG-ATA-TTC-GTC-CAT-CCG-AGC-CCG-TGG-CGG-GCT-TTA-GGA-CTC-TGC-GGG-CTT-CGCGGC-GCT-GTC-AGA-CTG-AAT-ATG-TCA-3'

Thrombin aptamer	5'-CCA-ACG-GTT-GGT-GTG-GTT-GG-3'

II.4. Experimental conditions

The enzymatic digestion was performed using a thermomixer (Eppendorf, Hamburg, Germany).

Enzymatic digestion was performed at 37 °C with stirring (240 rpm). In each experiment, the buffer described in **Table IV-3** was used with its corresponding aptamer, BOL009. All experiments were performed in duplicate or triplicate. The standard deviations are presented in the form of error bars. The pH of all buffers was measured with a Seveneasy pH meter (Mettler Toledo, Columbus, Ohio, USA) and was adjusted using either a 1 M NaOH solution or a 0.1 M HCl solution.

Table IV-3. Incubation conditions of thiabendazole with BOL009.

Aptamer	**Target**	**HEPES buffer composition**	**Interaction conditions**
BOL009	Thiabendazole	20 mM HEPES, 20 mM CH_3CO_2Na, 140 mM CH_3CO_2K, 3 $CH_3CO_22Mg4H_2O$ mM and 17% MeOH	1- Incubate BOL009 in HEPES buffer for 30 min at room temperature 2- Add thiabendazole and incubate 30 min at room temperature under gentle stirring in HEPES buffer
Thrombin aptamer	Thrombin	20 mM Tris-HCL, 120 mM NaCl, 1 mM MgCl2 et 10 mM KCL, pH 7,4.	1- Incubate thrombin aptamer in Tris buffer for 30 min at room temperature. 2- Add thrombin and incubate for 60 min at 25 °C under gentle stirring in Tris buffer.

II.5. Exonuclease I digestion and fluorescence spectroscopy

The interaction between the aptamer and its target results in delayed digestion of the oligonucleotide due to the formation of an aptamer/target complex impeding the enzymatic digestion[39–43]. The working principle of this method is described in **Figure IV-1**.

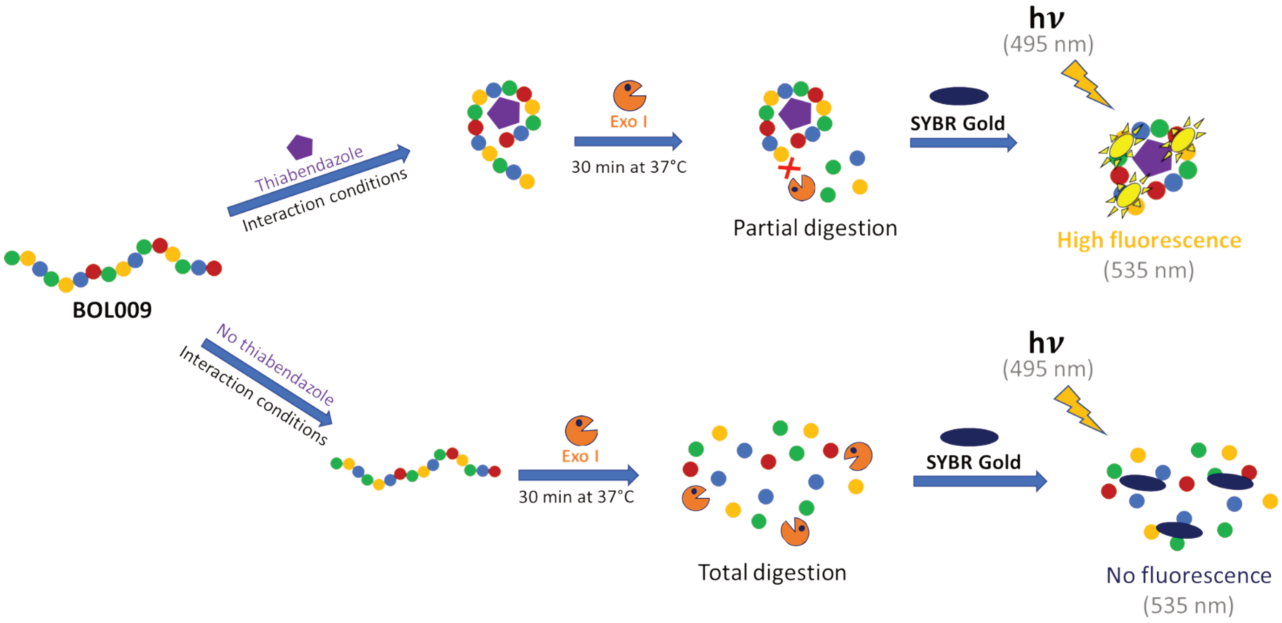

Figure IV-1. Principle of BOL009/thiabendazole interaction analysis using Exo I, followed by fluorescence spectroscopy.

In order to analyze the interaction of BOL009 with thiabendazole, the following experiment was performed: 10 µL of 10 µM BOL009 were drawn off and mixed with 90 µL of interaction buffer containing 17% MeOH. The whole set is incubated for 30 min at room temperature. The thiabendazole is then added to the reaction medium with a final concentration of 0.2 g L^{-1} and incubated for 30 min at room temperature. A control sample that doesn't contain thiabendazole is prepared as well. Once the incubation is finished, an optimized concentration of Exo I (C_f = 0.6 U μL^{-1}) is added to the reaction medium, and digestion is started at 37 °C for 30 min with gentle stirring in the thermomixer (Eppendorf, Hamburg, Germany). At the end of digestion, 5 µL of the samples were drawn off and loaded into the wells of a black 384-well microplate (Corning black, Thermo Fischer Scientific) containing 25 µL of stop solution (1.2X SYBR Gold, 12 mM Tris-HCl pH = 7.4, 48% formamide (v/v), 3.75 mM EDTA). Fluorescence was measured at 535 nm after excitation at 495 nm (Tecan Infinite M1000 Pro, Männedorf,

Switzerland). Fluorescence intensity is converted to the digestion yield via **Equation II-1**. The yield of digestion is lower when the target protects its aptamer.

II.6. Application of the enzymatic digestion method to detect other targets

The thrombin protein was considered in order to verify whether the enzymatic digestion method is applicable for the detection of other targets. The aptamer sequence is given in **Table IV-2**, and the interaction conditions are described in **Table IV-3**. The same protocol as described in **II.5** is applied for the detection of thrombin, considering the interaction conditions described below.

III. Results and Discussion

III.1. Inhibition of Exo I by thiabendazole

To assess the interaction between thiabendazole and BOL009, conventional fluorescence spectroscopy was used to follow Exo I digestion. However, it is well-established that pesticides can inhibit the activity of some enzymes, including AChE, butyrylcholinesterase (BChE)[54], tyrosinase[55,56], alkaline phosphatase[57,58], peroxidase[52], acid phosphatase[51,52], urease[36] and most recently Exonuclease I[44].

Therefore, prior to analyzing the interaction, it is essential to confirm that thiabendazole does not inhibit the activity of Exo I. For this purpose, since the glyphosate aptamer is not expected to interact with thiabendazole, we conducted glyphosate aptamer digestion by Exo I in the presence and absence of thiabendazole (**Figure IV-2**). The optimization of Exo I concentration was performed at first in order to reach the highest yield of GLY3 digestion possible (**Figure IV-S1**). The maximal percentage of digestion was obtained with 0.6 U μL^{-1}, it is therefore this concentration value which is selected to conduct the inhibition test.

As observed in **Figure IV-2**, Exo I performs over 80% of digestion in the presence and absence of thiabendazole which proves that Exo I is not inhibited by thiabendazole.

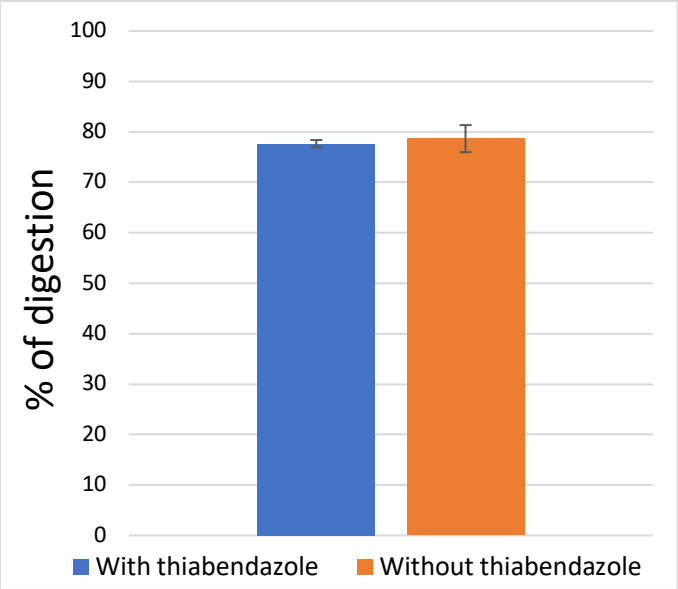

Figure IV-2. Digestion of glyphosate aptamer by Exo I in the presence and absence of 0.2 g L^{-1} thiabendazole.

III.2. Exo I digestion as a route for thiabendazole/BOL009 interaction analysis

Enzymatic digestion prior to fluorescence spectroscopy is widely used to analyze the interaction between an aptamer and its target[47–51]. As performed with the GLY3 aptamer, an optimization of Exo I concentration was done first with the BOL009 aptamer (**Figure IV-S2**).

Figure IV-S2 shows that 0.6 U µL is sufficient for the enzyme to achieve almost 95% of digestion, and it is, therefore, this concentration value that is chosen for BOL009 aptamer digestion analyses.

Figure IV-3 shows the percentage of digestion obtained upon enzymatic digestion of BOL009 by Exo I in the presence and the absence of 0.2 g L^{-1} thiabendazole.

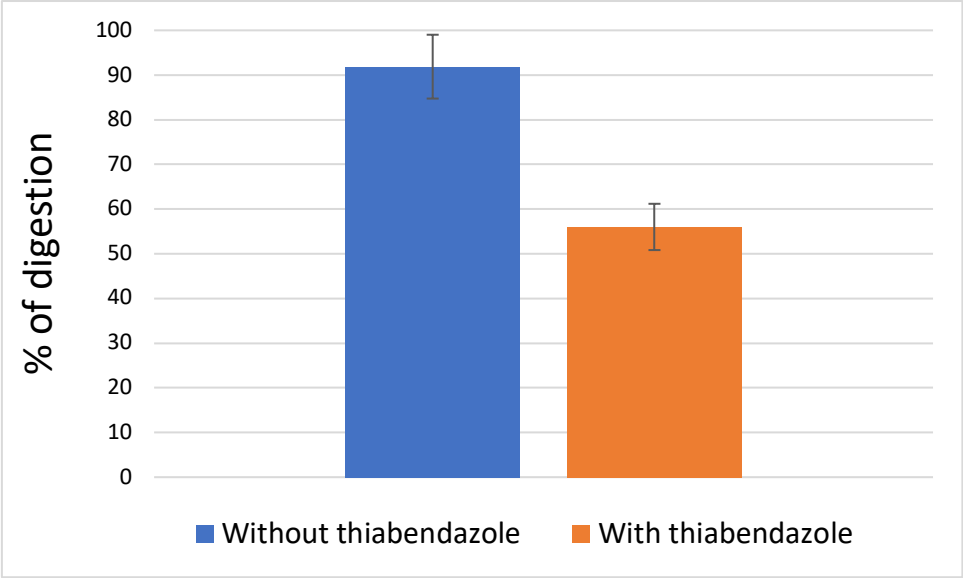

Figure IV-3. Digestion of BOL009 (1 µM) by Exo I (0.6 U µL-1) for 30 min at 37 °C in HEPES buffer in the presence and the absence of thiabendazole at 0.2 g L^{-1}.

The Exo I performs 92% of BOL009 digestion in the conditions described above, but only 56% in the presence of thiabendazole. The present experiment provides evidence that the presence of thiabendazole has a significant impact on the activity of Exo I digestion. Specifically, the results demonstrate that the activity of Exo I digestion is reduced in the presence of thiabendazole. This enzymatic activity reduction is directly related to the formation of a complex between BOL009 and thiabendazole. These findings provide confirmation that there is an interaction between BOL009 and thiabendazole, and that this interaction plays a critical role in modulating the activity of Exo I digestion.

III.3. Detection of thiabendazole using fluorescence spectroscopy in combination with Exo I digestion

After confirming the interaction between BOL009 and thiabendazole, we were able to detect thiabendazole using the method we are proposing. The reduction in enzymatic activity is directly proportional to the number of complexes formed between BOL009 and thiabendazole. Therefore, an increase in the number of complexes is expected to lead to a greater reduction in Exo I activity. Using these findings, we were able to detect thiabendazole by adding higher concentrations of the compound.

We conducted therefore an experiment in which BOL009 was digested at various concentrations of thiabendazole (0, 0.2, 2, 4, 8, 12, 16, and 20 mg L^{-1}) under the same conditions as described in materials and methods (**Figure IV-4**).

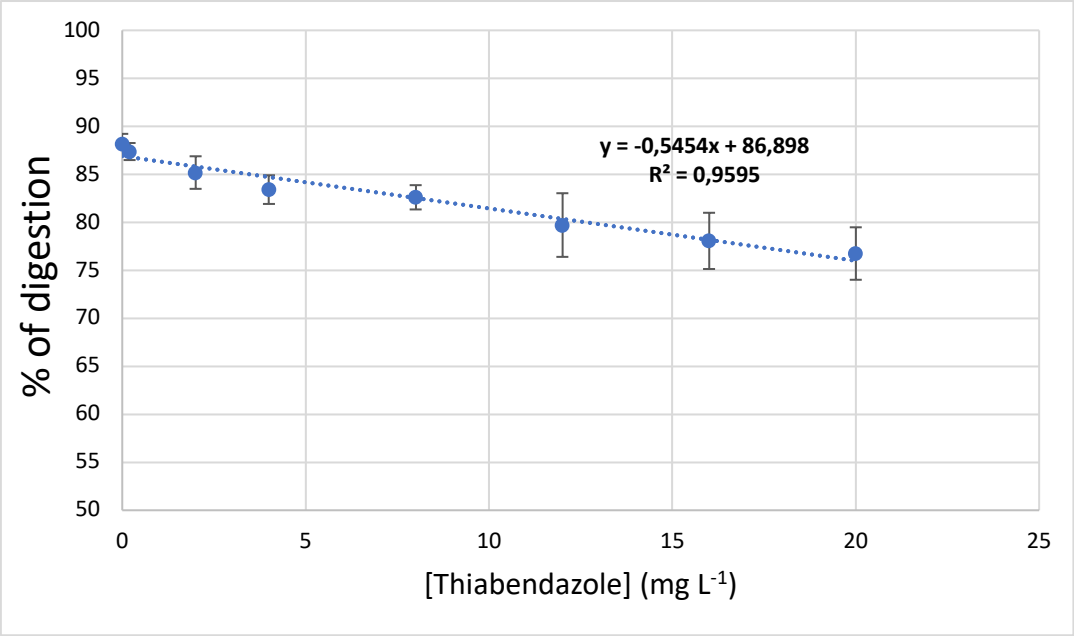

Figure IV-4. Digestion of BOL009 at 1 µM by Exo I (0.6 U µL-1) at 37 °C for 30 min in HEPES buffer in the presence of different concentrations of thiabendazole.

The results observed in **Figure IV-4** demonstrate that the concentration of thiabendazole has a direct impact on the activity of Exo I, resulting in a decrease in digestion efficiency. Our findings show that the reduction in enzymatic activity occurs within a linear range of 0 to 20 mg L^{-1} of thiabendazole concentrations, with a limit of detection of about 0.2 mg L^{-1}.

III.4. Specificity of interaction of BOL009 with thiabendazole

Is the interaction of the BOL009 aptamer specific to thiabendazole? In order to answer this question, other pesticide molecules, especially carbendazim that has a similar structure as thiabendazole with a benzimidazole group, were tested: glyphosate, aminomethylphosphonic acid (AMPA), simazine, atrazine, isoproturon and atrazine-desethyl.

Figure IV-5 shows the percentage of digestion of the BOL009 by Exo I in the absence and in presence of these pesticides.

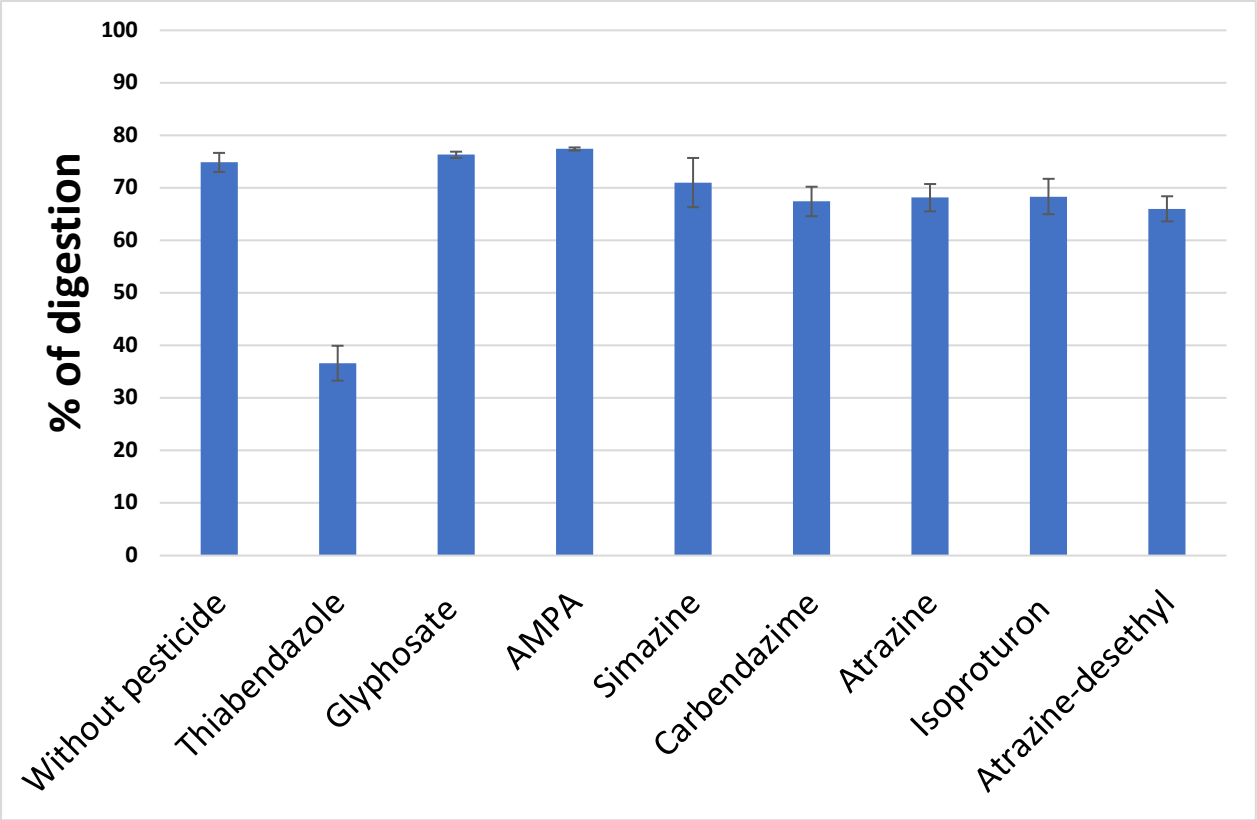

Figure IV-5. Digestion of BOL009 at 1 µM by Exo I (0.6 U µL^{-1}) at 37 °C for 30 min in HEPES buffer in the absence and the presence of different pesticide molecules at 1 mM.

As observed in **Figure IV-5**, only thiabendazole shows a significant reduction of Exo I activity, which means that the interaction with BOL009 aptamer is specific to thiabendazole.

III.5. Applicability of the enzymatic digestion method on another target

In order to verify whether the enzymatic digestion method is applicable for the detection of other target, the detection of thrombin molecule was tested. It should be recalled that the thrombin aptamer is a short 20-mer sequence, whereas thrombin is a large molecule. **Figure IV-6** shows the result of the interaction tests obtained.

Figure IV-6. Digestion of thrombin aptamer (1 µM) by Exo I (0.6 U µL^{-1}) for 30 min at 37 °C in Tris buffer in the presence and the absence of thrombin at 0.1 mM.

In the presence of thrombin, enzymatic digestion is reduced (52% of digestion) compared to the same condition without thrombin in which enzymatic digestion is optimal (97% of digestion).

This result shows clearly that the enzymatic digestion method is applicable to any target for which a specific aptamer has been selected and optimized.

IV. Conclusion

In conclusion, the findings of this study demonstrate the successful interaction of BOL009 aptamer with thiabendazole, resulting in a specific reduction of Exo I activity, as determined by fluorescence spectroscopy. This decrease in enzymatic activity is attributed to the formation of the BOL009/thiabendazole complex, indicating the high sensitivity and specificity of our method in detecting thiabendazole at low concentrations. Therefore, our approach offers a valuable rapid tool for the accurate detection of thiabendazole in various samples, with potential applications in food safety monitoring, environmental analysis, and pharmaceutical quality control. Furthermore, this method could be applied for the detection of any target for which a specific aptamer has been selected and optimized as demonstrated for thrombin which is a big protein recognized by a short sequence aptamer.

Acknowledgements:

We acknowledge grants from the Universite de Pau et de Pays de l'Adour through its project Energy and Environment Solutions supported by the Agence National pour la recherche (ANR OPE-2018-0020) and the Communauté d'agglomération de Pau Béarn Pyrénées (CDAPBP, OPE-2020-0032) and from the Région Nouvelle Aquitaine (CONV-2019-0227)

.

V. References

(1) Cooper, J.; Dobson, H. The Benefits of Pesticides to Mankind and the Environment. *Crop Protection* **2007**, *26* (9), 1337–1348. https://doi.org/10.1016/j.cropro.2007.03.022.

(2) Koutros, S.; Lynch, C. F.; Ma, X.; Lee, W. J.; Hoppin, J. A.; Christensen, C. H.; Andreotti, G.; Freeman, L. B.; Rusiecki, J. A.; Hou, L.; Sandler, D. P.; Alavanja, M. C. R. Heterocyclic Aromatic Amine Pesticide Use and Human Cancer Risk: Results from the U.S. Agricultural Health Study. *International Journal of Cancer* **2009**, *124* (5), 1206–1212. https://doi.org/10.1002/ijc.24020.

(3) Amr, S.; Dawson, R.; Saleh, D. A.; Magder, L. S.; St. George, D. M.; El-Daly, M.; Squibb, K.; Mikhail, N. N.; Abdel-Hamid, M.; Khaled, H.; Loffredo, C. A. Pesticides, Gene Polymorphisms, and Bladder Cancer Among Egyptian Agricultural Workers. *Archives of Environmental & Occupational Health* **2015**, *70* (1), 19–26. https://doi.org/10.1080/19338244.2013.853646.

(4) Alavanja, M. C. R.; Dosemeci, M.; Samanic, C.; Lubin, J.; Lynch, C. F.; Knott, C.; Barker, J.; Hoppin, J. A.; Sandler, D. P.; Coble, J.; Thomas, K.; Blair, A. Pesticides and Lung Cancer Risk in the Agricultural Health Study Cohort. *American Journal of Epidemiology* **2004**, *160* (9), 876–885. https://doi.org/10.1093/aje/kwh290.

(5) Beane Freeman, L. E.; Bonner, M. R.; Blair, A.; Hoppin, J. A.; Sandler, D. P.; Lubin, J. H.; Dosemeci, M.; Lynch, C. F.; Knott, C.; Alavanja, M. C. R. Cancer Incidence among Male Pesticide Applicators in the Agricultural Health Study Cohort Exposed to Diazinon. *American Journal of Epidemiology* **2005**, *162* (11), 1070–1079. https://doi.org/10.1093/aje/kwi321.

(6) Kole, R. K.; Banerjee, H.; Bhattacharyya, A. Monitoring of Market Fish Samples for Endosulfan and Hexachlorocyclohexane Residues in and Around Calcutta. *Bull. Environ. Contam. Toxicol.* **2001**, *67* (4), 554–559. https://doi.org/10.1007/s001280159.

(7) *USGS Scientific Investigations Report 2009-5132: Trends in Pesticide Concentrations in Corn-Belt Streams, 1996–2006*. https://pubs.usgs.gov/sir/2009/5132/ (accessed 2021-10-22).

(8) Alsammarraie, F. K.; Lin, M.; Mustapha, A.; Lin, H.; Chen, X.; Chen, Y.; Wang, H.; Huang, M. Rapid Determination of Thiabendazole in Juice by SERS Coupled with Novel

Gold Nanosubstrates. *Food Chemistry* **2018**, *259*, 219–225. https://doi.org/10.1016/j.foodchem.2018.03.105.

(9) Jamieson, J. D.; Smith, E. B.; Dalvie, D. K.; Stevens, G. J.; Yanochko, G. M. Myeloperoxidase-Mediated Bioactivation of 5-Hydroxythiabendazole: A Possible Mechanism of Thiabendazole Toxicity. *Toxicology in Vitro* **2011**, *25* (5), 1061–1066. https://doi.org/10.1016/j.tiv.2011.04.007.

(10) P100N28R.Pdf. https://nepis.epa.gov/Exe/ZyPDF.cgi/P100N28R.PDF?Dockey=P100N28R.PDF (accessed 2023-04-26).

(11) Rial-Otero, R.; Gaspar, E. M.; Moura, I.; Capelo, J. L. Chromatographic-Based Methods for Pesticide Determination in Honey: An Overview. *Talanta* **2007**, *71* (2), 503–514. https://doi.org/10.1016/j.talanta.2006.05.033.

(12) van der Hoff, G. R.; van Zoonen, P. Trace Analysis of Pesticides by Gas Chromatography. *Journal of Chromatography A* **1999**, *843* (1–2), 301–322. https://doi.org/10.1016/S0021-9673(99)00511-7.

(13) Núñez, O.; Moyano, E.; Galceran, M. T. LC–MS/MS Analysis of Organic Toxics in Food. *TrAC Trends in Analytical Chemistry* **2005**, *24* (7), 683–703. https://doi.org/10.1016/j.trac.2005.04.012.

(14) Sharma, S. K.; Sehgal, N.; Kumar, A. Biomolecules for Development of Biosensors and Their Applications. *Current Applied Physics* **2003**, *3* (2–3), 307–316. https://doi.org/10.1016/S1567-1739(02)00219-5.

(15) Pang, S.; Yang, T.; He, L. Review of Surface Enhanced Raman Spectroscopic (SERS) Detection of Synthetic Chemical Pesticides. *TrAC Trends in Analytical Chemistry* **2016**, *85*, 73–82. https://doi.org/10.1016/j.trac.2016.06.017.

(16) Chen, N.; Liu, H.; Zhang, Y.; Zhou, Z.; Fan, W.; Yu, G.; Shen, Z.; Wu, A. A Colorimetric Sensor Based on Citrate-Stabilized AuNPs for Rapid Pesticide Residue Detection of Terbuthylazine and Dimethoate. *Sensors and Actuators B: Chemical* **2018**, *255*, 3093–3101. https://doi.org/10.1016/j.snb.2017.09.134.

(17) Luo, Q.; Yu, F.; Yang, F.; Yang, C.; Qiu, P.; Wang, X. A 3D-Printed Self-Propelled, Highly Sensitive Mini-Motor for Underwater Pesticide Detection. *Talanta* **2018**, *183*, 297–303. https://doi.org/10.1016/j.talanta.2018.02.059.

(18) Vinoth Kumar, J.; Karthik, R.; Chen, S.-M.; Natarajan, K.; Karuppiah, C.; Yang, C.-C.; Muthuraj, V. 3D Flower-Like Gadolinium Molybdate Catalyst for Efficient Detection and Degradation of Organophosphate Pesticide (Fenitrothion). *ACS Appl. Mater. Interfaces* **2018**, *10* (18), 15652–15664. https://doi.org/10.1021/acsami.8b00625.

(19) Abnous, K.; Danesh, N. M.; Ramezani, M.; Alibolandi, M.; Emrani, A. S.; Lavaee, P.; Taghdisi, S. M. A Colorimetric Gold Nanoparticle Aggregation Assay for Malathion Based on Target-Induced Hairpin Structure Assembly of Complementary Strands of Aptamer. *Microchim Acta* **2018**, *185* (4), 216. https://doi.org/10.1007/s00604-018-2752-3.

(20) Palanivelu, J.; Chidambaram, R. Acetylcholinesterase with Mesoporous Silica: Covalent Immobilization, Physiochemical Characterization, and Its Application in Food for Pesticide Detection. *Journal of Cellular Biochemistry* **2019**, *120* (6), 10777–10786. https://doi.org/10.1002/jcb.28369.

(21) Long, Q.; Li, H.; Zhang, Y.; Yao, S. Upconversion Nanoparticle-Based Fluorescence Resonance Energy Transfer Assay for Organophosphorus Pesticides. *Biosensors and Bioelectronics* **2015**, *68*, 168–174. https://doi.org/10.1016/j.bios.2014.12.046.

(22) Lin, B.; Yu, Y.; Li, R.; Cao, Y.; Guo, M. Turn-on Sensor for Quantification and Imaging of Acetamiprid Residues Based on Quantum Dots Functionalized with Aptamer. *Sensors and Actuators B: Chemical* **2016**, *229*, 100–109. https://doi.org/10.1016/j.snb.2016.01.114.

(23) Sahub, C.; Tuntulani, T.; Nhujak, T.; Tomapatanaget, B. Effective Biosensor Based on Graphene Quantum Dots via Enzymatic Reaction for Directly Photoluminescence Detection of Organophosphate Pesticide. *Sensors and Actuators B: Chemical* **2018**, *258*, 88–97. https://doi.org/10.1016/j.snb.2017.11.072.

(24) Zor, E.; Morales-Narváez, E.; Zamora-Gálvez, A.; Bingol, H.; Ersoz, M.; Merkoçi, A. Graphene Quantum Dots-Based Photoluminescent Sensor: A Multifunctional Composite for Pesticide Detection. *ACS Appl. Mater. Interfaces* **2015**, *7* (36), 20272–20279. https://doi.org/10.1021/acsami.5b05838.

(25) He, L.; Jiang, Z. W.; Li, W.; Li, C. M.; Huang, C. Z.; Li, Y. F. In Situ Synthesis of Gold Nanoparticles/Metal–Organic Gels Hybrids with Excellent Peroxidase-Like Activity for Sensitive Chemiluminescence Detection of Organophosphorus Pesticides. *ACS Appl. Mater. Interfaces* **2018**, *10* (34), 28868–28876. https://doi.org/10.1021/acsami.8b08768.

(26) Ouyang, H.; Tu, X.; Fu, Z.; Wang, W.; Fu, S.; Zhu, C.; Du, D.; Lin, Y. Colorimetric and Chemiluminescent Dual-Readout Immunochromatographic Assay for Detection of Pesticide Residues Utilizing g-C3N4/BiFeO3 Nanocomposites. *Biosensors and Bioelectronics* **2018**, *106*, 43–49. https://doi.org/10.1016/j.bios.2018.01.033.

(27) Liu, B.; Zhou, P.; Liu, X.; Sun, X.; Li, H.; Lin, M. Detection of Pesticides in Fruits by Surface-Enhanced Raman Spectroscopy Coupled with Gold Nanostructures. *Food Bioprocess Technol* **2013**, *6* (3), 710–718. https://doi.org/10.1007/s11947-011-0774-5.

(28) Mu, T.; Wang, S.; Li, T.; Wang, B.; Ma, X.; Huang, B.; Zhu, L.; Guo, J. Detection of Pesticide Residues Using Nano-SERS Chip and a Smartphone-Based Raman Sensor. *IEEE J. Select. Topics Quantum Electron.* **2019**, *25* (2), 1–6. https://doi.org/10.1109/JSTQE.2018.2869638.

(29) Anirudhan, T. S.; Alexander, S. Design and Fabrication of Molecularly Imprinted Polymer-Based Potentiometric Sensor from the Surface Modified Multiwalled Carbon Nanotube for the Determination of Lindane (γ-Hexachlorocyclohexane), an Organochlorine Pesticide. *Biosensors and Bioelectronics* **2015**, *64*, 586–593. https://doi.org/10.1016/j.bios.2014.09.074.

(30) Li, H.; Wang, Z.; Wu, B.; Liu, X.; Xue, Z.; Lu, X. Rapid and Sensitive Detection of Methyl-Parathion Pesticide with an Electropolymerized, Molecularly Imprinted Polymer Capacitive Sensor. *Electrochimica Acta* **2012**, *62*, 319–326. https://doi.org/10.1016/j.electacta.2011.12.035.

(31) Madianos, L.; Skotadis, E.; Tsekenis, G.; Patsiouras, L.; Tsigkourakos, M.; Tsoukalas, D. Impedimetric Nanoparticle Aptasensor for Selective and Label Free Pesticide Detection. *Microelectronic Engineering* **2017**, *189*, 39–45. https://doi.org/10.1016/j.mee.2017.12.016.

(32) Fan, L.; Zhang, C.; Yan, W.; Guo, Y.; Shuang, S.; Dong, C.; Bi, Y. Design of a Facile and Label-Free Electrochemical Aptasensor for Detection of Atrazine. *Talanta* **2019**, *201*, 156–164. https://doi.org/10.1016/j.talanta.2019.03.114.

(33) Koukouvinos, G.; Tsialla, Z.; Petrou, P. S.; Misiakos, K.; Goustouridis, D.; Ucles Moreno, A.; Fernandez-Alba, A. R.; Raptis, I.; Kakabakos, S. E. Fast Simultaneous Detection of Three Pesticides by a White Light Reflectance Spectroscopy Sensing Platform. *Sensors and Actuators B: Chemical* **2017**, *238*, 1214–1223. https://doi.org/10.1016/j.snb.2016.09.035.

(34) Belenguer, J.; Estévez, M. C.; Lechuga, L. M.; Montoya, A.; Díaz, R. Development of an SPR-Based Immunoassay for the Detection of Thiabendazole. *International Conference on Food Innovation* **2010**.

(35) Estevez, M.-C.; Belenguer, J.; Gomez-Montes, S.; Miralles, J.; M. Escuela, A.; Montoya, A.; M. Lechuga, L. Indirect Competitive Immunoassay for the Detection of Fungicide Thiabendazole in Whole Orange Samples by Surface Plasmon Resonance. *Analyst* **2012**, *137* (23), 5659–5665. https://doi.org/10.1039/C2AN36094B.

(36) Blažková, M.; Rauch, P.; Fukal, L. Strip-Based Immunoassay for Rapid Detection of Thiabendazole. *Biosensors and Bioelectronics* **2010**, *25* (9), 2122–2128. https://doi.org/10.1016/j.bios.2010.02.011.

(37) Ruscito, A.; McConnell, E. M.; Koudrina, A.; Velu, R.; Mattice, C.; Hunt, V.; McKeague, M.; DeRosa, M. C. In Vitro Selection and Characterization of DNA Aptamers to a Small Molecule Target. *Current Protocols in Chemical Biology* **2017**, *9* (4), 233–268. https://doi.org/10.1002/cpch.28.

(38) Wang, H.; Cheng, H.; Wang, J.; Xu, L.; Chen, H.; Pei, R. Selection and Characterization of DNA Aptamers for the Development of Light-up Biosensor to Detect Cd(II). *Talanta* **2016**, *154*, 498–503. https://doi.org/10.1016/j.talanta.2016.04.005.

(39) Zheng, D.; Zou, R.; Lou, X. Label-Free Fluorescent Detection of Ions, Proteins, and Small Molecules Using Structure-Switching Aptamers, SYBR Gold, and Exonuclease I. *Anal. Chem.* **2012**, *84* (8), 3554–3560. https://doi.org/10.1021/ac300690r.

(40) Lv, L.; Li, D.; Liu, R.; Cui, C.; Guo, Z. Label-Free Aptasensor for Ochratoxin A Detection Using SYBR Gold as a Probe. *Sensors and Actuators B: Chemical* **2017**, *246*, 647–652. https://doi.org/10.1016/j.snb.2017.02.143.

(41) Gao, X.; Qi, L.; Liu, K.; Meng, C.; Li, Y.; Yu, H.-Z. Exonuclease I-Assisted General Strategy to Convert Aptamer-Based Electrochemical Biosensors from "Signal-Off" to "Signal-On." *Anal. Chem.* **2020**, *92* (9), 6229–6234. https://doi.org/10.1021/acs.analchem.0c00005.

(42) Li, H.; Song, S.; Wen, M.; Bao, T.; Wu, Z.; Xiong, H.; Zhang, X.; Wen, W.; Wang, S. A Novel Label-Free Electrochemical Impedance Aptasensor for Highly Sensitive Detection of Human Interferon-Gamma Based on Target-Induced Exonuclease Inhibition. *Biosensors and Bioelectronics* **2019**, *142*, 111532. https://doi.org/10.1016/j.bios.2019.111532.

(43) Guo, Z.; Lv, L.; Cui, C.; Wang, Y.; Ji, S.; Fang, J.; Yuan, M.; Yu, H. Detection of Aflatoxin B 1 with a New Label-Free Fluorescent Aptasensor Based on Exonuclease I and SYBR Gold. *Analytical Methods* **2020**, *12* (22), 2928–2933. https://doi.org/10.1039/D0AY00967A.

(44) Berkal, M. A.; Palas, Q.; Ricard, E.; Lartigau-Dagron, C.; Ronga, L.; Toulmé, J.-J.; Parat, C.; Nardin, C. Glyphosate-Exonuclease Interactions: Reduced Enzymatic Activity as a Route to Glyphosate Biosensing. *Macromol Biosci* **2023**, e2200508. https://doi.org/10.1002/mabi.202200508.

(45) Aptamer specifically bound with glyphosate and application. Aptamer Specifically Bound with Glyphosate and Application. 2015.

(46) Arduini, F.; Cinti, S.; Caratelli, V.; Amendola, L.; Palleschi, G.; Moscone, D. Origami Multiple Paper-Based Electrochemical Biosensors for Pesticide Detection. *Biosensors and Bioelectronics* **2019**, *126*, 346–354. https://doi.org/10.1016/j.bios.2018.10.014.

(47) de Lima, F.; Lucca, B. G.; Barbosa, A. M. J.; Ferreira, V. S.; Moccelini, S. K.; Franzoi, A. C.; Vieira, I. C. Biosensor Based on Pequi Polyphenol Oxidase Immobilized on Chitosan Crosslinked with Cyanuric Chloride for Thiodicarb Determination. *Enzyme and Microbial Technology* **2010**, *47* (4), 153–158. https://doi.org/10.1016/j.enzmictec.2010.05.006.

(48) Kim, G.-Y.; Kang, M.-S.; Shim, J.; Moon, S.-H. Substrate-Bound Tyrosinase Electrode Using Gold Nanoparticles Anchored to Pyrroloquinoline Quinone for a Pesticide Biosensor. *Sensors and Actuators B: Chemical* **2008**, *133* (1), 1–4. https://doi.org/10.1016/j.snb.2008.01.055.

(49) García Sánchez, F.; Navas Díaz, A.; Ramos Peinado, M. C.; Belledone, C. Free and Sol–Gel Immobilized Alkaline Phosphatase-Based Biosensor for the Determination of Pesticides and Inorganic Compounds. *Analytica Chimica Acta* **2003**, *484* (1), 45–51. https://doi.org/10.1016/S0003-2670(03)00310-6.

(50) Mazzei, F.; Botrè, F.; Montilla, S.; Pilloton, R.; Podestà, E.; Botrè, C. Alkaline Phosphatase Inhibition Based Electrochemical Sensors for the Detection of Pesticides. *Journal of Electroanalytical Chemistry* **2004**, *574* (1), 95–100. https://doi.org/10.1016/j.jelechem.2004.08.004.

(51) Mazzei, F.; Botrè, F.; Botrè, C. Acid Phosphatase/Glucose Oxidase-Based Biosensors for the Determination of Pesticides. *Analytica Chimica Acta* **1996**, *336* (1), 67–75. https://doi.org/10.1016/S0003-2670(96)00378-9.

(52) Chauhan, N.; Pundir, C. S. An Amperometric Biosensor Based on Acetylcholinesterase Immobilized onto Iron Oxide Nanoparticles/Multi-Walled Carbon Nanotubes Modified Gold Electrode for Measurement of Organophosphorus Insecticides. *Analytica Chimica Acta* **2011**, *701* (1), 66–74. https://doi.org/10.1016/j.aca.2011.06.014.

(53) Vaghela, C.; Kulkarni, M.; Haram, S.; Aiyer, R.; Karve, M. A Novel Inhibition Based Biosensor Using Urease Nanoconjugate Entrapped Biocomposite Membrane for Potentiometric Glyphosate Detection. *International Journal of Biological Macromolecules* **2018**, *108*, 32–40. https://doi.org/10.1016/j.ijbiomac.2017.11.136.

Supporting Informations

Rapid and specific detection of thiabendazole: Enzymatic digestion-enabled fluorescent aptasensor

*Mohamed Amine Berkal, Jean-Jacques Toulmé, Corinne Nardin**

M. A. Berkal, C. Nardin

Universite de Pau et des Pays de l'Adour, E2S UPPA, CNRS, IPREM, Pau, France

E-mail: corinne.nardin@univ-pau.fr

J. J. Toulmé

ARNA Laboratory, Inserm U1212, CNRS UMR5320, University of Bordeaux, 33076 Bordeaux, France

Novaptech, 146 rue Léo Saignat, 33076 Bordeaux, France

Keywords: Thiabendazole, oligonucleotide switching structures, enzymatic digestion, fluorescence spectroscopy, biosensing

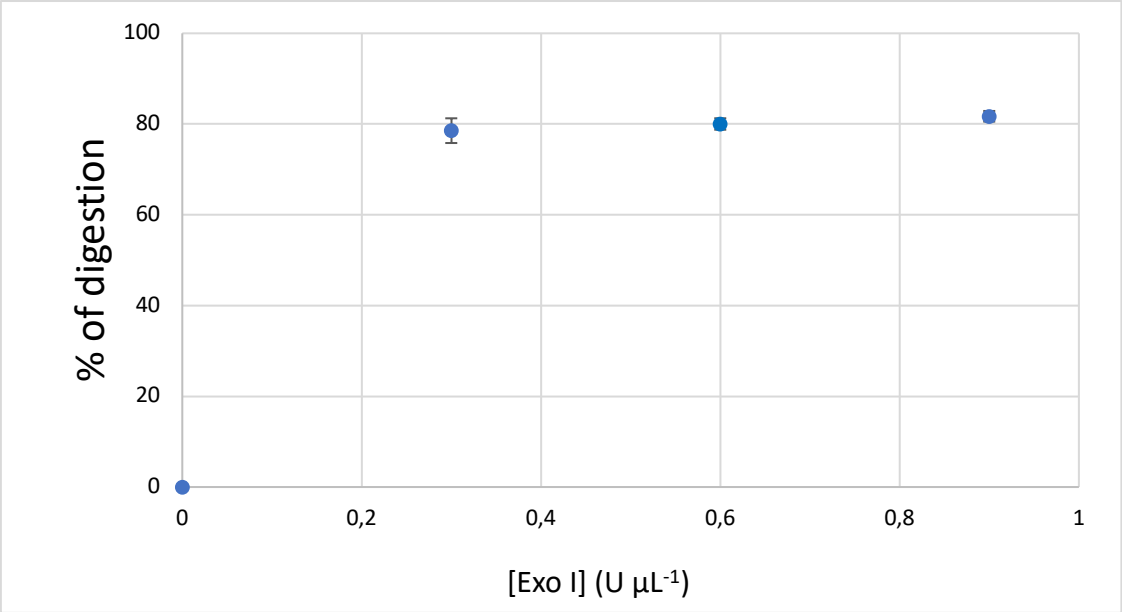

Figure IV-S1. Optimization of the Exo I concentration for GLY3 (1 µM) aptamer digestion.

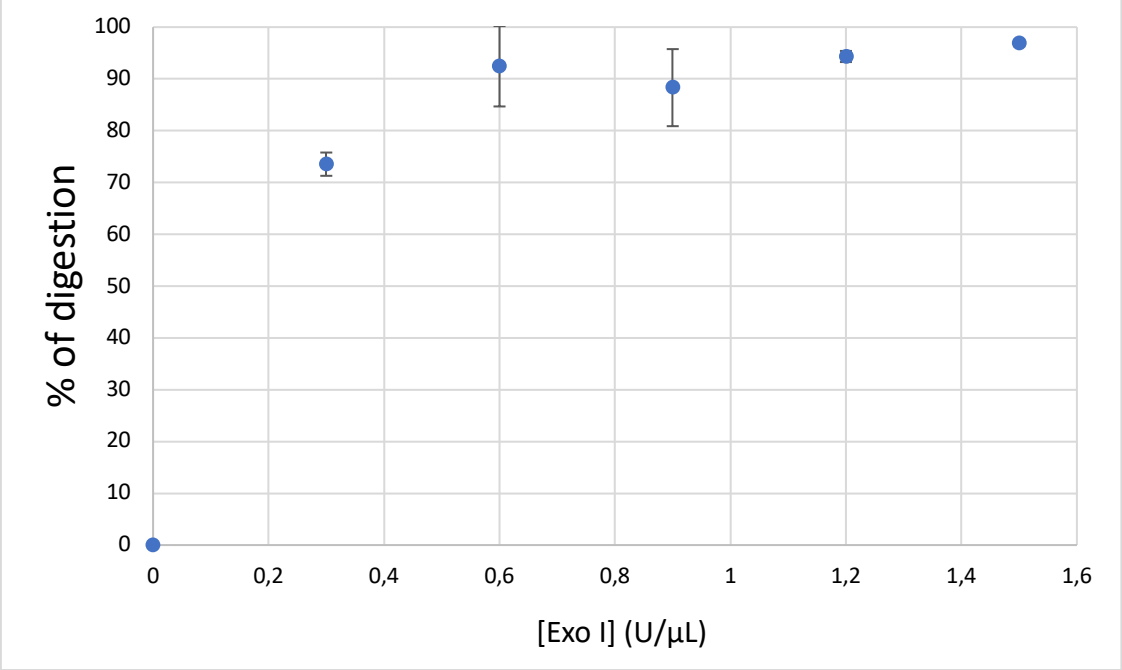

Figure IV-S2. Optimization of the Exo I concentration for BOL009 (1 µM) aptamer digestion.

Conclusion Générale et Perspectives

L'objectif principale de ce projet de thèse était de développer un biocapteur pour détecter, sur site et en temps réel, le glyphosate dans les eaux de surface. Après avoir réalisé une étude bibliographique approfondie (premier chapitre), les aptacapteurs électrochimiques se sont distingués parmi les autres types de biocapteurs de par leur capacité à fournir des mesures sensibles du fait de la détection électrochimique, couplée à la détection spécifique du fait de l'utilisation d'aptamère. Ces performances ont guidé notre choix vers le développement d'un aptacapteur électrochimique pour détecter le glyphosate. Le premier objectif était donc de sélectionner et optimiser un aptamère contre le glyphosate afin de pouvoir le combiner à une plateforme de détection électrochimique. Trois aptamères candidats ont pu être identifiés dans la littérature : GLY1, GLY2 et GLY3. L'interaction de ces aptamères candidats avec le glyphosate a été évaluée en utilisant la méthode de digestion enzymatique. Cette étude a été détaillée dans le deuxième chapitre. Malheureusement, aucun candidat n'a permis de démontrer une interaction avec le glyphosate. Suite à ce constat, une deuxième molécule cible, le thiabendazole, dont l'aptamère est fourni par l'entreprise Novaptech a été étudiée. Cet aptamère a été immobilisé sur une plateforme électrochimique qui a déjà permis la détection de la thrombine en utilisant son aptamère spécifique. Après avoir testé la détection du thiabendazole via cette plateforme, aucune variation de signal électrochimique n'a pu être obtenue. Bien que plusieurs optimisations aient été effectuées sur la plateforme électrochimique ainsi que sur la conception de l'aptamère, aucune détection n'a pu être observée. L'une des hypothèses les plus marquantes permettant d'expliquer ce résultat est celui stipulant qu'une molécule de haut poids moléculaire, après avoir été capturée par l'aptamère à la surface de l'électrode de travail, gène le flux d'électrons ce qui conduit à la réduction du flux des électrons et donc la détection de la thrombine. Or, pour le thiabendazole qui est une petite molécule, sa capture par l'aptamère semble n'engendrer aucune variation du signal par ce que la taille du thiabendazole est négligeable par rapport à l'aptamère et son interaction peut se faire dans une région définie sur l'aptamère n'engendrant aucun changement de conformation significatif, ni de propriétés physico-chimiques à la surface d'électrode permettant sa détection.

En résumé, notre étude démontre que les aptacapteurs électrochimiques sont adaptés à la détection de molécules de haut poids moléculaire qui provoquent des changements physico-chimiques notables à la surface de l'électrode. Cependant, pour les petites molécules, notre recherche suggère que la détection électrochimique n'est pas appropriée en l'état actuel des

connaissances. D’autres types d’électrodes toutefois plus coûteuse comme le SiC pourrait être considérées mais non qualifiable pour une utilisation sur le terrain à bas coût.

Les résultats décrits dans le dernier chapitre montrent, si cela était nécessaire, que les aptamères sont adaptés pour détecter les petites molécules en solution. Ceci s’explique par le fait que le principe de détection est différent de celui utilisé en électrochimie. La méthode de digestion enzymatique permet une détection simple, rapide et spécifique envers l’analyte. Cette méthode peut également être appliqué à n’importe quelle cible ayant son aptamère, que ce soit une longue séquence ou une courte séquence, ou bien une petite molécule ou une grande molécule, comme le prouve le test de détection de la thrombine considérée comme une grande molécule ayant un aptamère de courte séquence (20 bases nucléotidiques).

La limite de ces biocapteurs développés est leur faible sensibilité. Selon la législation, les eaux de consommation humaine (ECDH) sont considérées de qualité si les pesticides ne dépassent pas les MRL qui sont fixées à 0.1 µg L^{-1} pour chaque pesticide. Dans notre étude, les deux biocapteurs montraient des limites de détection autour de 16 mg L^{-1} et de 0.2 mg L^{-1} pour le glyphosate et le thiabendazole respectivement, ce qui est bien au-dessus des MRL établis par la législation. Pour remédier à ce problème, il est envisageable d'explorer d'autres conceptions de reconnaissance aptamère/cible en utilisant des oligonucléotides complémentaires ou des sondes de fluorescence plus sensibles. D’autres part, l'utilisation de séquences d'oligonucléotides marquées par des sondes, fluorophores ou chromophores, ainsi que l'exploration d'autres techniques telles que les nanoparticules d'or greffées par des aptamères, peuvent être étudiés pour détecter ces pesticides avec une meilleure sensibilité.

En fin de compte, notre travail ouvre des perspectives prometteuses pour l'utilisation des aptamères dans la détection de petites molécules en solution, offrant des avantages considérables en termes de simplicité, rapidité et de spécificité d’analyse. Ces découvertes sont susceptibles de contribuer de manière significative au domaine de la détection des pesticides et à ses applications pratiques. D’autre part, la détection électrochimique ne semble pas adaptée, d’après nos conclusions de recherche, à la détection des pesticides en utilisant leurs aptamères.

General conclusion and perspectives

The main objective of this thesis project was to develop a biosensor for the on-site and real-time detection of glyphosate in surface waters. After conducting an in-depth literature review (**Chapter I**), electrochemical aptasensors were stood out for their ability to provide sensitive measurements through the electrochemical detection, in combination to specificity when using aptamers as recognition element. These performances guided our choice towards the development of an electrochemical aptasensor for glyphosate detection. The first objective was therefore to develop an aptamer against glyphosate for use on the electrochemical platform. Three candidate aptamers were identified in the literature: GLY1, GLY2, and GLY3. The interaction of these candidate aptamers with glyphosate was evaluated using the enzymatic digestion method, as detailed in **Chapter II**. Unfortunately, none of the candidates demonstrated interaction with glyphosate.

Following this observation, a second target molecule, thiabendazole, for which the aptamer was selected and optimized by the company Novaptech, was studied. This aptamer had previously been successfully immobilized on an electrochemical platform, allowing the detection of thrombin using its specific aptamer. After testing the detection of thiabendazole via this developed electrochemical platform, no variation in electrical signal could be observed. Despite several optimizations of the electrochemical platform and aptamer design, no detection could be achieved. One of the most prominent hypotheses explaining this result is that a large molecule, once captured by the aptamer on the working electrode surface, hinders electron flow, leading to a reduction in electrical current and thus the detection of thrombin. However, for thiabendazole, which is a small molecule, its capture by the aptamer may not induce any signal variation because the size of thiabendazole is negligible compared to the aptamer, and its interaction can occur within a defined region on the aptamer without significant changes in conformation or physicochemical properties at the electrode surface allowing its detection.

In summary, our studies demonstrate that electrochemical aptasensors are suitable for the detection of large molecules that induce significant physicochemical changes at the electrode surface. However, for small molecules, our research suggests that electrochemical detection is not appropriate at the current stage and improvement of the electrode might enable to achieve the targeted detection but at prizes inappropriate on-site detection.

The results described in the last chapter (**Chapter IV**), if it were necessary, confirm that aptamers are well-suited for detecting small molecules in solution. This is explained by the fact that the detection principle differs from that needed for electrochemical detection. The enzymatic digestion method allows simple, rapid, and specific detection of the analyte. This method can also be applied to any other target if its aptamer has been selected and optimized, whether it is a long sequence or a short sequence, or a small or large molecule, as demonstrated by the thrombin detection test, considered as a large molecule with a short aptamer sequence (20 nucleotide bases).

The limitation of these developed biosensors is their low sensitivity. According to the legislation, human consumption water (ECDH) is considered to be of good quality if the pesticides do not exceed the MRLs, which are set at 0.1 µg L^{-1} for each pesticide. In our study, the two biosensors showed detection limits are around 16 mg L^{-1} and 0.2 mg L^{-1} for glyphosate and thiabendazole respectively, which is well above the MRLs set by the legislation. To overcome this problem, other aptamer/target recognition designs could be explored, using complementary oligonucleotides or more sensitive fluorescence probes. On the other hand, the use of oligonucleotide sequences labelled with fluorophore or chromophore probes, as well as the exploration of other techniques such as gold nanoparticles grafted with aptamers, could be studied to detect these pesticides with greater sensitivity.

Ultimately, our work opens up promising prospects for the use of aptamers in the detection of small molecules in solution, offering significant advantages in terms of simplicity, rapidity and specificity. These findings are likely to make a significant contribution to the field of pesticide detection and its practical applications in the future.